

**Using By-product Industrial Materials to Replace All Cement in
Construction Products**

Seema Karami

BEng and MSc in Civil Engineering

PhD Thesis

Faculty of Engineering and Computing

Coventry University

In collaboration with Lafarge Plasterboard

November, 2008

Abstract

At present, cementitious binders are used extensively in the construction industry and principally in concretes. They are also used in some applications like ground improvement. In these applications the cost of the binder, typically Portland cement, accounts for a considerable proportion of the total cost of the technique. In addition to the financial cost there is also the environmental impact of quarrying and processing of raw materials to produce Portland cements.

Gypsum waste, by-pass dust and fly ash by-products have been identified as the alternative sources of cementitious binder. Using these materials has two advantages: they have little or no production cost; and the re-use of such material would negate the need for expensive disposal.

This thesis describes a programme of laboratory testing and study on the possible field trials to investigate the possibility of using mentioned by-product materials as construction materials.

Laboratory trials carried out to investigate the properties of waste materials in different combinations; binary and ternary using the same water content.

Specimens were evaluated on the basis of Unconfined Compressive Strength at 3,7 and 28 days curing. It was found that pastes containing waste gypsums, Basic oxygen Slag and Run of station ash achieved the highest unconfined compressive strengths (up to 20 MPa) and five mixes of these groups were selected for further tests such as viscosity, permeability, expansion, XRD and freeze and thaw.

Data obtained from the ternary combinations were analyzed using two different methods, i.e. Response Surface method and Artificial Neural Network.

Two prediction models were created using MINITAB and MATLAB software and the predicted results were compared. It was concluded that the Artificial Neural Network had fewer errors than the response surface model.

The feasibility of using by-product materials in two field trials was also studied and the possibility of 100% cement replacement in low strength concrete used in subway backfilling (using 80%BOS-15% Plasterboard Gypsum-5%bypass dust) and light weight blocks (60% run of station ash-20%plaster board gypsum-20% bypass dust) was investigated.

It was found that waste gypsum could be used in both trials and the basic oxygen slag could be used for subway backfilling because it improved the flow. However it was not a good idea to use the steel slag in light weight products because of its density.

The thesis concludes that there are several potential applications for the use of the waste gypsums in combination with other waste materials in the construction industry but further work is required before it can be used commercially. However the sources and differing chemical contents of the by-product materials may have significant impact on the cementitious behaviour of by product materials.

Contents

1. Introduction	
1.1 Introduction	1
1.2 Background	2
1.3 Aims and Objectives	2
1.4 Project Overview	5
2. Literature Review	
2.1 Introduction	6
2.2 A summary about Portland cement	7
2.3 Sulphate activated Cement	8
2.4 Waste	8
2.4.1 Classification of waste	8
2.5 Previous Use of Wastes in Construction Industry	8
2.5.1 Wastes in Cements and Concretes	8
2.5.2 Gypsum Waste	9
2.5.2.1 Flue gas desulphurisation	9
2.5.2.2 Phosphogypsum	9
2.5.2.3 Plasterboard Gypsum	10
2.5.2.4 Red Gypsum	11
2.5.3 Ashes	12
2.5.3.1 Sources of Ash	12
2.5.3.2 Use of Ash as fill materials	13
2.5.3.3 Use of Ash in Concrete	13
2.5.3.4 Ternary Blend of PC-PFA-GGBS	14
2.5.3.5 Use of Ash in Wall board	15

2.5.3.6 Ash –Gypsum and Ash-CKD Mixes	15
2.5.4 Slag	16
2.5.4.1 Types of Slag	16
2.5.4.2 Hydraulic Activity of Slag	16
2.5.4.3 Uses of Slag	17
2.5.5 Cement Kiln Dust CKD	20
2.5.6 A summary of the Review	23
3. Experimental Method	
3.1 Introduction	24
3.2 Sources of Materials	24
3.3 Chemical Analysis	27
3.4 Particle Size	28
3.5 Density	28
3.6 Mill	29
3.7 Mixing procedure	29
3.8 Paste mixtures	30
3.9 Flow test	31
3.10 Viscosity of Concrete	33
3.11 Setting Time	35
3.12 pH Measurement	36
3.13 Casting	36
3.14 Curing	37
3.15 Compressive Strength Testing	38
3.16 Cube Crusher	39
3.17 Expansion	40

3.18 Freeze – Thaw Resistance	40
3.19 X-Ray Diffraction (XRD) test and Sample preparation and analysis	42
3.20 Scanning Electron Microscopy (SEM)	42
3.21 High Pressure Flow Test (Permeability)	43
3.22 Inductivity Coupled Plasma (ICP)	46
4. Test Programme and Results	
4.1 Testing	46
4.2 Chemical analysis of Materials	48
4.3 Particle size	49
4.4 Results of Step 1-Binary Mixes	51
4.4.1 Basic Oxygen Slag (BOS)- Run Of Station Ash(ROSA)	51
4.4.2 Basic Oxygen Slag (BOS) - Bypass Dust (BPD)	53
4.4.3 Basic Oxygen Slag (BOS) – Red Gypsum (RG)	54
4.4.4 Basic Oxygen Slag (BOS) – Plasterboard Gypsum (PG)	56
4.4.5 Bypass Dust (BPD) – Run of Station Ash (ROSA)	57
4.4.6 Run of Station Ash (ROSA)-Red Gypsum (RG)	58
4.4.7 Run of Station Ash (ROSA)-Plasterboard Gypsum (PG)	59
4.4.8 Bypass Dust (BPD)-Red Gypsum (RG)	60
4.4.9 Bypass Dust (BPD)-Plasterboard Gypsum (PG)	61
4.5 Results of Step 2-Ternary Mixes	62
4.5.1 Setting time	62
4.5.2 Compressive strength	63
4.6 Selected Binder Mixes	74
4.6.1 Effect of water content on compressive strength	74
4.6.2 Effect of particle size on compressive strength	76

4.6.3 Length change of five selected pastes (Expansion)	77
4.6.4 X-Ray Diffraction Analysis	80
4.6.5 Permeability (High Pressure Flow Test) and ICP	82
4.6.6 Water absorption	84
4.7 Concrete Samples	84
4.7.1 Viscosity	84
4.7.2 Freeze Thaw and Wet/Dry Testing	86
5. Data Analysis and Mathematical Modelling	
5.1 Introduction	87
5.2 Response Surface Method	88
5.2.1 Introduction	88
5.2.2 Mixture Design	89
5.2.3 Results of Mixture Design and Regression	92
5.3 Using Artificial Neural Network for Prediction	95
5.3.1 Introduction	95
5.3.2 Error Minimisation	97
5.4 Neural Network Model and Parameters	97
5.4.1 Architecture	98
5.4.2 Neuron Model	98
5.4.3 Feedforward Network	99
5.4.4 Training	100
5.4.5 Software and Transfer Function	101
5.5 Analysis of Results	102
5.6 Discussion and Conclusions	104

6. Field Trial Subway Backfilling in Coventry and Block Making	
6.1 Introduction	105
6.1.1 Material Preparations for subway backfilling	106
6.2 Light weight block	109
6.2.1 Specification for blocks	110
6.2.2 Mixes with BOS and Air entrainment	110
6.2.3 Air entrained mixes without BOS	113
6.2.4 Using Crushed Plasterboard as Light Weight Aggregate	114
6.2.5 Mixes with normal Ligh Weight Aggregate	117
6.2.6 Effect of source of waste products on characteristics of Light weight concrete	118
6.2.7 Effect of plasterboard particle size on compressive strength and density of block samples	121
6.2.8 Hanson Concrete samples	124
7. Discussion	
7.1 Introduction	125
7.2 Hydration mechanism in the pasts	125
7.3 Flow	127
7.4 Compressive Strength	134
7.5 Density	144
7.6 Achievements and Implications	145
8. Conclusions and Recommendations for future work	146

Figures

Figure 3- 1 Fresh Red Gypsum	25
Figure 3- 2 Plasterboard Gypsum before and after grinding	26
Figure 3- 3 Micromeritics AccuPyc 1330 Helium Pycnometer and Sample Cells	29
Figure 3- 4 Ball Mill	29
Figure 3- 5 From left: 2-litre mixer, 10-litre mixer, horizontal mixer	30
Figure 3- 6 Modified Flow table	31
Figure 3- 7 Slump Test Equipment	32
Figure 3- 8 Rheological behaviour of some viscous materials (Shames,1992:18)	33
Figure 3- 9 ICAR Rheometer	34
Figure 3- 10 Vicat Apparatus for determining the setting time of mortar	35
Figure 3- 11 50mm and 100 mm cubes	36
Figure 3- 12 (a and b) - Hammer drill with designed attached plate	37
Figure 3- 13 Sample curing container	37
Figure 3- 14 Lloyd computerised compressive strength testing machine	38
Figure 3- 15 Avery Denison Cube Crusher	39
Figure 3- 16 Length change test samples and apparatus	39
Figure 3- 17 Environmental Chamber	40
Figure 3- 18 Temperature Change in Freeze thaw cycle	41
Figure 3- 19 Permeability test apparatus	43
Figure 3- 20 Modifications to Hoek Cell for Concrete Permeability Measurements (Ganjian et al. 2004)	44
Figure 4- 1 Particle size analysis of ground (for two hours) and sieved red gypsum	49
Figure 4- 2 Particle size analysis of ground (for two hours) and sieved plasterboard gypsum.	49

Figure 4- 3 Particle size analysis of ground (for 4 hours) and sieved basic oxygen slag	50
Figure 4- 4 Particle size analysis of by-pass dust (2)	50
Figure 4- 5 Particle size analysis of run of station ash (Ratcliff power station)	50
Figure 4- 6 Compressive Strength of BOS - ROSA pastes at 3,7, and 28 days	52
Figure 4- 7 Compressive Strength of BOS – BPD pastes at 3,7, and 28 days	53
Figure 4- 8 Compressive Strength of BOS – RG pastes at 3,7, and 28 days	55
Figure 4- 9 Compressive Strength of BOS – PG pastes at 3, 7, and 28 days	56
Figure 4- 10 Compressive Strength of ROSA-BPD pastes at 3, 7, and 28 days	57
Figure 4- 11 Compressive Strength of ROSA – RG pastes at 3, 7, and 28 days	59
Figure 4- 12 Compressive Strength of ROSA – PG pastes at 3, 7, and 28 days	60
Figure 4- 13 Compressive Strength of BPD – RG pastes at 3, 7, and 28 days	61
Figure 4- 14 Compressive Strength of BPD – PG pastes at 3, 7, and 28 days	62
Figure 4- 15 (A and B)- BOS+ROSA+BPD strength (MPa) after 7 and 28 days	67
Figure 4- 16 (A and B)- BOS+ROSA+RG strength (MPa) after 7 and 28 days	68
Figure 4- 17 (A and B)- BOS+ROSA+PG strength (MPa) after 7 and 28 days	69
Figure 4- 18 (A and B)- BOS+BPD+PG strength (MPa) after 7 and 28 days	70
Figure 4- 19 (A and B)- BOS+BPD+RG strength (MPa) after 7 and 28 days	71
Figure 4- 20 (A and B)- ROSA+BPD+RG strength (MPa) after 7 and 28 days	72
Figure 4- 21 (A and B)- ROSA+BPD+PG strength (MPa) after 7 and 28 days	73
Figure 4- 22 Effect of w/b ratio on Compressive Strength at different ages	75
Figure 4- 23 Compressive strength development of semy-dry BOS-BPD-PG mix at 28 days with various w/c according to Ganjian et al. (2007) results	76
Figure 4- 24 Effects of Particle size on Compressive strength (MPa) of BOS-ROSA-PG/RG mixes	77
Figure 4- 25 Cracking was observed in samples during curing because of high water/binder ratio	78

Figure 4- 26 Length Change of Selected Paste and Mortar Samples at different ages	79
Figure 4- 27 XRD of BOS-ROSA-RG at 3 days-E=Ettringite, G=Gypsum, Q=Quartz	80
Figure 4- 28 XRD of BOS-ROSA-RG at 7 days-E=Ettringite, G=Gypsum, Q=Quartz	81
Figure 4- 29 XRD of BOS-ROSA-RG at 28 days-E=Ettringite, G=Gypsum, Q=Quartz	81
Figure 4- 30 Viscosity of cement replacement concrete and control mix	85
Figure 4- 31 Concrete sample BOS 30%-ROSA 60%-RG 10% burst after 10 freeze-thaw cycles	86
Figure 4- 32 Concrete sample BOS 30%-ROSA 60%-PG10% burst after 10 freeze-thaw cycles	86
Figure 5- 1 Simple Design diagram	90
Figure 5- 2 Different groups of mixes in Step 2	91
Figure 5- 3 Mixture Design Plot and Mixture Contour Plot For Mix BOS-ROSA-BPD	93
Figure 5- 4 Comparison between Predicted and Experimental 28 days Compressive strength for BOS-ROSA-BPD Group	95
Figure 5- 5 Schematic diagram of an artificial neuron	96
Figure 5- 6 log-Sigmoid Transfer Function	99
Figure 5- 7 Proposed NN model	101
Figure 5- 8 Network summary as it was created by MATLAB 6.1 software	102
Figure 5- 9 Performance Of training set of 80 paste design data	102
Figure 5- 10 Performance Of test set of 10 paste design data	103
Figure 6- 1 Sieve analysis of fine and coarse aggregate	107
Figure 6- 2 Shear stress at the end of subway	109

Figure 6- 3 (a,b) Effect of foaming on Compressive Strength and Density on mix (48%BOS-40%ROSA-12%RG)	111
Figure 6- 4 (a,b,c) Microscopic photos of air entrained samples with 0.5%,1% and 2% foaming agent	112
Figure 6- 5 Sample compaction using hammer drill for 50 mm cube	115
Figure 6- 6 Attached plate to hammer drill for better compaction	115
Figure 6- 7 Crushed plasterboard as aggregate in light weight samples	116
Figure 6- 8 Effect of using PG as aggregate on the compressive strength	117
Figure 6- 9 Effect of Sources of BPD on The Compressive Strength of pastes	120
Figure 6- 10 Effect of different sources of Ash on the compressive strength	121
Figure 6- 11 Effect of ROSA source and PG particle size on the compressive strength of specimens	123
Figure 6- 12 Effect of ROSA source and PG particle size on the density of specimens	123
Figure 6- 13 Fresh light weight concrete demoulded straight after concrete casting	124
Figure 7- 1 Hydration of a single Portland cement grain	126
Figure 7- 2 Effect of BOS on Flow in the binary mixes with other waste materials	128
Figure 7- 3 Effect of ROSA on Flow in the binary mixes with other waste materials	129
Figure 7- 4 Effect of BPD on Flow in the binary mixes with other waste materials	129
Figure 7- 5 Effect of waste material contents on the flow of the ternary pastes BOS-BPD-ROSA	130
Figure 7- 6 Effect of waste material contents on the flow of the ternary pastes BPD-BOS-RG	131
Figure 7- 7 Effect of waste material contents on the flow of the ternary pastes BPD-BOS-RG	132
Figure 7- 8 Effect of waste material contents on the flow of the ternary pastes BOS-ROSA-RG	133

Figure 7- 9 Effect of waste material contents on the flow of the ternary pastes BOS-ROSA-PG	133
Figure 7- 10 Relationship between Flow and Compressive strength of pasts containing BOS	135
Figure 7- 11 Relationship between Flow and Compressive strength pasts containing ROSA	138
Figure 7- 12 Relationship between Flow and Compressive strength pasts containing BPD	139
Figure 7- 13 Effect of Compressive Strength on Permeability of pastes	141
Figure 7- 14 Effect of Compressive Strength on setting time of pasts	142
Figure 7- 15 Effect of Compressive Strength on Length Change of samples at 28 days	143

Tables

Table 2-1 Main Compound of Portland cement (Neville 2000)	7
Table 4- 1 Summary of Tests of Step 1-Binary Combinations	46
Table 4- 2 Summary of Tests of Step 2-Ternary Combinations	47
Table 4- 3 Tests on Five Selected Mixes	47
Table 4- 4 Effect of Particle size and w/c on selected mixes	47
Table 4- 5 Chemical analysis of Raw materials	48
Table 4- 6 Characterisation of BOS and ROSA Mixes	51
Table 4- 7 Characterisation of BOS and BPD Mixes	53
Table 4- 8 Characterisation of BOS and RG Mixes	54
Table 4- 9 Characterisation of BOS and PG Mixes	56
Table 4- 10 Characterisation of BPD and ROSA Mixes	57
Table 4- 11 Characterisation of ROSA and RG Mixes	58
Table 4- 12 Characterisation of ROSA and PG Mixes	59
Table 4- 13 Characterisation of BPD and RG Mixes	60
Table 4- 14 Characterisation of BPD and PG Mixes	61
Table 4- 15 Setting time measurement	62
Table 4- 16 Characterisation of BOS, ROSA, and PBD Mixes	63
Table 4- 17 Characterisation of BOS, BPD, and RG Mixes	64
Table 4- 18 Characterisation of BOS, BPD, and PG Mixes	64
Table 4- 19 Characterisation of BOS, ROSA, and RG Mixes	65
Table 4- 20 Characterisation of BOS, ROSA, and PG Mixes	65
Table 4- 21 Characterisation of ROSA, BPD, and PG Mixes	65
Table 4- 22 Characterisation of ROSA, BPD, and RG Mixes	66

Table 4- 23 Selected mixes for further tests	74
Table 4- 24 Effect of water/binder ratio on Compressive Strength of samples	74
Table 4- 25 Effects of particle size on compressive strength of pastes	76
Table 4- 26 Permeability of samples	83
Table 4- 27 ICP analysis of solution from 5 selective mixes	83
Table 4- 28 Water absorption of pastes	84
Table 4- 29 Flow of concrete samples	85
Table 5- 1 BOS-ROSA-BPD mixture design and compressive strength at 28 days (laboratory data)	92
Table 5- 2 Predicted Response for New Design Points Using Model for 28 days	94
Table 5- 3 The different ANN that used to train the data of BOS,BPD,RG,PG, and ROSA in ternary mixes	101
Table 5- 4 Test set data (10 pastes) for prediction model	103
Table 6- 1 Mix Design with Coventry Novel Cement	107
Table 6- 2 Sieve Analysis of Coarse and Fine Aggregate	108
Table 6- 3 Properties of Coventry concrete mix for subway backfilling	108
Table 6- 4 Checking shear stress for subway ends	108
Table 6- 5 Sample (48%BOS-40%ROSA-12%RG)air entraining with different amount of Foaming Agent from Lafarge plasterboard	110
Table 6- 6 Mix design for light weight paste using foaming agent aggregate	114
Table 6- 7 Mix design for light weight paste using crushed plasterboard as light aggregate	114
Table 6- 8 Trial mixes for the light weight block	117
Table 6- 9 Light weight concrete trials using light weight aggregate	118
Table 6- 10 Chemical analysis of 4 different types of ROSA	119

Table 6- 11 Effect of BPD from same source and different batches on specimens	120
Table 6- 12 Compressive strength of 4 different Ashes	121
Table 6- 13 PG sieve analysis	122
Table 6- 14 Effect of ROSA source and PG size on compressive strength and density of specimens	122

List of Abbreviations

Basic Oxygen Slag: BOS

By-Pass Dust: BPD

Cement Kiln Dust: CKD

Compressive Strength: CS

Controlled Low Strength Material: CLSM

Engineering and Physical Sciences Research Council: EPSRC

Flue Gas Desulphurisation: FGD

Ground Granulated Blastfurnace Slag: GGBS

Inductively Coupled Plasma: ICP

Knowledge Transfer Networks: (KTNs)

Ordinary Portland cement: OPC

Plasterboard Gypsum: PG

Red Gypsum: RG

Run Of Station Ash: ROSA

Scanning Electron Microscopy: SEM

Waste and Resources Action Programme: WRAP

X-Ray Diffraction: XRD

X-Ray Fluorescence: XRF

1.INTRODUCTION

1.1 Introduction

The aim of this research was to investigate the potential to use by-product materials, especially red gypsum (from the production of titanium dioxide pigment) and plasterboard gypsum (from demolition sites) as construction raw materials. The focus of the research concentrated on developing and maximizing cementitious reactions of waste gypsum by mixing it with other by-product materials (Basic Oxygen Slag, Run of Station Ash and cement Bypass Dust), to create some cementitious binders for cement replacement. The ultimate objective was to find applications for the binders in the manufacturing of light weight blocks and low strength concrete to be used as backfilling material.

The use of waste materials in construction is increasing and has its own market and related standards. Pulverised Fly Ash (PFA) and Ground Granulated Blast Furnace Slag (GGBS) are examples of materials that used to be wastes and presently are used as construction materials. Fly ash and GGBS are used as partial replacements for cement in concrete manufacturing and are used in soil stabilization for road construction.

Studies have been carried out previously to investigate the uses of by-product materials which were used in this research within the construction industry. These are reviewed in Chapter 2.

This research was funded by the EPSRC as a part of the Resource Efficiency Knowledge Transfer Network (KTN)s scheme. The waste materials were selected according to the contract (appendix A).

The work was closely related to the Waste and Resources Action Programme (WRAP) contract in which a “Coventry Blend” binder (the binder materials were three by-product materials that were used in this research) was developed and three successful site trials were completed with it (Ganjian *et al.* 2007).

1.2 Background

Rapid industrialization in developing countries continues to attract growth in urbanized areas. New construction to support urbanization, such as buildings for housing and industries, mass transit for moving people, and facilities for handling water and sewage all require construction activities. The shortage of conventional building materials in developing countries and abundantly available industrial waste products has promoted the development of new building materials (Kumar 2002).

Traditionally most waste will go to landfill. Many research projects are aimed at alternatives to dumping waste and instead finding ways to successfully use materials and lessen environmental impacts. This project was part funded by producers of waste gypsum in order to find uses for this material.

One alternative to landfill is to reuse industrial wastes in construction. The successful research and development of a new building material, or component using wastes as raw materials, is a very complex and multidisciplinary task, having technical, environmental, financial, marketing, legal and social aspects (John 2001).

This research has been motivated by the economic and environmental concerns over the disposal of wastes with the costs of traditional engineering materials.

1.3 Aims and Objectives

The aim of this research was to study on the potential for using waste gypsum by mixing it with other available waste materials and water to maximize the strength gain. The final aim is to apply the results of this research to introduce a novel product that can be used in construction.

Three categories of tests were performed to achieve **the aim** of the project.

1. Optimization of the paste mixes

Tests were developed and executed to achieve the following:

- To study the chemical and physical characteristics of each waste material by chemical analyses, particle size and density measurements
- To develop binders using contaminated gypsum and other wastes with no cement or other materials with commercial value
- To carry out trial mixes incorporating red gypsum and/or waste plasterboard to see if the compressive strength of pastes was enough to be used in low strength light weight blocks (**3 day compressive strength ≥ 2.5 MPa with a density of 1600 kg/m^3**).
- To measure the compressive strength of the mixed materials in binary (**two component**) and ternary (**three component**) combinations.
- To determine the optimal composition of the materials used in each of the mixes for making light weight blocks and other construction materials.
- To analyze the results of the performed tests using Neural Networks to determine how changing the relative amount of each of the composing materials affects the 28 days **compressive strength** of the mixes. Then to compare the results **to the results** obtained from employing a mathematical model, (Response Surface) and to determine which model yields more accurate results for predicting **behavioural** characteristics of the mixes

2. Further testing of five mixes which yielded the acceptable results in preliminary tests, to check the following:

- The workability and viscosity of concrete binders
- The setting time of the binders
- To determine what minerals were formed within selected binders using X-Ray Diffraction (XRD) tests
- The leaching from novel binders using high pressure flow tests and analyze the solutions leached from samples using Inductively Coupled

Plasma (ICP) method to measure the amount of heavy metals and sulfate in the samples

- the response of the novel concrete to the freeze-thaw cycles
- The expansion of the pastes

3. Design for **possible** site trials for the following purposes:

- To assess the suitability of self compacted concrete with 100% cement replacement using Coventry novel cement for subway backfilling in Coventry City Centre
- To develop a binder for light weight concrete block construction by mixing either red or plasterboard gypsum with other waste materials and water with advantageous strength and density properties
- To determine the effect of using different sources of ash and treatment of gypsum on the strength of blocks

The following materials were considered in this research (**according to the contract of this project that can be found in the Appendix A**):

- Red Gypsum (**RG**)
- Plasterboard Gypsum (**PG**)
- Basic Oxygen Slag (**BOS**)
- Cement By Pass Dust (**BPD**)
- Run Of Station Ash (**ROSA**)
- Ordinary Portland cement (OPC) and aggregate (gravel, sand and light weight aggregate) also were used for control mixes and concrete.
- **Foaming agent from Lafarge plasterboard**

The detail of the sources of the materials and methods are explained in chapter 3, Experimental Methods. The following is the list of tests carried out which were performed in this research:

- Flow test
- Compressive Strength test
- Viscosity **measurement**

- Setting Time **measurement**
- pH Measurement
- Expansion **measurement**
- Freeze – Thaw Resistance **measurement**
- X-Ray Diffraction (XRD) **analysis**
- Scanning Electron Microscopy (SEM)
- High Pressure Flow Test (Permeability)
- Inductively Coupled Plasma (ICP) **analysis**

1.4 Project Overview

A review of previous research on using waste materials in civil engineering and industrial products is presented in chapter 2 of this thesis.

The testing methods and apparatus and experimental program are explained in chapter 3. Chapter 4 includes the tests and the results for the binders. The mathematical modeling and analysis of the results are presented in chapter 5 which include the predictions of the compressive strength of the binders.

The findings of the project and the feasibility analysis of industrial application of the results of this research are presented in chapter 6.

The discussions and conclusions of the research and recommendations for further work are presented in chapter 7.

2.LITERATURE REVIEW

2.1 Introduction

In the following chapter, the literature and the reports related to the raw materials used in this research are studied. Some research methods of the reviewed documents are also employed in this research.

The results of the previous researches are compared with the results of this research. However the specific combinations of the raw materials in this research were not found in any other documents.

Most of previous researches aimed to partially replace Portland cement in construction products though the purpose of this research was to replace all cement in them.

Millions of tonnes of industrial waste materials are currently landfilled and thus unused around the world. Alternative methods of recycling these materials in production, especially construction products, are much more variable environmentally friendly options.

The increasing cost of disposal in the UK stimulated industries to find new effective alternate uses for waste materials. Normally every government makes efforts to recycle paper, glass, and similar kinds of waste but these are only a small proportion of waste products. More kinds of wastes originate from industries. The construction industry, energy production, and mining produce millions of tones of waste annually. The construction industry uses high

volume of waste as backfill and in concrete production every year; therefore it should be an ideal industry to recycle and utilise further waste.

2.2 A summary about Portland cement

The main raw materials used in manufacturing of Portland cement consist of **lime, clay, gypsum and iron oxide**. Four compounds that **are** usually the major constituents of cement are shown in Table 2-1:

Table 2-1 Main Compound of Portland cement (Neville 1995)

Name of Compound	Oxide Composition	Abbreviation
Tricalcium silicate	$3\text{CaO}.\text{SiO}_2$	C_3S
Dicalcium silicate	$2\text{CaO}.\text{SiO}_2$	C_2S
Tricalcium Aluminate	$3\text{CaO}.\text{Al}_2\text{O}_3$	C_3A
Tertacalcium Aluminoferrite	$4\text{CaO}.\text{Al}_2\text{O}_3.\text{Fe}_2\text{O}_3$	C_4AF

Minor compounds such as MgO , TiO_2 , Mn_2O_3 , K_2O , and Na_2O also exist in Portland cement in addition to the main compounds. K_2O and Na_2O are known as the alkalis. They can show the reactivity with some aggregates and this reaction can cause disintegration of the concrete and can affect the rate of the gain of strength of cement. However the amounts of minor compounds are not more than a few percent of the mass of cement. Generally the alkalis increase the early strength development and reduce the long-term strength (Neville 1995).

The main cementitious compounds in cement are the two calcium silicates, (**C_2S and C_3S**). The physical behaviour of cement during hydration is similar to that of **the** two compounds alone (Neville 1995).

Gypsum **may be** added to the cement clinker when it is cooled and grinding to a fine powder. This should be very carefully **controlled** because an excess of gypsum leads to an expansion and disruption of the set cement paste. The gypsum content required increases with the C_3A content and also with the alkali content of the cement. The gypsum amount added to cement clinker is as

the mass of SO₃ percent which is limited to a maximum of 3.5%. In some cases higher amounts of gypsum, **are permitted** (Neville 1995).

2.3 Sulphate activated Cement

Waste Gypsum can be used in calcium sulphoaluminate cement production. Calcium sulphoaluminate based cements show faster hardening than Portland cement because of rapid formation of ettringite (C₆AS₃H₃₂) that originates in hydration reaction of calcium sulphoaluminate (C₄A₃S) and calcium sulphate. This ettringite develops large crystals that have the ability to produce high strength at early stages (Beretka *et al.* 1996).

2.4 Waste

2.4.1 Classification of Wastes

“Waste is described as unused discharge products generated from human life, social and industrial activity. Radioactive industrial waste is regulated separately” (Chandra 1997).

Wastes are classified in three different groups: the industrial wastes, residential wastes and business wastes. Separate collection has been applied for the convenience of treatment and recycling of wastes (Chandra 1997).

2.5 Previous Use of Wastes in Construction Industry

2.5.1 Wastes in Cements and Concretes

The different types of mineral **additives** which are normally used in concrete products are: ash (fly ash), blast furnace slag, pozzolans and silica fume.

For example volcanic ash and pumice blended cement **have** been developed and used (Hossain 2003). **The** development of high volume fly ash binders was reported by Malhotra (2000). The use of cement kiln dust (CKD) and blast furnace slag (GGBS) in blended cement has been studied by Konsta-Gdoutos *et al.* (2003).

The use of fly ash is increasing every year. A high percentage of the cement in concrete can be replaced by fly ash. Concrete properties would not be affected for specific applications. However, a high-percentage replacement of cement by fly ash may result in concrete that has such a low workability that it is unusable in common manufacturing processes (Berryman *et al.* 2005).

The pozzolanic activity of a material is its ability to react with calcium hydroxide when it mixes with water to form hydrates possessing cementitious properties (Chandra 1997).

2.5.2 Gypsum Waste

The different sources of by-product gypsum reported in the literature are:

- 1) Flue gas desulphurisation (FGD) gypsum from power stations is the largest source of waste gypsum.
- 2) Phosphogypsum is an industrial by-product from the phosphoric acid and fertilizer industry.
- 3) Red Gypsum (RG) from Titanium Oxide production.
- 4) Plasterboard Gypsum (PG) from demolition sites.

2.5.2.1 Flue gas desulphurisation

Papageorgiou *et al.* (2005) studied using FGD gypsum as retarder in cement. They found FGD gypsum as a suitable alternative to natural gypsum based on the setting and strength results. Gypsum dehydration and formation of hemihydrate occurs in industrial cement mill. It has various effects on setting time and compressive strength. The extent of dihydrate conversion to hemihydrate depends on the clinker temperature and the relative humidity within the mill (Papageorgiou *et al.* 2005).

2.5.2.2 Phosphogypsum

Normally gypsum (phosphogypsum) anhydrate reacts slowly with water. It has to be activated by alkali sulphate activators, carbonate activators or a

combination of a small amount of Portland cement, alkali sulphate and $\text{Ca}(\text{OH})_2$ (Singh and Garg 1995).

Degirmenci *et al.* (2007) found the potential of using phosphogypsum (PG) in soil stabilization. They used class C fly ash and Portland composite cement. Their results showed that the treatment of soil (A-7-5, AASHTO classified) with fly ash, PG and cement reduced the plasticity index that is an indicator of soil improvement. Also, unconfined compressive strength of unstabilized soil was lower than the stabilized soil with above material.

Singh (2002) studied treating phosphogypsum for cement industries. He found that the purified phosphogypsum can be used as an additive in the manufacture of ordinary Portland cement and Portland slag cement. He also found that the purified phosphogypsum can be used for gypsum plaster production to be used in building material.

2.5.2.3 Plasterboard Gypsum

Ganjian *et al.* (2007) used plasterboard gypsum waste in road bases, sub-bases and stabilised sub-grades. They concluded that crushed or ground plasterboard gypsum can be used as a source of sulphate activator with slag and kiln dust or by pass dust to form an activated pozzolan. They used 15% of ground plaster gypsum with 5% of by pass dust and 80% basic oxygen slag. The result was a high compressive strength material named Coventry Novel Cement to be used in road base and sub base construction.

In addition, they found that Run of Station Ash (ROSA) has satisfactory pozzolanic potential to be used with slag, plasterboard, and by pass dust. The lower water content resulted higher strength as with Portland cement. Sufficient time must be considered for setting slag and gypsum mix and it is slower than setting time of Portland cement concrete mixes.

2.5.2.4 Red Gypsum

Titanium Oxide pigment production yields 250 kt of red and 84 Kt white gypsum per year in the UK. Worldwide production of red gypsum is 1.25 Mt from one producer alone (Huntsman Tioxide, 2007). It is estimated that this one industry in Malaysia produces approximately 400Kt of this material annually. This waste product is disposed off in landfills close to titanium dioxide plants (Fauziah *et al.* 1996).

Hughes (2006) researched on the use of synthetic red gypsum as a construction material. He mixed both red gypsum - BOS and red gypsum-GGBS. He found that Red Gypsum-GGBS has more compressive strength than red gypsum-BOS. The optimum combination from his mixes was a mix with 10% RG and 90%GGBS. The 50:50 mix also achieved high strength. From his research, RG-GGBS binders could be effective in mass concrete production. Although the compressive strength of these mixes was lower than the strength achieved by the Portland cement, long term compressive strength of RG-GGBS would be as high as Portland cement.

Red gypsum needs more water to achieve workability and this causes lower compressive strength. The particle size and shape of the material being mixed have an effect on the final strength. Curing conditions are important for RG-GGBS mixes. If RG-GGBS is cured in a soaked condition, the compressive strength is lower than the strength of samples cured un-soaked (Hughes 2006).

He used 50:50 red gypsum-GGBS binder for soil stabilisation. This binder proved the potential to improve some kinds of soils. The strengths were sufficient to pass the civil engineering specifications for ground improvement in most cases. The main problem was slow rate of hardening.

He also mentioned that the durability of mix needs to be verified and tests such as freeze - thaw and wet dry tests should be done. From his results in a field trial it has been concluded that a RG-GGBS binder can be a possible substitution for Portland cement in the dry mix process without any modifications and no extra

operator training or personal equipment is required. The average of 7day strengths of the columns of this binder was similar to those OPC columns, but increasing the proportion of binder reduced the failure strain (Hughes, 2006).

2.5.3 Ashes

2.5.3.1 Sources of Ash

Electrical power is supplied by thermal power plants where the fuel is coal and the by-products of the combustion of pulverized coal are produced in large quantities. These materials consist of fly ash, bottom ash, and boiler slag. Physical and chemical properties of coal ashes depend on the type, source, and fineness of the fuel as well as the operating conditions of the power plant. Fly ash is extracted from the gases by using cyclone collectors and electronic precipitators or bags and stored to be used or be disposed. Bottom ash is collected from the bottom of the combustion chamber in a granular form. Molten Boiler slag may be collected from the bottom of the boiler and quenched in water (Churchill *et al.* 1999). The chemical composition of fly ash and bottom ash from the same batch of the power station are similar.

Fly ash consists of fine, glassy particles with some coarser crystalline and some unburned carbon particles. Bottom ash consists of unshaped, porous, glassy particles with the size between 50.8 mm to 0.075 mm (2 in and No. 200 standard sieve) (Churchill *et al.* 1999).

Fly ash has different environmental problems such as leaching and dusting. It also takes large disposal area. These problems and its pozzolanic characteristics made it as an attractive construction material. Bottom ash has a large particle size and higher porous surface compared with fly ash. So it needs higher water to react thus cause lower compressive strength. Therefore most bottom ash is disposed in landfills causing environmental problems.

Depending on the chemical composition, fineness, and unburned carbon content fly ash is divided into two types according to standard (ASTM C 618-03 2003):

Class C and class F. Class C has high calcium content that cause high reactivity with water with no lime addition. Class F fly ash contains lower percentage of lime. Class F fly ash is not as pozzolanic as type C.

Rice husks are wastes of rice paddy milling industries. For countries rice producers, rice husk is considered as environmental pollution (Chandra 1997).

2.5.3.2 Use of Ash as fill materials

White (2006) investigated the stabilization of class C fly ash with calcium activators such as hydrated lime; cement kiln dust (CKD) in construction of a structural pavement base layer. He found strength and freeze-thaw durability of the stabilized mix increased.

Ambarish *et al.* (2007) studied class F fly ash its modification with lime or gypsum. Their result showed adding up to 10% of lime to class F fly ash improved the shear strength of the mixture. Adding 0.5%, 5% and 15% of gypsum to lime modifies the mix and caused it to gain higher strength in the early curing period. If the fly ash was stabilized with only lime, it required a longer curing period, 45 days or more to gain considerable shear strength.

2.5.3.3 Use of Ash in Concrete

Different kinds of ash are produced by coal-fired power stations. Fly ash is a valuable mineral being used in cements and concretes (Jones and Mccarthy 2005) investigated the potential of using unprocessed run of station (low lime) ash from bituminous coal combustion in foamed concrete. They used coarse fly ash as a replacement for sand. Using run of station ash had a significant beneficial effect on foamed concrete properties i.e. compressive strength at 28 days (Jones and Mccarthy 2005).

Chai and Raungrut (2003) studied ground bottom ash pozzolanic characteristics when mixed with Portland cement. They dried and sieved bottom ash through sieve 16 and used it as it was and also ground and sieved through sieve 325. They used original or ground bottom ash for cement replacement at the rate of 10, 20

and 30% to make concrete. They found out that the original bottom ash mortar had higher water requirements than the cement mortar, but the ground bottom ash mortar needed less water. The initial setting time increased depending on the fineness of fly ashes compared to cement paste. They did not recommend using original bottom ash as a pozzolanic material; however, ground bottom ash had good pozzolanic characteristics.

2.5.3.4 Ternary Blend of PC-PFA-GGBS

Özkan *et al.* (2007) investigated the potential use of granulated blast furnace slag and coal bottom ash as a sand replacement in concrete mixtures. The results showed replacement with Granulated blast-furnace slag (GBFS) and Coal bottom ash (CBA) as fine aggregate in concrete mixtures generally decreases the compressive strength. They concluded that if the content of CBA and GBFS is limited to 20%, the small decreases in strength can be accepted for low strength concrete works.

Singh *et al.* (2008) researched the use of cement stabilized fly ash–(GBFS) mixes for road embankments, and for base and sub-base courses of highway pavements. Test results showed an increase of the amount of GBFS in the fly ash sample with fixed cement content improves the CBR value of the stabilized mix. In this study, the maximum CBR value of compacted fly ash–GBFS–cement (52:40:8) mixture obtained was 105%, indicating its suitability for use in base and sub-base courses in highway pavements with proper combinations of raw materials.

Ganjian *et al.* (2004) used lagoon ash in a landfill liner. Their mixes were made with cement kiln dust (CKD), ordinary Portland cement (OPC), granulated blast furnace slag (GBS) and ground granulated blast furnace slag (GGBS). Mixes made from these materials showed good chemical buffering capacity for landfill waste leachate.

Puertas *et al.* (2000) researched the strength behaviour fly ash/ slag cement alkali activation with NaOH solution. They used different ratios of fly ash/ blast furnace slag cement (100/0, 70/30, 50/50, 30/70, and 0/100) and NaOH

concentration 2 and 10 M with different curing temperatures (25 °C and 65 °C). They found, increasing the slag content increased the compressive strength and it is directly related to NaOH concentration (10 M solution generated higher compressive strength). Increase in curing temperature has a positive effect on the first day compressive strength. But for longer age the effect is different since the 28 day compressive strength was higher when the curing temperature was 25 °C.

2.5.3.5 Use of Ash in Wall board

Ramesh *et al.* (1992) replaced calcined gypsum with three different kinds of fly ashes in different amounts (10, 20, 30 and 40% fly ash by weight) to make wall boards. They concluded by increasing the amount of fly ash, the water requirement decreased. Different sources of fly ashes had different effects on setting time. Some of them accelerated the setting process and some of them retarded it. Replacement of gypsum with 30% fly ash caused very little loss of compressive strength in the wallboard sample. They also found out that the wallboards with fly ash had superior properties to calcined gypsum. Fly ash could increase the flexural strength and develop high core hardness and nail head pull resistance and have better water resistance.

2.5.3.6 Ash –Gypsum and Ash-CKD Mixes

Min *et al.* (2008) studied on fly ash-lime activation with calcined phosphogypsum. They found adding calcined phosphogypsum to fly ash-lime paste accelerated the pozzolanic reaction and improved early strength of the binder. The effect of calcined phosphogypsum on the fly ash-lime system is because of the formation of ettringite and gypsum in the system. The ettringite formation accelerated the pozzolanic reaction and improved the strength of the mix.

Babaian *et al.* (2003) researched the effects of mechanical and chemical (Mechanochemical) activations on strength of CKD-fly ash mixes. They used different kinds of CKDs and fly ashes in their research. They found the major crystalline hydration product of a CKD-fly ash binder was ettringite that

appeared stable at the age over 100 days. They also noticed that grinding process reduced both particle size and crystalline phases of the materials and it improved binder reactivity. Vibratory grinding for 4 hours provided the best mechanochemical activation among all of grinding methods they used in their research.

2.5.4 Slag

2.5.4.1 Types of Slag

The use of iron blast furnace slag as cementitious materials has been practiced since the late 1800s because of its excellent performance and durability (Tüfekçi *et al.* 1997).

The main kinds of slag from literature that are used in construction are:

- Basic Oxygen Slag: The conversion of pig iron to raw steel in a basic oxygen furnace (BOS). In every ton of crude steel, about 100-150 kg of slag is generated as waste material (Reddy *et al.* 2006).
- Ground Granulated Blast-Furnace Slag: This comes from the extraction of iron ore to pig iron in a blast furnace. If the molten slag is quenched sufficiently rapidly it forms a glassy material, when finely ground, called “ground granulated blast-furnace slag” or GGBS.
- Ladle slag: To further refine the steel after extraction from a basic oxygen furnace or an electric arc furnace, calcium aluminate or CaF_2 is added to the molten steel as a flux for further refining while in a ladle. This slag is called ladle slag (Shi and Hu 2003).

2.5.4.2 Hydraulic Activity of Slag

The hydraulic activity of slag strongly depends on its chemical composition such as glass content, particle size distribution. The glass content of slag is the most significant variable and the most critical parameter to hydraulicity. The most important variable that affects the nature of slag is the temperature at which the

furnace is tapped. The rate of quenching that influences the glass content which is one of the principal factors affecting the slag cement strength (Pal *et al.* 2003).

There is no exact correlation of glass content to hydraulicity that the higher glass content would produce more reactive slag cement however the glassy structure is necessary to reactivity. Research showed that slag samples with 30-65% glass content are suitable to show activation (Pal *et al.* 2003).

Basic Oxygen Slag has been used as a kind of well-known aggregate in civil engineering construction and road ballast but the main problem with using slag in civil engineering is the existing free lime. “The free lime of steel slag comes from two sources: residual free lime from the raw material and precipitated lime from molten slag” (Shi 2004).

When free lime or limestone hydrates, its volume increases and swelling will happen (Reddy *et al.* 2006). To obtain stability, several methods have been employed such as weathering of the slag outside in slag pits or treatment of liquid slag by injecting oxygen and silica and autoclaving slag in baskets (Reddy *et al.* 2006).

2.5.4.3 Uses of Slag

Different kinds of steel slag are used in hydraulic structures. Some examples are:

- “1- Dams and dikes;
- 2- Stabilisation of river bottoms
- 3- Refilling of erosion areas on river bottoms; and
- 4- stabilisation of river banks “(Motz and Geiseler 2001)

Usually aggregates with size > 10 mm are used to prevent erosion. The high density, high level of strength and abrasion of steel slag aggregates ensure a long term resistance to dynamic forces from river flow (Motz and Geiseler 2001).

When it used in road construction it is claimed that the following results could be achieved:

“1-The crushed and rough surface of processed steel slag aggregate mixtures provide a stronger bearing capacity directly after compaction that is higher than when using other aggregates.

2- There is no influence of heavy rain on the bearing capacity of unbound layers built with steel slag mixtures.

3- The carbonatic solidification leads to an increase of bearing capacity.

4- The aggregate mixtures are permanently stable if the requirements for the volume stability have been fulfilled.

5- The asphaltic surface layers remain permanently level even under heavy traffic.

6- The resistance to polishing of asphaltic surface layers remains on a high level over a long-term period.

7- Roads built with steel slags as an unbound or bituminous bound aggregate do not influence the environment by leaching”(Motz and Geiseler 2001).

Mahieux *et al.* (2008) carried out a study on using BOS in hydraulic road binders. They used BOS and GGBFS from the same plant. The study found that although BOS in cement-based mortars had a poor hydraulic activity with no pozzolanic properties, the ternary blended binder mixing BOS, GGBFS and catalyst was successful. The mix with 52.5% of GGBFS, 42.5% of BOS and 5% of catalyst had compressive strength higher than 10 MPa at 28 days. It also had no problem with expansion.

Ladle slag can not be used as a cementitious material or Portland cement replacement by itself because it contains free lime. A study on cementitious properties of ladle slag under autoclave conditions for construction products was

done by Shi and Hu (2003). They found by using a small amount of cement or hydrated lime, the strength of the binder improved. They mixed different amount of ladle slag with Portland cement and ground quartz and placed the mixes in autoclave condition for curing. They also noticed that mixing fly ash with ladle slag is not suitable while using silica flour instead gave a compressive strength of 23 MPa however this is significantly lower than typical commercial production for autoclave concrete blocks that is 76.2 MPa.

The autoclave condition that they recommended was over 175°C and the time for constant temperature did not need to be more than 4h to achieve the compressive strength (Shi and Hu 2003).

Shi (2004) found the potential cementitious property of ladle slag can be increased significantly by using chemical activators under room temperature curing conditions. He mixed ground blast furnace slag and chemical activator with ladle slag cement based materials. He found the strength of the mix much lower than the Portland cement, and also found the finer ladle slag showed higher compressive strength. It showed very low strength at 3 days but a slightly higher strength gain rate than Portland cement after 7 days.

Generally, increasing fineness results in higher strength. The particle size of GGBS is a very important parameter for on energy saving and economical considerations and affects the reactivity of GGBS in concrete, early strength development of concrete and water requirement (Pal *et al.* 2003).

Ground granulated blast furnace slag does not react with water at room temperature without an activator. Portland cement clinker or lime are normally used as alkali activators (Heikal *et al.* 2002).

The main activators used in slag cements are Portland cement (Blastfurnace cements) or mixtures of Portland cement and calcium sulphate(super sulphated cements) (Taylor 1997). Other activators used in addition of water are sodium and potassium hydroxides, and mixtures of salts of high pH (Taylor 1997).

Blast furnace slag can give much higher strength than conventional cements by using proper alkaline activators. Ground steel slag also shows much better cementitious properties by using alkaline activators. Because of the potential of high content of free CaO and MgO, some cementitious materials that can use free CaO and MgO such as fly ash and blast furnace slag should be used together with steel slag (Shi 2004).

The hydration products found in slag-lime mixtures are usually calcium silicate hydrates and calcium aluminate hydrates with varying compositions. For slag-cement there is a consumption of calcium hydroxide from hydration of Portland cement clinker and residual alkalis in the slag (Heikal *et al.* 2002).

Heikal, *et al.* (2002) researched the setting time (initial and final) of Portland cement, granulated slag and by-pass cement dust composites. They found that the setting time of slag-cement paste was extended with slag content. An additional 2.5% mass by-pass cement dust increased the initial and final setting time of some mixes and decreased the final setting time of some other mixes.

Monshi and Kasiri (1999) used iron and steel slag as a raw material for Portland cement. Using iron slag, calcined lime, and steel slag (49:43:8) gave a compressive strength of concrete above standard values for OPC type I.

Shih *et al.* (2004) found the potential of using waste steel slag in making bricks. They found that if an appropriate amount of steel slag (less than 10%) added to the mixture using for brick making, the firing temperature would reduce. The compressive strength of this kind of brick and the shrinkage would drop if the amount of slag increases. The water absorption increased by increasing the slag content.

2.5.5 Cement Kiln Dust CKD

Cement kiln dust (CKD) and Cement By-Pass Dust (BPD) are by-products of the cement manufacturing process that are produced in high volumes. Studying the possibility of using it instead of landfilling is worthwhile because it is a by-

product from Portland cement industries and as long as cement is manufactured it would be produced.

There are two different kinds of cement kiln dust:

CKD: that is from chimney stack electrostatic precipitator that is sometimes recycled back into the kiln feed.

BPD: is from the kiln by-pass. The by-pass cement dust is produced as a solid waste during the manufacture of Portland cement clinker by using the dry process as a result of the presence of some volatile constituents in the kiln feed and it is not recycled back into the kiln feed.

The main difference between CKD and BPD is the temperature at which these materials are produced. CKD is taken out of the initial length of the kiln where the temperature is about 300 °C. BPD is from the kiln where the temperature is about 1000 °C. Therefore BPD has more a cementitious character than CKD that is more calcium carbonate (Ganjian *et al.* 2007).

However in some publications CKD and BPD mean same waste materials. K.S. Al-Jabri *et al.* (2006) named cement by-pass dust as cement kiln dust (CKD) in concrete production.

Al-Jabri *et al.* (2006) studied the effect of copper slag and cement by-pass dust on the mechanical properties of concrete. They did different trial mixes with different water to binder ratios 0.5, 0.6, and 0.7. Their results showed that 5% copper slag (No BPD) substitution for Portland cement had similar strength to their control mixture (only OPC and aggregate) especially at lower w/b ratios of 0.5 and 0.6. Higher amount of copper slag (13.5% with 1.5% of BPD as an activator) cement replacement had adverse effects on strength.

Taha *et al.* (2007) did an investigation to use (BPD) mixing with copper slag, incinerator ash, sand and cement to make controlled low strength materials

(CLSMs). (Engineered materials that have a specified compressive strength between 0.1 MPa and 8.3MPa at 28 days)

CLSM may be used in backfilling walls or trenches for bedding material for pipes, it also is used as void fillings i.e. Sewers, tunnel shafts and some other underground structures. They compared the mixes without waste cementitious materials and mixes with waste materials and cement. The results indicated that all of their mixes produced a CLSM with a compressive strength that can be excavated manually with good mechanical properties with a good mix design. Mixes using the waste material, cement and sand yielded higher compressive strength than those mixes using waste materials as full replacement for cement. They recommended the waste material from their research should always be used in combination with cement in order to achieve their pozzolanic activity (Taha *et al.* 2007).

Lachemi, *et al* (2008) investigated mixing various CKDs from four different sources or manufacturers with OPC and obtained different mechanical properties of CLSM. They found out that the chemical composition of CKD can vary from different sources depending on the kiln process (Dry or Wet) raw materials and the location and method of dust collection system used by different manufacturers (Lachemi, Hossain, Shehata *et al.* 2008). They concluded increasing CKD content increased the w/c ratio of the CLSM mix for achieving specific flow. Also, setting time increased with increasing CKD content. The compressive strength of CLSM increased if the CKD content increased. Using CKD and OPC together in a CLSM mix had higher compressive strength than the mix derived only from CKD.

Sreekrishnavilasam *et al.* (2007) researched using CKD in soil treatment. The soils used in this research were low plasticity clays. They compare the laboratory results from two fresh and one land filled CKD. Only one of the fresh CKDs with 2-5% of lime was found to be useful for soil stabilization. Using CKD for soil stabilization depend on the percentage of its free lime. The lower loss on ignition (LOI) alone is not a good parameter for CKD reactivity estimation,

since the 3 different kinds of CKDs had LOI near each other but their behaviour was completely different. Atterberg limits of soil-CKD mixtures, changing in plastic limit (PL) may be better indicator to find out the potential of CKD in soil stabilization.

They found that adding 10-20% of CKD (by dry mass of soil) to the soil at very high water content (outside the range of compatibility) could cause compaction without difficulties and without needing drying. It meant the CKD could be effectively used as “drying” agent for treating subgrades in cold seasons when the drying of soil might be difficult.

2.5.6 A summary of the Review

Waste materials have been used in construction with acceptable performance according to this review. The waste materials in this research were used in several research projects. Some researches’ objectives were close to the objectives of this project and the results and ideas from them led to many ideas about waste materials which are used in this research about their characteristics and behaviour. For example Ganjian *et al.* (2006) research on material from similar sources to the raw materials used in this research (BOS-PG) and their results were useful for this project. Hughes (2006) used RG in his research on construction products which was similar to one of the wastes used in this research. Even though other researchers used different waste materials, their aspects and ideas or methodologies were useful in this research.

3. Experimental Method

3.1 Introduction

The previous research on by-product materials was studied in the literature review chapter. Some of the methods and tests of the previous projects had good potential to be applied in this project. Other tests such as freeze-thaw test were carried out as the previous research recommended (Hughes 2006).

This chapter describes the testing methods applied in this research including material characterisation, binder development, laboratory works and concrete trials for block making.

3.2 Sources of Materials

Red Gypsum (RG)

The red gypsum supplier in this project was from Huntsman Tioxide, which manufactures titanium dioxide. The amount of RG collected for this research was 100 kg. RG must be first dried and ground before it can be made to a mix. Figure 3-1 illustrates the wet RG (as it was picked up from Huntsman Tioxide). Titanium oxide pigment production yields 250kt of “red” and 84kt of clean “white” gypsum per year in the UK (Huntsman Tioxide 2005).

The dark green colour inside the fresh gypsum is the result of oxidisation of the iron that exists in the mix, which changes from dark green to red.



Figure 3-1 Fresh Red Gypsum

Plasterboard Gypsum (PG)

The plasterboard used in this research was from the Lafarge Plasterboard recycling plant in Bristol. Approximately 250 kg of plasterboard gypsum (as it was) was collected from the plant (as it was) to be used in the lab. Almost 400 kg of ground plasterboard was collected again to be used in light weight block making.

It is estimated that around 300,000 tonnes of waste plasterboard as off-cuts, and from 500,000 tonnes to more than 1 Mtpa of waste plasterboard arising from demolition projects are generated each year (Ganjian *et al.* 2007).

Generally plasterboard gypsum was collected from demolition sites and contained crushed glass and paper. For the binary combinations of by-product materials, the plaster board was cleaned and ground before making samples. First, the bigger particles, papers and glasses were removed by hand and the gypsum was put in the tray to be dried. The dried plasterboard gypsum was ground and passed through 500 μm sieves. The dried plasterboard was kept in a sealed bucket (to prevent it from absorbing moisture from the air).

In step two (the ternary combinations of the raw materials that will be explained in this chapter) the plasterboard was pre-crushed and sieved by Lafarge. Figure 3-2 shows the waste plasterboard before and after the grinding process.



Figure 3- 2 Plasterboard Gypsum before and after grinding

Basic Oxygen Slag (BOS)

Steel slag dust is a by-product produced when manufacturing steel and Corus currently produces about half a million tonnes of it every year according to Tarmac (2006). The slag used in this research was obtained from Corus at Scunthorpe works. Approximately 250 kg of slag was collected to be used in the lab.

The slag was ground before it was used in mixtures. The grinding of the slag was done using a laboratory ball mill and sieved through a 600 micron sieve.

By Pass Dust (BPD)

Several kinds of BPDs were used in this project. The BPDs varied in both the physical and the chemical characteristics. Generation of BPD (CKD) is estimated at approximately 30 million tonnes worldwide per year (Sreekrishnavilasam *et al* 2007).

The BPDs used in this research were obtained from Castle Cement, Clitheroe, Lancashire. Collections were made four times and the amount of collected BPD was between 300 to 500 kg each time.

Run Of Station Ash (ROSA)

Run Of Station Ash from Ratcliff power station was used in step 2 and 3 of this research. Another kind of ROSA from Rugeley power station was used for the final

block trial. The amount of ROSA collected each time was around 500 kg and for the light weight block production around 750 kg of ROSA was collected for the block trial. According to the Rugeley Power Station reports (2007), 255 thousand tonnes of ash was landfilled during the year 2007. This amount was increased 238 thousand tonnes from 1999 to 2007.

Ordinary Portland Cement (OPC)

OPC from Castle Cement was used for making control samples.

Light weight aggregate

The light weight aggregate used in this research to be used for light weight block was Perlite that was supplied by Hanson. Perlite is foamed slag, formed by directing jets of water, steam and compressed air on the molten slag from blast furnace (Illston and Domone 2006).

Aggregate

Gravel was used as coarse aggregate and sand was used as fine aggregate in the concrete samples of this research.

Supper Plasticiser

Sika ViscoCrete 10 (GB), Multi-Functional Readymix Admixture was used for light weight blocks trials to improve the early strength.

Foaming Agent

This was supplied from Lafarge Plasterboard and is used for gypsum foaming.

3.3 Chemical Analysis

Chemical analysis of the raw materials was carried out using X-ray fluorescence (XRF) to determine the chemical composition of the materials.

XRF determines the composition of major alloying elements (Fe, Si, Mn ...) for metallography by bombarding with high-energy X-rays or gamma rays. It is used for elemental analysis and chemical analysis in the investigation of metals, glass, ceramics and building materials, and for research in geochemistry, forensic science and archaeology (Wise 1995).

The XRF test was carried out three times for each raw materials and the average of the data was reported in this research.

3.4 Particle Size

Particle size measurement of materials is an important parameter in most branches of industry. The chemical reactivity, flow and material strength of many materials are affected by the size and characteristics of the particles within them.

The particle size of the materials was measured using a Malvern Mastersize 2000 laser analyzer with accuracy of $\pm 1\%$.

3.5 Density

The density of the raw materials was measured using Micromeritics AccuPyc 1330 helium pycnometer. The helium pycnometer measures the volume and true density of solid objects, without damaging samples. The Micromeritics AccuPyc 1330 helium pycnometer determines powder and solid densities. Sample was prepared by drying for 24hr at 30° C before density measurement. After preparing the sample and, helium gas fills the sample chamber and pressure is measured. The helium then enters another empty chamber and the pressure in both chambers is measured. The sample volume is calculated based on these pressures and then with the known weight of the sample, the density is then calculated. The helium is able to fill all spaces. The measurement is repeated three times for each material.

Figure 3-3 shows the Micromeritics AccuPyc 1330 helium pycnometer and its sample cells.



Figure 3- 3 Micromeritics AccuPyc 1330 Helium Pycnometer and Sample Cells

3.6 Mill

A ball mill grinder was used to grind BOS, RG and PG. A cylindrical shell rotates around a horizontal axis, filled with material and sets of grinding **steel** balls of different sizes (12 mm, 20 mm and 25 mm). The shell is rotated at a speed of 0.8 (cycles per second) which causes reduction in particle size by impact. Figure 3-4 shows the ball mill grinder.



Figure 3-4 Ball Mill

3.7 Mixing procedure

A mechanical mixer (KENWOOD) with the capacity of 2- litres **was** used to make pastes and concrete for 50 mm moulds with different rotating speeds. Normal mixes were made in 5 minutes mixing time. First the materials were mixed dry for 1 minute and **whilst the blade was rotating water was added**. For semi-dry pastes the mixing time was extended to 7 minutes.

Concrete samples for 100-mm specimens were prepared with a 10-litre capacity mixer. The procedure was similar to the small mixes.

A horizontal mixer was used to make large concrete mixes for 100 mm and cylindrical specimens. The mixers are shown in figure 3-5.



Figure 3- 5 From left: 2-litre mixer, 10-litre mixer, horizontal mixer

3.8 Paste mixtures

Mixture preparation for the 50-mm cubes was carried out according to the following mixing procedure:

- 1- Dry mixing of materials (PG, RG, BOS, BPD, and ROSA whichever applicable) for 1 minute at low speed (from speed number 1, 2 and 3 it was kept 1).
- 2- Half of the mixing water was added during the first 30 seconds of mixing.
- 3- For the first 30 seconds mixing was at medium speed (2).
- 4- In the middle of mixing time, one or two times, depending on the flow of mix, the mixer was stopped and the mixture scraped off the sides of the mixing bowl and blades.

- 5- The rest of the mixing water was added and mixing was carried out for an additional two minutes or more, depended on the mixture, at high speed (3). Total mixing time for all mixes was approximately 5 minutes.

The 50 mm samples were easier to handle and were less likely to be damaged due to relatively smaller amount of mortars that was needed, which resulted in a smaller storage and curing space.

For the final mixes specimens were cast in both 50 mm and 100 mm moulds and the tests showed that the compressive strength of 50 mm is 75-80% of 100 mm specimens. More than 1500 of 50 mm cubes and around 50 of 100 mm cubes were designed and tested in this experiment.

3.9 Flow test

The flow of the pastes was measured by a modified flow table. Paste was poured in a 78 mm diameter 70 mm Height cylinder in 3 layers and compacted with 10 tamps using a small rod (5 mm diameter). After compaction the table was jolted 5 times using the handle and the diameter of the mixture was measured to show the flow. A paste was considered to be flowable when the spread was 510 mm to 620 mm in diameter in the standard flow table test. This corresponds to 110 mm to 210 mm in diameter for the small modified flow table. Figure 3-6 shows the small modified flow table.



Figure 3- 6 Modified Flow table

Another test that was used to measure the flow of the concrete mixes is the slump test. The slump test was performed according to part II of BS1881.



Figure 3-7 Slump Test Equipment

3.10 Viscosity of Concrete

An important property of fluid is viscosity. “For a well-ordered flow that fluid particles move in straight, parallel lines (parallel flow) the law states that for certain fluids, called Newtonian fluids” (Shames,1992).

Concrete and other cement-based materials, such as cement paste or mortar, are usually considered to be a Bingham fluid. The rheological properties of concrete can be identified with Bingham model (Erdogan *et al.* 2008):

$$\tau = \tau_0 + \mu\dot{\gamma} \quad \text{Equation 3- 1}$$

There is a linear relationship between shear stress τ , and shear strain rate $\dot{\gamma}$ that can be defined by plastic viscosity μ and a minimum stress τ_0 (yield stress). The yield stress is necessary for flow to occur (Erdogan *et al.* 2008).

Studying the response of materials to stress is called rheology. Newtonian and Non-Newtonian fluids are viscous materials. The shear stress is related to the shear rate.

In linear Bingham materials there is a fixed displacement for shear stress less than a value τ_1 and for Newtonian viscous behaviour when shear stress exceeds τ_1 . This behaviour is shown in figure 3-8. The equation for this behaviour is:

$$\tau = \tau_1 + \mu \frac{dV}{dy} \quad \text{Equation 3- 2 (Shames 1992)}$$

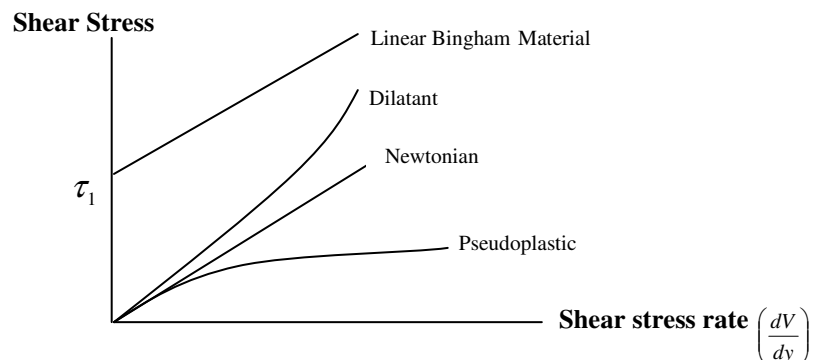


Figure 3- 8 Rheological behaviour of some viscous materials (Shames 1992)

Many materials possess a combination of viscous and elastic characteristics. These materials are viscoelastic materials. Plastics at room temperature under load are samples of viscoelastic materials.

Concrete is not a perfect Bingham fluid since the relationship between shear stress and shear strain rate may not be linear. For example the viscosity may increase with shear rate (shear thickening) or decrease with shear (shear thinning). Ordinary fresh concrete is almost like a Bingham fluid. Plastic viscosity is the most relevant rheological parameter for Bingham behaviour (Erdogan *et al.* 2008).

Coarse and fine aggregate content are important factors affecting concrete rheology. The morphological aggregate properties such as shape influence the rheological properties (plastic viscosity and yield stress) of the concrete mixture. Cubic particles have higher plastic viscosity than spherical particles. The coarse aggregate particle

shape has a much greater influence on the relative mixture viscosity than surface texture (Erdogan *et al.* 2008).

The plastic viscosity of a mixture is influenced more by increasing the amount of coarse aggregate than yield stress of the mixture because the yield stress is based on more static state of the mixture while viscosity is measured in dynamic state with particle interaction (Erdogan *et al.* 2008).

A decrease in yield stress of the paste increases the slump (Lachemi *et al.* 2003).

Flow increases with increasing W/C ratio. An increase in mixing time increases the flow of paste. Chindaprasirt *et al.* (2006) found **that** if yield stress and plastic viscosity of a paste increased the flow of paste would decrease.

An ICAR Rheometer was used to measure the viscosity of the selected concretes. Figure 3-9 shows the ICAR Rheometer used in this research.



Figure 3- 9 ICAR Rheometer

3.11 Setting Time

Setting Time is the term that is used to describe the stiffening of a cement paste (Neville, 1996). The setting time reflects the time in which the cement paste changes from a fluid to a rigid state. In practice, the initial set and the final set are used to describe the setting stages.

Initial setting time:

To determine the initial set, a round needle with a diameter of 1.13 ± 0.05 mm is used and when the paste stiffens enough for the needle to penetrate no deeper than 5 ± 1 mm from the bottom, the initial set has occurred.

Final setting time:

The final setting time was determined by observing the penetration of the vicat needle according to EN 480-2:2006.

Figure 3-10 shows the apparatus used for measuring the initial setting time of the tested pastes.



Figure 3- 10 Vicat Apparatus for determining the setting time of mortar

3.12 pH Measurement

The hydrogen activity or pH is a chemical property that is a measure of the acidity or alkalinity of a solution. Hydration of cements and pozzolanic materials is pH dependent. The pH value determination test is an important test to understand the various reactions of pozzolanic materials reaction with each other.

pH measurement of each material and paste was carried out using a pH meter. Solutions of the pastes were prepared and the pH meter was placed and kept in the solution until the pH level shown by the meter stopped rising. The last reading of the meter was the pH level recorded. The solutions were prepared the same way for all samples to have better result comparisons.

3.13 Casting

To prepare samples the 50 mm moulds were used to cast paste mixes and the 100 mm moulds were used to cast concrete samples. Moulds were filled with paste or concrete in three layers and compacted using a mechanical vibrating table. For semi-dry mixes, the mixes were tamped using a small rod (20 mm × 20 mm). A modified vibrating drill was employed to compact the dry 50 mm and 100 mm samples. A special mixing plate which was designed in the university lab for this purpose was attached to a vibrating drill. Figure 3-11 shows the 50 mm and 100 mm cube moulds and Figure 3-12 (a and b) shows the hammer drill.



Figure 3- 11 50mm and 100 mm cubes

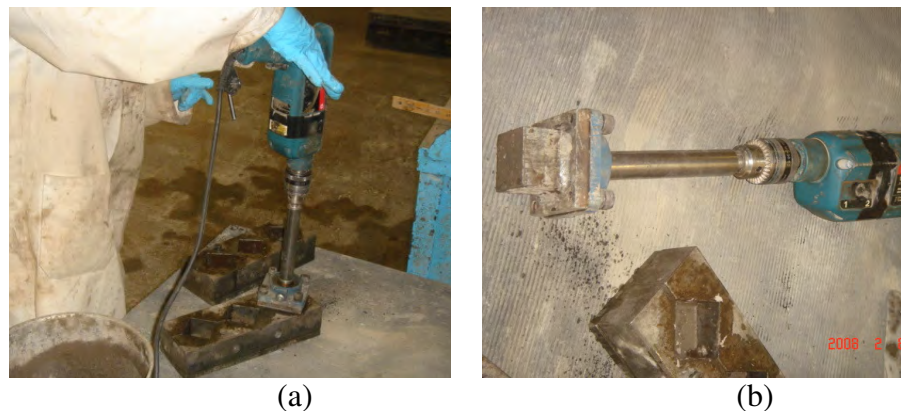


Figure 3- 12 (a and b) - Hammer drill with designed attached plate

3.14 Curing

The paste samples were stored in curing containers. The containers were filled partially with water and were covered with a plastic lid. The humidity in the containers was measured as approximately 98% RH. All containers were kept in temperature controlled room at 20 ± 2 °C.

Concrete samples were stored in a tank partially filled with water and covered with a lid to provide a curing condition of 98% RH at 20 ± 2 °C.

Figure 3-13 shows the container for sample curing.



Figure 3-13 Sample curing container

3.15 Compressive Strength Testing

The paste specimens were tested for compressive strength using Lloyd computerised testing machine. The loading rate was kept constant at 10mm/min and results were reported in MPa or N/mm². Figure 3-14 shows the Lloyd machine used in this test.



Figure 3- 14 Lloyd computerised compressive strength testing machine

3.16 Cube Crusher

A cube crusher was used for the concrete sample crushing with a maximum load of 2000Kg. The data were collected and saved in computer. Figure 3-15 shows the Avery Denison machine with the computer controller. The loading rate of this machine was set 5 kN/s.



Figure 3- 15 Avery Denison Cube Crusher

3.17 Expansion

Length changes, both increases and decreases, were measured along the longitudinal axis. The expansion test was performed according to the ASTM C 490-00 standard. Figure 3-16 shows the apparatus and the samples for the length change test. Samples for expansion were 25×25×285 mm and were made using prism moulds with steel inserts fitted at both ends of every sample.

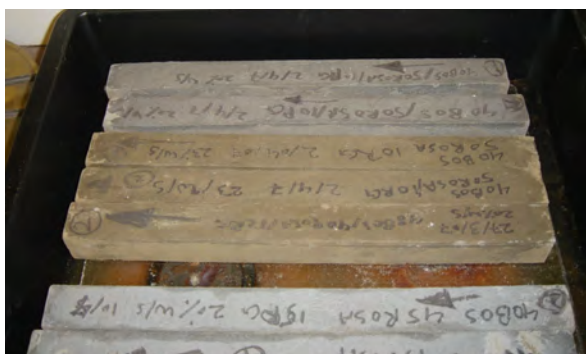


Figure 3- 16 Length change test samples and apparatus

3.18 Freeze–Thaw Resistance

The freeze thaw tests performed in this study were based on the ASTM procedure C666-97. An environmental chamber was used for the freeze up programme as shown in figure 3-17.

The program was run up to 300 cycles. Each cycle took about 5 hours (285 minutes). The samples were exposed to 300 cycles of freezing at -17.8°C , and thawing at 4.4°C .

After 28 days of curing, the concrete blocks were subjected to freeze–thaw cycles. Results of the test were saved on the computer.

Figure 3-18 shows the temperature changing during freeze-thaw cycles. Samples were taken using mould $230\text{ mm} \times 78\text{ mm} \times 78\text{ mm}$.



Figure 3- 17 Environmental Chamber

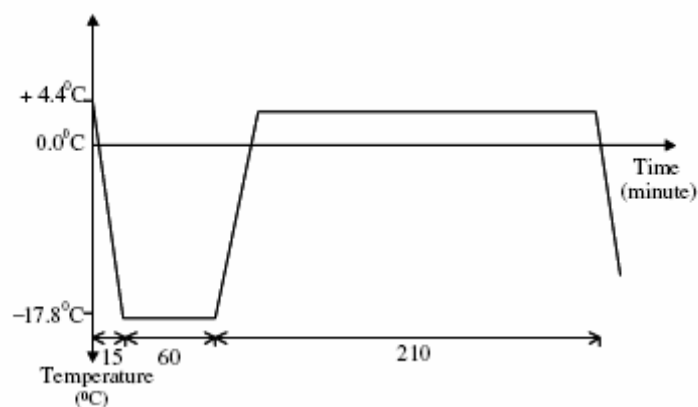


Figure 3- 18 Temperature Change in Freeze thaw cycle

3.19 X-Ray Diffraction (XRD) test and sample preparation and analysis

The X-ray diffraction is a technique where a focused beam of X-ray is directed at a powder sample of material and the pattern of the diffracted rays is recorded. The pattern can be used to identify the mineralogy of crystal grains in the powder.

Three specimens of 2 gram of each sample were selected and finely ground for XRD analysis. Test was using a pestle and mortar to pass a 75 μ m sieve. The ground powder was mounted and spread flat into sample holders and then inserted into the powder diffractometer where x-ray beam was fired at them.

For this study, XRD testing was performed by Philips PW1830 X-ray Powder diffractometer and using CuK α radiation at 40KV and 30 m A between 2 θ position of 5° and 90° at 0.6° min⁻¹.

During each test, the x-ray diffraction data was collected electronically and stored in a computer connected to the machine as a data files.

3.20 Scanning Electron Microscopy (SEM)

The scanning electron microscope (SEM) is a type of electron microscope that images the sample surface by scanning it with a high-energy beam of electrons across the sample surface.

The SEM was used in materials science and it has many applications in cement and concrete petrography (John *et al.*1998).

All samples must be in an appropriate size to fit in the specimen chamber and are generally mounted rigidly on a specimen holder called a specimen stub. Sample size for this test was selected from inside of the paste and with dimensions less than 5 mm.

SEM test is used to view the effect of the amount of the foaming agent on the porosity and the size of the voids generated by foaming agent.

3.21 High Pressure Flow Test (Permeability)

Permeability (k) is one of the porous material properties and it shows their ability to transmit fluids under a pressure (Shames 1992). The rate of flow is calculated with Darcy's law:

$$v = \frac{Q}{A} = \frac{k}{\mu} \frac{dP}{dL} \quad \text{Equation 3- 3}$$

Where:

V = velocity of flow (m/s)

Q = volume flow rate (m³/s)

A = area of cross section (m²)

dP = pressure loss(Pa) over the flow path of length dL (m)

μ = viscosity of the fluid (Pa.s)

k = intrinsic permeability of the porous medium (m²)

k shows the permeability of the porous material and it is related to hydraulic conductivity (K) of the fluid. The relationship between k and K is in equation 4:

$$K = \frac{kg\rho}{\mu} \quad \text{Equation 3- 4}$$

Where

ρ = density of liquid (kg/m³)

g = gravitational acceleration (m²/s)

The specimens used in the high pressure flow test were made using a cylindrical mould and were first cut on a cutting lathe.

Samples of 55mm diameter and 25mm height were cast for permeability testing in a high pressure flow test. This test was carried out to check the long-term stability of mixes and also check the leaching of the specimen in regards to the environment. Figure 3-19 shows Hoek cell in which the distilled water is eluted through a column of test material under a pressure gradient. A sample solution was collected from each specimen in the Hoek cell and analysed using Inductive Couple Plasma (ICP) apparatus.



Figure 3- 19 Permeability test apparatus

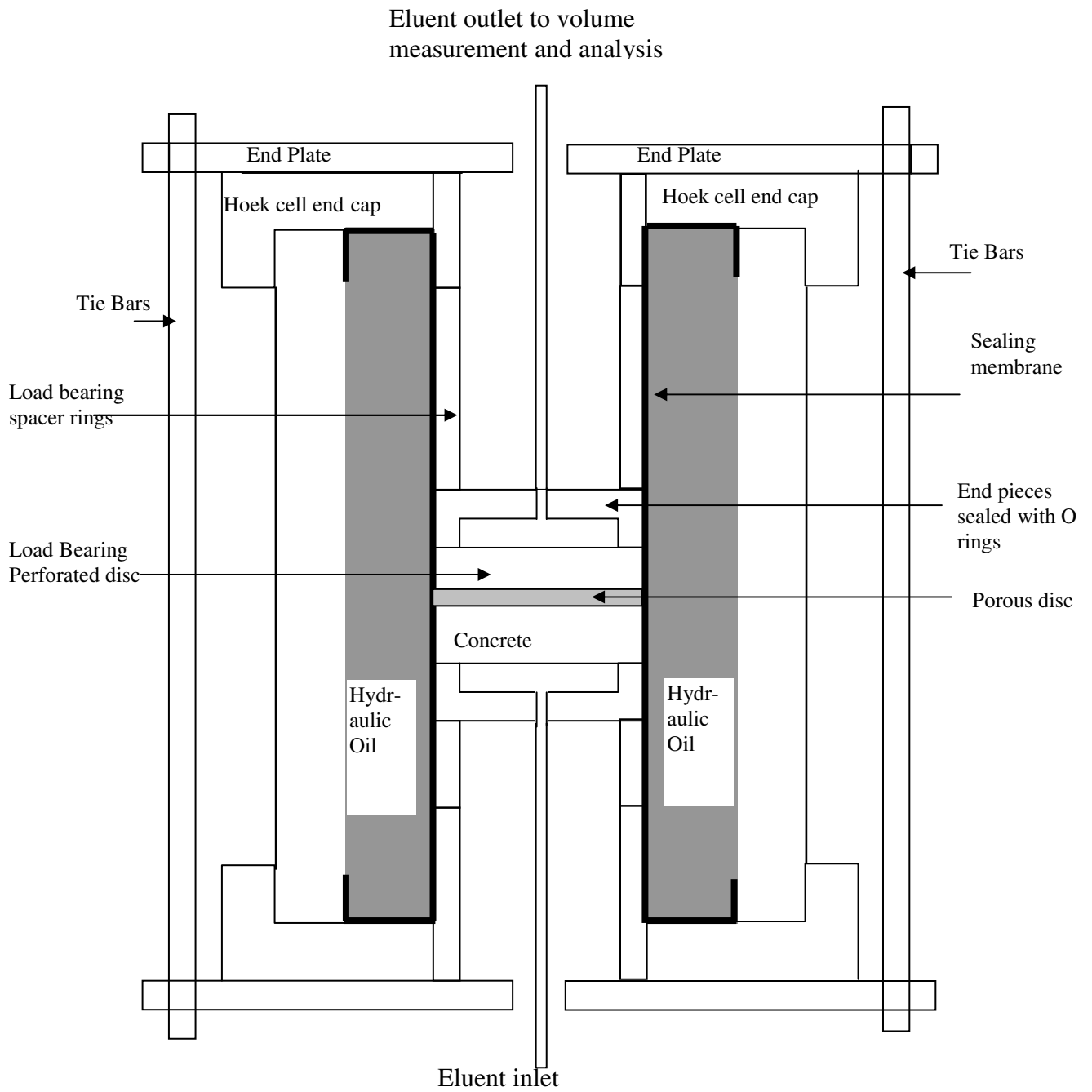


Figure 3-20 Modifications to Hoek Cell for Concrete Permeability Measurements (Ganjian *et al.* 2004)

3.22 Inductively Coupled Plasma (ICP)

Inductively Coupled Plasma (ICP) is an analytical technique which is used for detecting trace metals in environmental samples. The primary goal of ICP is to get elements to emit characteristic wavelength specific light which can then be measured. The technology for the ICP method was first employed in the early 1960's with the intention of improving upon crystal growing techniques. This test was done in Coventry University, Department of Chemistry using a Perkin Elmer, Optima Emission Spectrometer 5300DV. The test is to find the elements in the sample. The machine works on atomic emission. The results of the test are the amounts of the element in mg/l.

4. Test Programme and Results

4.1 Introduction

Results of the tests that were carried out using the various apparatuses are presented in this chapter. The results of each step are presented in this chapter.

Tests were carried out on two different, binary and ternary, combinations. The amount of each material in ternary combination was chosen according to the results of binary results. For all pastes, the density and the compressive strength were measured.

Summaries of the tests are shown in Tables 4-1 and 4-2 for Step 1 and Step 2 of paste samples and Table 4-3 shows the other tests on 5 selected samples.

Table 4-1 Summary of Tests of Step 1-Binary Combinations

Materials	Number of Types of samples	Test Ages (Days)	Number of Samples	Flow	Compressive Strength
BOS-BPD	7	3,7 and 28	72	×	×
BOS-ROSA	8	3,7 and 28	63	×	×
BOS-RG	4	3,7 and 28	36	×	×
BOS-PG	4	3,7 and 28	36	×	×
ROSA-BPD	4	3,7 and 28	36	×	×
ROSA-RG	3	3,7 and 28	27	×	×
ROSA-PG	4	3,7 and 28	36	×	×
BPD-RG	4	3,7 and 28	36	×	×
BPD-PG	4	3,7 and 28	36	×	×
Sum	42	3	378		

Where:

BOS : Basic Oxygen Slag
ROSA : Run of Station Ash

PG: Plasterboard Gypsum
RG: Red Gypsum

BPD: Bypass Dust
x: Done

Table 4-2 Summary of Tests of Step 2-Ternary Combinations

Tests	Number of Types of samples	No of tests Ages	Number of Samples	Flow	Compressive Strength
BOS-ROSA-BPD	14	3	126	×	×
BOS-BPD-RG	12	3	108	×	×
BOS-BPD-PG	12	3	108	×	×
BOS-ROSA-RG	11	3	99	×	×
BOS-ROSA-PG	11	3	99	×	×
ROSA-BPD-PG	11	3	99	×	×
ROSA-BPD-RG	11	3	99	×	×
Sum	82		738		

Table 4-3 Tests on Five Selected Mixes

	SlumpOf Concrete	Viscosity Of Concrete	Setting time	High Pressure flow	ICP	Expansion	XRD	Water Absorption	Freeze -Thaw
OPC	1	1	1	2	1	2	-	3	2
48%BOS-40%ROSA-12%RG	1	1	1	2	1	2	3	3	2
40%BOS-50%ROSA-10%RG	1	1	1	2	1	2	3	3	2
30%BOS-60%ROSA-10%RG	1	1	1	2	1	2	3	3	2
40%BOS-50%ROSA-10%PG	1	1	1	2	1	2	3	3	2
30%BOS-60%ROSA-10%PG	1	1	1	2	1	2	3	3	2

Table 4- 4 Effect of Particle size and w/c on selected mixes

	W/C	Particle size
OPC	-	-
48%BOS-40%ROSA-12%RG	-	-
40%BOS-50%ROSA-10%RG	-	-
30%BOS-60%ROSA-10%RG	9	9
40%BOS-50%ROSA-10%PG	-	-
30%BOS-60%ROSA-10%PG	9	9

Further tests for subway backfilling and block making are reported in Chapter 6.

4.2 Chemical analysis of Materials

The chemical analysis of the raw materials was carried out using XRF method. Three samples of each raw material were selected to be analysed and the average of three data points for each raw materials is reported in Table 4-5.

Table 4-5 Chemical analysis of Raw materials

Sample	% OPC	% BOS	% ROSA	% CKD	% PG	% BPD ₁	% PD ₂	% RG
SiO ₂	20.00	11.43	45.91	9.89	2.43	21.86	19.92	12.71
TiO ₂	-	0.39	1.41	0.14	0.03	0.29	0.15	0.39
Al ₂ O ₃	6.00	1.60	26.51	3.72	0.81	3.85	3.23	1.72
Fe ₂ O ₃	3.00	28.24	5.23	1.24	0.36	2.57	1.86	17.36
MnO	-	4.35	0.08	0.02	<0.01	0.02	0.01	2.66
MgO	1.50	8.27	2.13	0.94	0.40	1.13	0.77	6.18
CaO	63.00	41.29	6.88	40.42	37.30	53.40	38.79	35.89
Na ₂ O	1.00	0.02	0.61	0.43	0.03	0.41	1.22	<0.01
K ₂ O	1.00	0.02	1.35	6.36	0.24	3.64	15.04	0.02
P ₂ O ₅	-	1.48	0.98	0.08	0.02	0.08	0.06	1.62
SO ₃	2.00	0.44	1.37	5.59	53.07	7.10	8.25	11.31
LOI	0.50	3.12	7.11	30.99	4.09	5.64	9.65	10.14

Where:

BPD₁, BPD₂ : different batches of by-pass dust from Castle cement

4.3 Particle size

Particle size analyses of the waste materials are shown in Figures 4-1 to 4-5.

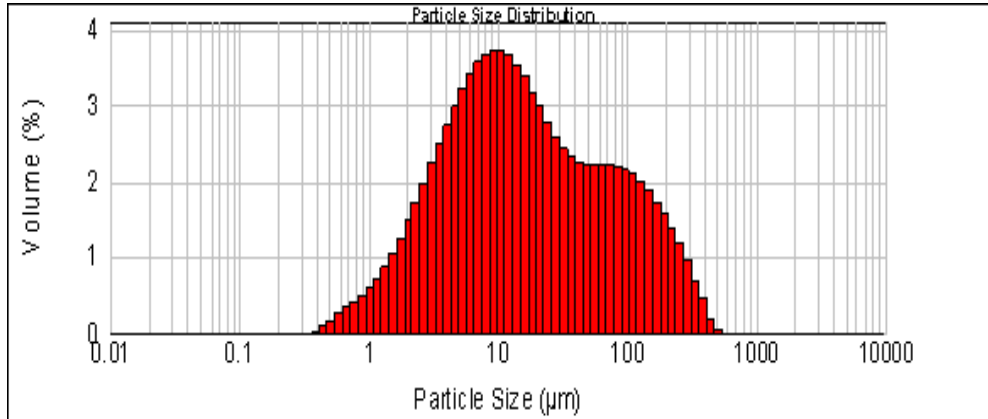


Figure 4- 1 Particle size analysis of ground (for two hours) and sieved red gypsum

Particle size analysis of the plasterboard gypsum was carried out and the results of such analysis are shown in figure 4-2.

The range in the particle size was caused by impurities in the PG sample.

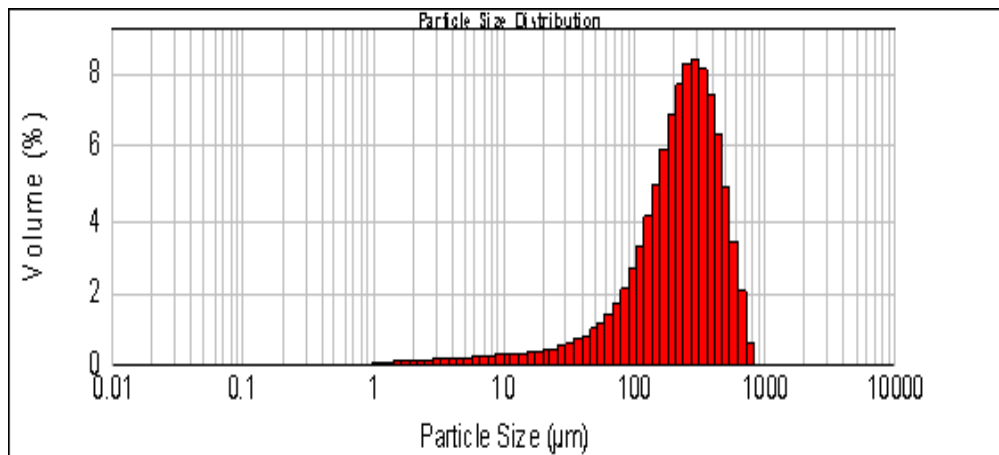


Figure 4- 2 Particle size analysis of ground (for two hours) and sieved plasterboard gypsum

Figure 4-3 depicts the results of the particle size analysis of the ground slag.

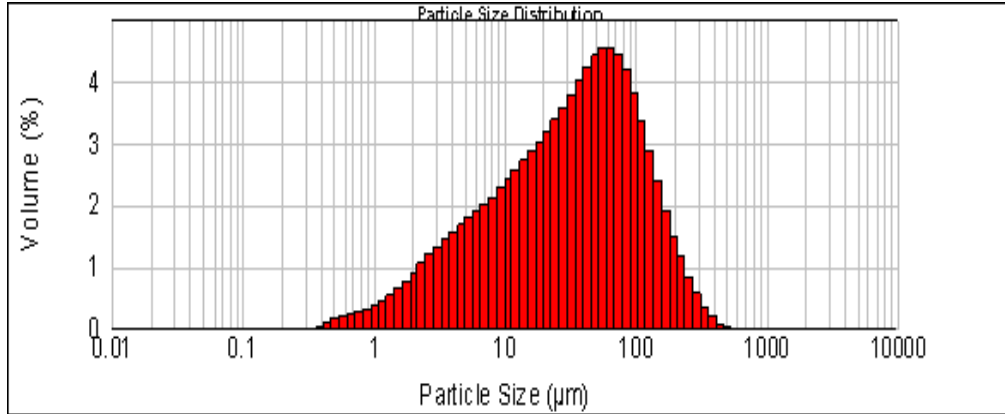


Figure 4- 3 Particle size analysis of ground (for 4 hours) and sieved basic oxygen slag

Figure 4-4 shows the particle size of Castle cement BPD that was used in most mixes including the final mixes.

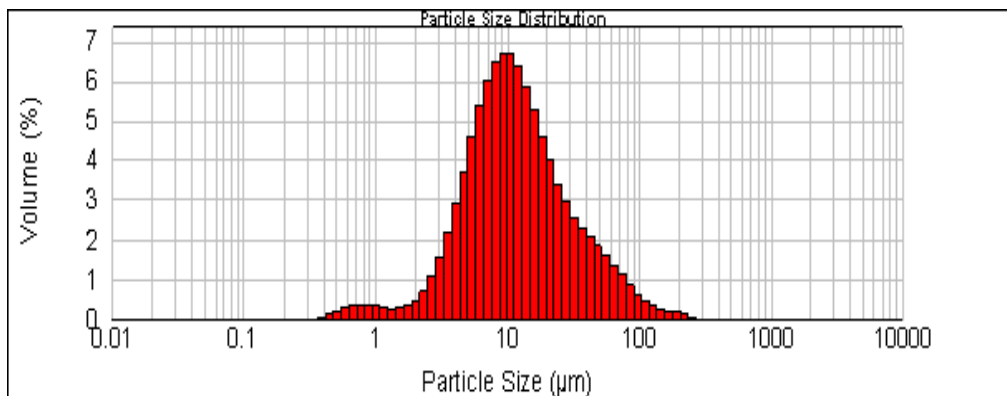


Figure 4- 4 Particle size analysis of by-pass dust (2)

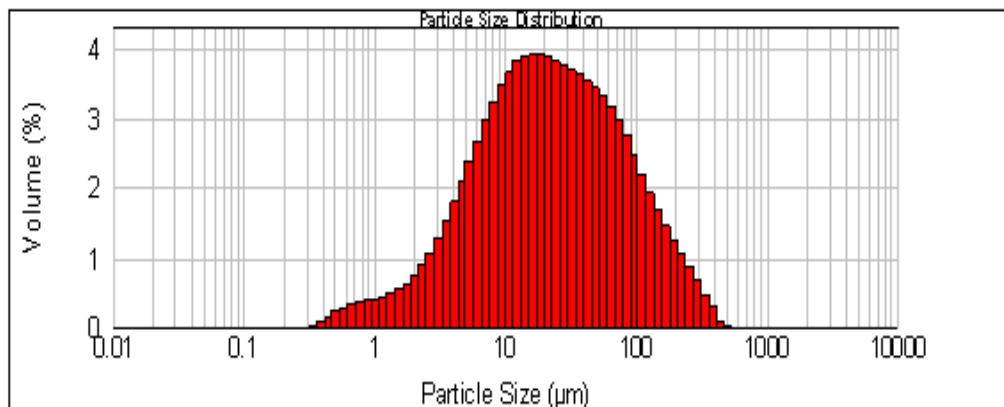


Figure 4- 5 Particle size analysis of run of station ash (Ratcliff power station)

4.4 Results of Step 1-Binary Mixes

The 9 groups of mixes show the effect of each material on other materials. The results were helpful to find out whether each material could be used as an activator for others.

The results of compressive strength at 3, 7, and 28 days, flow, density, and mixing time of pastes made in step 1, are given in tables 4-6 to 4-14. Error bars are shown as the average of the standard deviations for each series of tests.

The w/c ratio was 0.3 for all mixes.

4.4.1 Basic Oxygen Slag (BOS)- Run Of Station Ash(ROSA)

Table 4-6 Characterisation of BOS and ROSA Mixes

Materials		Compressive Strength MPa.			Density	Flow	Mixing Time
BOS%	ROSA%	3 days	7 days	28 days	Kg/m ³	mm	min
0	100	0.6	0.9	2.0	1640	No Flow	5
10	90	0.5	0.8	2.0	1760	No Flow	5
20	80	0.4	0.5	0.9	1808	80	5
40	60	0.3	0.5	1.3	1864	116	5
60	40	0.3	0.5	2.0	2160	162	5
80	20	0.2	0.4	3.7	2200	High Flow	5
90	10	0.4	0.8	4.7	2240	High Flow	5
100	0	0.0	0.3	2.8	2320	High Flow	5

BOS-ROSA

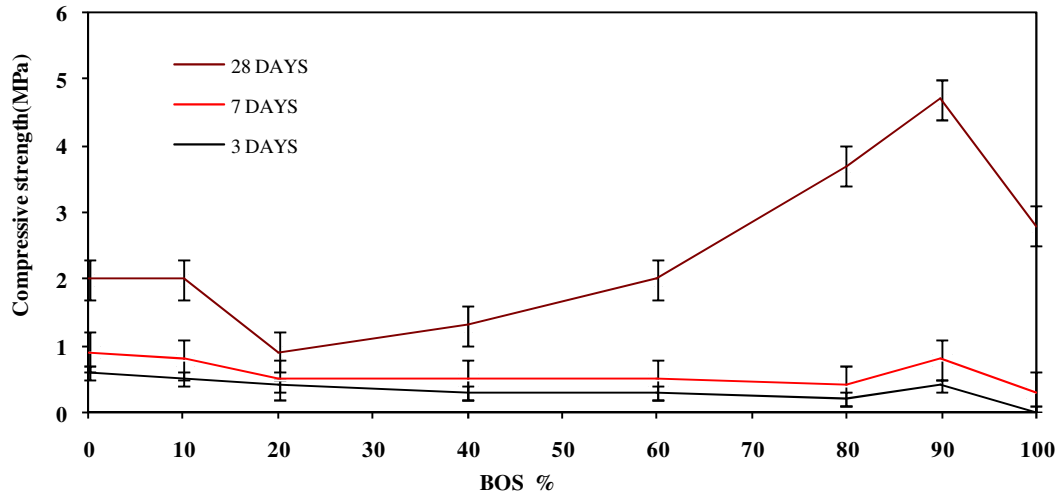


Figure 4- 6 Compressive Strength of BOS - ROSA pastes at 3,7 and 28 days

Figure 4-6 demonstrates the effect of BOS on the compressive strength of the BOS, ROSA mixtures. A significant increase in these mixes occurred from 20% of BOS to 90% of BOS. The maximum compressive strength was for 90% BOS and 10% ROSA. In all mixes the compressive strength increased with time.

The flow of the mixes was decreased by increasing ROSA. Water was absorbed by ROSA during mixing however a part of the absorbed water was slowly being returned to the mix after 3 minutes of mixing that slightly increased the flow.

The paste using only BOS did not set at 3 days with 30% of water. However its compressive strength was more than ROSA paste at 28 days.

The compressive strength of the optimum mix, 90%BOS-10%ROSA, was increased 55% from 3 days to 7 days of casting and was increased 93% from 3 days to 28 days.

4.4.2 Basic Oxygen Slag (BOS) - Bypass Dust (BPD)

Table 4-7 Characterisation of BOS and BPD Mixes

Materials		Compressive Strength MPa.			Density	Flow	Mixing Time
BOS%	BPD%	3 days	7 days	28 days	Kg/m ³	mm	min
0	100	3.4	5.9	13.1	1752	122	5
10	90	3.2	5.5	12.0	1858	125	5
20	80	2.3	4.0	9.3	2056	126	5
40	60	2.3	2.5	8.8	2120	134	5
60	40	1.3	2.8	9.0	2208	140	5
80	20	0.8	1.5	6.5	2264	147	5
90	10	0.7	1.0	4.0	2287	High Flow	5
100	0	0.0	0.3	2.8	2320	High Flow	5

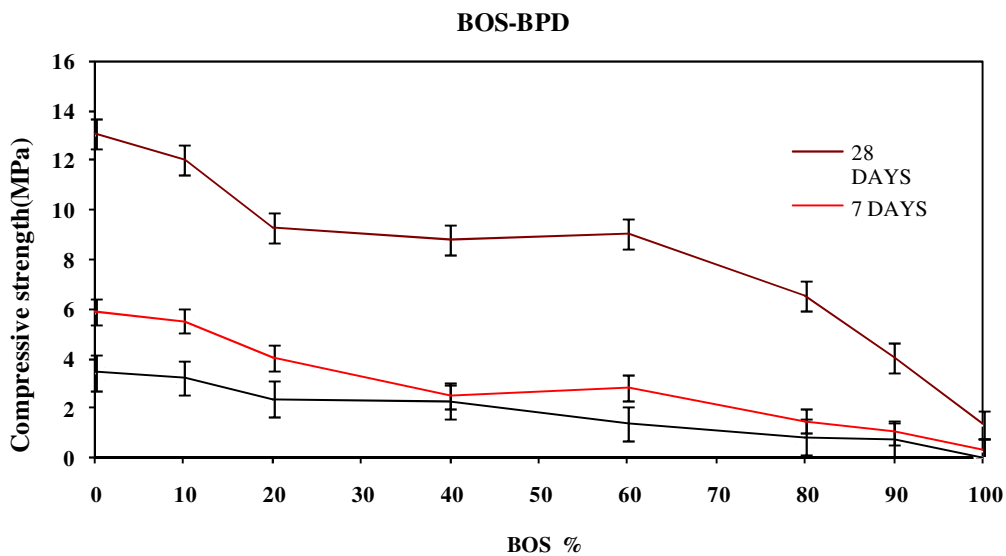


Figure 4-7 Compressive Strength of BOS – BPD pastes at 3,7 and 28 days

Figure 4-7 demonstrates the effect of BOS content on the compressive strength of the BOS-BPD mixtures. Although in the paste with 0% BOS-100% BPD had the highest compressive strength. **There was no optimum point for BOS-BPD pastes. The more the BPD the more the compressive strength of pastes were.**

The reason could be described that BPD had the Portland cement characteristics. The chlorides, sulphates and alkalis in the BPD activated the slag (Heikal *et al.* 2002).

Strength development of pastes was the result of the hydration of both C₃S and C₃A and the formation of the C-S-H and ettringite-ferrite (Aft) phases. In the presence of Ca²⁺ and SO₄²⁻ in the liquid phase, the hydration of C₃A and C₄AF in the initial preinduction period is reduced and ettringite-ferrite phase (AFt) is formed during hydration. When the gypsum is consumed and nothing remains to form ettringite, C₄AH₁₃ is produced, and this reacts with ettringite already produced to form monosulphate and it happens during final set (Heikal *et al.* 2002).

The setting time of BPD-BOS paste was extended with slag content due to the low hydraulic properties of granulated slag in comparison with BPD. The setting process is associated with the formation of calcium sulphoaluminate hydrate (C-S-H). The formation of these hydrates depends on the reaction velocity of the aluminate compounds, amount of the phases, calcium sulphate retarder and calcium hydroxide. The BPD (upon hydration) acts as a source of calcium hydroxide that gives the correct alkalinity to form ettringite (Heikal *et al.* 2002).

The high free lime content of CKD (BPD) improves the hydration process and accelerates hydration and forming more crystalline hydration products (Konstantinos *et al.* 2003).

The mix with 60% BOS and 40% BPD was considered to be a reasonable optimum mix among BOS-BPD mixes. In all pastes the compressive strength increased with time.

4.4.3 Basic Oxygen Slag (BOS) – Red Gypsum (RG)

Table 4-8 Characterisation of BOS and RG Mixes

Materials		Compressive Strength MPa.			Density	Flow	Mixing Time
BOS%	RG %	3 days	7 days	28 days	Kg/m ³	mm	min
20	80	0.8	1.9	4.1	1800	No Flow	5
40	60	1.0	2.8	5.5	1912	No Flow	5
60	40	1.4	2.8	8.8	2056	95	5
80	20	0.5	1.4	9.0	2208	121	5
100	0	0.0	0.3	2.8	2320	High Flow	5

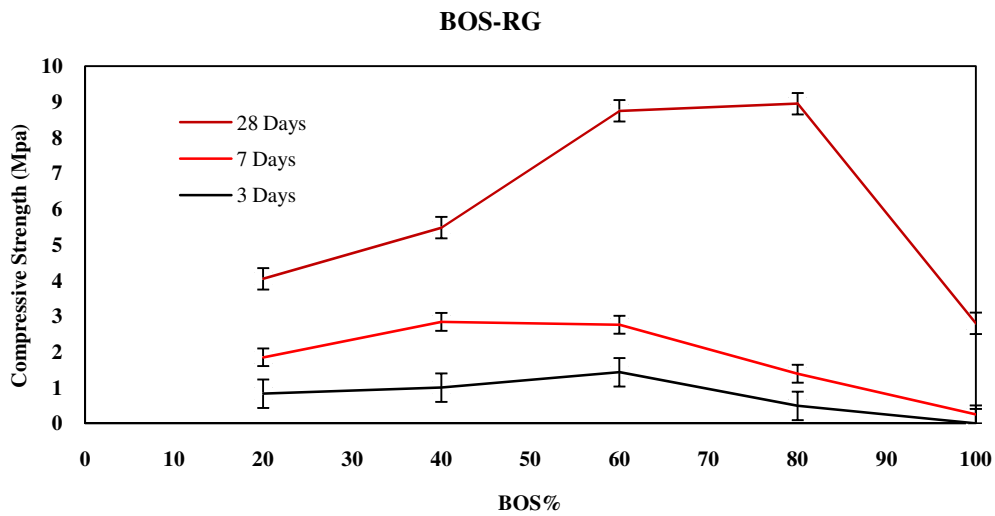


Figure 4-8 Compressive Strength of BOS – RG pastes at 3,7, and 28 days

Figure 4-8 demonstrates the effect of BOS on the compressive strength of the BOS-RG mixtures. The compressive strength of mixes increased from 0% RG and 100% BOS and reached its highest point for the 80% BOS-20% RG mix, then it decreased in compressive strength for the mix using only BOS. In all mixes the compressive strength increased with time. The compressive strength of the optimum mix at 7 days was increased by 65% compared to the 3 day compressive strength and it increased by 81% at 28 days.

The increase in compressive strength of BOS-RG pastes could be a results for a pozzolanic reaction had taken place between RG and BOS to produce dicalcium silicate (Hughes, 2006). RG water absorption in all mixes leading to less flow and BOS did not absorb water and by increasing BOS in each mix, the flow was increased.

The high free lime content of RG (almost equal to BPD) could improve the hydration process and accelerate hydration and forming more crystalline hydration products.

4.4.4 Basic Oxygen Slag (BOS) – Plasterboard Gypsum (PG)

Table 4-9 Characterisation of BOS and PG Mixes

Materials		Compressive Strength MPa.			Density	Flow	Mixing Time
BOS%	PG%	3 days	7 days	28 days	Kg/m ³	mm	min
20	80	0.4	1.0	3.9	1928	No Flow	5
40	60	0.8	1.2	4.2	2056	81	5
60	40	0.8	1.6	6.3	2144	102	5
80	20	1.0	2.3	9.5	2184	130	5
100	0	0.0	0.3	2.8	2320	High Flow	5

BOS-PG

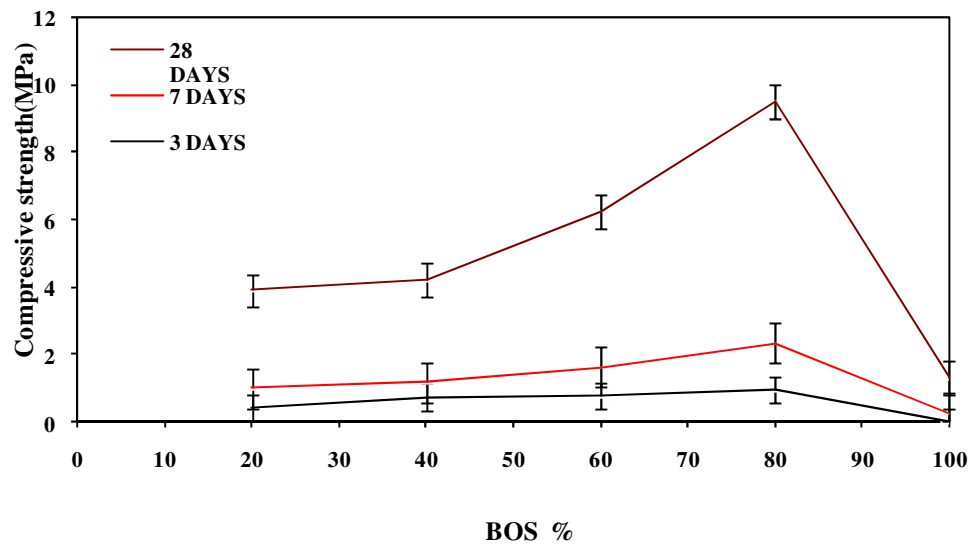


Figure 4-9 Compressive Strength of BOS – PG pastes at 3, 7, and 28 days

Figure 4-9 demonstrates the effect of BOS content on the compressive strength of the BOS- PG pastes. In combination of BOS and gypsum, gypsum performs as a sulphate activator and forms crystalline phase of Al (OH)₃. The sulfur in slag acts as an autoactivator for pozzolanic reactions (Pouya *et al.* 2007).

The compressive strength of mixes increased from 0% PG and 100% BOS and reached its highest point with 80% BOS and 20% PG then it decreased for mix using only BOS. The compressive strength of the optimum mix was increased by 60% at 7 days and 90% at 28 days compared to the 3 days.

The compressive strength of BOS is increased by adding PG as an activator. In all mixes the compressive strength was increased by time. The flow of mixes is increased by increasing the amount of BOS.

4.4.5 Bypass Dust (BPD) – Run of Station Ash (ROSA)

Table 4-10 Characterisation of BPD and ROSA Mixes

Materials		Compressive Strength MPa.			Density	Flow	Mixing Time
ROSA%	BPD%	3 days	7 days	28 days	Kg/m ³	mm	min
0	100	3.4	5.9	13.1	1752	122	5
20	80	2.0	4.6	16.0	1920	118	5
40	60	1.3	4.2	19.6	1888	100	5
60	40	0.9	7.2	22.0	1880	98	5
80	20	0.7	5.6	16.5	1740	87	5
100	0	0.6	0.9	2.0	1640	No Flow	5

ROSA-BPD

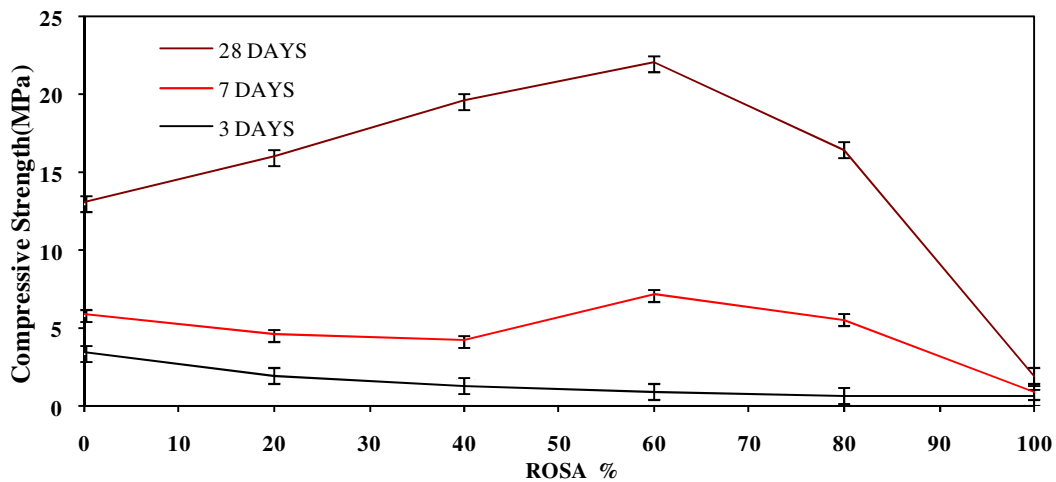


Figure 4-10 Compressive Strength of ROSA-BPD pastes at 3, 7, and 28 days

Figure 4-10 demonstrates the effect of ROSA on the compressive strength of the ROSA-BPD pastes. The compressive strength of mixes increased from the mix with 0% ROSA - 100% BPD to mix with 60% ROSA - 40% BPD. The highest compressive strength was for the mix 60% ROSA - 40% BPD then it decreased to

the mix with 100% of ROSA. The compressive strength of the optimum mix increased 85% from 3 to 7 days and it was increased 97% from 3 to 28 days.

The high compressive strength of this mix at 7 days (7.17 MPa) might be attributed to the influence of rapid hydration at early age on microstructure of the ROSA-BPD paste.

In all mixes the compressive strength increased with curing time. The flow of mixes decreased by increasing the amount of ROSA because ROSA absorbed water immediately after water added to the binder. However, it released water later to the paste and the flow increased.

ROSA-BPD had a higher compressive strength than other by-product combinations. This higher compressive strength at early age was also considered for use in light weight blocks mix design in this research. **Using 40% BPD was not feasible because BPD did not have similar chemical characteristics in different batches even if it was collected from the same source. These caused variations in the compressive strength of pastes. Therefore, BPD content should be limited to 15-20%.**

4.4.6 Run of Station Ash (ROSA) - Red Gypsum (RG)

Table 4- 11 Characterisation of ROSA and RG Mixes

Materials		Compressive Strength MPa.			Density	Flow	Mixing Time
ROSA%	RG%	3 days	7 days	28 days	Kg/m ³	mm	min
60	40	0.5	0.8	1.6	1480	82	5
80	20	0.7	1.3	2.6	1576	83	5
90	10	0.6	1.7	3.3	1623	85	
100	0	0.6	1.9	2.0	1640	No Flow	5

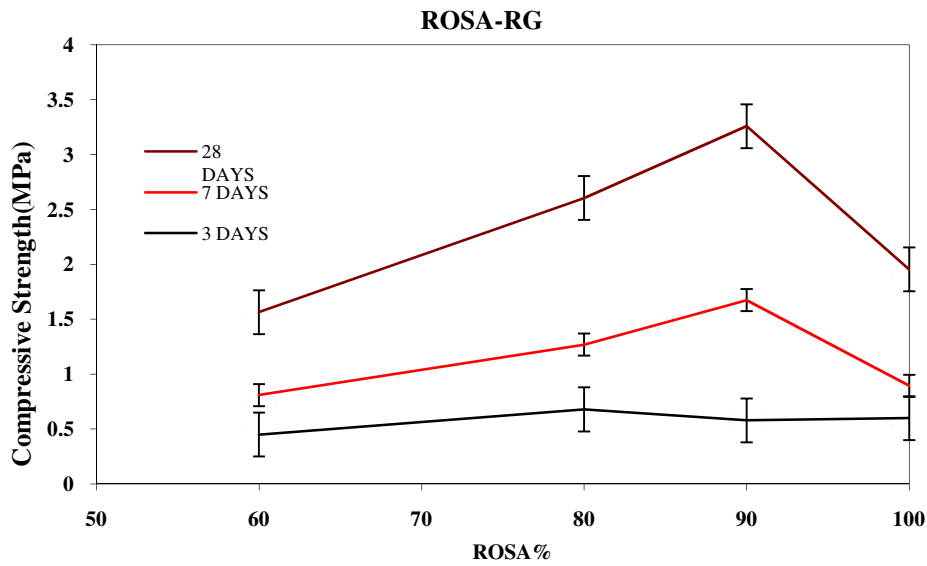


Figure 4- 11 Compressive Strength of ROSA – RG pastes at 3, 7, and 28 days

Figure 4-11 demonstrates the effect of ROSA content on the compressive strength of the ROSA-RG. Due to RG having a low compressive strength at high content and causing very sticky and dry paste, RG was limited to 40% with ROSA. The highest compressive strength was for mix 90% ROSA-10% RG. The compressive strength of this mix was increased 65% from 3 days to 7 days and it was increased 82% from 3 days to 28 days.

In all mixes the compressive strength increased with time. The flow of pastes decreased when ROSA content was increased.

4.4.7 Run of Station Ash (ROSA) - Plasterboard Gypsum (PG)

Table 4- 12 Characterisation of ROSA and PG Mixes

Materials		Compressive Strength MPa.			Density	Flow	Mixing Time
ROSA %	PG %	3 days	7 days	28 days	Kg/m ³	mm	min
40	60	0.3	1.0	2.0	1752	85	5
60	40	0.8	1.6	3.4	1744	85	5
80	20	1.2	3.0	6.3	1732	86	5
90	10	0.5	2.5	6.5	1724	87	5
100	0	0.6	1.9	2.0	1640	No Flow	5

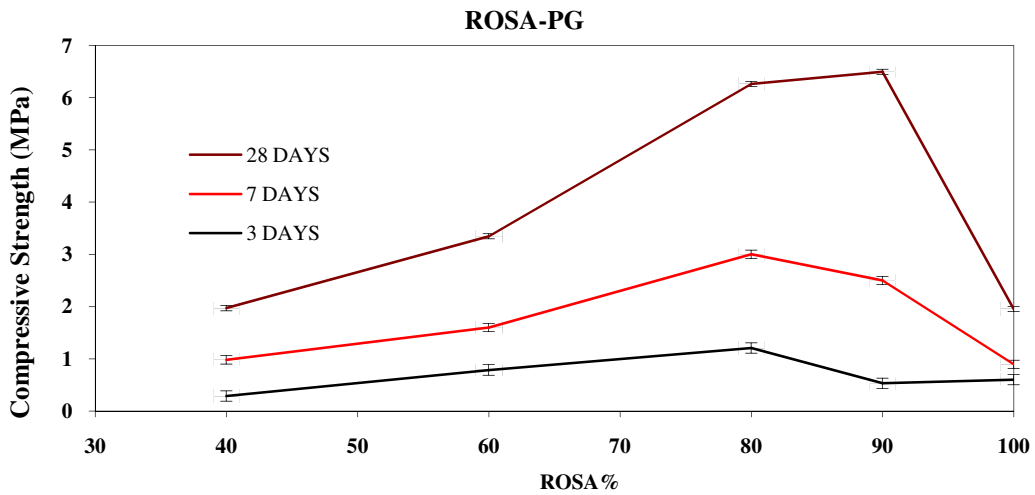


Figure 4- 12 Compressive Strength of ROSA – PG pastes at 3, 7, and 28 days

Figure 4-12 demonstrates the effect of ROSA content on the compressive strength of the ROSA- PG pastes. The compressive strength of mixes increased from 60% ROSA to 90% of ROSA and the highest compressive strength was for the mix 90% ROSA-10% PG (similar to RG mixes). The compressive strength grow was 79% and 92% from 3 days to 7 and 28 days.

In all pastes the compressive strength increased with time. The flow of pastes decreased when ROSA content increased.

4.4.8 Bypass Dust (BPD) - Red Gypsum (RG)

Table 4-13 Characterisation of BPD and RG Mixes

Materials		Compressive Strength MPa.			Density	Flow	Mixing Time
BPD%	RG%	3 days	7 days	28 days	Kg/m ³	mm	min
50	50	1.3	3.1	6.3	1960	87	5
60	40	1.4	2.8	6.7	1944	91	5
80	20	1.4	2.8	7.0	1916	98	5
90	10	2.2	3.0	7.9	1894	116	5
100	0	3.4	5.9	13.1	1752	122	5

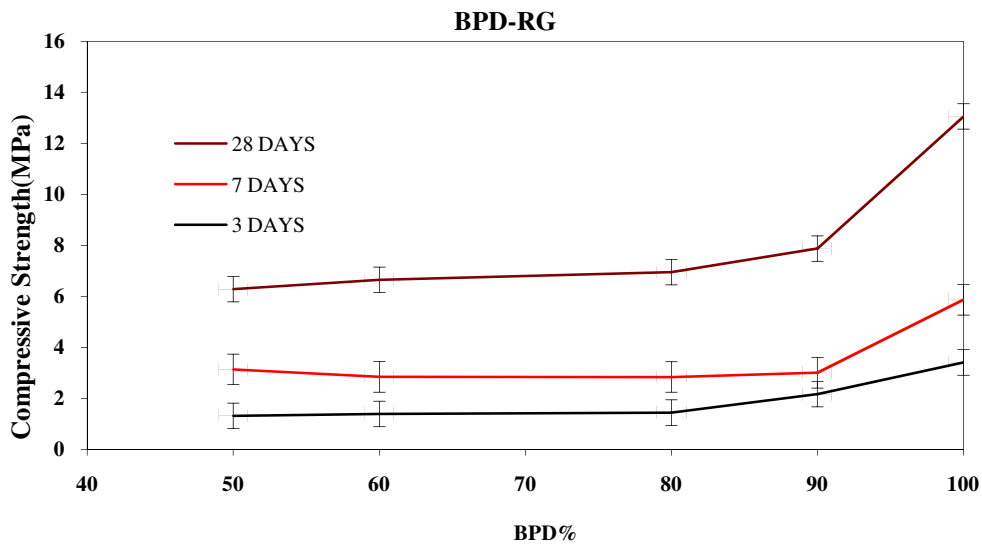


Figure 4-13 Compressive Strength of BPD – RG pastes at 3, 7, and 28 days

Figure 4-13 demonstrates the effect of BPD content on the compressive strength of the BPD-RG mixtures. The compressive strength of mixes increased from 50% BPD to 100% BPD. The highest compressive strength was for the paste 100% BPD. In all mixes the compressive strength increased with time. The flow of the mixes increased when BPD content increased.

An attempt was made to mix 60% RG with 40% BPD, **however** the mix was too stiff and **therefore** 50:50 RG: BPD mix was **used** instead.

The BPD content was limited to 15-20% **owing to** the variability of the BPD supply.

4.4.9 Bypass Dust (BPD) - Plasterboard Gypsum (PG)

Table 4-14 Characterisation of BPD and PG Mixes

Materials		Compressive Strength MPa.			Density	Flow	Mixing Time
BPD%	PG%	Kg/m ³	7 days	28 days	Kg/m ³	mm	min
40	60	0.9	1.3	2.5	1830	90	5
60	40	1.4	2.2	4.7	1805	95	5
80	20	2.3	3.7	8.0	1777	103	5
90	10	3.1	5.5	12.6	1765	118	5
100	0	3.4	5.9	13.1	1752	122	5

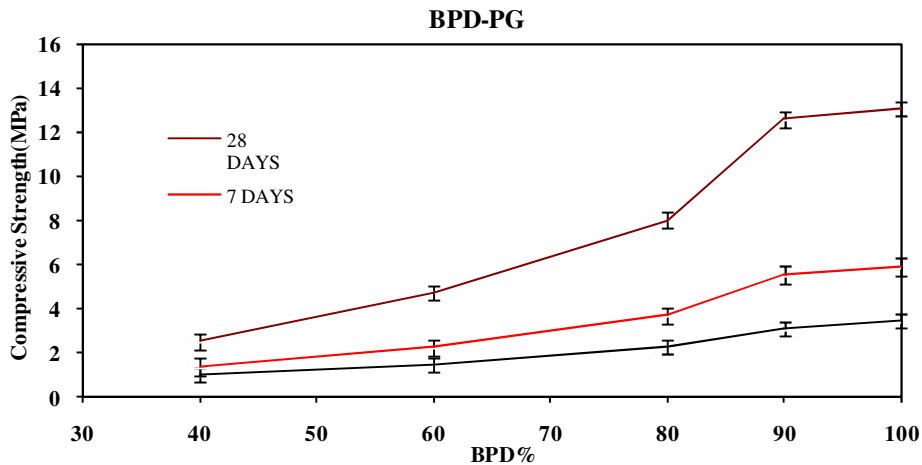


Figure 4- 14 Compressive Strength of BPD – PG pastes at 3, 7, and 28 days

Figure 4-14 demonstrates the effect of BPD content on the compressive strength of BPD-PG mixtures. The compressive strength of the mixes increased with adding BPD from 40% to 100%. The highest compressive strength is for the paste 100% BPD. In all mixes the compressive strength increased with time. The flow of the mixes increased when BPD content was increased.

4.5 Results of Step 2- Ternary Mixes

4.5.1 Setting time

The time taken for the pastes was determined by measuring the setting time which was measured using Vicat apparatus in BS EN 196-3:2005. Setting time is measured to predict the workability of fresh concrete.

The pastes were made with a 0.3 w/c ratio. The results for setting time are presented in table 4-15.

Table 4-15 Setting time measurement

Mixes	w/b ratio	Initial Setting time (Minutes)	Final Setting time (Minutes)
48%BOS-40%ROSA-12%RG	0.3	470 ± 5	745 ± 3
40%BOS-50%ROSA-10%RG	0.3	440 ± 3	705 ± 4
30%BOS-60%ROSA-10%RG	0.3	380 ± 4	670 ± 3
40%BOS-50%ROSA-10%PG	0.3	360 ± 5	620 ± 4
30%BOS-60%ROSA-10%PG	0.3	310 ± 5	595 ± 4

Pastes containing PG had shorter setting times than mixes containing RG. Using the same amount of RG or PG, mixes with more ROSA had shorter setting times. Also, the mix with 48% BOS took longer to set.

4.5.2 Compressive strength

The results from step 1 were used for step 2 paste mixtures. The materials in step 2 (the ternary combinations) were BOS, ROSA, BPD, PG, and RG. Different combinations were used for mixes. The result of compressive strength at 3, 7, and 28 days are shown in Tables 4-16 to 4-22.

Table 4- 16Characterisation of BOS, ROSA and PBD Mixes

Materials			Compressive Strength (MPa).			Flow mm	Mixing Time min
BOS%	ROSA%	BPD%	3 days	7 days	28 days		
76	19	5	0.2	1.0	8.7	High Flow	5
72	18	10	0.2	1.9	8.2	155	5
64	16	20	0.2	1.8	7.2	143	5
48	12	40	0.3	0.9	5.7	134	5
32	8	60	0.3	0.8	4.5	125	5
50	45	5	0.5	2.9	11.1	152	5
35	55	10	0.9	4.3	15.0	132	5
27	68	5	0.6	1.4	8.2	123	5
30	30	40	0.3	1.1	10.0	130	5
15	80	5	0.5	2.6	8.0	83	5
18	10	72	0.6	1.5	6.3	No Flow	7
16	20	64	0.6	1.9	8.2	86	7
12	40	48	0.7	2.4	12.5	94	7
8	60	32	0.6	3.4	18.5	96	7

Table 4-16 shows the flow and compressive strength of BOS-ROSA-BPD mixes. There was an increase in compressive strength with curing time.

BPD is an alkali activator for both BOS and ROSA. It had better pozzolanic activation with ROSA therefore the highest compressive strength was achieved with higher ROSA content than BOS. The highest compressive strength at 28 days was for the mix with BOS 8%, ROSA 60% and 32% BPD. Flow increased by increasing the amount of BOS. Higher amounts of ROSA and BPD decreased the flow.

Table 4- 17 Characterisation of BOS, BPD and RG Mixes

Materials			Compressive Strength (MPa).			Flow mm	Mixing Time min
BOS%	BPD%	RG%	3 days	7 days	28 days		
85	10	5	0.4	0.7	9.3	High Flow	5
85	5	10	0.3	0.7	9.2	High Flow	5
80	10	10	0.3	1.0	6.2	High Flow	5
76	5	19	0.4	0.9	6.0	High Flow	5
76	19	5	0.5	1.3	9.4	High Flow	5
72	10	18	0.5	0.9	8.7	High Flow	5
72	18	10	0.5	1.1	6.8	High Flow	5
68	15	17	0.2	1.1	5.7	155	5
68	17	15	0.3	1.1	5.9	144	5
65	10	25	0.4	0.9	6.0	86	7
64	20	16	0.4	1.0	5.3	134	5
60	20	20	0.4	1.0	5.0	No Flow	7

Table 4- 18 Characterisation of BOS, BPD and PG Mixes

Materials			Compressive Strength (MPa).			Flow mm	Mixing Time min
BOS%	BPD%	PG%	3 days	7 days	28 days		
85	10	5	0.3	1.0	10.1	High Flow	5
85	5	10	0.2	0.9	10.0	High Flow	5
80	10	10	0.3	1.1	7.0	High Flow	5
76	19	5	0.5	1.0	6.3	High Flow	5
76	5	19	0.5	1.4	10.5	134	5
72	18	10	0.6	1.4	9.2	High Flow	5
72	10	18	0.3	1.3	7.2	High Flow	5
68	17	15	0.4	1.2	6.2	155	5
68	15	17	0.4	1.3	6.3	150	5
65	10	25	0.4	1.1	6.2	86	7
64	20	16	0.4	1.3	5.8	144	5
60	20	20	0.6	1.2	5.3	110	7

Tables 4-17 and 4-18 demonstrate the compressive strength and flow of different mixes with BOS-BPD-RG and PG. In every mix the compressive strength increased with curing time. Pastes using PG had more compressive strength compared with pastes RG in combination with BOS-BPD with the same percentage. This could be because of the role of PG as a sulphate activator for BOS and ROSA. The higher the amount of BOS, the more the flow was in most cases. Higher amounts of RG or PG lead to lower flow.

The compressive strength in ternary mixes did not change linearly. Any changes of RG or BPD in mixes could be affected by two other materials. For example the minimum compressive strength at 28 days was for the mix with 19% of BPD (5% RG and 76% BOS) while higher compressive strength was for the mix contain 20% BPD (60%BOS and 20%RG) that was near the maximum strength of this group of pastes.

Table 4- 19 Characterisation of BOS, ROSA and RG Mixes

Materials			Compressive Strength (MPa)			Flow mm	Mixing Time min
BOS%	ROSA%	RG%	3 days	7 days	28 days		
76	19	5	0.4	1.3	6.7	High Flow	5
75	15	10	0.2	0.8	9.7	High Flow	5
64	20	16	0.3	1.8	11.8	147	5
50	45	5	0.3	2.0	13.8	148	5
48	40	12	0.6	3.2	17.6	120	5
40	30	30	0.9	2.6	17.9	115	5
40	50	10	0.7	2.4	19.3	123	5
35	45	20	0.9	4.0	15.4	100	5
30	60	10	0.7	2.5	18.9	87	5
20	72	8	0.7	2.9	12.5	No Flow	5
15	80	5	0.7	4.5	10.2	No Flow	5

Table 4- 20 Characterisation of BOS, ROSA and PG Mixes

Materials			Compressive Strength (MPa)			Flow mm	Mixing Time min
BOS%	ROSA%	PG%	3 days	7 days	28 days		
76	19	5	0.2	0.8	8.9	High Flow	5
75	15	10	0.2	1.0	5.9	High Flow	5
64	20	16	0.4	1.1	11.5	High Flow	5
50	45	5	0.6	2.1	13.4	136	5
48	40	12	0.4	1.6	7.1	153	5
40	30	30	0.4	1.1	10.6	119	5
40	50	10	0.6	2.3	18.8	131	5
35	45	20	0.5	1.7	15.5	130	5
30	60	10	0.5	2.4	18.6	95	5
20	72	8	0.6	3.9	13.4	90	5
15	80	5	0.5	3.3	9.1	85	5

Tables 4-19 and 4-20 demonstrate the compressive strength and flow of different mixes with BOS, ROSA, RG and PG. The compressive strength increased with time. The flow decreased by decreasing the amount of BOS.

There was no significant increase by increasing the amount of BOS. The highest compressive strength in both kinds of mixes happened in ROSA 60% and this result agrees with step one.

Table 4- 21 Characterisation of ROSA, BPD and PG Mixes

Materials			Compressive Strength (MPa)			Flow mm	Mixing Time min
ROSA%	BPD%	PG%	3 days	7 days	28 days		
85.5	5	9.5	0.8	2.5	14.0	No Flow	7
85	10	5	0.7	2.5	14.3	No Flow	7
81	10	9	0.6	2.3	15.8	No Flow	7
76.5	15	8.5	0.8	2.1	18.0	No Flow	7
76	19	5	0.5	2.1	17.0	No Flow	7
75	5	20	0.6	2.4	9.8	No Flow	7
72	18	10	0.7	2.3	16.3	No Flow	7
70	10	20	0.7	2.4	16.0	No Flow	7
68	17	15	0.9	1.8	15.4	No Flow	7
65	15	20	0.6	2.0	10.1	No Flow	7
60	20	20	1.1	2.3	5.4	No Flow	7

Table 4- 22 Characterisation of ROSA, BPD and RG Mixes

Materials			Compressive Strength (MPa)			Flow mm	Mixing Time min
ROSA%	BPD%	RG%	3 days	7 days	28 days		
85.5	5	9.5	1.2	3.5	7.0	No Flow	7
85	10	5	0.7	2.8	12.2	No Flow	7
81	10	9	1.0	4.3	8.0	No Flow	7
76.5	15	8.5	1.0	3.3	10.0	No Flow	7
76	19	5	0.6	3.8	8.2	No Flow	7
75	5	20	0.6	2.0	8.9	No Flow	7
72	18	10	1.0	2.9	13.5	No Flow	7
70	10	20	0.7	2.5	11.0	No Flow	7
68	17	15	0.8	4.5	12.0	No Flow	7
65	15	20	0.8	3.5	9.2	No Flow	7
60	20	20	1.0	2.1	4.9	No Flow	7

Tables 4-21 and 4-22 demonstrate the compressive strength and flow of different mixes with ROSA, BPD, RG and PG. In both mixes the compressive strength increased with time.

Figures 4-15 to 4-21 illustrate the curves for the 7 and 28 day compressive strength of the ternary combinations of raw materials. In these figures each axis show percentage of two raw materials and remaining percentage (that was not shown in the graph) of each mixture is the percentage of the third raw material. The compressive strength of mixes can be observed in each graph. For instance from figure 4-15 B it can be observed that the compressive strength of mix 30% BOS-30% ROSA and 40% of BPD is around 10 MPa at 28 days.

SURFER 8 software has been used to draw these graphs.

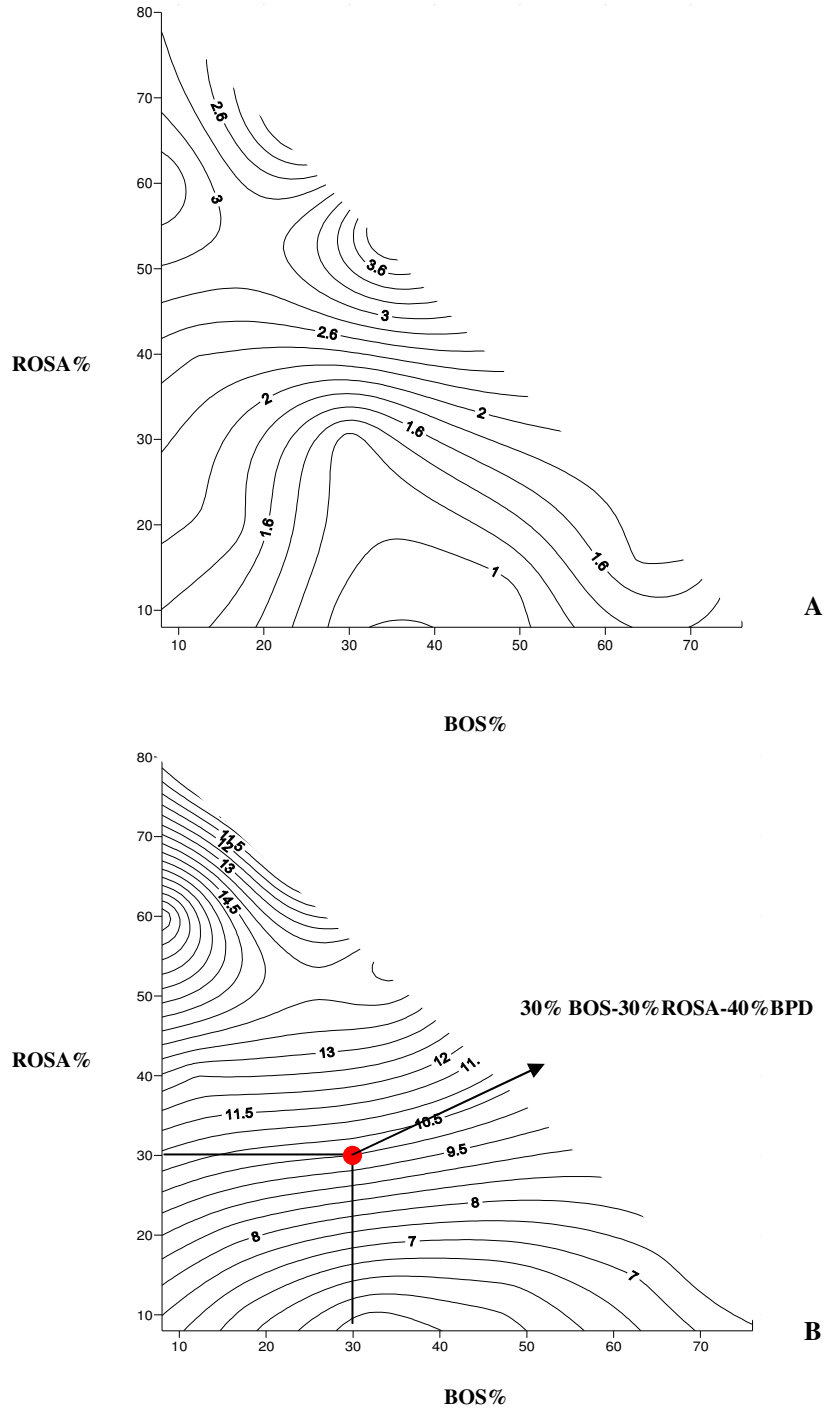


Figure 4- 15 (A and B)- BOS+ROSA+BPD strength (MPa) after 7 and 28 days

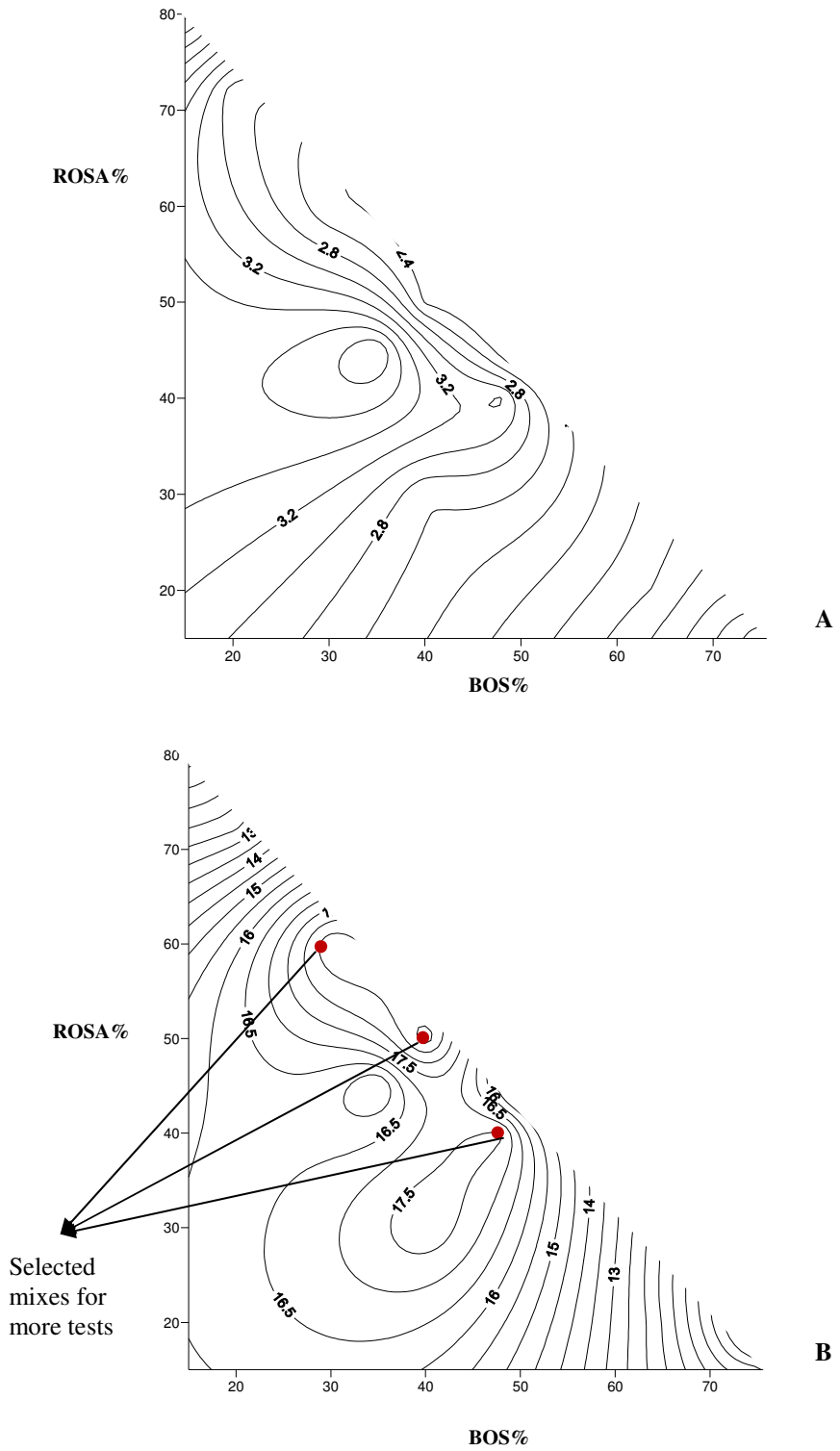


Figure 4- 16 (A and B)- BOS+ROSA+RG strength (MPa) after 7 and 28 days

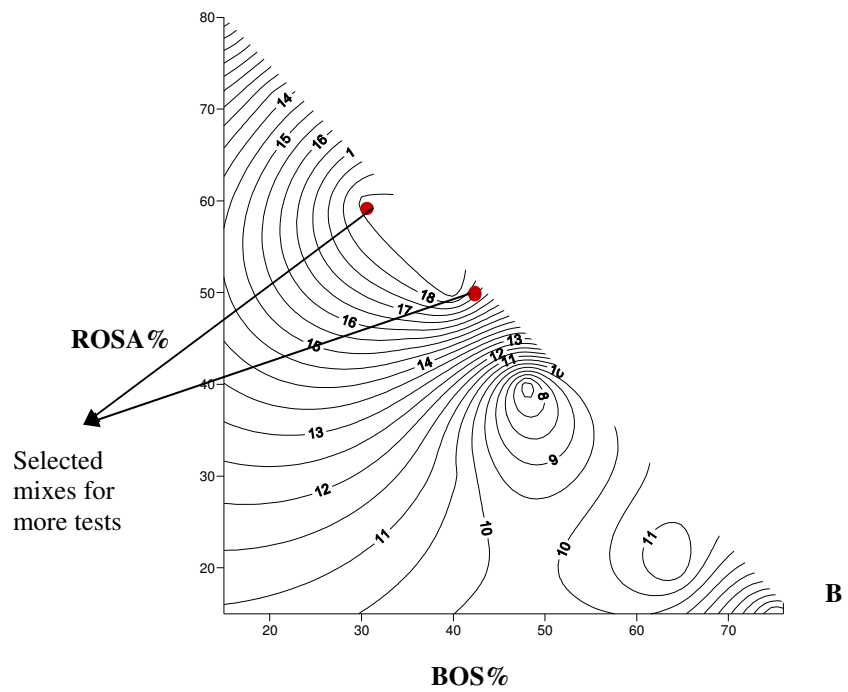
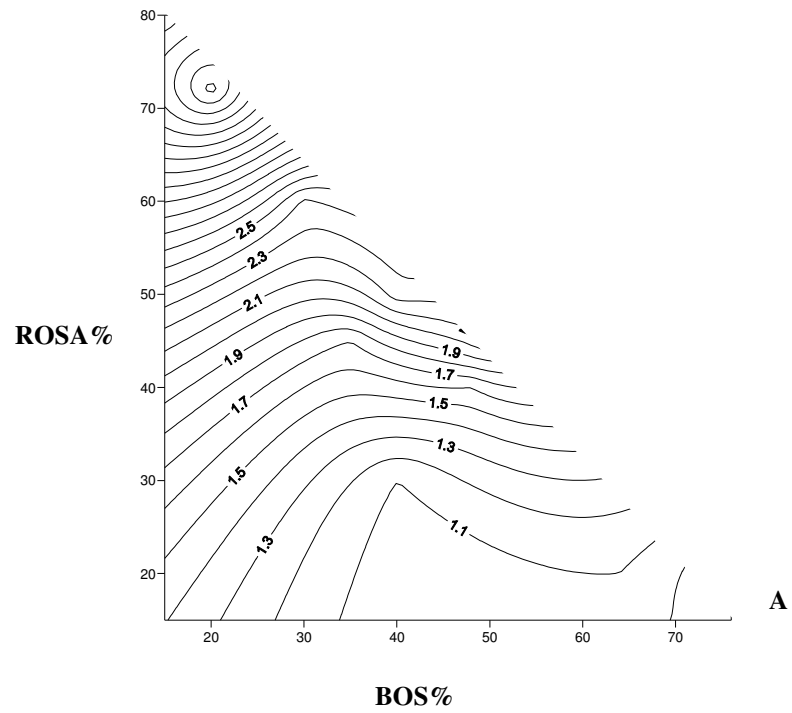


Figure 4- 17 (A and B)- BOS+ROSA+PG strength (MPa) after 7 and 28 days

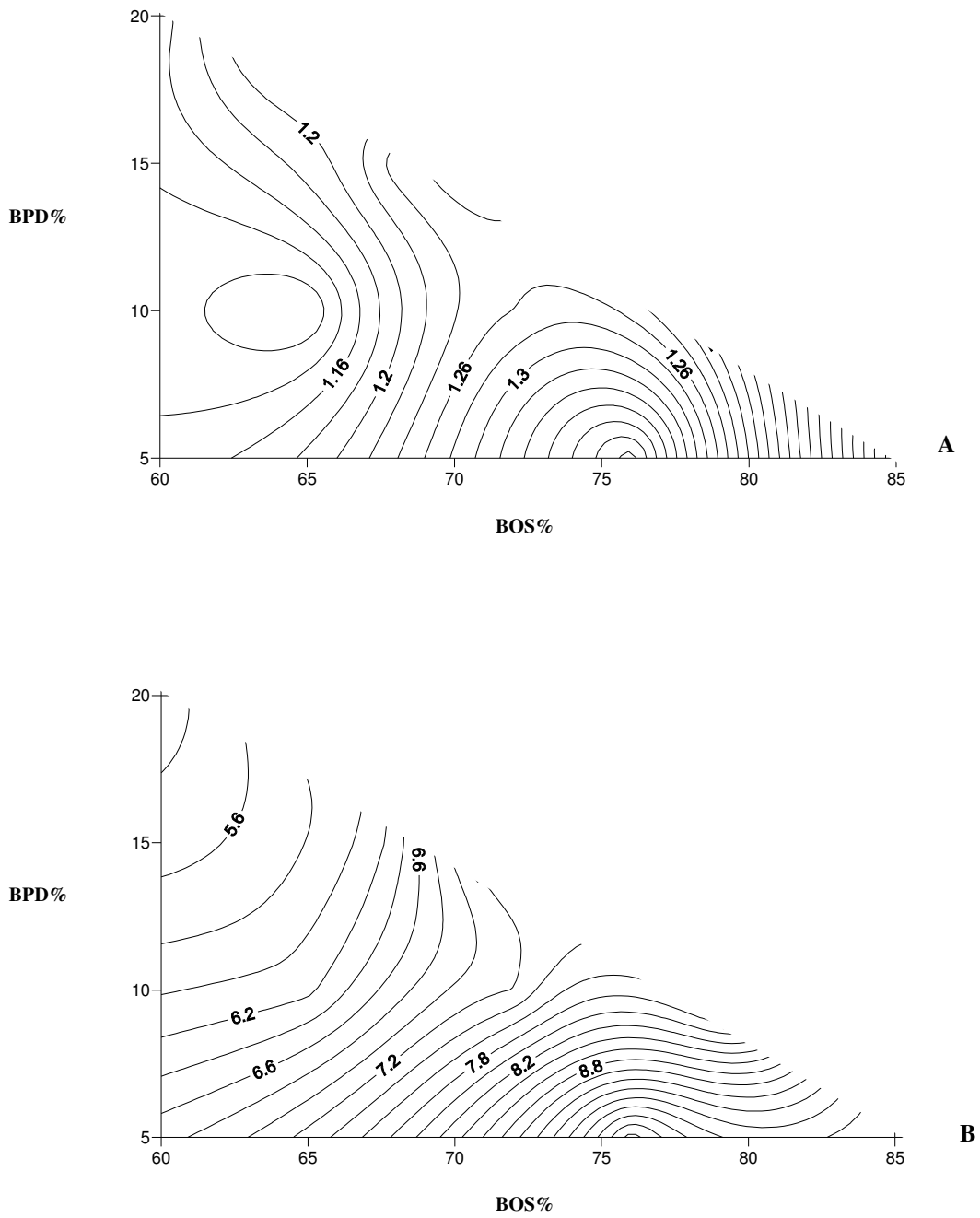


Figure 4- 18 (A and B)- BOS+BPD+PG strength (MPa) after 7 and 28 days

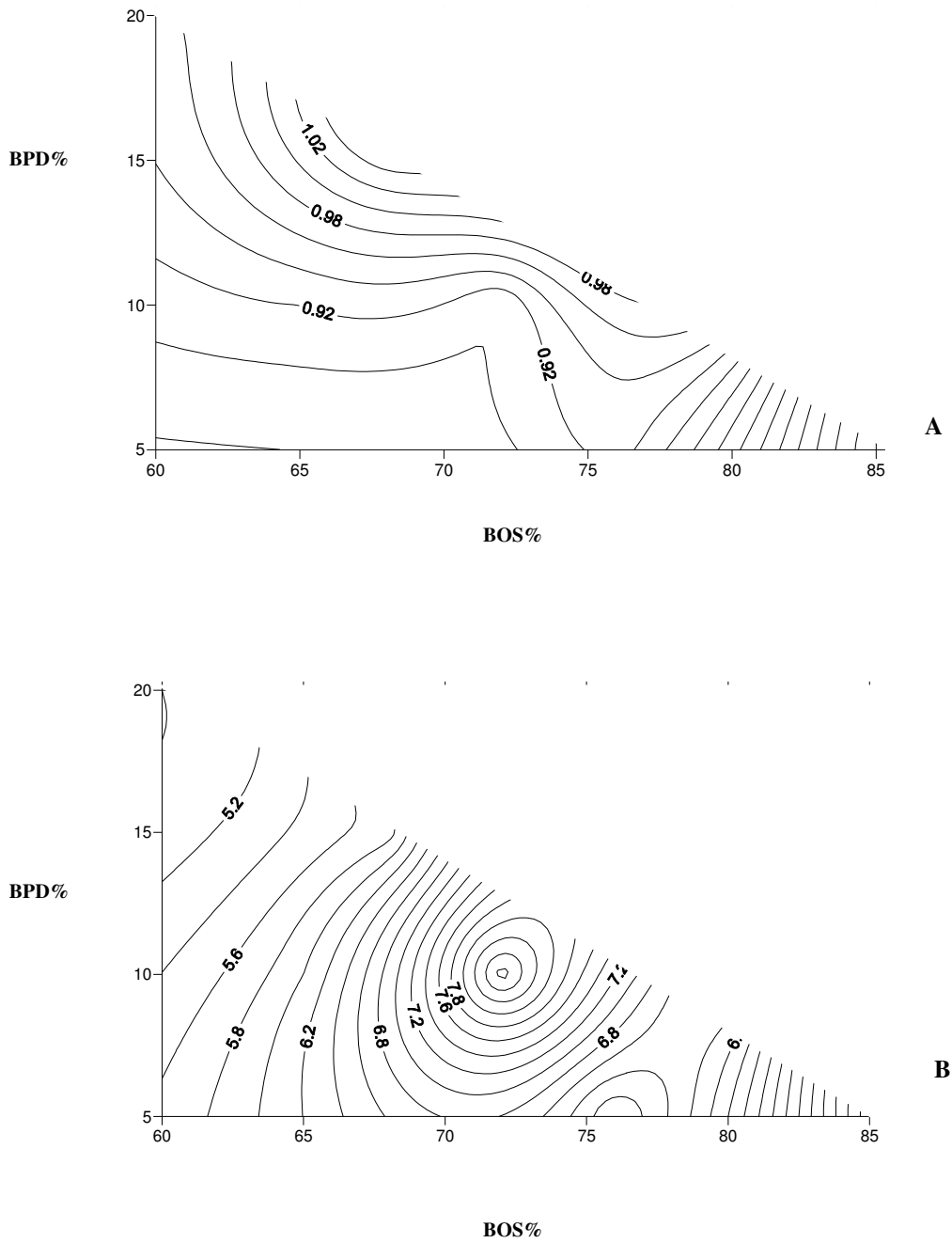


Figure 4- 19 (A and B)- BOS+BPD+RG strength (MPa) after 7 and 28 days

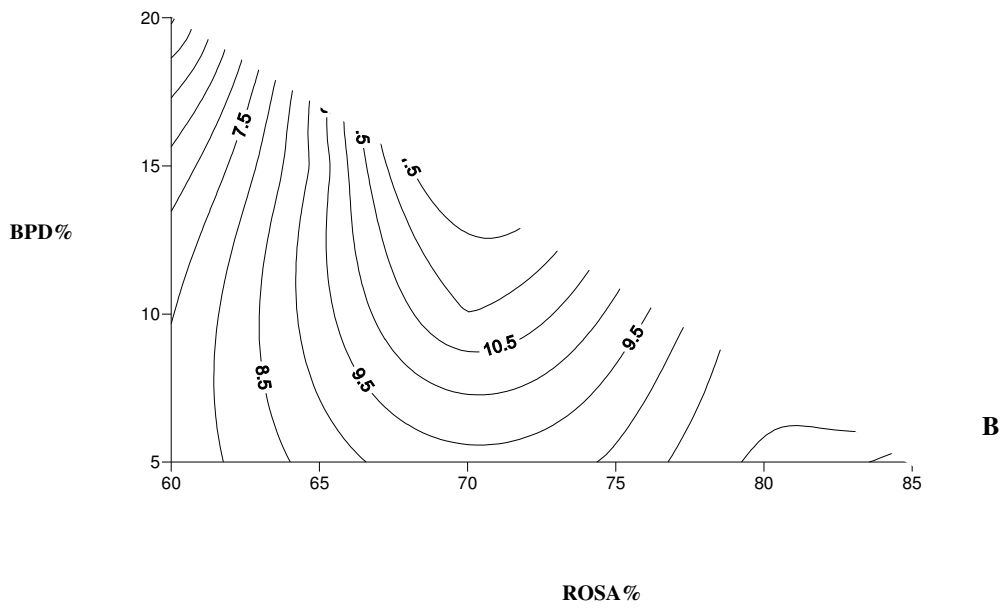
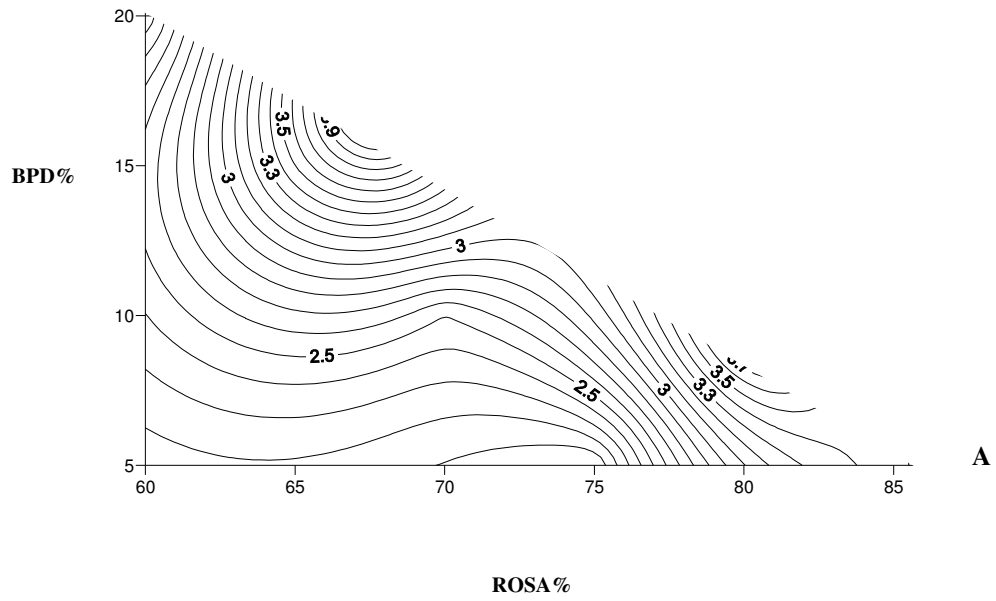


Figure 4- 20 (A and B)- ROSA+BPD+RG strength (MPa) after 7 and 28 days

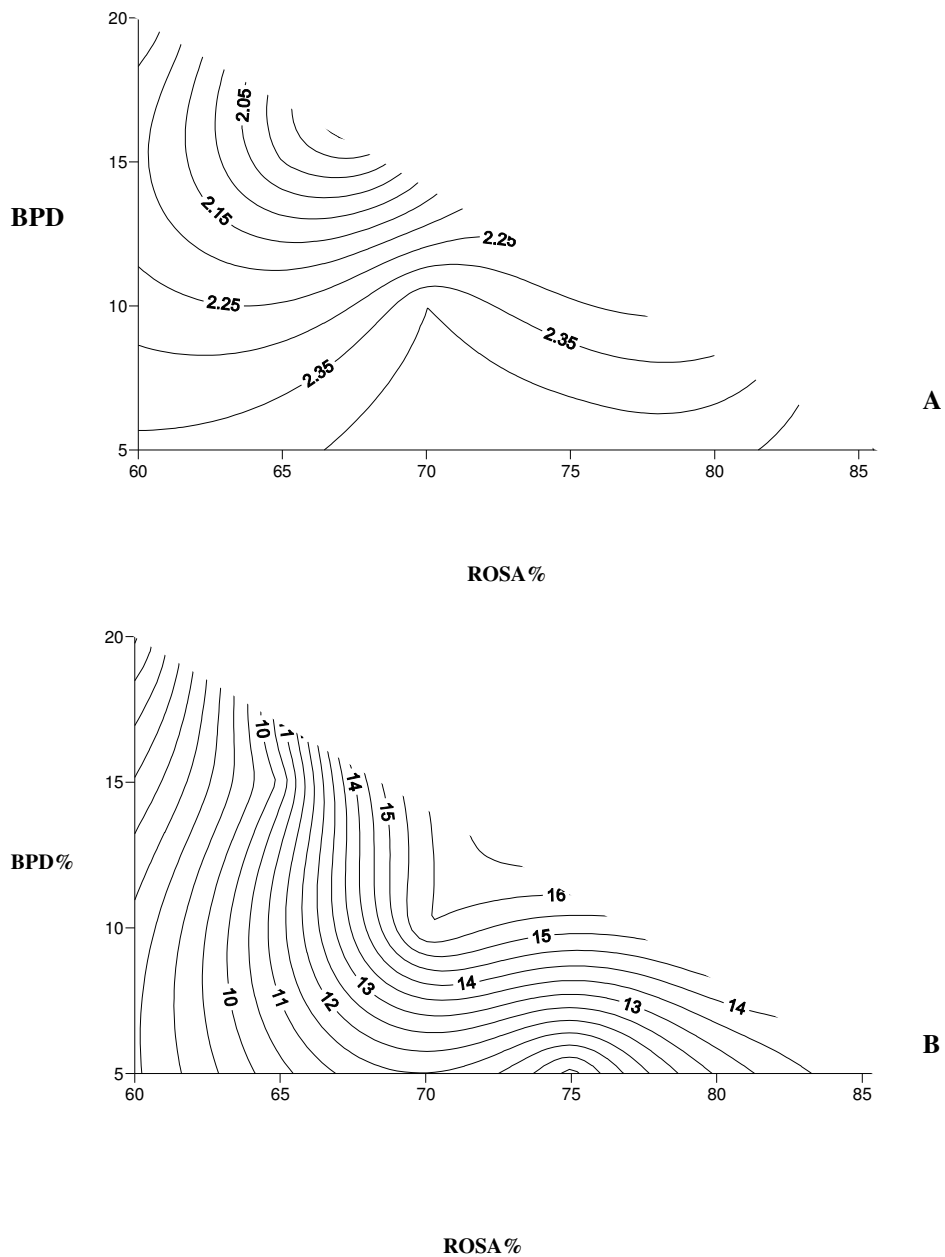


Figure 4- 21 (A and B)- ROSA+BPD+PG strength (MPa) after 7 and 28 days

The compressive strength of all mixes in ternary mixes was increased by curing time. The maximum compressive strength in both 7 and 28 days has occurred in the same area of the contours. **In another words**, mixes with higher compressive strength at 7 days had higher compressive strength at 28 days.

4.6 Selected Binder Mixes

From step 2 ternary mix design, 5 mixes with the highest compressive strength were selected for other tests. The mix designs and results of tests from step 2 are presented in table 4-23.

Table 4- 23 Selected mixes for further tests

Mix	w/b Ratio	3 Day Compressive Strength (MPa)	7 Day Compressive Strength (MPa)	28 Day Compressive Strength (MPa)
48%BOS-40%ROSA-12%RG	0.3	0.6	3.2	17.6
40%BOS-50%ROSA-10%RG	0.3	0.7	2.4	19.3
30%BOS-60%ROSA-10%RG	0.3	0.7	2.5	18.9
40%BOS-50%ROSA-10%PG	0.3	0.6	2.3	18.8
30%BOS-60%ROSA-10%PG	0.3	0.5	2.4	18.6

4.6.1 Effect of water content on compressive strength

All mixes in step one and two, binary and ternary mixes were mixed with a 30% water/binder ratio. The reduction in water content led to higher compressive strength. Table 4-24 presents the compressive strength results of 2 selected ternary mixes with various water/binder ratios and flows.

Table 4- 24 Effect of water/binder ratio on Compressive Strength of samples

Mixes	3 Day Compressive Strength (MPa)	7 Day Compressive Strength (MPa)	28 Day Compressive Strength (MPa)
30BOS-60ROSA-10RG (0.3 w/b)	2.0	3.7	19.8
30BOS-60ROSA-10PG (0.3 w/b)	1.7	3.6	19.2
30BOS-60ROSA-10RG (0.2 w/b)	2.8	4.9	22.5
30BOS-60ROSA-10PG (0.2 w/b)	2.5	4.7	21.7

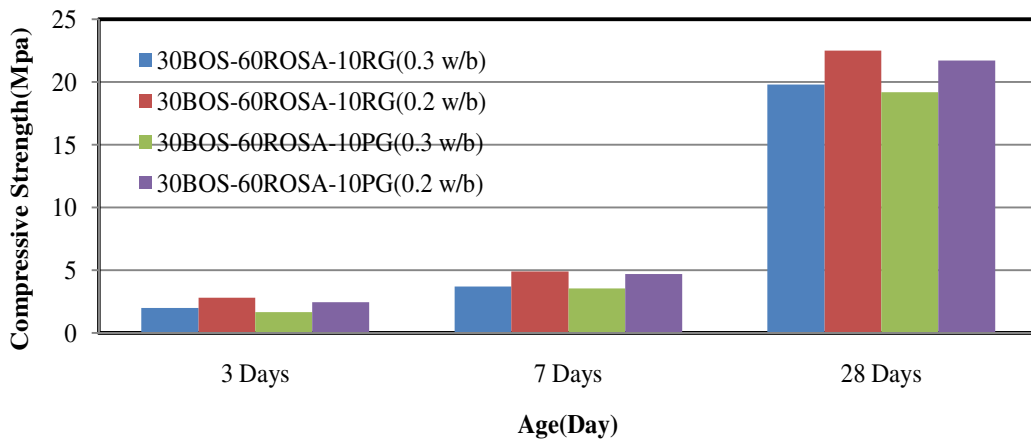


Figure 4- 22 Effect of w/b ratio on Compressive Strength at different ages

From figure 4-22, it can be seen that the higher w/c ratio gave less compressive strength for paste with RG and PG.

Further reductions in w/c ratio caused very dry mixes that caused less hydration and pozzolanic activities led to less compressive strength.

The reduction of the 28 day compressive strength by increasing w/c from 0.2 to 0.3 was 12% for the mix containing RG and 11.5% for the mix containing PG and it is typical for ordinary cement (Neville 1995)

The optimum w/b ratio as it is shown in Figure 4-23 was also studied for the Coventry novel cement (80%BOS, 15%PG, 5%BPD) (Ganjian *et al.* 2007) and it was 13% for semi dry paste.

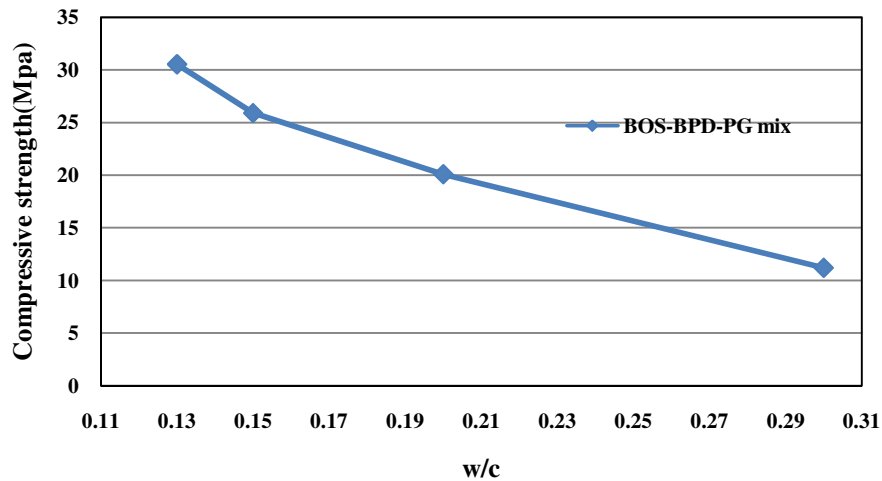


Figure 4- 23 Compressive strength development of sem-dry BOS-BPD-PG mix at 28 days with various w/c ratios according to Ganjian *et al.* (2007)

4.6.2 Effect of particle size on compressive strength

Using BOS, PG and RG with different particle sizes had effects on compressive strength of pastes in every age. BOS, PG and RG were sieved through sieve 500µm and 600 µm. Results of compressive strength of pastes BOS-ROSA-PG and BOS-ROSA-RG in different particle size are presented in table 4-26.

Table 4- 25 Effects of particle size on compressive strength of pasts

Mixes	3 Day Compressive Strength (MPa)	7 Day Compressive Strength (MPa)	28 Day Compressive Strength (MPa)
30%BOS-60%ROSA-10%RG (600µm)	0.7	2.5	18.9
30%BOS-60%ROSA-10%PG (600µm)	0.5	2.4	18.6
30%BOS-60%ROSA-10%RG (500µm)	2.0	3.7	19.8
30%BOS-60%ROSA-10%PG (500µm)	1.7	3.6	19.2

Figure 4-24 shows the effects of particle size on compressive strength at 3, 7, and 28 days. The compressive strength was increased by reducing particle size. This could be because of more interaction and higher surface area to react.

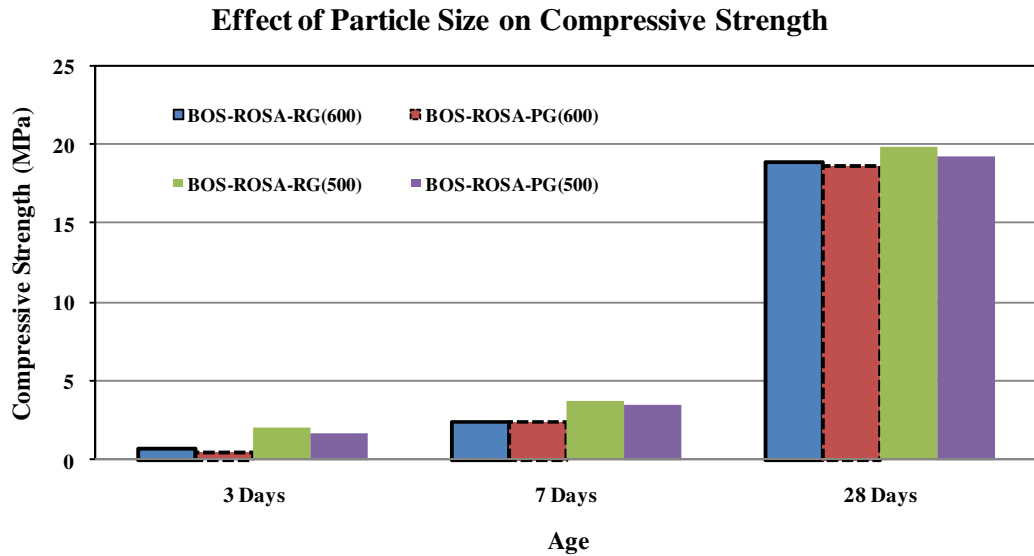
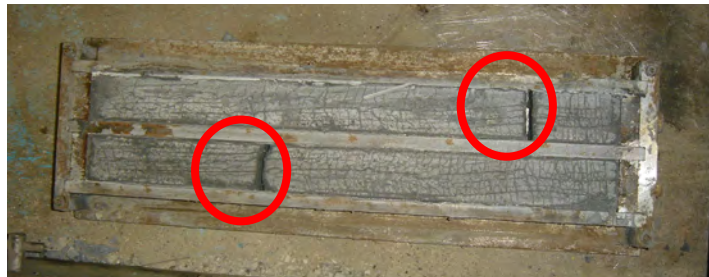


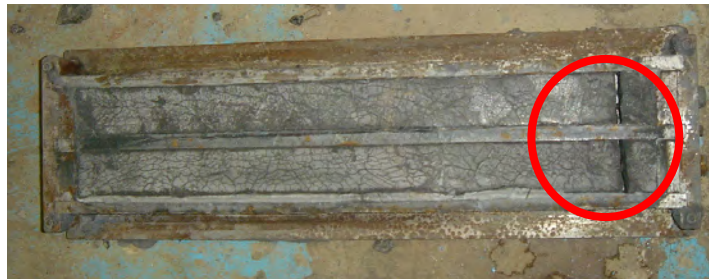
Figure 4- 24 Effects of Particle size on Compressive strength of BOS-ROSA-PG/RG mixes

4.6.3 Length change of five selected pastes (Expansion)

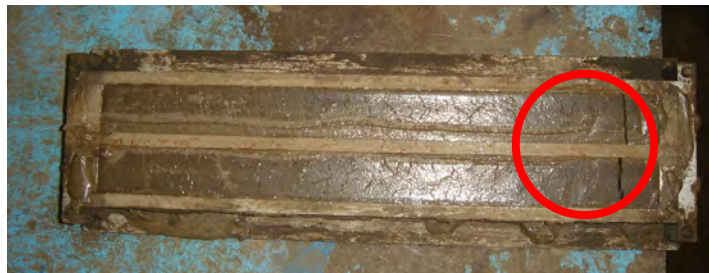
In order to investigate the long term durability of the five selected mixes from step 2, the length changes of paste samples were measured according to ASTM C151. The control mortar using Portland cement with 0.5 w/c ratio was made to compare the results. Making a sample for this test was not possible with 0.3 w/b ratio because they cracked in the first day after casting. The amounts of water were reduced to 0.23 to achieve sound samples. Some of the cracking is shown in Figure 4-25. By reducing w/c ratio, cracks slowly were disappeared.



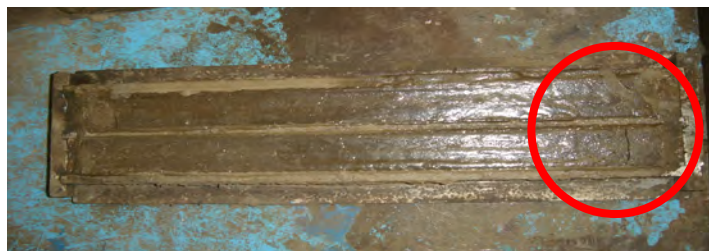
40BOS+50ROSA+10PG+0.30 L/S



40BOS+45ROSA+15PG+0.30 L/S



40BOS+50ROSA+10RG+0.27 L/S



40BOS+50ROSA+10RG+0.25 L/S

Figure 4- 25 Cracking was observed in samples during curing because of high water/binder ratio

The maximum allowed expansion or shrinkage of any mix depends on the application of the mix.

A second set of samples was cast and the length change of every sample was measured at 7, 14 and 28 days and every two weeks after that up to 26 weeks age. Results were compared as percentage of length change at different ages. The allowed expansion or shrinkage of paste limits to 0.1% at 26 weeks age according to ASTM C1260. This limit is for destructive alkali silica reaction in concrete.

A control sample with Portland cement was cast for comparison. Pastes and mortars were made using w/c ratio of 0.23%. OPC was made using the same sand/binder ratio of 2.7 and 0.5% w/c ratio.

All samples were cured at 20 °C and 98% RH.

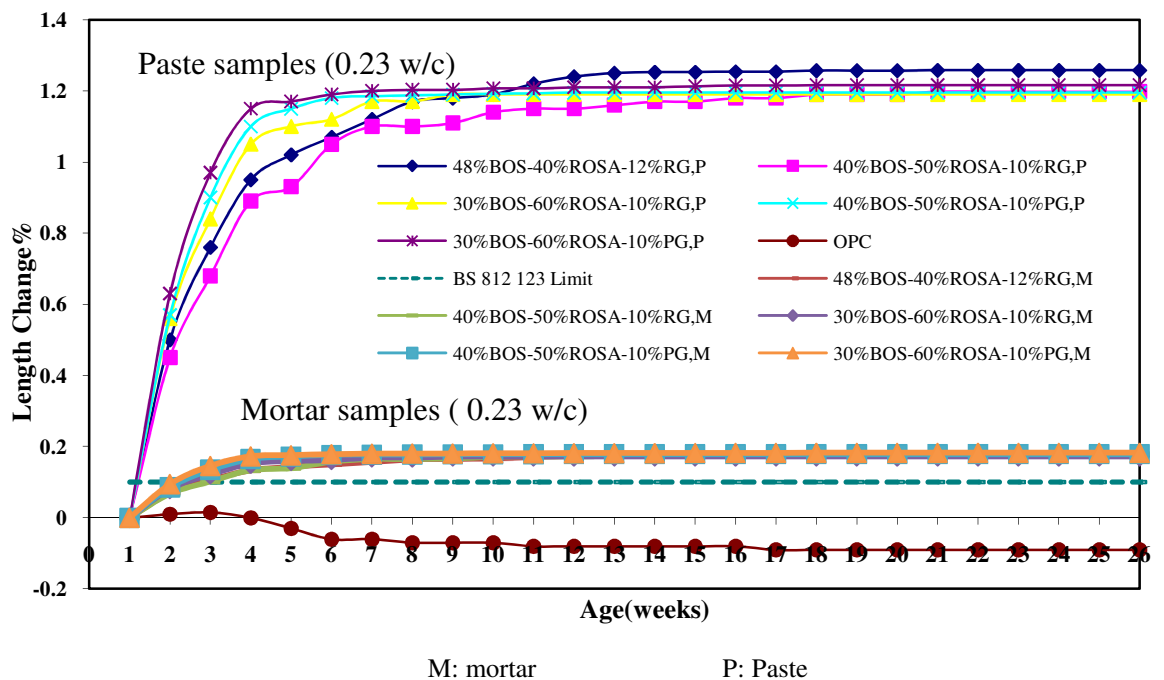


Figure 4- 26 Length Change of Selected Paste and Mortar Samples at different ages

From Figure 4-26, it can be seen that the OPC sample shrank from week 4 to week 6 and remained the same length at early age. Other samples exceeded the limit of expansion that is indicated in BS 812 123. The reason of expansion could

be because of ettringite formation and the high MgO content of BOS might responsible for increased expansion in BOS samples.

The expansion of mortar samples was around 15% of the paste samples (Ganjan *et al.* 2007) and it was used as a coefficient for pastes' expansion. However their expansion was still more than the BS limit.

4.6.4 X-Ray Diffraction Analysis

The results of XRD test showed the existence of four minerals which were effected in compressive strength.

Figures 4-27 to 4-29 shows the XRD results of paste BOS48%-ROSA40%-RG12% at 3, 7 and 28 days.

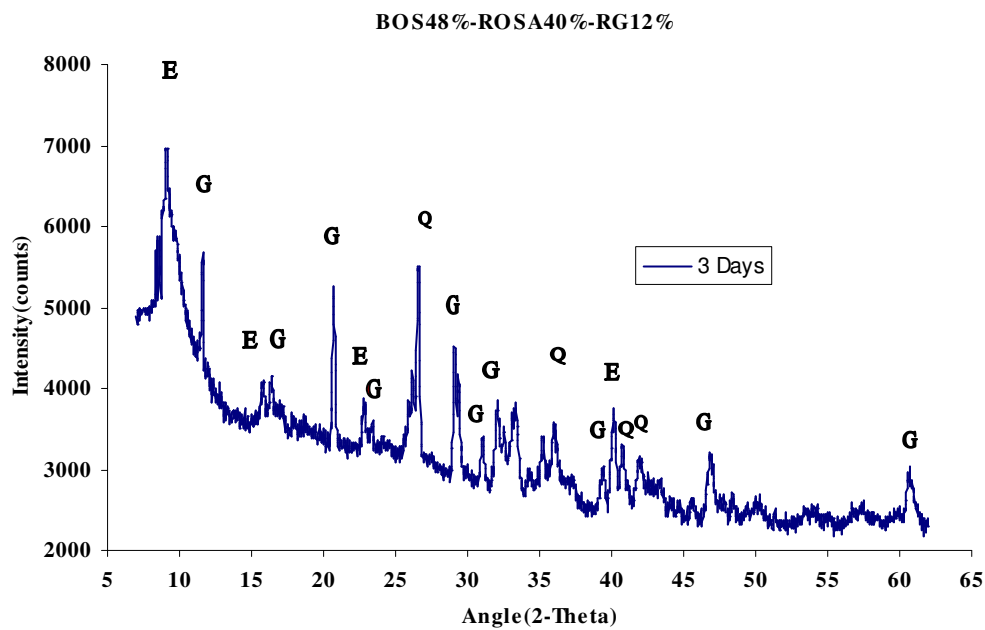


Figure 4- 27 XRD of BOS-ROSA-RG at 3 days-E=Ettringite, G=Gypsum, Q=Quartz

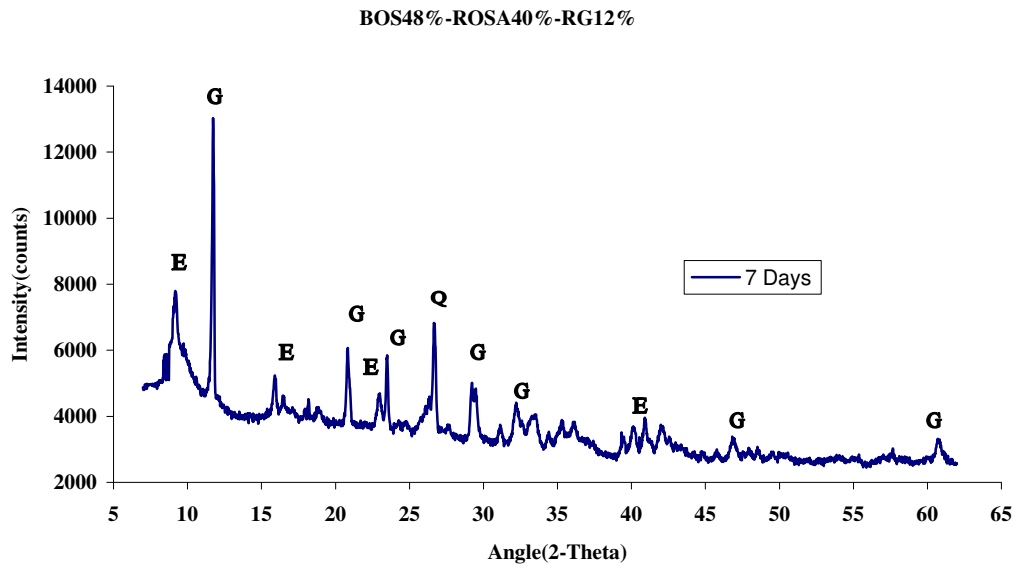


Figure 4- 28 XRD of BOS-ROSA-RG at 7 days-E=Ettringite, G=Gypsum, Q=Quartz

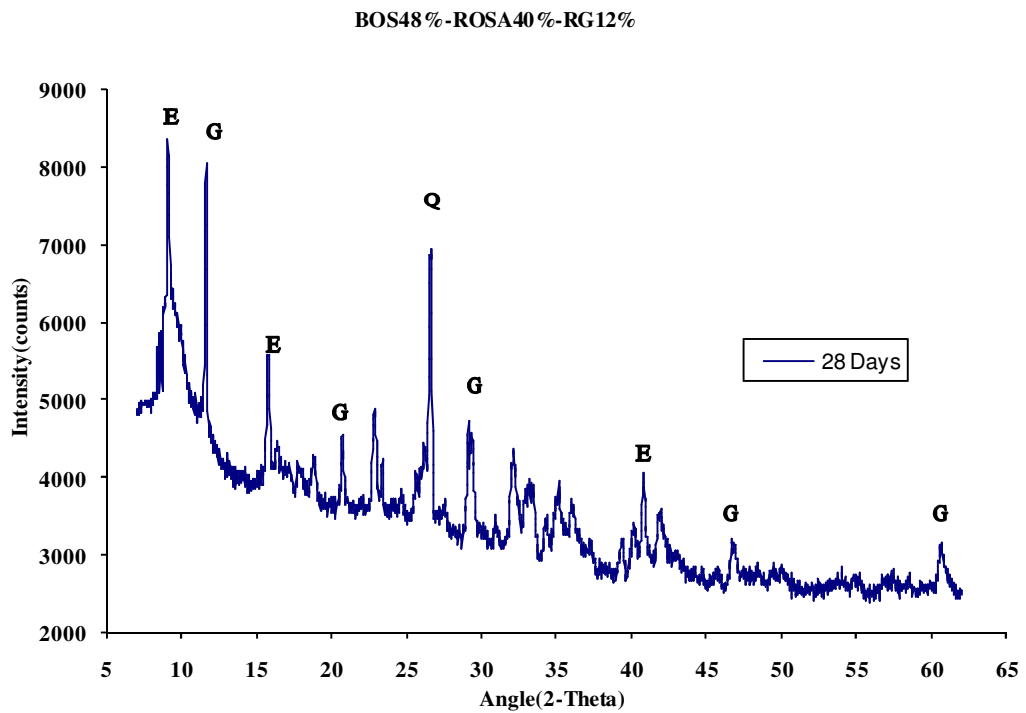
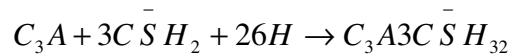


Figure 4- 29 XRD of BOS-ROSA-RG at 28 days-E=Ettringite, G=Gypsum, Q=Quartz

The initial reaction between gypsum and C₃A is:



The product name is calcium sulphoaluminate that is also known as ettringite. Ettringite reaction is much slower than C₃A alone. The ettringite is gradually transformed to calcium mono sulphoaluminate that has lower sulphate content. The formation of ettringite can accelerate the pozzolanic reaction of ROSA that could improve both early and late strength of the mixes (Min *et al.* 2008).

Gypsum was also formed in all samples and that contributed to early strength. From Figures 4-27 to 4-29 it can be seen that the peak associated with ettringite after 3 days, compare to 7 and 28 days, corresponding lower strength of paste in that age. The initial setting and early age strength is related to the formation of ettringite as a result of reaction between aluminium and calcium dissolved from BOS and with sulphate from gypsum (Ganjian *et al.* 2007) The ettringite prevents Portland cement from setting quickly and with time is replaced by calcium monosulfoaluminateb (John *et al.* 1998).

At later age, in all five samples, more ettringite was found in the mixture and higher strength was also achieved in later age (7 and 28 days). The XRD of all samples in every ages shows the growth of ettringite as time progressed giving peaks at 9.096 °, 15.79 ° and 17.83 ° on 2θ and the strongest intensity was measured at 9.096°.

XRD results for other mixes are in appendix B.

4.6.5 Permeability (High Pressure Flow Test) and ICP

Samples of the selected pastes were made using cylindrical moulds for the high pressure flow test. The coefficient of permeability of laboratory pastes was measured using the high pressure through flow test. Table 4-26 presents the results of permeability test.

An OPC sample was made as a control paste for comparison. w/c in all mixes were 0.23 and it was 0.5 in OPC mix.

Table 4- 26 Permeability of samples

Mix	Coefficient of Permeability (m/s)
OPC Sample	6.03E-10
48%BOS-40%ROSA-12%RG	6.22E-10
40%BOS-50%ROSA-10%RG	7.72E-10
30%BOS-60%ROSA-10%RG	6.91E-10
40%BOS-50%ROSA-10%PG	6.28E-10
30%BOS-60%ROSA-10%PG	6.90E-10

Pastes with RG had greater coefficient than PG pastes with the same amount of BOS-ROSA.

All pastes had bigger coefficient than the OPC because of the strength (37 Mpa). Sample solutions were collected from the specimens tested and analysed using Inductive Coupled Plasma (ICP). The results of chemical analysis of solutions are presented in table 4-27.

Table 4- 27 ICP analysis of solution from 5 selective mixes

Element	48BOS- 40ROSA- 12RG	40BOS- 50ROSA- 10RG	40BOS- 50ROSA- 10PG	30BOS- 60ROSA- 10RG	30BOS- 60ROSA- 10PG	Control Mix OPC
Na	297.6	23.4	47.2	245.2	115.3	43.3
Mg	<1.0	<1.0	<1.0	<1.0	<1.0	<0.1
Al	<0.1	<0.1	<0.1	<0.1	<0.1	<0.1
Ba	<0.1	<0.1	<0.1	<0.1	<0.1	<0.1
Ca	276.0	589.5	522.0	598.9	560.2	154.0
K	448.9	140.5	110.6	398.8	230.6	35.1
Cr	<0.1	<0.1	<0.1	<0.1	<0.1	<0.1
Ni	<0.1	<0.1	<0.1	<0.1	<0.1	<0.1
Pb	<0.1	<0.1	<0.1	<0.1	<0.1	<0.1
S	137.1	127.4	124.8	184.0	159.0	14.5
Si	27.3	3.8	5.8	6.3	3.5	<0.1
Sr	<1.0	<1.0	<1.0	<1.0	<1.0	<0.1
P	<1.0	<1.0	<1.0	<1.0	<1.0	<0.2

From Table 4-27, it can be seen that no heavy metal elements leached from samples.

Also, the concentration of Potassium was higher than OPC in all samples; that could be because of K₂O in PG and RG.

4.6.6 Water absorption

Water absorption testing for samples was done according to BS EN 771-4:2003 and the results of the test are presented in table 4-28.

Table 4- 28 Water absorption of pastes

Mixes	Weight Before soaking(g)	Weight After Soaking(g)	Weight gain %	Compressive Strength (MPa) before soaking	Compressive Strength (MPa) after soaking	Compressive strength loss %
48% BOS-						
40% ROSA- 12% RG	234.3	239.0	2.0	17.6	16.3	7.4
40% BOS-						
50% ROSA- 10% RG	232.3	236.1	1.6	19.3	17.4	9.8
30% BOS-						
60% ROSA- 10% RG	232.7	237.5	2.1	18.9	17.3	8.5
40% BOS-						
50% ROSA- 10% PG	226.0	228.0	0.9	18.8	17.5	6.9
30% BOS-						
60% ROSA- 10% PG	232.7	232.8	<0.1	18.6	17.2	7.5

The compressive strength of all pastes was reduced after soaking in water. **The reason was the unsoaked samples were harder and soaking made samples softer.** Samples absorbed water in soaking conditions (2% maximum weight gain).

4.7 Concrete Samples

4.7.1 Viscosity

The viscosity of the selected mixes from step 2 is shown in Figure 4-30. The viscosity of mixes using plasterboard gypsum is around twice that of mixes using red gypsum.

Table 4- 29 Flow of concrete samples

Mixes	Binder kg/m ³	Water (kg/m ³)	w/c	Coarse Agg (kg/m ³)	Fine Agg (kg/m ³)	Slump (mm)	Density kg/m ³	Concrete 28 day compressive strength (MPa)
OPC control mix	360	180	0.5	1240	620	75	2400	23.0
48%BOS- 40%ROSA- 12%RG	360	180	0.5	1240	620	190	2400	7.8
40%BOS- 50%ROSA- 10%RG	360	180	0.5	1240	620	189	2400	6.5
30%BOS- 60%ROSA- 10%RG	360	180	0.5	1240	620	193	2400	6.4
40%BOS- 50%ROSA- 10%PG	360	180	0.5	1240	620	195	2400	6.7
30%BOS- 60%ROSA- 10%PG	360	180	0.5	1240	620	193	2400	7.0

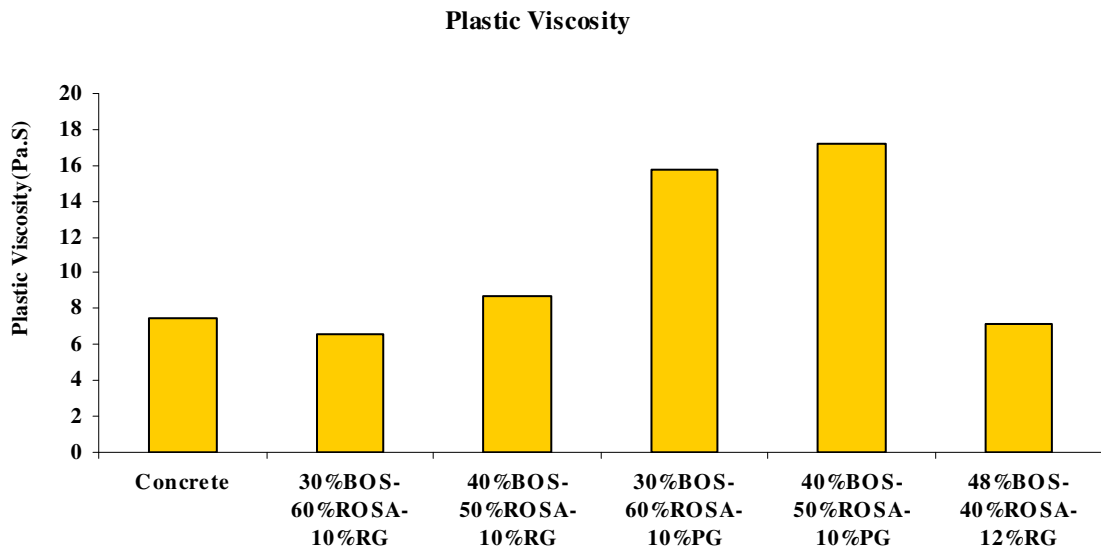


Figure 4- 30 Viscosity of cement replacement concrete and control mix

4.7.2 Freeze Thaw and Wet/Dry Testing

All samples failed to resist the freeze-thaw cycles. The samples were damaged and destroyed in the first 10 freeze-thaw cycles. Figures 4-31 and 4-32 show the condition of the samples under the freeze and thaw cycles.



Figure 4- 31 Sample BOS 30%-ROSA 60%-RG 10% burst after 10 freeze-thaw cycles



Figure 4- 32 Sample BOS 30%-ROSA 60%-PG10% burst after 10 freeze-thaw cycles

5. Data Analysis and Mathematical Modelling

5.1 Introduction

Casting all combinations of raw materials was not possible due to the time consuming and shortage of space. To have better understanding about the compressive strength of unmade pastes, two prediction models are used in this chapter. These two models will predict the 28 day compressive strength of the ternary combinations of the raw materials.

The Response Surface Method (RSM) and Artificial Neural Networks (ANN) were used for prediction of compressive strength of pastes. These two methods were found to be the most appropriate methods for analysing the data of this research and they were recommended by the literature and by the mathematical department of Coventry University.

According to literatures, during recent decades much effort has been directed towards finding efficient statistical methods for reliable analysis of experimental results. Response Surface and Artificial Neural Network techniques are the two recent approaches for solving complex problems.

RSM: The Response Surface Method is considered to be one of the most widely used methods in data analysis. RSM provides important applications in the design, development and formulation of new products, as well as in the improvement of existing product designs (Montgomery 2005).

RSM has been used to optimise products in chemical (biochemical processes) (Bas and Boyaci 2007), manufacturing (Nikolaidis *et al.* 2000) and other industries. But

its use has been limited in the concrete and cement industry and modelling compressive strength of molasses-cement sand system (Mandal and Roy 2006).

ANN: In a research programme experiments are conducted at predetermined levels and, based on analysis of variance, models developed are validated. Modification of the statistical model by incorporating new random data is not feasible. This limitation can be addressed effectively with the artificial neural networks (ANN). Neural networks can be trained effectively with random data in the solution space, and new data can be used at any stage to refine the model further.

Both methods were used for data analysis and prediction of 28 day compressive strength of pastes of ternary combinations. Using results from step 1 and step 2 (binary and ternary) produced unreasonable errors in prediction modelling with RSM. But using only the data of ternary mixes the compressive strength was estimated with lower error. This might be because each material had chemical reactions with other material and the results from binary and ternary blends made conflicts in modelling. The comparison of using data from binary and ternary mixing in the model and using only ternary mixes for prediction is shown in appendix C.

75 results used for ANN and RSM were only the data from ternary mixes to make the results comparable.

5.2 Response Surface Method

5.2.1 Introduction

The Response Surface Methodology (RSM) is a collection of statistical and mathematical techniques that is useful for analysis and modelling of problems. A response is influenced by several variables and the objective of the method is to minimize this response (Montgomery 2005).

In this section a brief of background of mixture design and the results for 7 groups of pastes is provided. The effect of each component on 28 day compressive strength of pastes has been analysed.

5.2.2 Mixture Design

Mixture experiments are a special class of response surface design in which the product under investigation is made up of several components or ingredients and the factors are the components or ingredients of a mixture. Consequently their levels are not independent. In another word, if x_1, x_2, \dots, x_p denote the proportions of p components of a mixture, then

$$0 \leq x_i \leq 1 \quad i=1,2,\dots,p \quad \text{Equation 5- 1}$$

And

$$x_1 + x_2 + \dots + x_p = 1 \quad (\text{i.e., 100 percent}) \quad \text{Equation 5- 2}$$

(Montgomery 2005)

For three-component mixtures, the mixture space is a triangle with vertices corresponding to formulations that are pure blends (mixture that is 100% of a single component).

In mixtures considered in this research, constraints on the individual components arise. Lower and upper bound constraints of the form

$$l_i \leq x_i \leq u_i \quad i=1, 2, \dots, p \quad \text{Equation 5- 3}$$

are fairly common (Montgomery 2005).

To correlate the effects of the variables and the response factor the standards forms of the mixture model that normally used are:

Linear: $E(y) = \sum \beta_i x_i \quad i=1,2,\dots,p \quad \text{Equation 5- 4}$

Quadratic: $E(y) = \sum \beta_i x_i + \sum \sum \beta_{ij} x_i x_j \quad i=1,2,\dots,p, i < j \quad \text{Equation 5- 5}$

Full Cubic:

$$E(y) = \sum \beta_i x_i + \sum \sum \beta_{ij} x_i x_j \quad i < j < k \quad \text{Equation 5- 6}$$

$$+ \sum \sum \delta_{ij} x_i x_j (x_i - x_j) + \sum \sum \sum \beta_{ijk} x_i x_j x_k$$

Special Cubic:

$$E(y) = \sum \beta_i x_i + \sum \sum \beta_{ij} x_i x_j \quad i < j < k \quad \text{Equation 5- 7}$$

$$+ \sum \sum \sum \beta_{ijk} x_i x_j x_k$$

In above equations, the parameter β_i presents the expected response to the pure blend $x_{i=1}$ and $x_{i=0}$ when $j \neq i$. The portion $\sum \beta_i x_i$ is called the linear blending portion.

A Quadratic polynomials model has been used in this research for the response surface because it gives better results in prediction than linear and the linear model is only valid in the absence of interaction effects between components. Quadratic models have been used in previous studies had reasonable results in prediction (Gomes *et al.* 2004 and Mandal 2006).

Cubic models are complex and it was not possible to derive the most efficient design. Mixture points lie within the equilateral triangle as a mixture space with the name of simplex design (Montgomery 2005). Figure 5-1 shows this triangle.

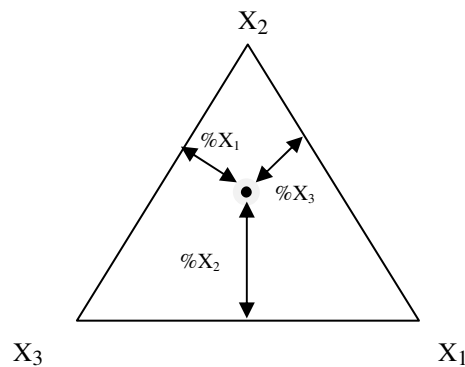


Figure 5- 1 Simplex Design diagram

The main aim of this section is to predict the 28 day compressive strength of ternary combinations by using experimental data. For this purpose, the quadratic form was chosen to develop the model of different combinations of RG, PG, BOS, BPD, and ROSA.

Since, each mix is a combination of three waste materials; the design had been done for the following ternary groups shown in figure 5-2:

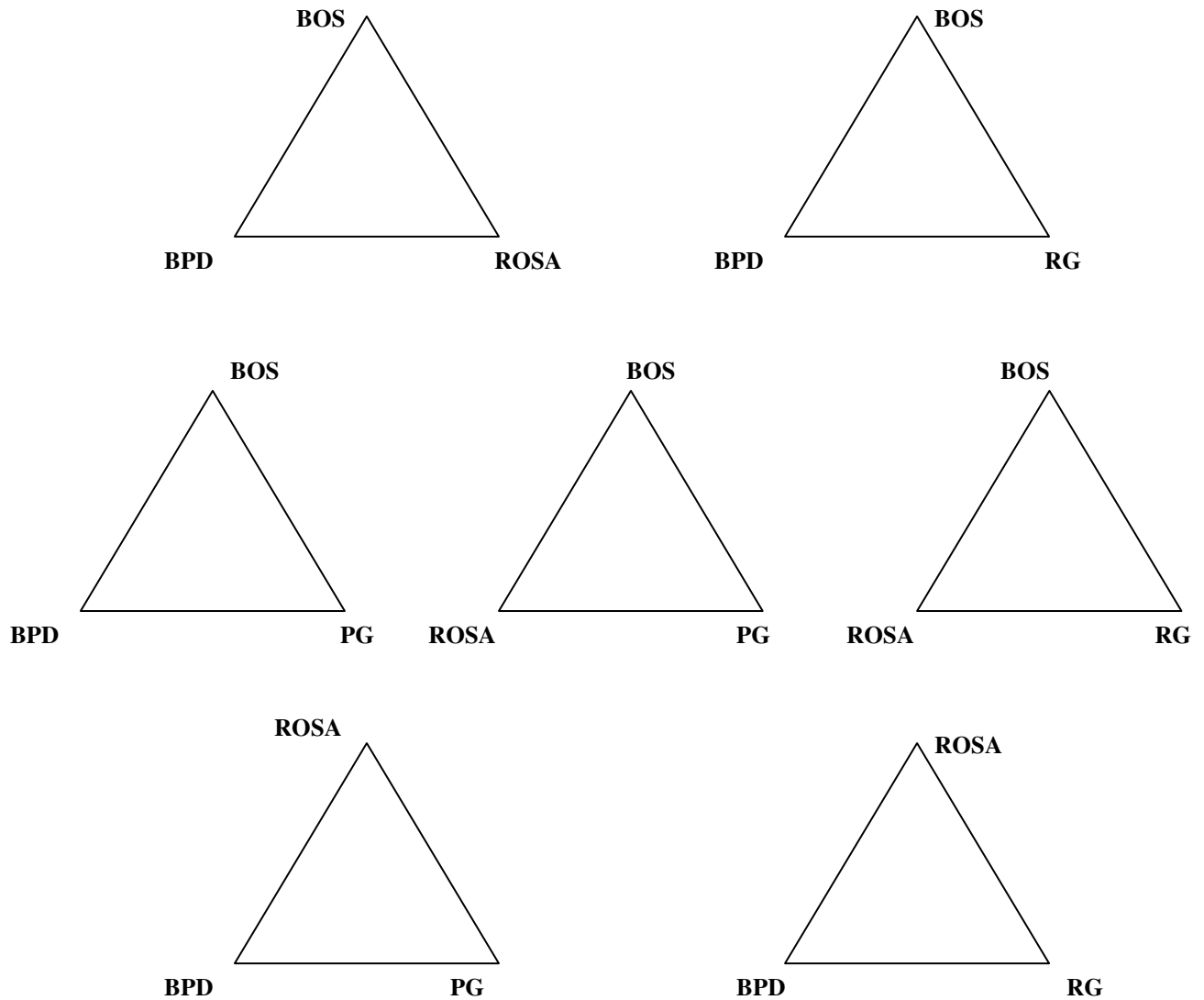


Figure 5- 2 Different groups of mixes in Step 2

Mixes for each group were analysed using MINITAB 14 software. This software has a special section for mixture design.

The quadratic model was used for prediction of results. Then the material content and the 28 day compressive strength of experimental mixes were analysed. The results and outputs from the software are presented in this section and appendix C of this report.

5.2.3 Results of Mixture Design and Regression

Mix design and mixture contour plots were drawn using MINITAB 14 software and are presented in this chapter. A Prediction model as a quadratic equation has been produced for each group and is presented separately for each group of mixing. The amount of error has been calculated for every mix.

$$Error\% = \frac{ABS (experimental\ CS - estimated\ CS)}{(experimental\ CS * 100)} \quad \text{Equation 5- 8}$$

Where:

CS=28 day Compressive Strength

The data analysis and model for the BOS-ROSA-BPD combination is presented in this chapter. Other group mixture analysis and prediction models are presented in Appendix C.

BOS-ROSA-BPD

Table 5- 1 BOS-ROSA-BPD mixture design and compressive strength at 28 days (laboratory data)

Mix No	BOS	ROSA	BPD	28 days CS (MPa)
1	76	19	5	8.7
2	72	18	10	8.2
3	48	12	40	5.7
4	32	8	60	4.5
5	35	55	10	15
6	27	68	5	8.2
7	30	30	40	10
8	15	80	5	8
9	18	10	72	6.3
10	16	20	64	8.2
11	12	40	48	12.5
12	8	60	32	18.5

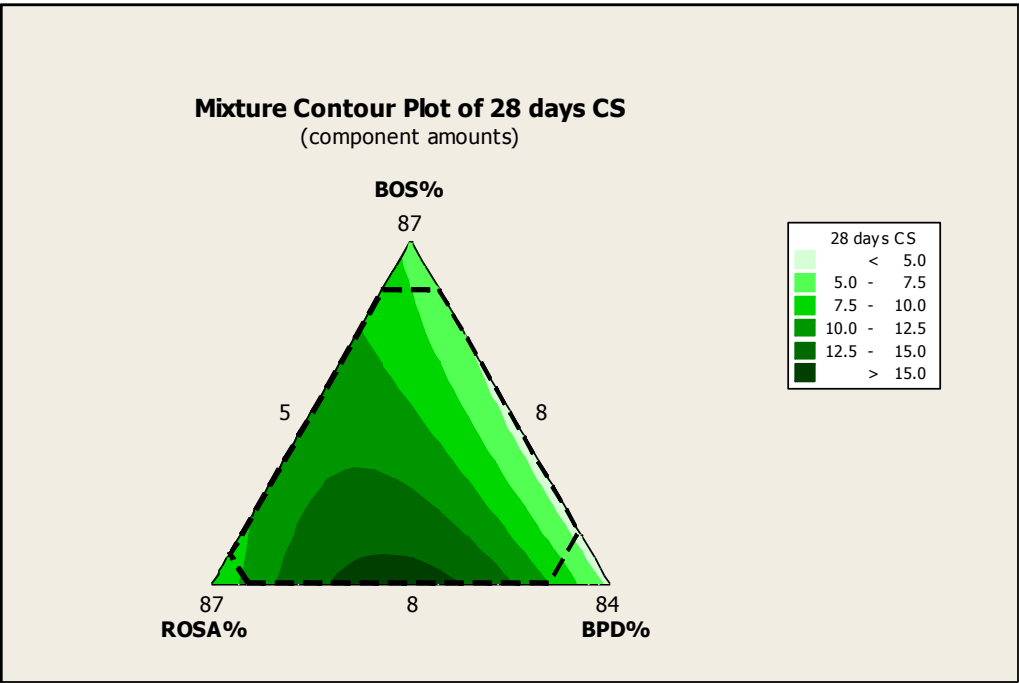
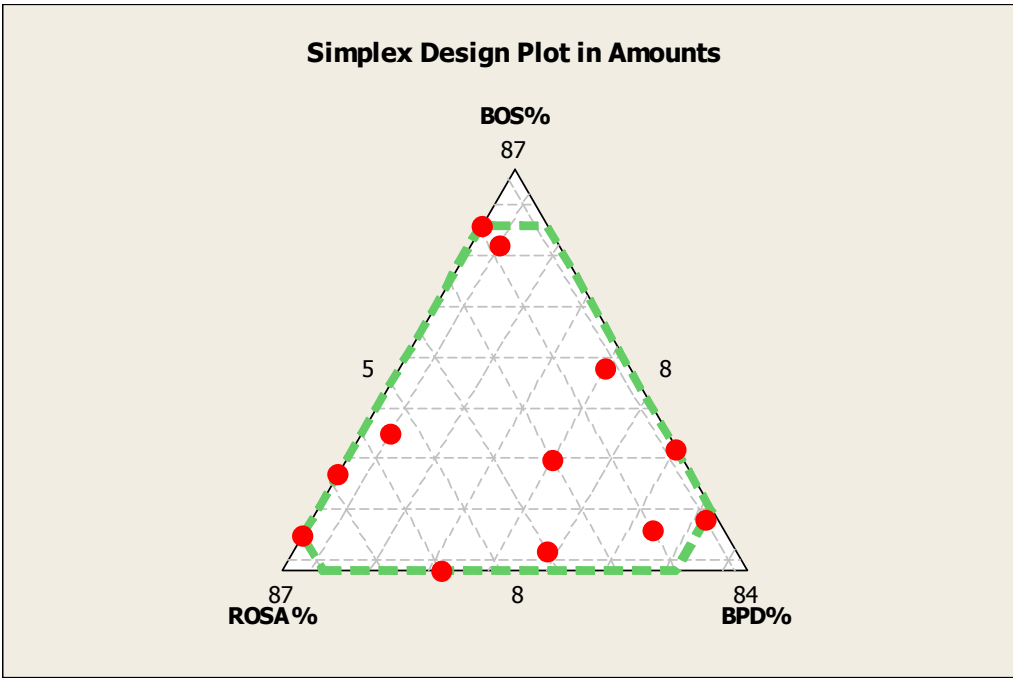


Figure 5- 3 Mixture Design Plot and Mixture Contour Plot For Mix BOS-ROSA-BPD

Quadratic model Coefficients using MINITAB 14:

Equation 5- 9

$$CS=0.055*BOS+0.03*ROSA+(-0.0045)*BPD+0.0026*BOS*ROSA+(-8.7*E-4)*BOS*BPD+0.0065*ROSA*BPD$$

Table 5- 2 Predicted Response for New Design Points Using Model for 28 days

Mix No	BOS	ROSA	BPD	28 days CS (MPa)	Predicted Compressive Strength (Mpa)	Error%
1	76	19	5	8.7	8.8	1.4
2	72	18	10	8.2	8.4	1.7
3	48	12	40	5.7	5.8	1.2
4	32	8	60	4.5	3.8	14.7
5	35	55	10	15.0	11.8	21.6
6	27	68	5	8.2	10.3	26.0
7	30	30	40	10.0	11.4	14.2
8	15	80	5	8.0	8.8	10.2
9	18	10	72	6.3	5.0	21.1
10	16	20	64	8.2	9.4	14.3
11	12	40	48	12.5	14.8	18.4
12	8	60	32	18.5	15.5	16.1
Test Data	64	16	20	7.2	7.6	5.6
Test Data	50	45	5	11.1	11.2	1.1

Figure 5-4 shows the experimental compressive strength and predicted compressive strength at 28 days and the error as percentage. The average error was 9% for this group\of ternary combination.

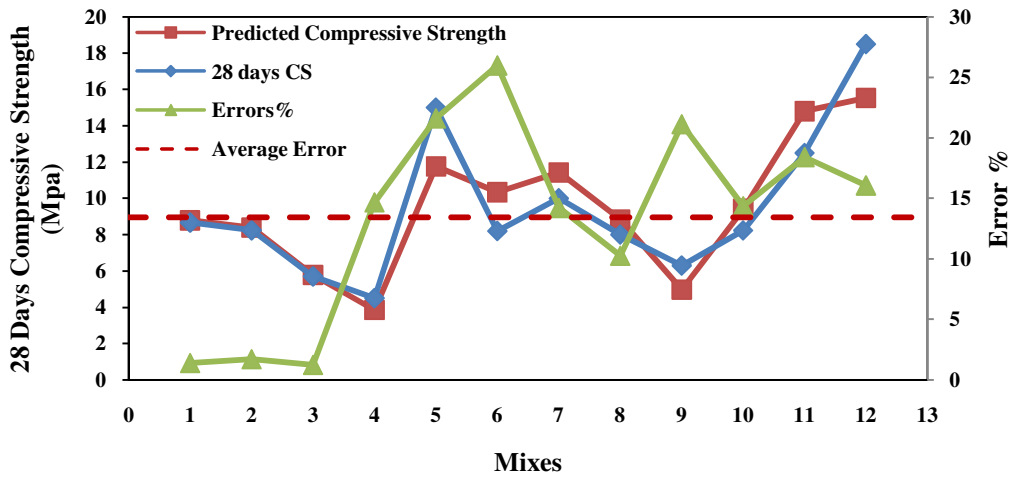


Figure 5- 4 Comparison between Predicted and Experimental 28 days Compressive strength for BOS-ROSA-BPD Group

5.3 Using Artificial Neural Network for Prediction

5.3.1 Introduction

An artificial neural network (ANN), often just called a "neural network" (NN), is a mathematical model or computational model based on biological neural networks. It consists of an interconnected group of artificial neurons and processes information using a connectionist approach to computation. In most cases an ANN is an adaptive system that changes its structure based on external or internal information that flows through the network during the learning phase (Tarassenko 1998).

Neural Networks can't solve every problem. Sometimes traditional mathematical methods may have better results. However, most neural networks, when they are used wisely, perform at least as well as the most appropriate traditional methods and they are significantly better in some other cases (Tarassenko 1998).

The success in the results of a neural network depends on knowledge about the problem and the network architecture and the training of the neural network.

An elementary neuron with n inputs is shown in figure 5-5. Each input is weighted with an appropriate weight w . The sum of the weighted inputs and the bias forms the

input to the transfer function f . Neurons can use any differentiable transfer function f to generate their output.

To have better understanding of neural network expressions, they have been summarised in Appendix C in alphabetic order.

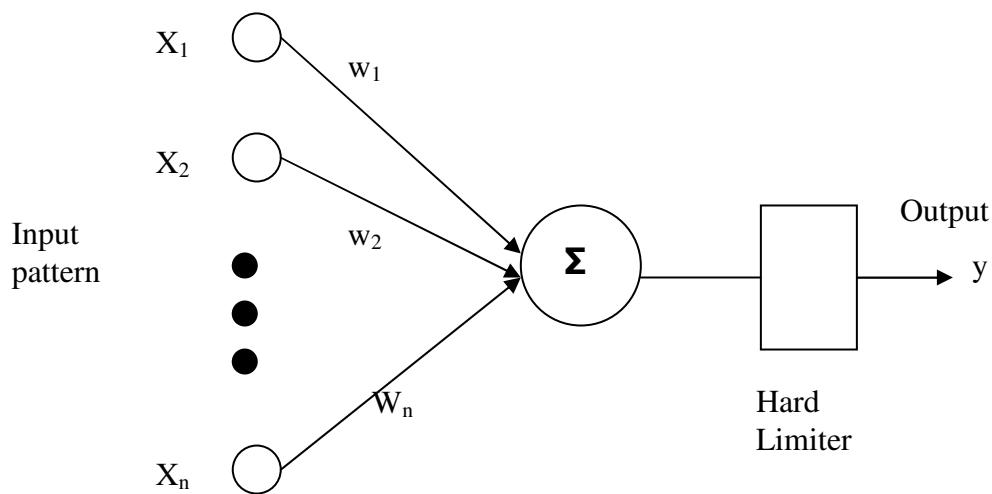


Figure 5- 5 Schematic diagram of an artificial neuron

The neurons that are input patterns, represented by the vector of numbers $x=(x_1, x_2, \dots, x_n)$ (Tarassenko 1998).

$$y=f_h(\sum_{i=1}^n w_i x_i) \qquad \text{Equation 5- 10}$$

Where y is the neuron output (± 1) and f_h is a hard limiting or threshold function and known as the neuron's activation function. When $\sum w_i x_i$ is greater than zero the output would be +1 and if $\sum w_i x_i$ is less than or equal to zero the activation function gives -1 output (Tarassenko 1998).

Learning consists of adjusting w_i weights and the neuron performs the classification task as close as possible to it. The word "learning" may cause misleading the idea of a strong association with the process of human, or animal learning. Learning is the minimisation of a cost function, such as the mean square error at the output(s) (Tarassenko 1998).

5.3.2 Error Minimisation

To minimise the error for solving the problem, Tarassenko (1998) used error feedback to adjust the weights during training. This is to measure an error E at the network output and minimise it by gradient of descent. Therefore the gradient of the error for weight w_i is $\partial E/\partial w_i$.

The change in weight from the current weight to the new weight is given by:

$$\Delta w_i = -\eta \partial E/\partial w_i \quad \text{Equation 5- 11}$$

Where η is a small parameter which sets the step size (usually called learning rate). If η is too large, then error correction process can overshoot and divergent oscillation may occur. If it is too low, then the weights take a very long time to converge.

5.4 Neural Network Model and Parameters

An Artificial Neural Network (ANN) model for predicting the compressive strength of waste binder mixes using five different raw materials (BOS, BPD, ROSA, PG, and RG) has been developed.

The training of the network performed using 75 experimental data sets for training set and 8 data for validation and test set. These data have been selected and normalised from the experiments that are shown in appendix C.

The back-propagation algorithm was used to develop the neural Network. The term backpropagation refers to the manner in which the gradient is computed for nonlinear multilayer networks. It is widely used as a learning algorithm in feed-forward multilayer neural networks and it is applied to feed-forward ANNs with one or more than one hidden layer.

Based on this algorithm, the network learns a distributed associative map between the input and output layers (Mandal and Roy 2006). The network is trained by repeatedly using a set of input-target data. The network learns the relationship between the input and target data by adjusting the weights to minimize the error between the input and target values. The major advantages of BPNN over the regression technique are (Mandal and Roy 2006):

- “no mathematical model is required;
- capable of modelling highly non-linear relationships;
- capable of using dispersed data in the solution domain;
- Existing models can be refined using new data sets easily through training.”

In spite of the advantages it has over the regression models, there are a number of drawbacks. Some of them are:

- No theoretical basis exists to determine the number of hidden layers and number of neurons therein.
- Different configurations of BPNN have great effects on the predicted results.
- Scaling of the data to suit the non-linearity function (usually sigmoid) has a great effect on predicted results.

Back-propagation networks were constructed and trained using the neural network toolbox of the software package MATLAB 6.1.

5.4.1 Architecture:

This section explains the architecture of the network most commonly used with the backpropagation algorithm-the multilayer feedforward network.

5.4.2 Neuron Model:

The most popular function that has been used in simulation is the sigmoid function. The Sigmoid function works as follows (Demuth *et al.* 2006):

$$F(\text{net}_j) = 1/(1 + e^{-\text{net}_j})$$

$$\text{net}_j = \sum_i W_{ji} a_i$$

Equation 5- 12

Where:

w_{ij} = weights of each neuron

The sigmoid transfer function shown below takes the input, which can have any value between plus and minus infinity, and squashes the output into the range 0 to 1. This transfer function is commonly used in backpropagation networks, in part because it is differentiable (Demuth *et al.* 2006).

The logsig transfer function is shown in Figure 5-6.

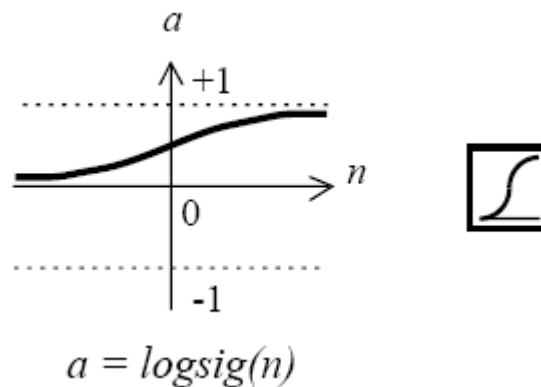


Figure 5- 6 log-Sigmoid Transfer Function

If the last layer of a multilayer network has sigmoid neurons, then the outputs of the network are limited to a small range. If linear output neurons are used the network outputs can take on any value.

In backpropagation it is important to be able to calculate the derivatives of any transfer functions used.

5.4.3 Feedforward Network

Feedforward networks often have one or more hidden layers of sigmoid neurons followed by an output layer of linear neurons. Multiple layers of neurons with non linear transfer functions allow the network to learn nonlinear and linear relationships between input and output vectors. The linear output layer lets the network produce values outside the range -1 to $+1$ (Demuth *et al.* 2006).

On the other hand, to constrain the outputs of a network the output layer should use a sigmoid transfer function.

All data should first be calculated from the training examples. The normalised value of x_i is then given by equation 5-13:

$$x_i^* = (x_i - x_{min}) / (x_{max} - x_{min}) \quad \text{Equation 5-13}$$

Once these transformation parameters have been computed, they are applied to all input patterns presented to the network, whether from the training, validation or test set, therefore all patterns would be in the same normalisation.

5.4.4 Training

The Network can be trained for function approximation (nonlinear regression), pattern association, or pattern classification. The training process requires a set of examples of proper network behaviour, network inputs and target outputs.

The Neural Network developed in this research has five neurons (variable percentage of raw materials) in the input layer and one neuron in output layer as illustrated.

There are generally four steps in training process (Demuth *et al.* 2006):

- Assemble the training data
- Create the network object
- Train the network
- Simulate the network response to new inputs

From the literature and trial and error, two hidden layers for the neural network were selected. The first hidden layer has 20 units and the second one has 21 units as illustrated in figure 5-7.

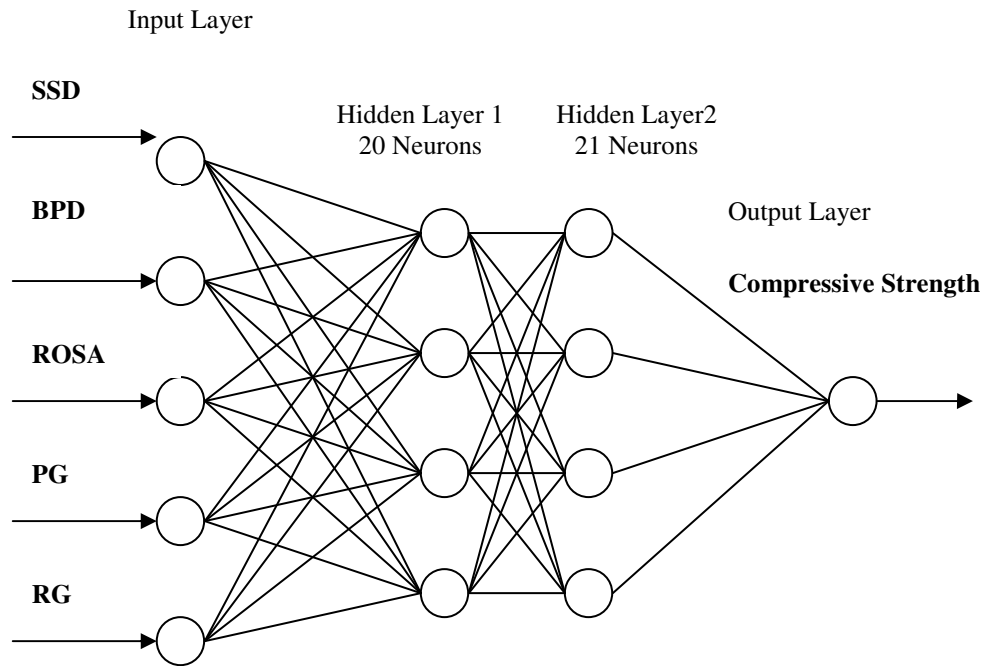


Figure 5- 7 Proposed NN model

5.4.5 Software and Transfer Function

The data simulation for this project was done by using MATLAB 6.1 software. The transfer function that was used in this thesis for simulation of the data was tan-sigmoid that is one of the MATLAB 6.1’s function data sets.

The configurations of the neural networks that were trained are given in Table 5-3. The input and target data are scaled within the range 0 to +1. The scaled values of the training sets are given in Appendix C.

Table 5- 3 The different ANN that used to train the data of BOS, BPD, RG, PG and ROSA in ternary mixes

Network	Number Inputs	Number of Epoch	Number of Hidden Layer	Number of Neurons in Layer 1	Number of Neurons in Layer 2	Number of Outputs	Average of Error in Validation Set
1-1	5	1000	2	20	21	1	17.10

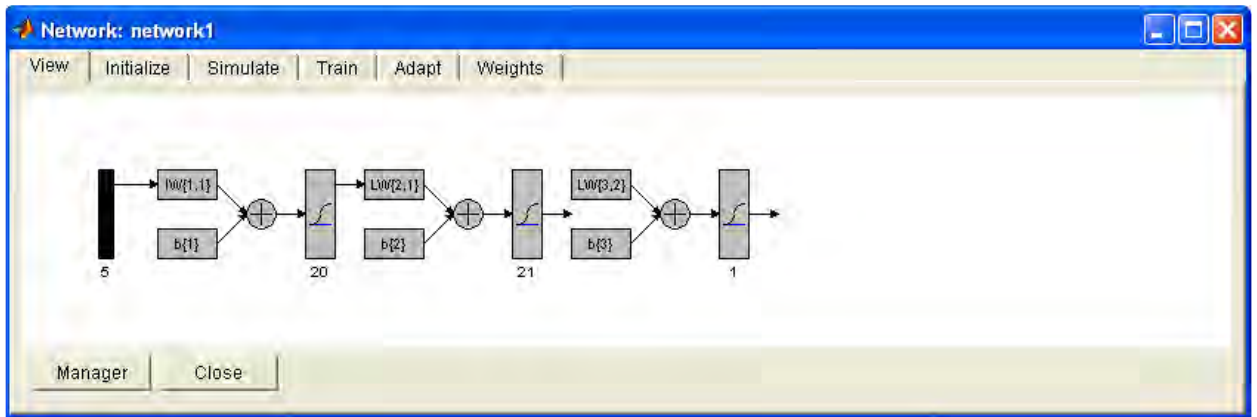


Figure 5- 8 Network summary as it was created by MATLAB 6.1 software

5.5 Analysis of Results

Results of estimation with neural network model from the learning set (75 results from step 2) are given in Figure 5-9.

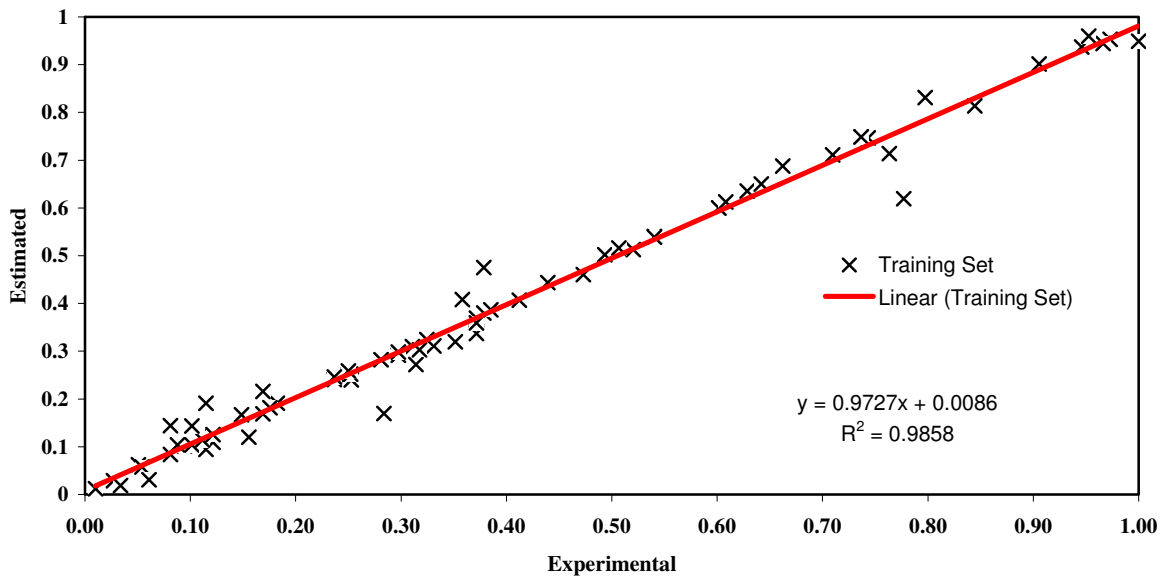


Figure 5- 9 Performance Of training set of 80 paste design data.

Results from 8 experimental mixes were selected for testing the neural network. Table 5-4 shows the selected mixes for used test set.

Table 5- 4 Test set data (10 pastes) for prediction model

BOS%	ROSA%	BPD%	RG%	PG%	28 days CS (MPa)	28 Days CS (MPa) predicted by ANN	Error%
50	45	5	0	0	0.45	0.46	4.45
76	0	5	0	19	0.41	0.33	18.82
48	40	0	12	0	0.89	0.58	34.33
0	65	15	20	0	0.32	0.34	7.88
0	76	15	0	9	0.91	0.77	15.42
64	16	20	0	0	0.18	0.17	3.74
68	0	17	15	0	0.09	0.04	49.57
64	20	0	0	16	0.47	0.46	2.64

Figure 5-10 shows that the neural network in this research was capable of generalizing between variables (materials) and outputs (compressive strength) and it made good predictions.

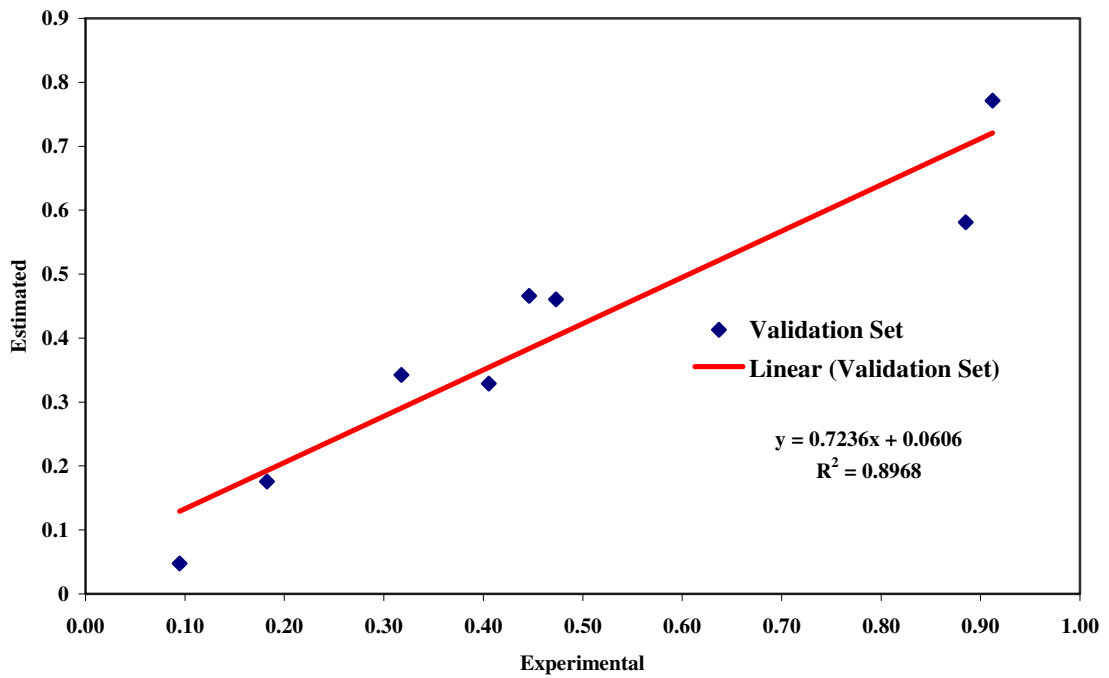


Figure 5- 10 Performance Of test set of 10 paste design data

5.6 Discussion and Conclusions

Data analysis and prediction modelling was done in this chapter for ternary mixes of 7 different groups.

Although numerical optimisation along with graphical analysis can provide useful information, it is not a substitute for subject matter expertise. Therefore, it is necessary to use relevant background information, theoretical principles, and knowledge gained through observation or previous experimentation when applying these methods.

The prediction results from Artificial Neural Network had less error than RSM and were more accurate compared to the Response Surface results because it presents nonlinearities in a much better and reliable way. However, both techniques are often used for predicting optimum process conditions (Dutta *et al.* 2004).

The results of these two methods of prediction were not used for mix optimisation because the sources of waste materials were change and it changed the result of the compressive strength.

6. Field Trial Subway Backfilling in Coventry and Block Making

6.1 Introduction

A ternary combination of the raw materials 80% steel slag, 15% plasterboard gypsum and 5% bypass dust 50 tonnes which remained from the last trials of Coventry University (Ganjian *et al.* 2007) was chosen to be used in the subway backfilling. However the site trial was not carried out during the time of this project.

From the results of experiments of chapter 4, one of the mixes of the 5 selected mixes from the results of ternary combinations (48% BOS- 40% ROSA- 12% RG) was selected to be used in the light weight block making. The density of the mix was too high due to the BOS. A kind of foaming agent was used to reduce the density of the mix. Using foaming agent reduced the density and the compressive strength of the mix therefore BOS was replaced by ROSA and BPD. Therefore the mix from the ternary combinations of 60% ROSA- 20% PG or RG- 20% BPD was chosen to be used for the block trials (3 day compressive strength 1.6 MPa with the density 1600-1700 kg/m³).

Foam concrete is often used to backfill disused pedestrian subways. Since the foam concrete does not have high compressive strength, the novel cement, Coventry blend (80% BOS- 15% PG- 5% BPD) could be a suitable replacement and a feasible option to be used in subway backfilling. Jacobs Ltd., Coventry Council asked **Coventry University** to develop a concrete with the minimum 1.0 MPa compressive strength at 28 days. For this chapter the feasibility study of that project has been described.

Another idea for using waste materials was to make lightweight blocks with 100% Portland cement replacement. The main characteristic required for the block was gaining acceptable compressive strength at 3 days that could be moved without any damage to the edges and surfaces.

6.1.1 Material Preparations for subway backfilling

The slump of the concrete to be used for subway backfilling was required to be at least 100 mm.

Coventry blend was selected for subway backfilling because 50 tonnes of Coventry Blend were left over from the previous site trials (Ganjian *et al.* 2007). The blend had been prepared at the Ryder Point Processing Plant for a previous project in Coventry University. The blended powder consisted of 80% ground BOS, 15% ground PG and 5% BPD. The BOS and PG were dried before grinding. Both BOS and PG passed through a 500 µm mesh and then were blended with BPD. The plasterboard was supplied by Lafarge and contained paper. However, since the ground PG was sieved before blending, the majority of the paper was removed in the grinding and sieving process. The pre-blended powder was easy to use like ordinary cement without any further work or preparation.

The pre-blended mixture was mixed with coarse and fine aggregates for subway backfilling using a similar design as in Portland cement concrete.

The sieve analysis of fine and coarse aggregates is shown in Table 6-1 and Figure 6-1.

Table 6-1 Sieve Analysis of Coarse and Fine Aggregate

Coarse Aggregate					
ASTM	Mesh (mm)	Retain on sieve (gram)	% Retain	Sum of retain%	% pass
1/2"	19.1	0.0	0.0	0.0	100.0
	13.2	13.9	0.7	0.7	99.3
3/8"	9.5	364.6	18.2	18.9	81.1
No 4	4.8	1437.5	71.9	90.8	9.2
bottom		184.0	9.2	100.0	0.0
	Sum	2000.0	100		

Fine Aggregate					
ASTM	Mesh (mm)	Retain on sieve (gram)	% Retain	Sum of retain%	% pass
3/8"	9.5	0.0	0.0	0.0	100.0
4	5.0	18.1	1.2	1.2	98.8
8	2.4	174.8	11.7	12.9	87.1
16	1.2	114.4	7.6	20.5	79.5
30	0.6	223.5	14.9	35.4	64.6
50	0.3	748.0	49.9	85.3	14.7
100	0.2	164.1	10.9	96.2	3.8
bottom		57.1	3.8	100.0	0.0
	Sum	1500.0	100.0		

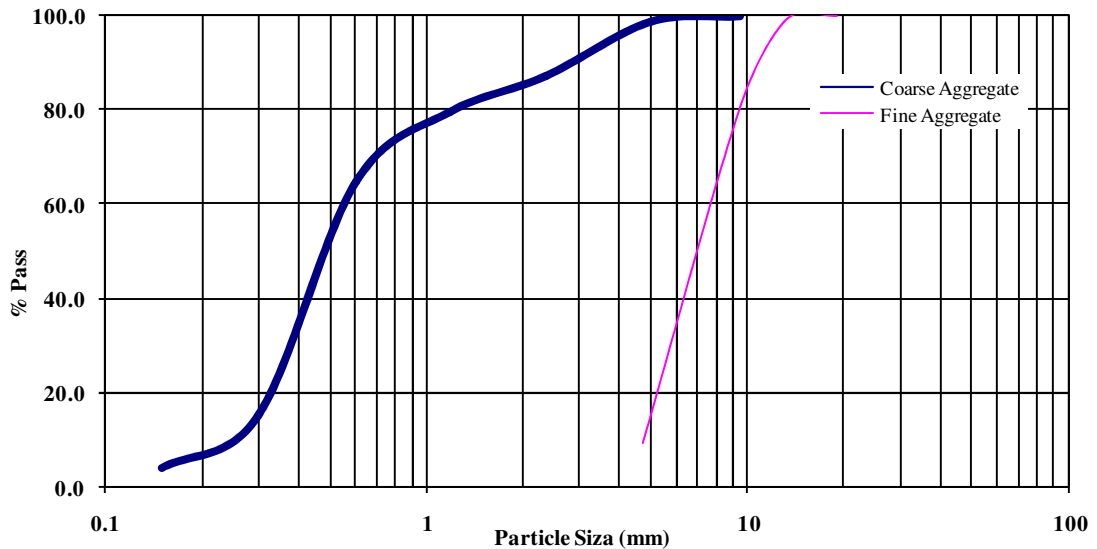


Figure 6-1 Sieve analysis of fine and coarse aggregate

The composition of the concrete is presented in Table 6-2.

Table 6-2 (Concrete) Mix Design using Coventry Novel Cement

Mix Proportions (Kg)		
Blended Novel Binder (Coventry Blend)	Fine Aggregate	Coarse Aggregate
400	300	900

Different w/c ratios were tried to find the appropriate slump as shown in Table 6-3.

Table 6- 3 Properties of Coventry concrete mix for subway backfilling

W/C	Slump (mm)	3 days CS MPa (50mm)	7 days CS MPa (50mm)	28 days CS MPa (50mm)	28 days CS MPa (100mm)
0.7	50	0.7	1.0	1.8	-
0.9	100	0.5	0.9	1.7	1.6
1.0	107	0.2	0.6	1.1	1.1

The third mix with w/c = 1 was selected because it satisfied the criteria for slump.

The stability of the Coventry mix concrete against shear strength was checked. The maximum shear strength was calculated for the wedges at the end of the subway. The calculations and the schematic plan of the concrete are shown in Table 6-4 and Figure 6-2.

Table 6-4Checking shear stress for subway ends

α°	x	$V(m^3)=X^3/2$	$M(kg) = 2000*V$	Stress (Mpa)
1	0.05	0.000	0.91	0.00003
2	0.11	0.002	3.66	0.00012
3	0.16	0.004	8.24	0.00027
4	0.21	0.007	14.70	0.00049
..
30	1.73	0.500	1000.00	0.00250
..
45	3.00	1.500	3000.00	0.00500
..
60	5.20	4.500	9000.00	0.00750
..
75	11.2	20.892	41784.61	0.00933

$\rho = 2000 \text{ kg/m}^3$

α = crack angle

X = the distance to the end of subway

V = volume of wedge concrete

M = weight of wedge concrete

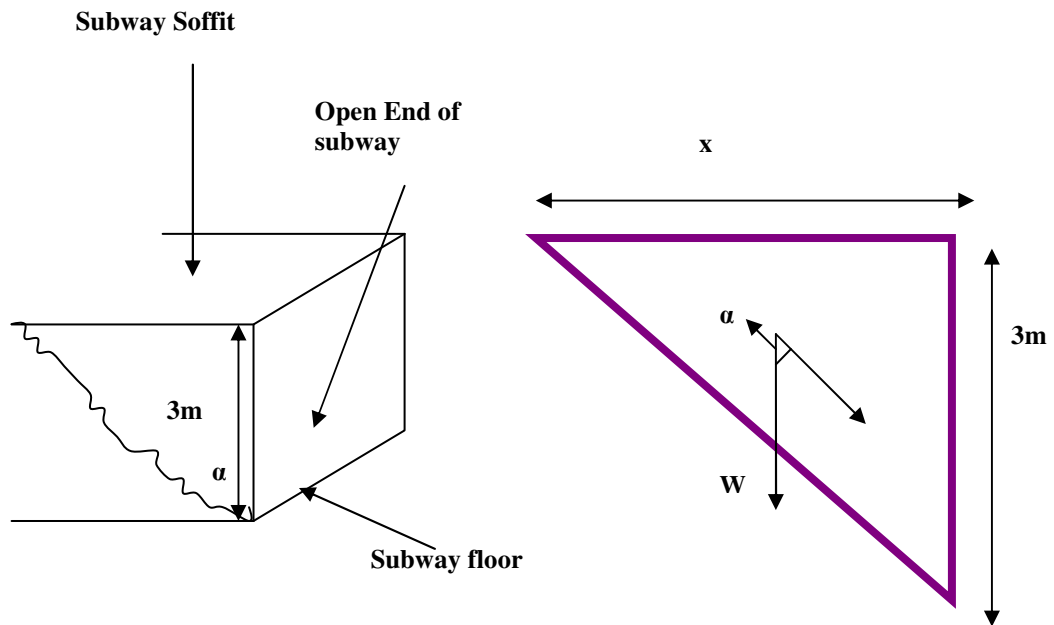


Figure 6- 2 Shear stress at the end of subway

Based on calculations, cracks would not occur at the edges, because the shear stress in the wedge was less than the concrete's shear stress during its early age when it was not fully hardened. This study showed that using Coventry novel cement in subway backfilling was a feasible option.

6.2 Light weight block

Light weight blocks can be used for non load-bearing purposes, such as in making curtain walls and partitions. Curtain walls and partitions should be light and have low sound transmission characteristics and durability. Only in the case of components forming load-bearing walls is strength the main criterion (Kumar, 2002).

Light weight block making from waste materials was one of the objectives of this research. The following two methods were used to find the lightest product with the highest compressive strength.

- Foaming Agent
- Light Weight Aggregate

Also, increasing water to binder ratio would cause the paste to have lower density and lower compressive strength.

Coventry blend could not be used for making light weight blocks because it contained a high amount of BOS (80%) which made it heavy. It also failed to meet the 3 days compressive strength requirements of at least 2.5 MPa. Therefore a lighter mix with higher compressive strength at 3 days was chosen for study.

6.2.1 Specification for blocks

Hanson Block Company asked for a product with a compressive strength of 2.5 MPa at 3 days. The product should have smooth surfaces with enough compressive strength with low density (1600 to 1700 kg/m³) to be easy to be moved in 3 days.

6.2.2 Mixes with BOS and Air entrainment

To make light weight block samples with these selected mixes a foaming agent was added to the mix. The results are shown in Table 6-5. The density of this mix before using foaming agent was 2045 Kg/m³.

Table 6-5 Sample (48%BOS-40%ROSA-12%RG) air entraining using different amount of Foaming Agent from Lafarge plasterboard

Foam Agent%(paste)	BOS	ROSA	RG	3 Day	7 Day	28 Day	Density(Kg/m ³)
0	48	40	12	0.93	3.23	17.6	2045
0.5	48	40	12	0.42	1.15	14.14	1680
1	48	40	12	0.38	1.04	12.6	1376
2	48	40	12	0.23	0.98	11.9	1432

The foaming agent was added to the water and then added to the mix to achieve better reaction on materials.

Figures 6-3 (a and b) shows the effect of three different percentage of foaming agent on the compressive strength and the density of 48%BOS-40%ROSA-12%RG mix.

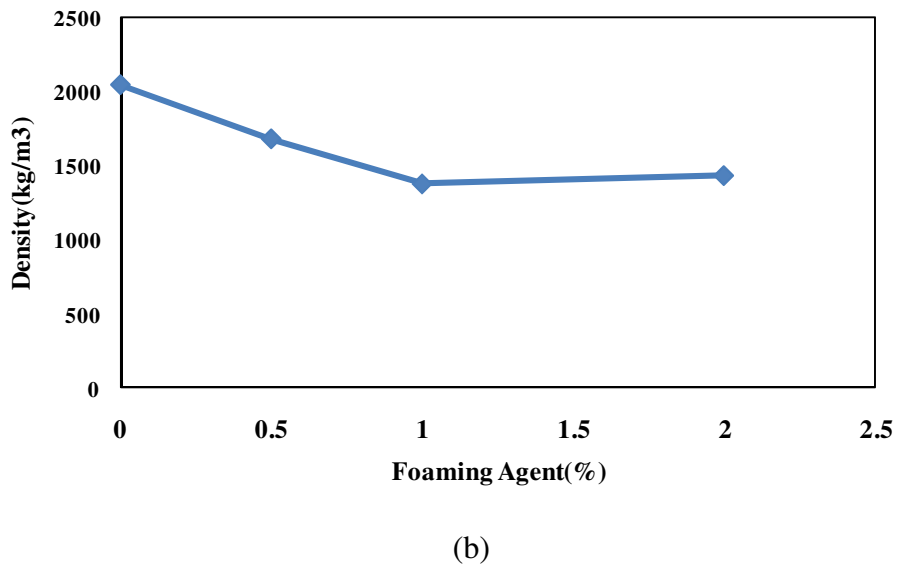
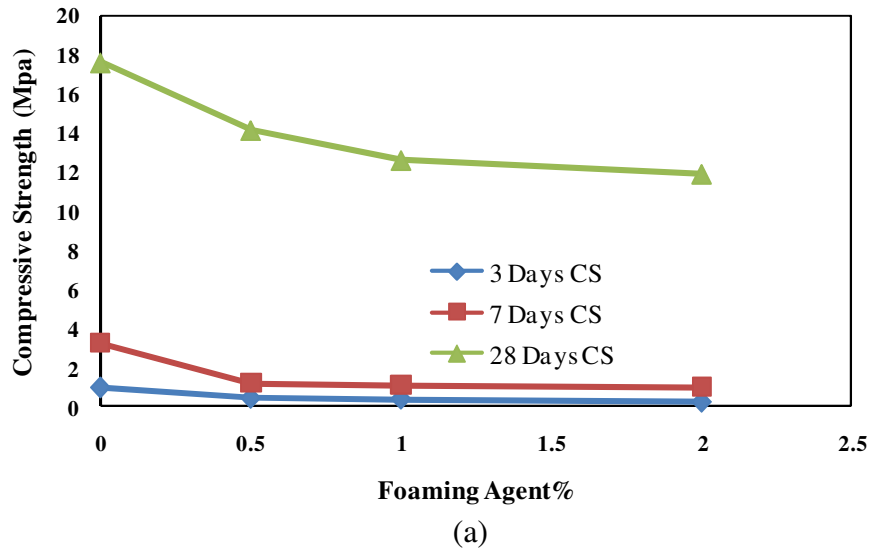
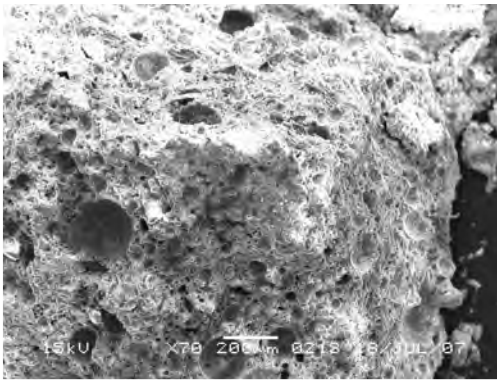


Figure 6-3 (a,b) Effect of foaming on 28 day compressive strength and bulk density of mix 48% BOS-40% ROSA-12% RG

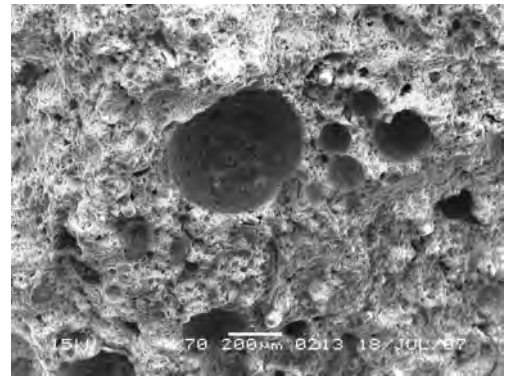
From figures 6-3 (a, b) it can be seen that the compressive strength of pastes at every age was decreased by increasing the amount of foaming agent.

The figures 6-4 (a, b, c) show the effect of foaming agent on the voids in a paste sample. Microscopic photographs show 200µm scale voids. This scale was big enough to show the voids in samples but the crystalline structure of minerals were not observed during this test and it required bigger scale.

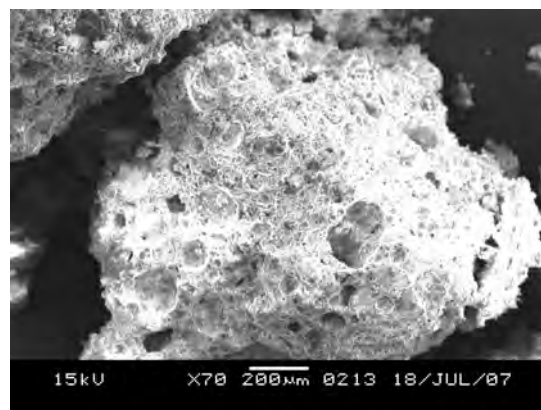
The figures show increasing foaming agent from 0.5% to 1% causing more voids in sample. The lowest density (highest amount of voids) occurred by adding 1% of foaming agent.



(a) 0.5% Foaming agent



(b) 1% Foaming agent



(c) 2% Foaming agent

Figure 6-4 (a,b,c) Microscopic photos of air entrained samples with 0.5%,1% and 2% foaming agent

The foaming agent used in these trials was supplied by Lafarge Plasterboard. This foaming agent works well with anhydrate gypsum. However it did not produce the same results for the by-product plasterboard gypsum. Although using the foaming agent made the samples lighter, it caused the compressive strength of samples to drop significantly.

The results showed reduction in density of paste, but the pastes were more fragile than the previous pastes with no foaming agent.

6.2.3 Air entrained mixes without BOS

One of the mixes with high compressive strength at 3 days from step 2 of this project was selected for the trial. The trial was carried out on pastes instead of concrete since the compressive strength of the concrete is influenced by the compressive strength of the paste. According to Lafarge's recommendation, the amount of the foaming agent should be between 0.2% and 1% of the total weight of the gypsum. In this case, the amount of the foaming agent exceeded the recommended range of 0.2% to 1%. The proportions of 0.5%, 1% and 2% foaming agent to the binder mass were tested.

The foaming agent was mixed with water before the water was poured into the blend.

The red gypsum was wet and coarse, thus extra drying and grinding process would have been needed to make it useable in binder mixing. Therefore ready to use, ground and sieved plasterboard gypsum was selected for this study.

Reviewing the pastes from step 2 of this study and the effect of each material on the compressive strength revealed that by-pass dust will achieve higher initial compressive strength. It was used for this experiment.

Details of the results are presented in Table 6-6.

Table 6- 6 Mix design for light weight paste using foam agent

Mix	W/C	Foam agent% by cement weight	C S at 3 day (MPa)	C S at 7 day (MPa)	C S at 28 day (MPa)	Density Kg/m ³
60%ROSA-20%PG-20%BPD	0.25	0	2.3	4.2	6.5	1785
60%ROSA-20%PG-20%BPD	0.25	0.5	0.74	2.1	3.5	1630
60%ROSA-20%PG-20%BPD	0.25	1	0.65	1.9	3.35	1564
60%ROSA-20%PG-20%BPD	0.25	2	0.64	1.75	3.2	1470

CS: Compressive Strength

Using 20% **by- pass dust**, 20% plasterboard or red **gypsum** and 60% of run of station ash produced acceptable results. Air entraining reduced the compressive strength at every age, and that was a problem for the final product. Using light weight aggregate is another option to consider. Using a higher binder to aggregate ratio led to higher compressive strength and smoother surface.

6.2.4 Using Crushed Plasterboard as Light Weight Aggregate

The initial idea was to use crushed plasterboard as light weight aggregate. If that idea were feasible, it could lead to consumption of more waste plasterboard. Several trials were **undertaken** in this research to study the feasibility of this idea. Table 6-7 shows the results of the trials.

Table 6- 7 Mix design for light weight paste using crushed plasterboard as light aggregate

Mixes	Aggregate* Kg/m ³	Cement Kg/m ³	Density Kg/m ³	3 day compressive strength (MPa)	7 day compressive strength (MPa)	28 day compressive strength (MPa)
60%ROSA-20%PG-20%BPD	727	727	1860	0.75	2.1	4.4
60%ROSA-20%PG-20%BPD	275	1103	1720	0.95	2.7	5.1

*Crushed plasterboard gypsum (pass 9 remain 4.5)

w/c was 0.2 in all mixes

Because the mixes were semi-dry, using the vibration table was not a suitable method for samples' compaction. Also, because PG as aggregate was brittle and

tamping would crush the aggregate, using the vibrating table would have caused lower compressive strength. Therefore concrete samples were compacted using a hammer drill and attached plate (for both 50 mm and 100 mm cubes) in 3 compacted layers. Figures 6-5 and 6-6 show the compaction method of concrete samples.



Figure 6- 5 Sample compaction using hammer drill for 50 mm cube



Figure 6- 6 Attached plate to hammer drill for better compaction

The trial mixes with plasterboard gypsum had insufficient compressive strength at 3 days. Plasterboard gypsum was too fragile to be used as light weight aggregate, because it was crushed during vibration with the drill hammer. The crushing reduced the compressive strength of the mix. It also contained crushed glass and paper that made the mixture **inhomogeneous**, which could be one of the reasons for lower compressive strength. If used only as aggregate, it also increased the density that was undesirable for light weight blocks. Figure 6-7 shows crushing plasterboard gypsum during compaction.

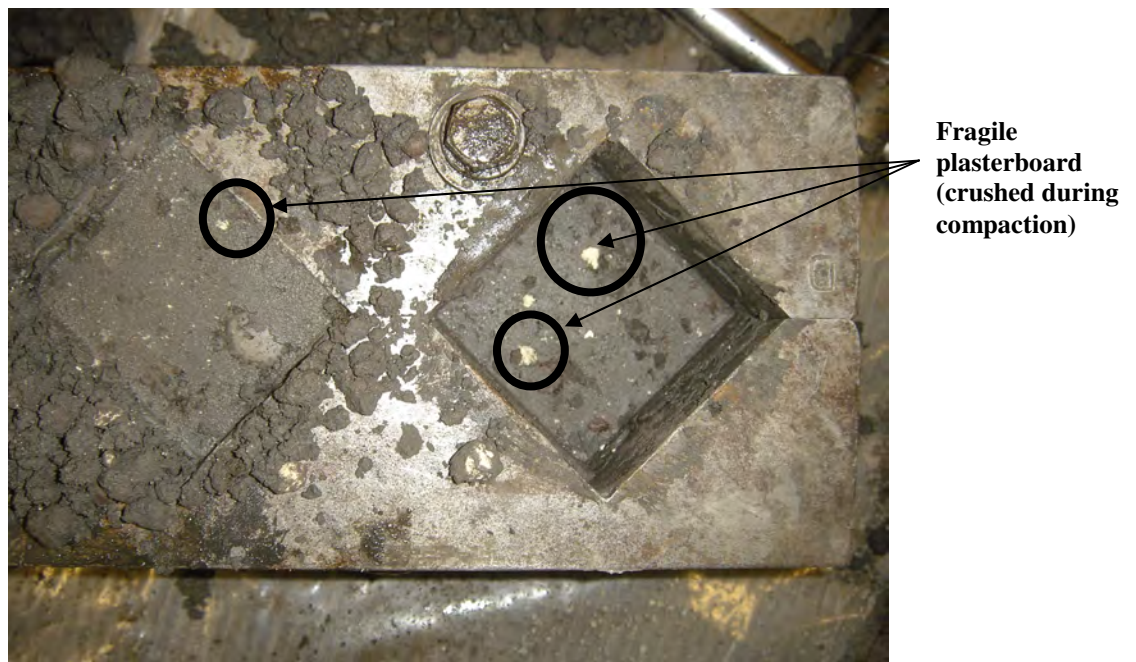


Figure 6-7 Crushed plasterboard as aggregate in light weight samples

Although using crushed plasterboard gypsum as aggregate for concretes containing BOS reduced the density, it was not a good option to be used replacement of aggregate because it reduced the compressive strength of the pastes. PG as aggregate absorbed water during mixing and these characteristics also reduced the density and **reduced** compressive strength.

Figure 6-8 shows the effect of PG as aggregate on the density of the trial concretes however the cementitious paste was not similar in some of the mixes according to Table 6-8.

Table 6-8 Trial mixes for the light weight block

BOS%	ROSA%	BPD%	RG%	Density (Kg/m ³)	w/c	PG (kg) in each m ³
30	60	0	10	1660	0.7	1200
25	65	0	10	1700	0.8	1250
30	60	0	10	1728	0.5	1000
20	5	70	5	1776	0.4	1200
30	60	0	10	1784	0.4	1000
80	0	10	10	1840	0.4	1200
30	55	5	10	1850	0.5	1000
30	60	0	10	2010	0.3	0

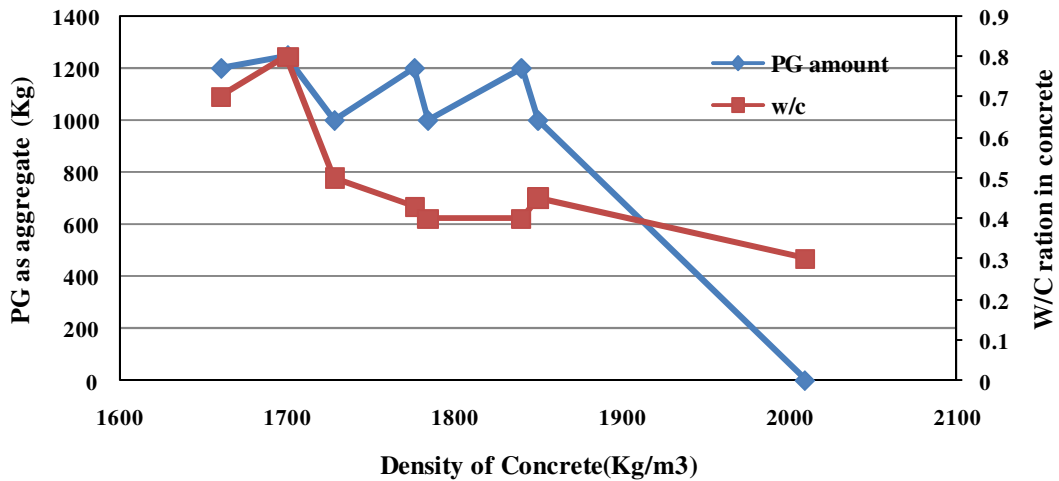


Figure 6- 8 Effect of using PG as aggregate on the compressive strength

It can be seen in figure 6-8, that increasing the PG, as aggregate, reduced the density because it decrease the amount of cementitious material that contained BOS. Therefore by omitting BOS from mixes and using waste materials with lower density and replacing PG with conventional light weight aggregate the final light weight sample for block making was tested.

6.2.5 Mixes with normal Light Weight Aggregate

Hanson lightweight aggregate was used. This aggregate was obtained from the block plant on Shawell Rugby. Table 6-9 shows the compressive strength and

the density of the light weight aggregate concrete made with paste 60%ROSA-20%PG-20%BPD.

Table 6- 9 Light weight concrete trials using light weight aggregate

Mixes	Aggregate Kg/m ³	Cement Kg/m ³	Density Kg/m ³	3 day compressive strength (MPa)	7 day compressive strength (MPa)	28 day compressive strength (MPa)
60%ROSA- 20%PG-20%BPD	727	727	1640	2.1	4.5	6.2
60%ROSA- 20%PG-20%BPD	571	857	1760	2.8	4.9	7.5
60%ROSA- 20%PG-20%BPD	275	1103	1820	2.4	4.3	8.3

w/c was 0.2 in all mixes ROSA: Rugeley Ash (I)

6.2.6 Effect of source of waste products on characteristics of Light weight concrete

Working with waste materials is not as easy as working with standard materials such as Ordinary Portland cement. Every batch of by-product materials has its own physical and chemical characteristics. Therefore it is essential to check such characteristics and for each batch used in the experimentation and compare the results with the previous batches.

The effect of ROSA and BPD sources were studied for block making. Four different ROSA batches were used in block making trials, 2 different batches of Rugeley Ash (Indonesian coal (I) and mixed Indonesian coal with Russian coal (II)) and two different batches of Ratcliff Ash. Two different kinds of BPD from Castle Cement (collected in different dates) were also used. The chemical analyses of the ashes materials are shown in Table 6-10.

Table 6-10 Chemical analysis of 4 different types of ROSA

Sample	Rugeley Ash (I)	Rugeley Ash (II)	Ratcliff Ash (I)	Ratcliff Ash (II)
SiO ₂	33.30	39.32	46.38	47.16
TiO ₂	0.82	1.02	1.05	1.04
Al ₂ O ₃	14.60	19.81	25.25	24.33
Fe ₂ O ₃	16.89	9.25	8.33	8.86
MnO	0.16	0.10	0.18	0.16
MgO	8.32	4.52	2.42	2.22
CaO	19.62	12.58	5.27	4.71
Na ₂ O	0.29	0.36	0.88	0.70
K ₂ O	1.01	1.19	2.08	2.14
P ₂ O ₅	0.27	0.82	0.64	0.53
SO ₃	1.32	1.01	0.70	0.50
LOI	3.56	9.63	6.33	7.22

The results of compressive strength testing of the specimens were completely different. Rugeley ash (I) showed more reactivity with BPD and PG in early age (3 days). The compressive strength of the specimens using Rugeley ash type (II) was almost double those of Rugeley ash type (I). That was because of high lime content (CaO) in Rugeley ash type (I) which is the reason why type C fly ash (to ASTM classification) with high lime content shows more pozzolanic activity than fly ash type F (to ASTM classification).

Ruggedly ash (II) needed a higher w/c and its density was lower than Rugeley ash (I). Obviously the benefit was using more binder in concrete without increasing the product's density.

Rugeley ash (I) was brown in colour, which could have been due to higher Fe₂O₃ content. Rugeley ash (II) was gray.

Ratcliff ashes had similar physical and chemical characteristics with gray colour. Their reactivity was the same and their compressive strength was close to each other.

Similar differences were observed by changing the source of BPD. Tables 6-11 and 6-12 show the effects that different types of fly ash (ROSA) and BPD had on the compressive strength of the light weight block trials.

Figure 6-9 shows the effect of BPD on the compressive strength of samples.

Table 6- 11 Effect of BPD from same source and different batches on specimens

Mix	Aggregate /Cement	Cement Kg/m ³	Density Kg/m ³	w/c	3 days CS MPa (50 mm)	7 days CS MPa (50 mm)	28 days CS MPa (50 mm)
60%ROSA _{Ru(II)} - 20%BPD _(I) -20%PG _G	275	1103	1750	0.25	2.4	4.3	8.3
60%ROSA _{Ru(II)} - 20%BPD _(II) -20%PG _G	275	1103	1560	0.25	1.5	2.6	8.8

Ru=Rugeley Ash G=Ground plasterboard

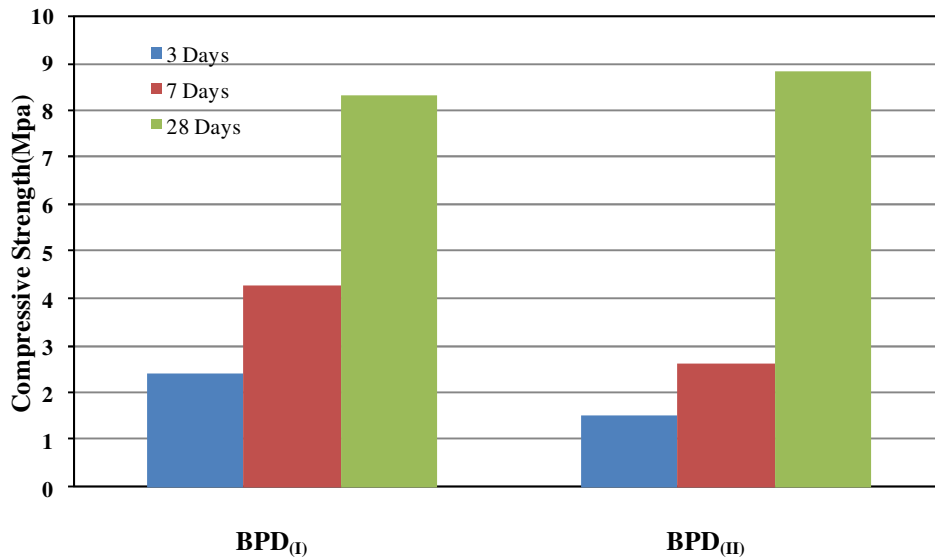


Figure 6- 9 Effect of Sources of BPD on the Compressive Strength of pastes

Table 6-12 Compressive strength of 4 different Ashes

Mix	Aggregate /Cement	Cement Kg/m ³	Density Kg/m ³	w/c	3 day CS MPa (50 mm)	7 day CS MPa (50 mm)	28 day CS MPa (50 mm)
60% ROSA _{RU(I)} +20% BPD(I) -20% PGG	275	1103	1820	0.25	5.3	6.2	9.5
60% ROSA _{RU(II)} +20% BPD(I) -20% PGG	275	1103	1750	0.25	2.4	4.3	8.3
60% ROSA _{RA(I)} +20% BPD(I) +20% PGG	267	1067	1670	0.25	0.7	1.5	8.5
60% ROSA _{RA(II)} +20% BPD(I) +20% PGG	267	1067	1667	0.25	1.6	2.8	9.3

RU=Rugeley Ash

RA=Ratcliff Ash

G=Ground plasterboard

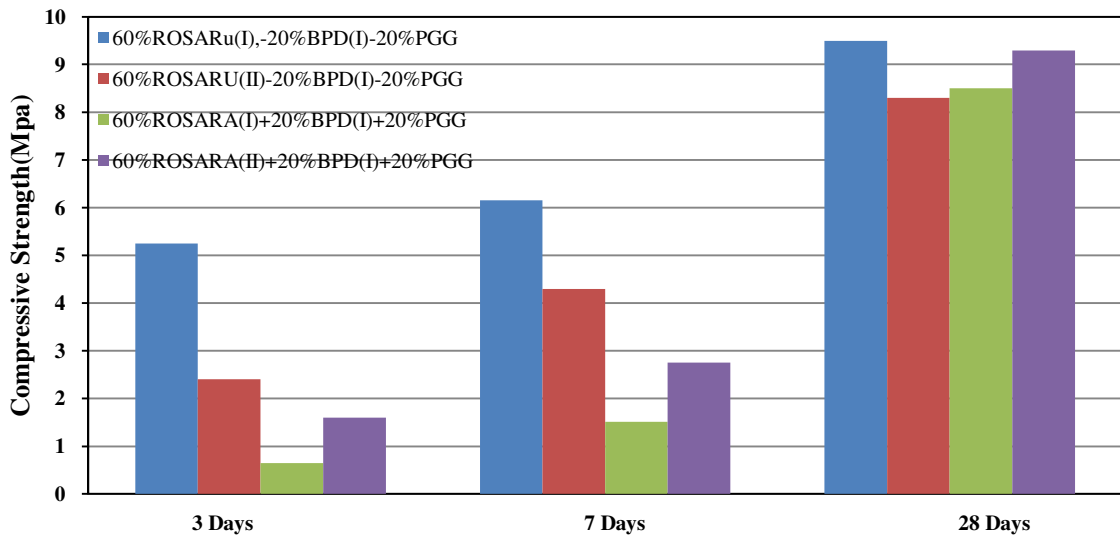


Figure 6- 10 Effect of different sources of Ash on the compressive strength

6.2.7 Effect of plasterboard particle size on compressive strength and density of block samples

Plasterboard gypsum that was obtained from Lafarge for the site trial was not ground. The plasterboard did not have as much paper and crushed glass that it normally does. It might have been cleaned before it was sent to Coventry University. The sieve analysis of crushed plasterboard is shown in Table 6-13. Sieves were selected according to the size of the particles.

Previously PG was ground and sieved through a 600 μ m sieve.

Both plasterboard types were used to make mixes and study the effect of the plasterboard particle size on the compressive strength. It was assumed that more finely ground and sieved PG would have higher compressive strength than the coarser one.

Table 6- 13 PG sieve analysis

BS mm	remain%	pass%
5.00	21.8	78.2
2.36	16.0	62.2
0.60	38.1	24.1
remain	24.1	
Sum	100.0	

The effect of the plasterboard particle size on the compressive strength of the block mixes is shown in Table 6-14.

Table 6- 14 Effect of ROSA source and PG size on compressive strength and density of specimens

Mix	Aggregate /Cement	Cement Kg/m ³	Density Kg/m ³	w/c	3 day CS MPa (50 mm)	7 day CS MPa (50 mm)	28 day CS MPa (50 mm)
60%ROSA _{RA(I)} +20%BPD+20%PG _C	267	1067	1660	0.25	0.73	1.50	6.45
60%ROSA _{RA(I)} +20%BPD+20%PG _G	267	1067	1670	0.25	0.65	1.51	8.50
60%ROSA _{RU(II)} +20%BPD+20%PG _C	267	1067	1663	0.25	1.52	2.64	8.80
60%ROSA _{RU(II)} +20%BPD+20%PG _G	267	1067	1667	0.25	1.60	2.75	9.30
RA=Ratcliff Ash	RU:Rugeley Ash				C:Crushed PG	G:Ground PG	
CS= Compressive Strength							

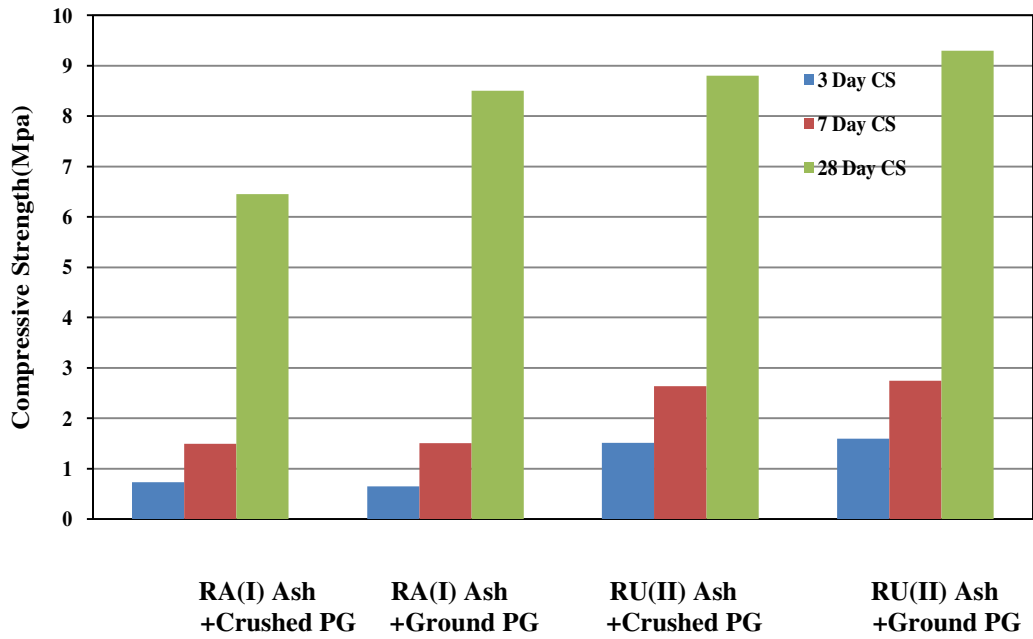


Figure 6- 11 Effect of ROSA source and PG particle size on the compressive strength of specimens

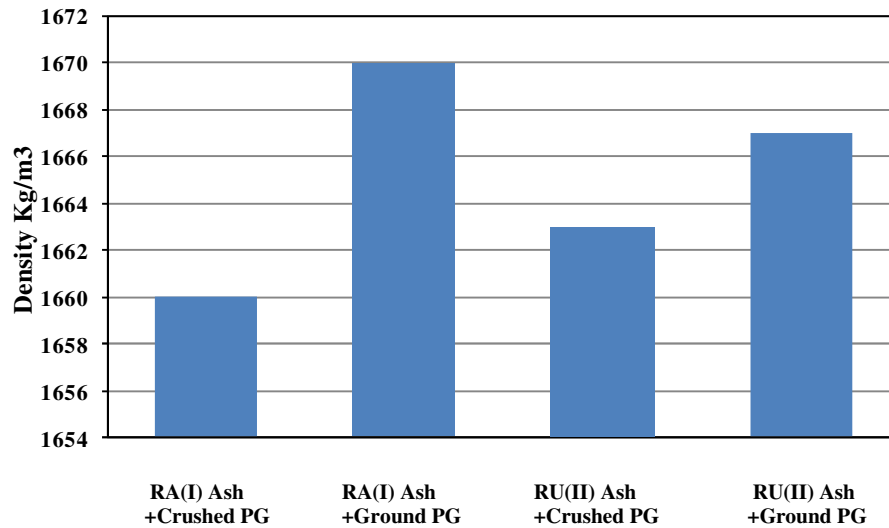


Figure 6- 12 Effect of ROSA source and PG particle size on the density of specimens

Figures 6-11 and 6-12 show the effect of PG particle size on the compressive strength and the density of the light weight concrete. Samples made with ground

and sieved PG had slightly higher compressive strength than those made with coarser PG. However the difference in compressive strength at 3 days was not significant enough justify the amount of time, energy and money that was needed to grind and sieve the coarse PG for block making.

6.2.8 Hanson Concrete samples

Prior to the site trial in Hanson block manufacturing, the stability of the final mix at very early age was tested in simulated works conditions with hammer drill compaction. However the compressive pressure and vibration in a factory would be much higher than that of the hammer drill. Figure 6-13 shows the 100 mm stable sample demoulded after casting.



Figure 6-13 Fresh light weight concrete demoulded straight after concrete casting

As shown in Figure 6-13, the mix was stable after demoulding and did not have any changes in dimensions after it was cured. The sample was hard enough after 3 days to be moved with no damage in edges, however its compressive strength at 3 days was 1.6 MPa instead of 2.5 MPa. It is suggested that compressive strength may not be the only factor which prevents damage in the block handling machine and this highly cohesive mix might be adequate.

7. Discussion

7.1 Introduction

This chapter discusses about **all the** results of the research which led to the conclusions **and** how this research met the objectives. Two major results were about the flow and the compressive strength of pastes made of waste materials. The relationships between these two characteristics of the pastes are explained in this chapter. Then the relationship between all other results on the five selected mixes is discussed.

7.2 Hydration mechanism in the pastes

The hydration process takes place at the solid-liquid interface. Solid products start to be generated and grow around a core of unhydrated cementitious materials. This assumption can describe the reaction between BOS-RG/PG-ROSA directly after mixing with water. The soluble ions, Ca^{2+} , Al^{3+} , Si^{4+} , Mg^{2+} , SO_4^{2-} from gypsum compounds and Run of Station Ash and released ions from slag enter the solution. OH^- and alkali are also available in the system in the early minutes of hydrations.

Two main hydration products (known as gel) include an amorphous mass, mainly Calcium Sulphate Hydrate (C-S-H), in the form of irregular fibrous particles and large hexagonal crystals of calcium hydroxide (Illston and Domone 2006).

Figure7–1 illustrates the hydration of Portland cement (Illston and Domone 2006)

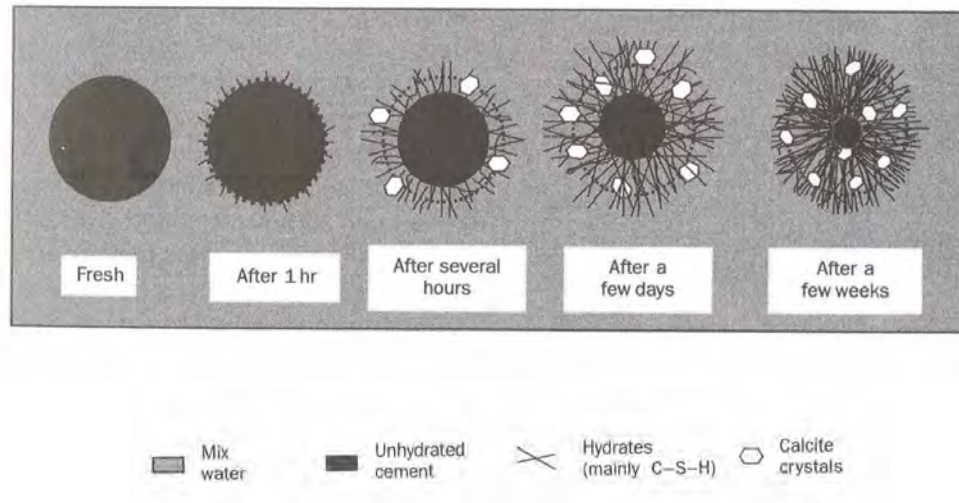


Figure 7-1 Hydration of a single Portland cement grain

The main part of the hydration of the by-product raw materials, generation of C-S-H gel and calcium hydroxide, is assumed to be similar with Portland cement.

It is also worth mentioning that the rate of hydration decreases due to the increased difficulty of diffusion of water into the hydration product to the unhydrated part of cementitious particle. That is the reason for the products deposited near the fresh cement/water interface (inner products) being denser than those deposited further away (outer products). Therefore even after many years there will be a residual core of the unhydrated cement (Illston and Domone 2006).

C-S-H would be formed on the surface of slag grains by time (Ganjian *et al.* 2007).

Ca^{2+} , Al^{3+} , Si^{4+} from ROSA and OH^- ions are assumed to be gradually removed from the solution by hydration process. It caused an increase in sulphate ions in the pour solution to balance the charge of alkali ions. By increasing the hydration, the amount of C-S-H gel augments and in order to maintain the chemical balance between liquid and solid in the mixture corrosion happens in

the slag. In the conducted tests of this research, the pH of the pastes was measured and the values were between 10.9 and 12.3, the formation of ettringite crystals ($C_6A\bar{S}_3H_{32}$) was possible (Neville 1995). Fairly large quantities of crystallised ettringite within the cementitious matrix could cause expansion of pastes that was shown in figure 4-26 of chapter 4.

7.3 Flow

Flow of pastes is measured because it is important when the concrete needs to be pumped. In subway backfilling, especially it is important because self compacted concrete is needed with the slump of more than 100 mm.

The results of experiments showed the flow of binary mixes changes with changing the amount of each component. Mixes with flow ≥ 180 mm were classified as high flow and the mixes with flow ≤ 79 mm were classified as low flow.

Figure 7-2 shows the flow of all binary mixes containing BOS increased with increasing BOS content.

BOS particles surfaces are smooth and absorb less water. It is not a good material in block making since it causes paste to have higher flow and be unstable. Even with lower water content it was unsuitable because the materials could not react well with a low amount of water. The BOS-RG mixes had the least flow in all mixes. Mixes with RG needed more water to achieve workability. This was observed by Hughes (2006).

RG made the paste sticky when the content in the mix was increased. This might be because of the particle size of RG that was finer than other materials except BPD. Fineness increases the particles' surface areas which increases the friction between grains and leads higher viscosity and less flow.

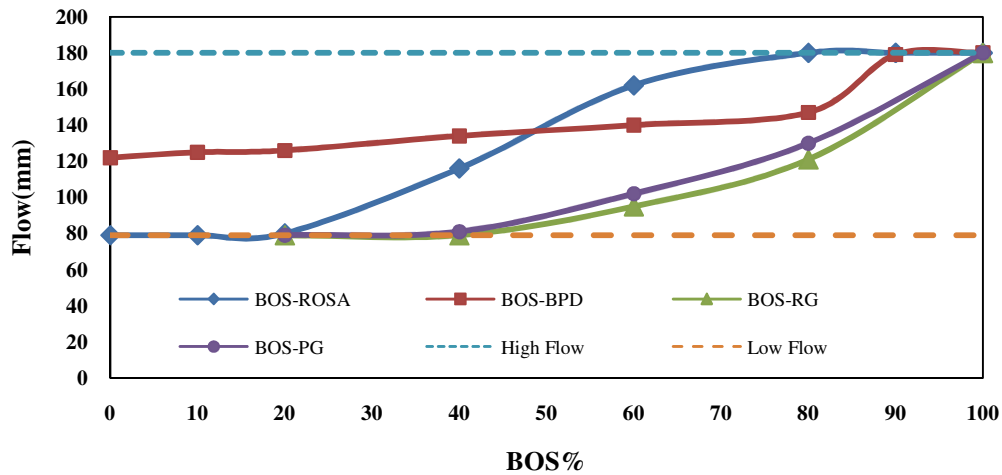


Figure 7-2 Effect of BOS on Flow in the binary mixes with other waste materials

Figure 7-2 illustrates that the flows of the pastes containing PG were less than those of those containing ROSA. This might be because of the existence of paper in PG dissolved in water during mixing and made pulp which had high viscosity.

Flow decreased when ROSA increased in mix with all other waste materials. ROSA absorbed water during mixing. Figure 7-3 shows the effect of ROSA content on flow of pastes. It needed higher water to react because of a higher porous surface compared with fly ash. This was observed by Kiattikomol *et al.* (2001).

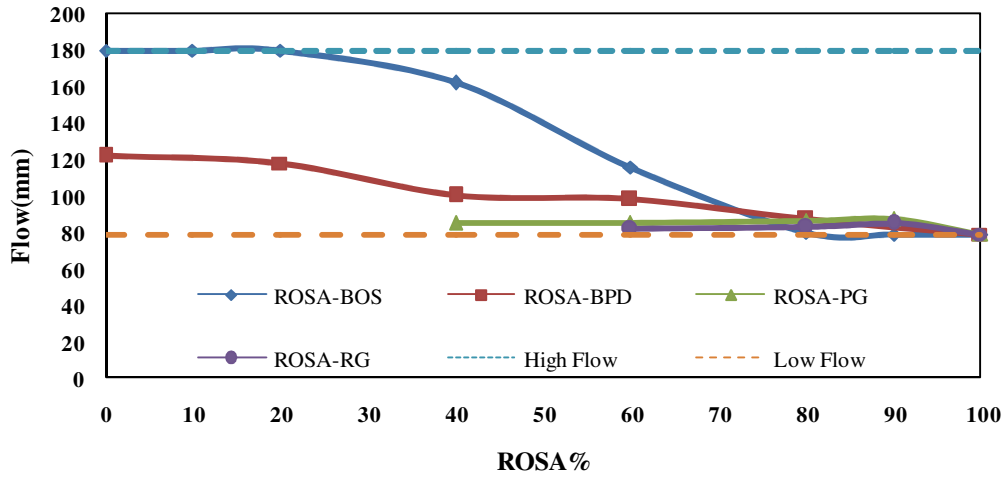


Figure 7-3 Effect of ROSA on Flow in the binary mixes with other waste materials

The flow of pastes BPD-ROSA, BPD-RG and BPD-PG was increased by increasing BPD. Figure 7-4 shows how the flow of pastes was changed by increasing BPD.

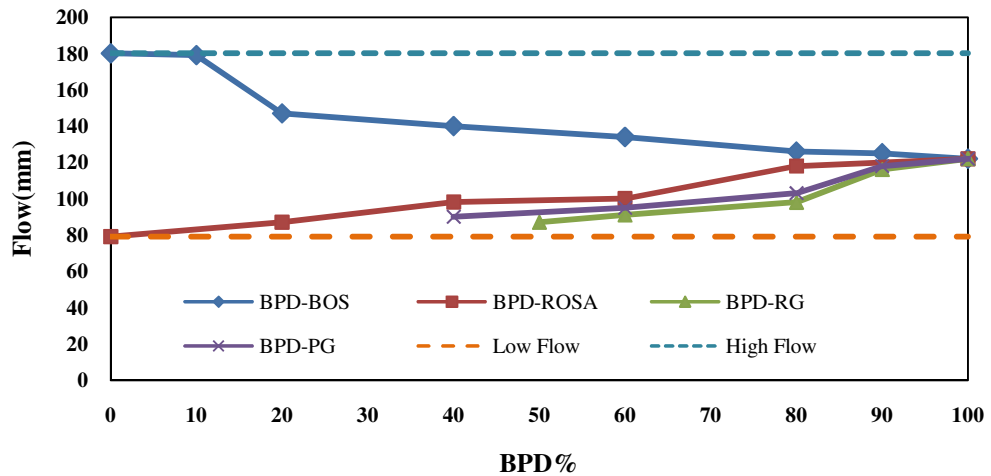


Figure 7-4 Effect of BPD on Flow in the binary mixes with other waste materials

From these results it is concluded that whenever a mix needs to have more flow, it should have BOS. This helps in selecting mixes for subway backfilling or any other purposes that needs higher slump. It is also concluded; pastes with ROSA-PG/RG were stable and had less flow when made semi-dry. This is important in block making. Blocks should be stable after demoulding and high

flow pastes or dry pastes were not suitable for that purpose even in low water content.

In ternary combinations of the waste materials BOS-ROSA-BPD selected waste content, the amount of each material had significant affect on the flow of the paste. For example the flow was not decreased only by decreasing BOS. In figure 7-5 it can be seen that by increasing BPD (to 72%) and decreasing BOS (to 18%), the mix had the lowest flow. However by decreasing BOS (to 15%), the flow was increased because ROSA amount changed from 10% to 80% and that change led higher flow. So, in ternary combination flow was not affected directly by one material.

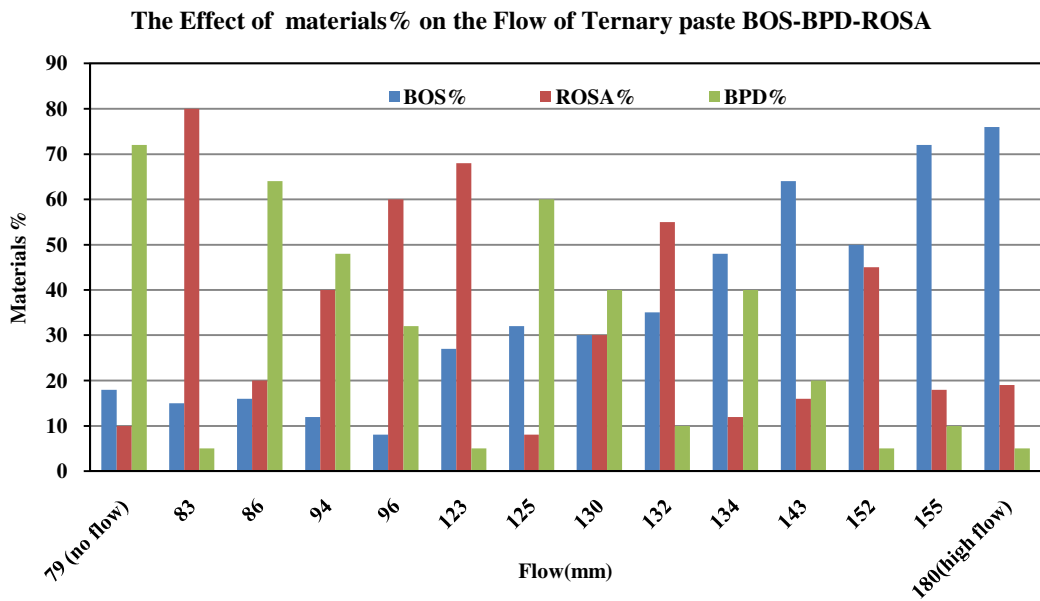


Figure 7-5 Effect of waste material contents on the flow of the ternary pastes BOS-BPD-ROSA

In ternary combinations of BOS-BPD-RG, the flow of paste changed depending on all three materials. For example by increasing BOS from 64% to 65%, the flow of paste was increased 48mm because RG was decreased 9% and the change in RG content had a significant affect on flow. In other words, as it was concluded for BOS-ROSA-BPD ternary combinations, the flow of pastes was influenced by changing of all materials. Figure 7-6 shows changes

in flow by changing the amount each the material in the flow of ternary combination of BOS-BPD-RG. It also can be seen in this figure that by reducing RG only 4% from 20% to 16% with the same amount of BPD that was 20% and increasing BOS only 4%, the flow changed 55mm. This condition could be considered as binary combination that by increasing RG the flow decreased. So, the flow of the ternary mixes with same amount of one material change similar to the flow of the binary mixtures.

Figure 7-7 shows the flow changes by material content. From this figure it may be seen the flow of paste changes depending on all three materials.

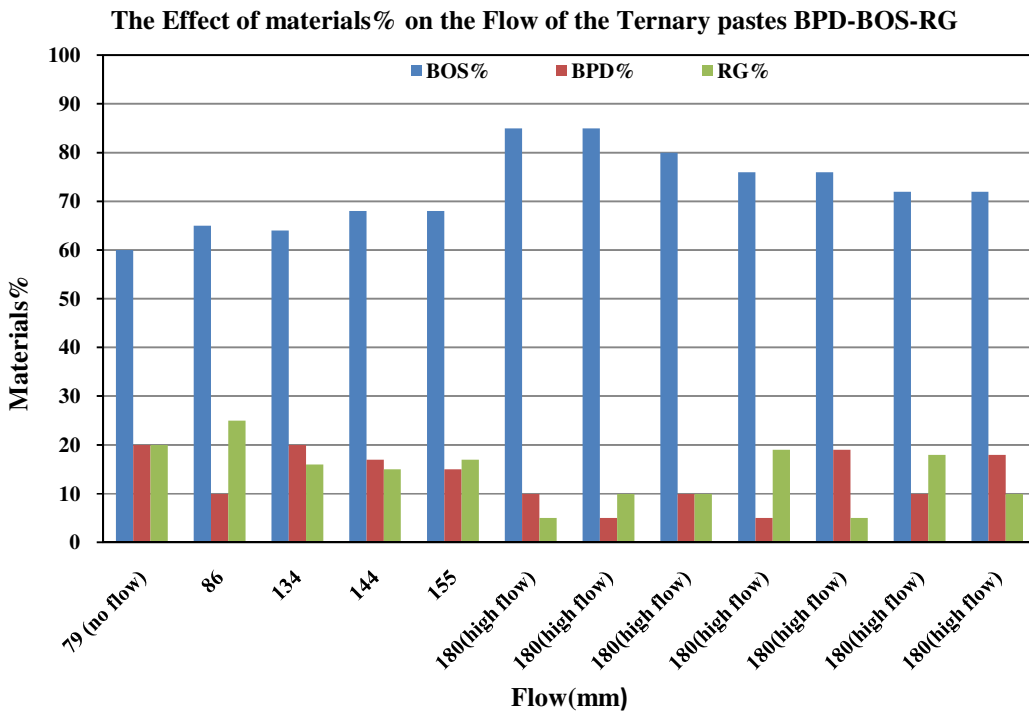


Figure 7-6 Effect of waste material contents on the flow of the ternary pastes BPD-BOS-RG

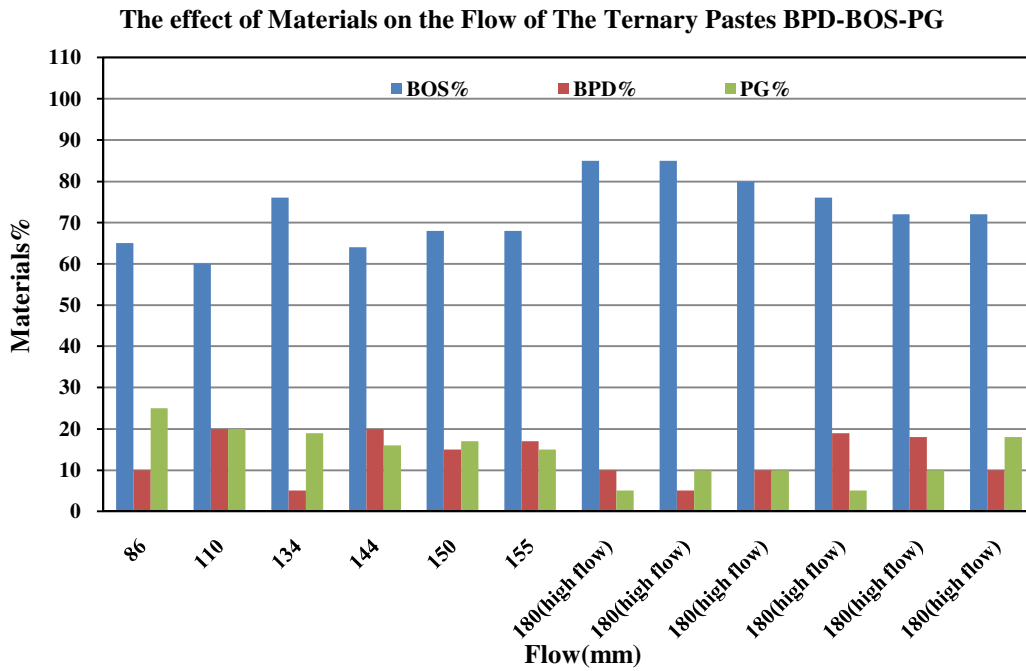


Figure 7-7 Effect of waste material contents on the flow of the ternary pastes BPD-BOS-RG

The flow of ternary pastes of BOS-ROSA-RG depended on changes of all materials content. However two pastes that had equal amount of one material (e.g. BOS 40%) the flow changes similar to binary combination. Figure 7-8 shows the changes of flow by changing material content. By decreasing RG from 30% to 12% and increasing ROSA from 30% to 50% with the same amount of BOS, the flow increased, that is similar to a binary combination of ROSA-RG.

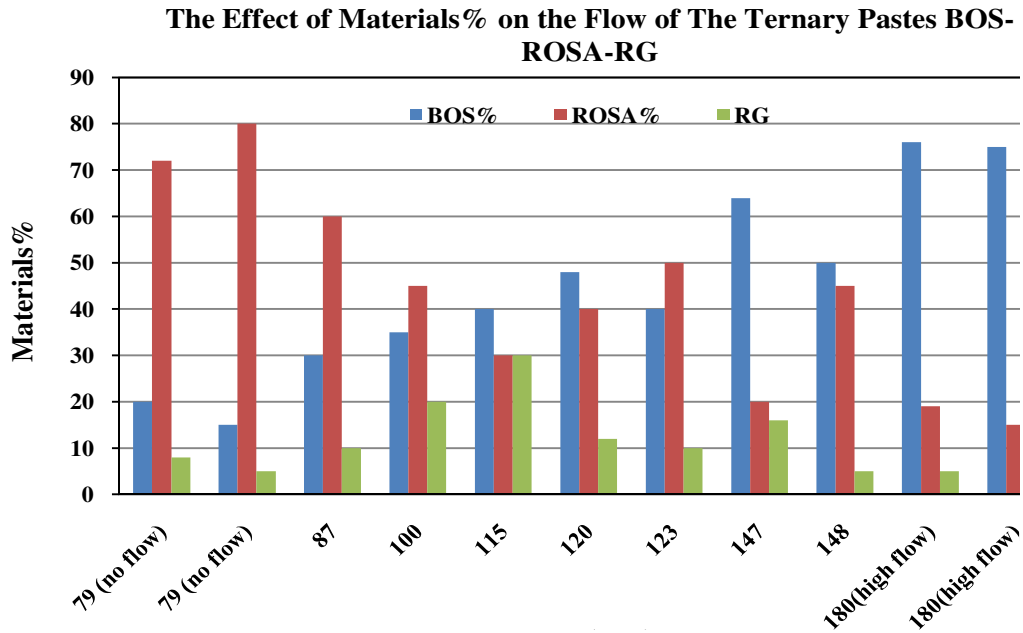


Figure 7-8 Effect of waste material contents on the flow of the ternary pastes BOS-ROSA-RG

The flow changes of the ternary combinations of BOS-ROSA-PG are shown in figure 7-9. It can be seen that the flow of pastes depended on changes of each material. Increasing or decreasing of each material did not have direct effects on the flow as in the other ternary groups.

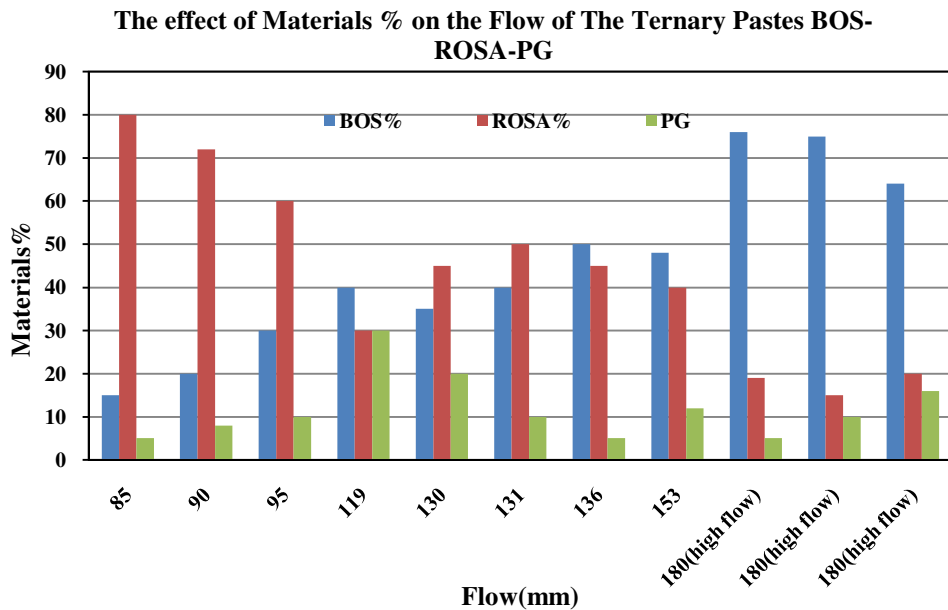


Figure 7-9 Effect of waste material contents on the flow of the ternary pastes BOS-ROSA-PG

All of ternary combinations of ROSA-BPD-RG/PG were semi-dry pastes with flow ≤ 79 mm (no flow). The reason could be because ROSA content was higher than BOS and it affected on the flow. These combinations were really dry that mixing times were increased to let ROSA release the water to the mixes.

However since they were semi-dry, they could be stable after demoulding. This helped in selecting paste for block making. The sample of concrete using lightweight aggregate (267 kg/m^3) and paste 60% ROSA-20% BPD-20% PG (1067 kg/m^3) using 0.20-25% of w/c ratio was completely stable after demoulding as it was discussed in chapter 6.

It was concluded pastes containing BOS were not suitable for light weight block making for two main reasons; higher density and more flow. However those pastes could be useful in subway backfilling and road bases as Ganjian *et al.* (2007) used in his research.

7.4 Compressive Strength

All selected waste materials had pozzolanic activity and some could be used as activators for others such as BPD. ROSA seemed to be an alkali activator for BOS. PG also had the role of sulphate activator for BOS.

Pastes of binary mixes containing BOS

The mixes using BOS showed less compressive strength at early age (3 days) because BOS showed its pozzolanic activities slowly. The mixes containing BOS had higher density compared to the mixes without BOS. Therefore by increasing BOS, the density of mixes was increased. The difference in density depended to other waste materials in the pastes.

Optimum compressive strength of pastes containing BOS and other waste materials in binary mixes were as follows:

90%BOS-10%ROSA, BOS-BPD had no optimum, 80%BOS-20%RG, and 80%BOS-20%PG.

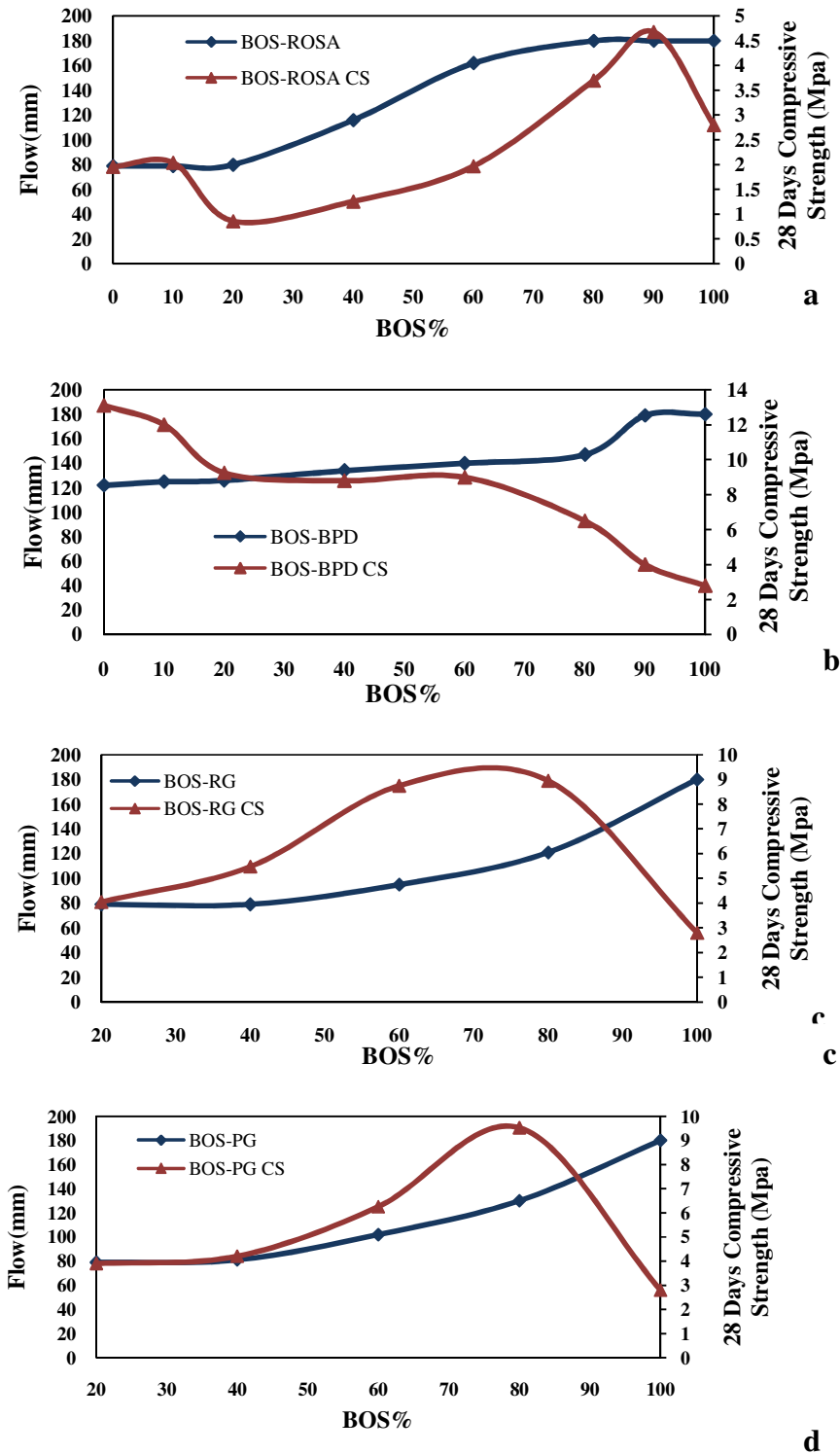


Figure 7-10 Relationship between Flow and Compressive strength of pasts containing BOS

The relationship between flow and compressive strength of cementitious pasts containing BOS is shown in figure 7-10.

This figure illustrates that the flow and the compressive strength of cementitious pastes were not related to each other. For instance, by increasing BOS, flow increased and compressive strength was gained and it had its optimum (figure 7-10 a, c, and d). However, flow was increased by increasing BOS and compressive strength was decreased by increasing the flow (figure 7-10 b). It can be concluded that both flow and compressive strength of the pastes were dependant on both materials. Therefore the flow of paste can be optimized.

Pastes of binary mixes containing ROSA

ROSA reacted with BPD, BOS, PG and RG. High calcium ROSA was more reactive than the low calcium ROSA. In the presence of water and BOS, its alkalinity reduced (Neville, 1996). This fact could explain the reduction in compressive strength of BOS-ROSA mixes when BOS is less than 60% (Figure 4-6). The paste 20% BOS-80% ROSA had the least compressive strength. Then by increasing the amount of BOS the compressive strength of paste increased (more than the compressive strength of mix 100% ROSA) when the BOS content was more than 60%.

The mixes using ROSA-BPD had the highest compressive strength among all binary combinations. The glassy materials in ROSA could be broken down when the pH value of the pore water was at least 13.2 (Neville, 1996). BPD could produce it because it contained high alkalinity (pH 12.6). This could be the reason that BPD-ROSA combination had the highest pozzolanic reaction that led to its compressive strength.

Reasonable amounts of alkalis K_2O and Na_2O in ROSA led to higher early strength in pastes however its alkali content was less than that of BPD therefore it had less early strength compared with BPD.

Sources of coal had specific effects on the compressive strength of pastes. Ash of burning Indonesian coal had lime and had higher compressive strength even with no activator. It could be classified as ASTM Fly ash type C and it showed good reactions with BPD.

Optimum compressive strength of pastes using ROSA were in mixes; 60% ROSA-40% BPD, 90% ROSA-10% RG, and 90% ROSA-10% PG.

Pastes of binary mixes containing BPD

Using BPD in the paste led to a higher early compressive strength compared with pastes without using BPD. Because BPD was the waste from cement industries and chemical analysis showed it contained more K_2O and Na_2O than any other waste materials and it gave higher compressive strength at early ages. Furthermore, it had higher alkalis K_2O and Na_2O than OPC (1% K_2O and 1% Na_2O) that could increase the early strength development and reduce the long-term strength (Neville, 1996).

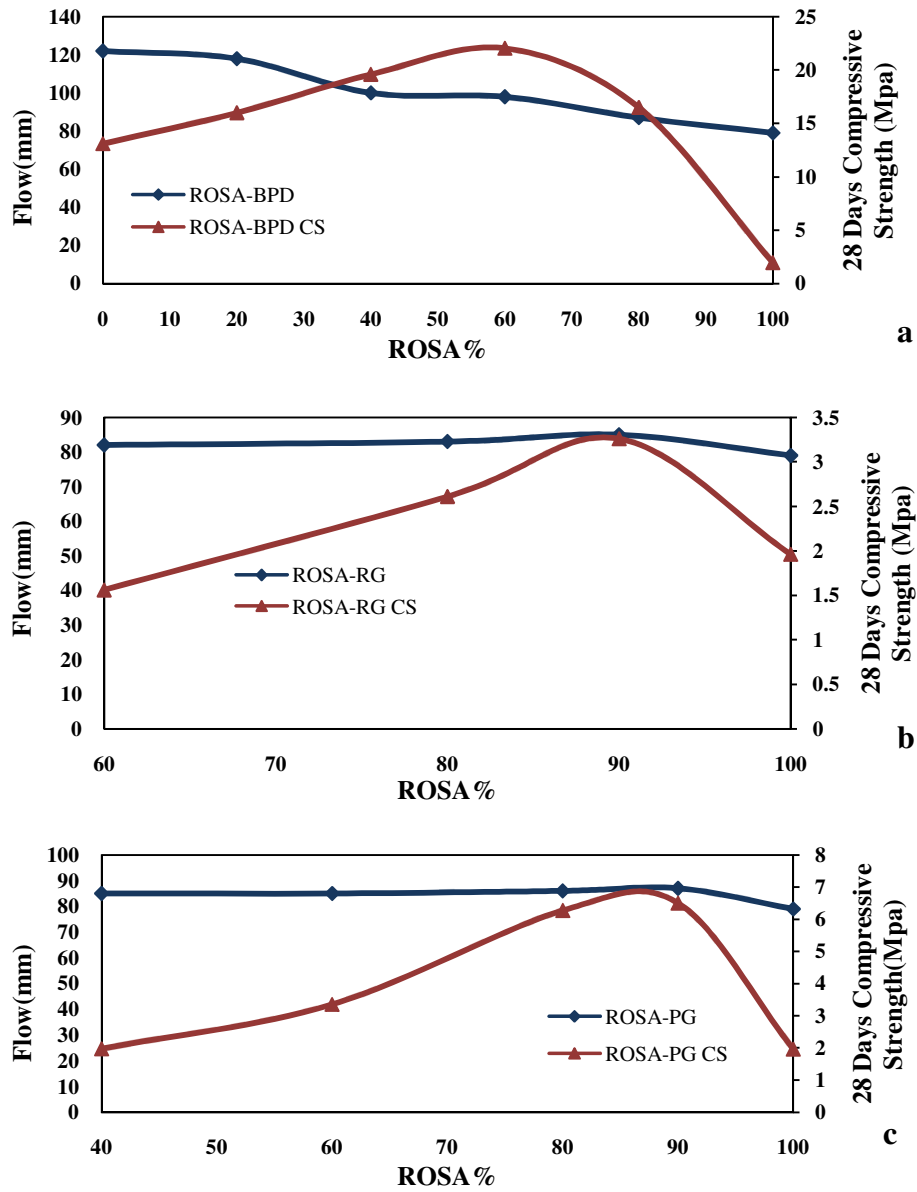


Figure 7-11 Relationship between Flow and Compressive strength pasts containing ROSA

Figure 7-11 (a to c) shows the relationship between flow and compressive strength of pasts containing ROSA. Similar to mixes containing BOS, there is no specific relationship between flow and compressive strength of these series of mixes.

BPD was finer than other waste materials from the results of sieve analysis and this may be considered as a reason to show more reaction with other materials

in presence of water. However its characteristics changed in each batch even if it was collected from the same source. Therefore when it was used for the final product of this research, the light weight block, its content was limited to 20%. BPD had no optimum compressive strength in binary mixes with PG and RG. The reason was because the origin of BPD was by-product of Portland cement so it had the main role in the process of hydration and strength build up. In other word, the compressive strength of BPD-PG and BPD-RG pastes were increased by increasing BPD.

BPD contributed to pozzolanic activity with RG, PG and BOS. The compressive strength of pastes using BPD in the fist three days of hydration grew faster than those samples with no BPD. Therefore BPD was used for the ternary mixes to gain the highest possible compressive strength for the light weight block design.

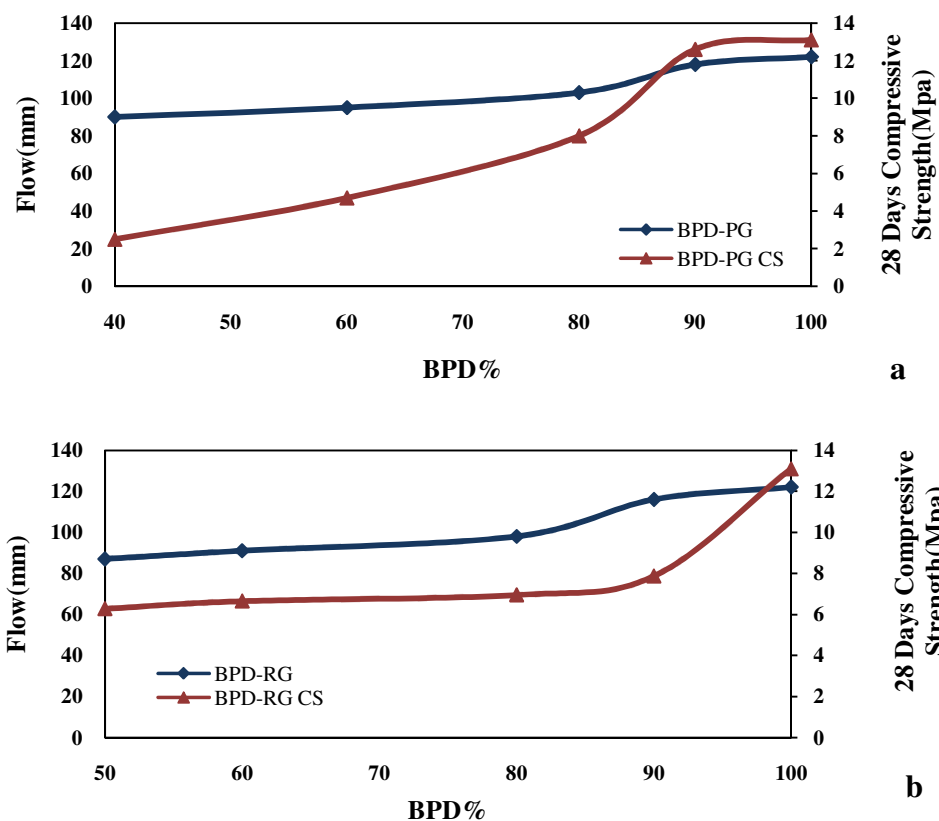


Figure 7-12 Relationship between Flow and Compressive strength pasts containing BPD

Figure 7-12 (a and b) shows compressive strength and flow are similar in BPD- gypsum (RG or PG) pastes. **Compressive strength was increased by increasing the flow in these pastes.** However from figures 7-10 (b) and 7-11 (a) there was no relationship between flow and compressive strength of the pastes.

In all mixes containing red gypsum, the increase in the amount of RG, led to **the mix being** sticky especially in RG-ROSA mixes.

Similar to ordinary Portland cement, the compressive strength of all binary and ternary pastes increased with time.

The five mixes that were selected from step 2 and are shown in Table 4-23 in chapter 4 are discussed in this section.

The compressive strength of cementitious pastes was changed with different water/cement ratios. The lower the water content, the higher the compressive strength of **the** paste. **These** results were agreed with **those** of Ganjian *et al.* (2007). **However** in this **study** each paste had an optimum w/c ratio to gain its maximum compressive strength.

Particle size of waste materials was an effective parameter in **the** compressive strength **prediction**. The lower the particles size of materials, the higher was the compressive strength. That was due to more surface area for chemical reaction between materials. This was similar to the results of Shi (2004).

Figure 7-13 shows that the **permeability coefficient** of pastes **did** not decrease by increasing the compressive strength of pastes. It was slightly higher **with the** pastes containing PG compared **to** the pastes containing RG with the same ratio.

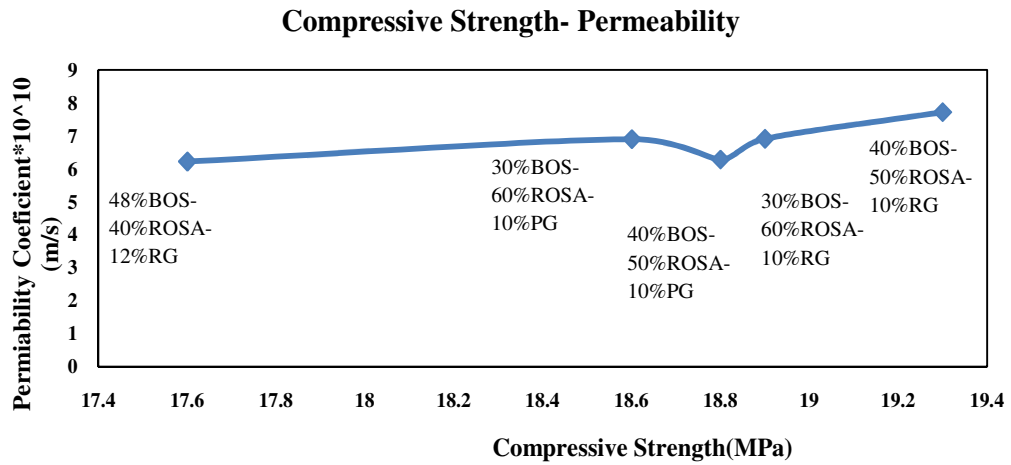


Figure 7- 13 Effect of Compressive Strength on Permeability of pastes

All pastes had a higher permeability coefficient than the OPC sample. However in the real condition the effect will be less critical than the high pressure water conditions in the test and also if the mixes were used as interior products permeability would not be relevant.

ICP analysis of solutions from the permeability test showed, Na, Ca, S, and Si which are considered as ordinary components of soil and rocks. Although the level of sulfate and calcium leached from the samples was more than that for OPC, due to the lower hydration rates, in the high pressure cell through flow test, the condition was more accelerated than normal conditions so the ions are not expected to leach from the products in real life conditions.

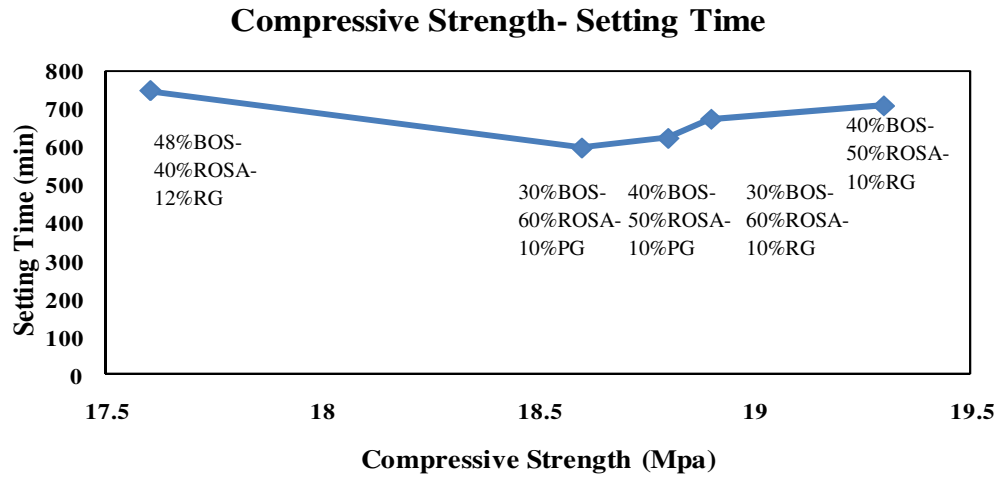


Figure 7-14 Effect of Compressive Strength on Setting Time of Pastes

The setting time of all pastes was slower than OPC which agreed with Ganjian *et al.* (2007) and Hughes (2006).

Figure 7-14 shows that the setting time of samples using PG with same BOS-ROSA ratio was less than those using RG. It could be because PG had more sulphate than RG and that reduced the setting time.

PG was preferred instead of RG for block making because setting time and early compressive strength was important as was explained in chapter 6.

Bypass dust showed pozzolanic activations in the early age of samples and increased the early compressive strength. Although it was not used in the five selected pastes for more tests, it could reduce the setting time of pastes due to its chemical compositions that were close to the Portland cement compositions. Bypass dust was used for the final mix for, light weight blocks, since it increased the early compressive strength.

Figure 7-15 shows all pastes with RG/PG-BOS-ROSA had expansion in the first 3 months of curing. The expansion slowly ceased after 3 months. The expanding reaction in most cases was because of the formation of a calcium aluminate hydrate. The expansive agent could be ettringite (Taylor 1997)

which was observed by XRD test. The expansion reduction would be explained by existence of slag in the mixture (Taylor 1997).

Figure 7-15 shows the length changes of five selected samples. Each line shows the compressive strength at 28 days. It can be seen that compressive strength of samples was not related to the length change. However, the differences in the compressive strength of the selected samples were not high.

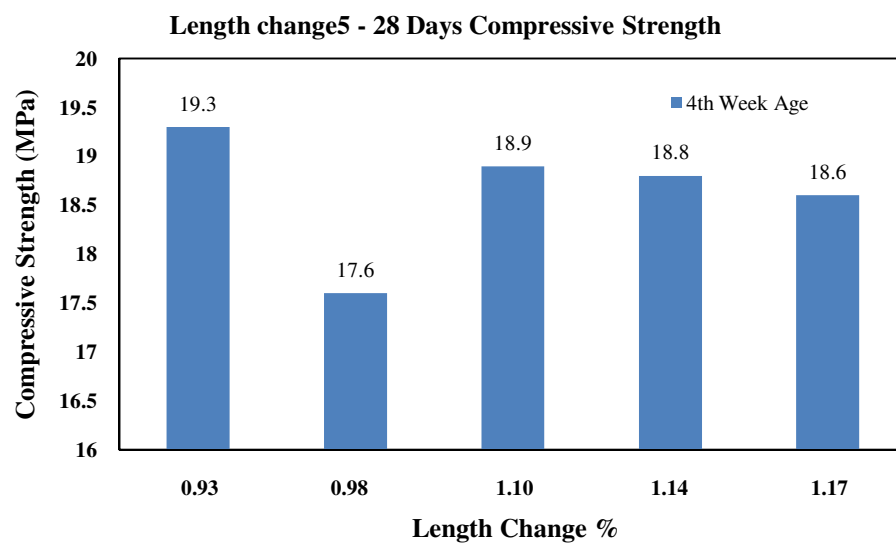


Figure 7-15 Effect of Compressive Strength on Length Change of samples at 28 days

The reduction in water/binder ratio from 0.30 to 0.23 reduced shrinkage of samples. Samples made of 0.30 w/b ratio cracked before demoulding. This was because of water evaporation and shrinkage of the paste in the early age and during setting. Because both sides of pastes were fixed with bolts into the moulds the samples were cracked (Figure 4-24).

The compressive strength of all samples was reduced after soaking in water that was agree with Hughes (2006) results. However as noted earlier the products might not be in the vicinity of water since they assumed to be used as interior products or road construction.

Viscosity of concrete using PG was around 2 times more than those of mixes using RG. The reason that mixes with plaster board gypsum had more viscosity could be because of the shape of PG particles and existing paper in waste PG.

The results of SEM on the samples using foaming agent showed an increase of voids in the samples and the increase in the foaming agent was parallel to the increase in voids.

Since the samples had low compressive strength compare to OPC, they did not bear freeze-thaw cycles and therefore cracked in the first 6-10 cycles. This should be noted if the product considered to be used for some product that will be placed in freezing conditions or low temperature areas such as paving blocks.

7.5 Density

Density of the pastes was an important factor in this research due to its role in the light weight block production. The density of slag was 2300 kg/m³. Slag also increased the flow of the pastes. However it had a major effect on the compressive strength improvement at 28 days. Therefore, slag was not used as a raw material for the final product of this research, for light weight blocks.

Slag is an appropriate material to be used in backfilling projects and road construction, where the density of the materials is not a factor for selecting materials.

7.6 7.6 Achievements and Implications

Block making

This work has significant implications in block making. It was noted in the introduction that currently used mixes (concretes) with cement have significant environmental impacts. The possible reductions in this will be limited by:

Strength limitations: The materials could be used for the low strength products with the 28 day compressive strength less than 20 MPa.

Transport Cost: most of by-product materials should be collected from a special works in the UK e.g. run of station ash from Rugeley Power Station. However Portland cement is available in many locations throughout the UK.

Processing Cost: Some of by-product materials such as waste plasterboard gypsum need to be dried and ground before using.

The benefits of using by-product materials will include reduction in volume of landfilling the by-product materials and the reduced cost.

Backfilling mix

The by-product materials as a cementitious mix have the opportunity to be used for backfilling instead of foam concrete which is normally used as a backfill material. The mix could be pumped and it does not need any special precautions other than standard foam concrete. It has the advantage that there is no risk of the strength increasing to levels which would require re-excavation with structural excavators.

Although cement replacement with by-product materials is an environmentally friendly idea regarding to reduction of CO₂, the existence of heavy metals in the solution leached from the mix during its service life might be one of the Environment Agency's concerns. This was checked in this research with the Inductively Coupled Plasma (ICP) and no heavy metals were found in the solutions. Nevertheless the Environment Agency remains cautious and may delay the work.

8. Conclusions and Recommendations for future work

The following conclusions were made from this research:

- **Manufacture** of light weight block with 100% cement replacement using light weight aggregate **is** a feasible project that can consume by-product materials. The mix 60%ROSA-20%PG-20%BPD has the **potential to be used for light weight block making within the specification set by Hanson. The density of the product (1600-1700 kg/m³ and its compressive strength at 3 days (1.6 MPa) met the criteria.**
- The Coventry blend 80%BOS-15%PG-5%BPD (Ganjian *et al.* 2007) could be used in subway backfilling. **This blend could be used as 100% cement replacement for low strength the concrete in backfilling projects.**
- The source of by-product materials in different batches, even from the same source, can affect physical and chemical characteristics of materials. Therefore the result of each research project may not be reliable and useful for other projects. **Therefore, for every novel product using waste materials as raw material, checking tests should be carried out. For industrial processes in-line analysis should be used as in cement manufacture.**
- Chemical analysis of the waste materials, **Basic Oxygen Slag, By-Pass Dust, Run Of Station Ash, Red Gypsum and Plaster board Gypsum**, shows the chemical compositions of waste materials such as BPD and ROSA from different sources or different batches from one source **were** different.

This affected **the** pozzolanic characteristics and cementitious properties of waste materials.

- Dry-ground red gypsum and crushed plasterboard gypsum could be used as a source of **sulphate** activator with slag, bypass dust and run of station ash to form low compressive strength cementitious pastes without using Ordinary Portland cement.
- ROSA and RG absorbed water during mixing with other materials. They reduced the flow of mixes. However the water absorbed by ROSA was returned to the mix after 3 minutes of mixing.
- BOS did not absorb water when it mixed with other by-product materials. This increased the flow of paste.
- Waste materials may need to be modified. **Physical** properties such as drying, grinding and sieving should be used to make them more effective. For instance PG and RG needed to be dry and ground before sieving. BOS needed to be ground and sieved before mixing to **create a better reaction**.
- The results of binary combinations of the by-product materials showed that ROSA-BPD mixes had the highest compressive strength compare to the other combinations of the raw materials. The highest compressive strength of the binary combinations belonged to the mix 60% ROSA - 40% BPD (22 MPa at 28 days).
- Pastes having BOS could not be used for light weight concrete because the density of the pastes was more than the density of light weight product criteria (1600 kg/m³). Using foaming agent up to 2% of paste weight could reduce the density of the pastes contained BOS. **H**owever foaming agent **also** reduced the compressive strength of the paste. It was concluded that using paste with lighter waste materials such as ROSA other than BOS in paste, and using light weight aggregate could be better option for the light weight products.

- This research showed that waste red gypsum and plasterboard gypsum can be mixed with other waste materials and the mix have the potential to be used in subway backfilling and light weight blocks.
- The five types of selected samples had less compressive strength when soaked in water than the samples cured in containers in the measured humidity of 98% RH.
- Selected samples had higher expansion than the OPC and standard limit. This expansion could be reduced by using aggregates. Mortars had less expansions compare to the pastes. This expansion is not an important factor when the materials are used as backfill materials for mines or wells.
- The results of XRD of all selected mixes showed existence of ettringite in all ages. The ettringite is one of the minerals results compressive strength.
- Artificial neural networks and response surface methods could predict the compressive strength of pastes. However the errors of ANN were less than the other method's errors.
- The results of two methods for predicting the compressive strength were not used for selecting 5 mixes with the highest compressive strength because the sources of some of waste materials (ROSA and BPD) were changed. The models could predict the 28 day compressive strength of the pastes using by-product materials from the same source with the same chemical compositions.

Suggested further work that should be carried out for future research

- The mechanism of chemical reactions of only five pastes were tested in this research, however some other pastes had good potential for more investigation and it is recommended for future researchers to use SEM to find a more accurate model of chemical reactions of waste materials.

- Other construction products can be made using waste gypsum such as paving blocks and mass concrete that can be an ideal topic of a new research.
- Longer curing periods can be used for some pastes, especially those containing BOS, to find out the long term effect of BOS on compressive strength if the paste can be used in other construction products than those with low compressive strength.
- As more tests were carried out on the selected samples, the effect of each material on characteristics of pastes could not be studied. It is recommended that tests are carried out in future studies. For instance, the effect of BOS or other material content on the expansion of samples could be studied.

References

- Adhikary, B. B. and Mutsuyoshi, H. (2006) 'Prediction of Shear Strength of Steel Fiber Rc Beams Using Neural Networks.' *Construction and Building Materials* 20, (9) 801-811
- Akkurt, S., Tayfur, G. and Can, S. (2004) 'Fuzzy Logic Model for the Prediction of Cement Compressive Strength.' *Cement and Concrete Research* 34, (8) 1429-1433
- Al-Jabri, K. S., Taha, R. A., Al-Hashmi, A. and Al-Harthy, A. S. (2006) 'Effect of Copper Slag and Cement by-Pass Dust Addition on Mechanical Properties of Concrete.' *Construction and Building Materials* 20, (5) 322-331
- Ambarish, G. and Chillara, S. (2007) 'Strength Characteristics of Class F Fly Ash Modified with Lime and Gypsum.' *Journal of Geotechnical and Geoenvironmental Engineering* 133, (7) 757-766
- American Society for Testing and Materials (2005) *Standard Test Method for Autoclave Expansion of Hydraulic Cement*. ASTM C151:2005. ASTM International, West Conshohocken, PA, available from <www.astm.org>
- American Society for Testing and Materials (2004) *Standard Practice for Use of Apparatus for the Determination of Length Change of Hardened Cement Paste, Mortar, and Concrete*. ASTM C490:2004. ASTM International, West Conshohocken, PA, available from <www.astm.org>
- American Society for Testing and Materials (2007) *Standard Test Method for Potential Alkali Reactivity of Aggregates (Mortar-Bar Method)*. ASTM C1260:2007. ASTM International, West Conshohocken, PA, available from <www.astm.org>

-
- Andrade, L. B., Rocha, J. C. and Cheriaf, M. (2007) 'Evaluation of Concrete Incorporating Bottom Ash as a Natural Aggregates Replacement.' *Waste Management* 27, (9) 1190-1199
- Babaian P.M, Kejin Wang, Alex Mishulovich, Sankar Bhattacharja and Sh, S. P. (2003) 'Effect of Mechanochemical Activation on Reactivity of Cement Kiln Dust-Fly Ash Systems.' *Materials Journal,ACI* 100, (1), 55-62
- Baro, J., Sanchez-Reyes, A., Chinchon, J. S., Lopez-Soler, A., Vazquez, E. and Yague, A. (1988) 'Natural Radiation in Fly Ashes from Coal Thermal Power Stations in Spain.' *Cement and Concrete Research* 18, (1) 131-137
- Bas, D. and Boyaci, I. H. (2007) 'Modeling and Optimization Ii: Comparison of Estimation Capabilities of Response Surface Methodology with Artificial Neural Networks in a Biochemical Reaction.' *Journal of Food Engineering* 78, (3) 846-854
- Bayramov, F., Tasdemir, C. and Tasdemir, M. A. (2004) 'Optimisation of Steel Fibre Reinforced Concretes by Means of Statistical Response Surface Method.' *Cement and Concrete Composites* 26, (6) 665-675
- Beretka, J., Cioffi, R., Marroccoli, M. and Valenti, G. L. (1996) 'Energy-Saving Cements Obtained from Chemical Gypsum and Other Industrial Wastes.' *Waste Management* 16, (1-3) 231-235
- Berryman, C., Zhu, J., Jensen, W. and Tadros, M. (2005) 'High-Percentage Replacement of Cement with Fly Ash for Reinforced Concrete Pipe.' *Cement and Concrete Research* 35, (6) 1088-1091
- British Standards Institution (1983) *Testing concrete. Method for determination of slump.* BS 1881-102:1983. London: B British Standards Institution

-
- British Standards Institution (2003) *Specification for masonry units. Autoclaved aerated concrete masonry units*. BS EN 771-4:2003. London: B British Standards Institution
- British Standards Institution (2005) *Methods of testing cement: Determination of setting time and soundness*. BS EN 196-3:2005. London: B British Standards Institution
- Buenfeld, N.R. and Stegemann J. A. (1999) 'A Glossary of Basic Neural Network Terminology for Regression Problems ' *Neural Computing & Applications*, 8, (4), 290-296
- Camilleri, J., Sammut, M. and Montesin, F. E. (2006) 'Utilization of Pulverized Fuel Ash in Malta.' *Waste Management* 26, (8) 853-860
- Chai, J. and Raungrut, C. (2003) 'Development of Bottom Ash as Pozzolanic Material.' *Journal of Materials in Civil Engineering* 15, (1) 48-53
- Chandra S., (1997) *Waste Materials Used in Concrete Manufacturing*. NOYES PUBLICATIONS, Westwood, New Jersey, U.S.A., 289 pages
- Churchill E. V., Amirkhanian S. N, (1999) 'Coal Ash Utilization in Asphalt Concrete Mixtures' *Journal of Materials in Civil Engineering*, (11), 4, 295-301
- Cliff, K. D., Green, B. M. R. and Miles, J. C. H. (1985) 'The Levels of Radioactive Materials in Some Common Uk Building Materials.' *The Science of The Total Environment* 45, 181-186
- Çolak, A. (2000) 'Density and Strength Characteristics of Foamed Gypsum.' *Cement and Concrete Composites* 22, (3) 193-200

-
- Davies, D. R. and Kitchener, J. N. (1996) 'Massive Use of Pulverised Fuel Ash in Concrete for the Construction of a U.K. Power Station.' *Waste Management* 16, (1-3) 169-180
- Degirmenci, N., Okucu, A. and Turabi, A. (2007) 'Application of Phosphogypsum in Soil Stabilization.' *Building and Environment* 42, (9) 3393-3398
- Degirmenci, N. (2008) 'Utilization of Phosphogypsum as Raw and Calcined Material in Manufacturing of Building Products.' *Construction and Building Materials* 22, (8) 1857-1862
- Demuth, H., Beale, M. and Hagan, M. (2006) *Neural Network Toolbox for Use with Matlab, User's Guide.* Version 5, The MathWorks, Inc., available from <www.mathworks.com>
- Dias, W. P. S. and Pooliyadda, S. P. (2001) 'Neural Networks for Predicting Properties of Concretes with Admixtures.' *Construction and Building Materials* 15, (7) 371-379
- Dutta, J. R., Dutta, P. K. and Banerjee, R. (2004) 'Optimization of Culture Parameters for Extracellular Protease Production from a Newly Isolated Pseudomonas Sp. Using Response Surface and Artificial Neural Network Models.' *Process Biochemistry* 39, (12) 2193-2198
- Eleni Vassiliadou, C. and Serji, N. A. (1999) 'Coal Ash Utilization in Asphalt Concrete Mixtures.' *Journal of Materials in Civil Engineering* 11, (4) 295-301
- Emery, J. J., "Slag Utilization in Pavement Construction," *Extending Aggregate Resources.* ASTM Special Technical Publication 774, American Society for Testing and Materials, 1982, pp. 95-118

-
- Erdemir, E. T., Batta, R., Spielman, S., Rogerson, P. A., Blatt, A. and Flanigan, M. (2008) 'Location Coverage Models with Demand Originating from Nodes and Paths: Application to Cellular Network Design.' *European Journal of Operational Research* 190, (3) 610-632
- Erdogan, S. T., Martys, N. S., Ferraris, C. F. and Fowler, D. W. (2008) 'Influence of the Shape and Roughness of Inclusions on the Rheological Properties of a Cementitious Suspension.' *Cement and Concrete Composites* 30, (5) 393-402
- Fauziah, I., Zauyah, S. and Jamal, T. (1996) 'Characterization and Land Application of Red Gypsum: A Waste Product from the Titanium Dioxide Industry.' *Science of The Total Environment* 188, (2-3) 243-251
- Felix, F. U. and Abdul, H. (2002) 'Strengths of Cement Kiln Dust Concrete.' *Journal of Materials in Civil Engineering* 14, (6) 524-526
- Freidin, C. (2007) 'Cementless Pressed Blocks from Waste Products of Coal-Firing Power Station.' *Construction and Building Materials* 21, (1) 12-18
- Ganjian, E., Claisse, P. and Pouya, H. S. (2007) *The Use of Plaster Board and Gypsum Waste in Road Bases, Sub-Bases and Stabilised Sub-Grade*. Final Report Coventry University, Project Code BPD5-002, 148 pages
- Ganjian, E., Claisse, P., Tyrer, M. and Atkinson, A. (2004) 'Preliminary Investigations into the Use of Secondary Waste Minerals as a Novel Cementitious Landfill Liner.' *Construction and Building Materials* 18, (9) 689-699
- Gomes, H. M. and Awruch, A. M. (2004) 'Comparison of Response Surface and Neural Network with Other Methods for Structural Reliability Analysis.' *Structural Safety* 26, (1) 49-67

-
- Heikal, M., Aiad, I. and Helmy, I. M. (2002) 'Portland Cement Clinker, Granulated Slag and by-Pass Cement Dust Composites.' *Cement and Concrete Research* 32, (11) 1805-1812
- Hossain, K. M. A. (2003) 'Blended Cement Using Volcanic Ash and Pumice.' *Cement and Concrete Research* 33, (10) 1601-1605
- Hughes, P. (2006) '*The Use Off Synthetic Red Gypsum as a Construction Material*' PhD thesis, Newcastle University
- Illston J.M. and Domone, P. L. J. (2006) *Construction Materials Their Nature and Behaviour*. London and New York: Spon Press, 3, 554 pages
- Ji, T., Lin, T. and Lin, X. (2006) 'A Concrete Mix Proportion Design Algorithm Based on Artificial Neural Networks.' *Cement and Concrete Research* 36, (7) 1399-1408
- John, D. A. S. and Sims, A. B. P. A. I. (1998) *Concrete Petrography a Handbook of Investigative Techniques*. First edn.: John Wiley and Sons
- John V.M. Zordan S.E. (2001), 'Research & development methodology for recycling residues as building materials— a proposal.' *Waste Management*, 21, (3) 213-219
- Jones, M. R. and Mccarthy, A. (2005) 'Utilising Unprocessed Low-Lime Coal Fly Ash in Foamed Concrete.' *Fuel* 84, (11) 1398-1409
- Jones, M. R., Mccarthy, A. and Booth, A. P. P. G. (2006) 'Characteristics of the Ultrafine Component of Fly Ash.' *Fuel* 85, (16) 2250-2259

-
- Kiattikomol, K., Jaturapitakkul, Ch., Songpiriyakij, S., Chutubtim, S. (2001) 'A study of ground coarse fly ashes with different finenesses from various sources as pozzolanic materials' *Cement and Concrete Composites* 23, (4-5), 335-343
- Konsta-Gdoutos, M. S. and Shah, S. P. (2003) 'Hydration and Properties of Novel Blended Cements Based on Cement Kiln Dust and Blast Furnace Slag.' *Cement and Concrete Research* 33, (8) 1269-1276
- Kumar, S. (2002) 'A Perspective Study on Fly Ash-Lime-Gypsum Bricks and Hollow Blocks for Low Cost Housing Development.' *Construction and Building Materials* 16, (8) 519-525
- Kumar, S. (2003) 'Fly Ash-Lime-Phosphogypsum Hollow Blocks for Walls and Partitions.' *Building and Environment* 38, (2) 291-295
- Kuo, S. T. (1996) 'Experiences of Coal Ash Artificial Reefs in Taiwan.' *Fuel and Energy Abstracts* 37, (3) 185-1406
- Kurama, H. and Kaya, M. (2008) 'Usage of Coal Combustion Bottom Ash in Concrete Mixture.' *Construction and Building Materials* 22, (9) 1922-1928
- Lachemi, M., Hossain, K. M. A., Shehata, M. and Thaha, W. (2008) 'Controlled Low Strength Materials Incorporating Cement Kiln Dust from Various Sources.' *Cement and Concrete Composites* 30, (5) 381-392
- Lachemi, M., Hossain, K. M. A., Lambros V., Nkinamubanzi, P. -C., Bouzoubaâ N., (2004) Performance of new viscosity modifying admixtures in enhancing the rheological properties of cement paste *Cement and Concrete Research*, 34, (2) 185-193
- Luxan, M. P., Sanchez De Rojas, M. I. and Frias, M. (1989) 'Investigations on the Fly Ash-Calcium Hydroxide Reactions.' *Cement and Concrete Research* 19, (1) 69-80

-
- Mahieux, P. Y., Aubert, J. E. and Escadeillas, G. (2008) 'Utilization of Weathered Basic Oxygen Furnace Slag in the Production of Hydraulic Road Binders.' *Construction and Building Materials*, 23, (2), 742-747
- Malhotra, A. B. A. V. M. (2000) 'High-Volume Fly Ash System: Concrete Solution for Sustainable Development.' *ACI* 97, (1)
- Mandal, A. and Roy, P. (2006) 'Modeling the Compressive Strength of Molasses-Cement Sand System Using Design of Experiments and Back Propagation Neural Network.' *Journal of Materials Processing Technology* 180, (1-3) 167-173
- Micah Hale, W., Freyne, S. F. and Russell, B. W. (2008) 'Examining the Frost Resistance of High Performance Concrete.' *Construction and Building Materials* 23, (2) 878-888
- Min, Y., Jueshi, Q. and Ying, P. (2008) 'Activation of Fly Ash-Lime Systems Using Calcined Phosphogypsum.' *Construction and Building Materials* 22, (5) 1004-1008
- Mohd, S., Wah, C. K., Lim, P. Y. and Zingoni, A. (2001) 'Development of Artificial Lightweight Aggregates.' In *Structural Engineering, Mechanics and Computation*. Oxford: Elsevier Science: 1399-1406
- Monshi, A. and Kasiri Asgarani, M. (1999) 'Producing Portland Cement from Iron and Steel Slags and Limestone.' *Cement and Concrete Research* 29, (9) 1373-1377
- Montgomery, D. C. (2005) *Design and Analysis of Experiments*. 6th edn. John Wiley & Sons Inc.
- Motz, H. and Geiseler, J. (2001) 'Products of Steel Slags an Opportunity to Save Natural Resources.' *Waste Management* 21, (3) 285-293

-
- Mun, K. J., Hyoung, W. K., Lee, C. W., So, S. Y. and Soh, Y. S. (2007) 'Basic Properties of Non-Sintering Cement Using Phosphogypsum and Waste Lime as Activator.' *Construction and Building Materials* 21, (6) 1342-1350
- Neville A. M. (1995) *Properties of Concrete*. Fourth edn.: Longman Group Limited, 864 pages
- Ni, H.-G. and Wang, J.-Z. (2000) 'Prediction of Compressive Strength of Concrete by Neural Networks.' *Cement and Concrete Research* 30, (8) 1245-1250
- Nikolaidis, E., Long, L. and Ling, Q. (2000) 'Neural Networks and Response Surface Polynomials for Design of Vehicle Joints.' *Computers & Structures* 75, (6) 593-607
- Nisnevich, M., Sirotnin, G., Schlesinger, T. and Eshel, Y. A. (2008) 'Radiological Safety Aspects of Utilizing Coal Ashes for Production of Lightweight Concrete.' *Fuel* 87, (8-9) 1610-1616
- Özkan, O., Yuksel, I. and Muratoglu, O. (2007) 'Strength Properties of Concrete Incorporating Coal Bottom Ash and Granulated Blast Furnace Slag.' *Waste Management* 27, (2) 161-167
- Öztaş, A., Pala, M., Özbay, E., Kanca, E., Çağlar, N. and Bhatti, M. A. (2006) 'Predicting the Compressive Strength and Slump of High Strength Concrete Using Neural Network.' *Construction and Building Materials* 20, (9) 769-775
- Pal, S. C., Mukherjee, A. and Pathak, S. R. (2003) 'Investigation of Hydraulic Activity of Ground Granulated Blast Furnace Slag in Concrete.' *Cement and Concrete Research* 33, (9) 1481-1486
- Papageorgiou, A., Tzouvalas, G. and Tsimas, S. (2005) 'Use of Inorganic Setting Retarders in Cement Industry.' *Cement and Concrete Composites* 27, (2) 183-189

-
- Picton, P. (1994) *Introduction to Neural Network*. First edn. The Macmillam Press Ltd London
- Pouya H. S., Ganjian E., Claisse P., and Karami S. (2007) 'Strength Optimization of Novel Binder Containing Plasterboard Gypsum Waste' *Materials Journal* 104, (6) 653-659
- Puertas, F., Martínez-Ramírez, S., Alonso, S. and Vázquez, T. (2000) 'Alkali-Activated Fly Ash/Slag Cements: Strength Behaviour and Hydration Products.' *Cement and Concrete Research* 30, (10) 1625-1632
- Ramesh, C. J., Joonu, O. T. and Rex, B. A. (1992) 'Properties of Gypsum Wallboards Containing Fly Ash.' *Journal of Materials in Civil Engineering* 4, (2) 212-225
- Reddy, A. S., Pradhan, R. K. and Chandra, S. (2006) 'Utilization of Basic Oxygen Furnace (Bof) Slag in the Production of a Hydraulic Cement Binder.' *International Journal of Mineral Processing* 79, (2) 98-105
- Rugeley Power Station (2007), available from <http://www.rugeleypower.com/Pages/envi%202.htm>
- Shi, C. (2004) 'Steel Slag- Its Production, Processing, Characteristics, and Cementitious Properties.' *American Society of Civil Engineers (ASCE)*, 16, (3), 230-236
- Shi, C. and Hu, S. (2003) 'Cementitious Properties of Ladle Slag Fines under Autoclave Curing Conditions.' *Cement and Concrete Research* 33, (11) 1851-1856
- Shih, P.-H., Wu, Z.Z. and Chiang, H.-L. (2004) 'Characteristics of Bricks Made from Waste Steel Slag.' *Waste Management* 24, (10) 1043-1047

-
- Singh, M., Garg, M. (1995) 'Activation of Gypsum Anhydrate-Slag Mixture.' *Cement and Concrete Research* 25, (2), 332-338
- Singh, M. (2002) 'Treating Waste Phosphogypsum for Cement and Plaster Manufacture.' *Cement and Concrete Research* 32, (7) 1033-1038
- Singh, S. P., Tripathy, D. P. and Ranjith, P. G. (2008) 'Performance Evaluation of Cement Stabilized Fly Ash-Gbfs Mixes as a Highway Construction Material.' *Waste Management* 28, (8) 1331-1337
- Sonebi, M. (2004) 'Medium Strength Self-Compacting Concrete Containing Fly Ash: Modelling Using Factorial Experimental Plans.' *Cement and Concrete Research* 34, (7) 1199-1208
- Sreekrishnavilasam, A., Rahardja, S., Kmetz, R. and Santagata, M. (2007) 'Soil Treatment Using Fresh and Landfilled Cement Kiln Dust.' *Construction and Building Materials* 21, (2) 318-327
- Swamy, R. N. and Lambert, G. H. (1983) 'Mix Design and Properties of Concrete Made from Pfa Coarse Aggregates and Sand.' *International Journal of Cement Composites and Lightweight Concrete* 5, (4) 263-275
- Taha, R. A., Alnuaimi, A. S., Al-Jabri, K. S. and Al-Harthy, A. S. (2007) 'Evaluation of Controlled Low Strength Materials Containing Industrial by-Products.' *Building and Environment* 42, (9) 3366-3372
- Tam, V. W. Y., Tam, C. M. and Wang, Y. (2007) 'Optimization on Proportion for Recycled Aggregate in Concrete Using Two-Stage Mixing Approach.' *Construction and Building Materials* 21, (10) 1928-1939

Tarassenko, L. (1998) *A Guide to Neural Computing Applications*. Published by Butterworth-Heinemann, New York, 139 pages

Tarmac (2006), available from <<http://www.tarmac.co.uk/STEELINDUSTRYBY-PRODUCTFINDSANEWUSETREATINGCONTAMINATEDLAND.aspx>>

Taylor, H. F. W. (1997). *Cement Chemistry*. Thomas Telford, London, 459 pages

Tüfekçi M., Demirbas, A. and Genc, H. (1997) 'Evaluation of Steel Furnace Slags as Cement Additives.' *Cement and Concrete Research* 27, (11) 1713-1717

White D.J., (2006) 'Reclaimed Hydrated Fly Ash as a Geomaterial' *Journal of Materials in Civil Engineering*, (18), 2, 206-213

Wise, D.L. Trantolo, D.J. , Altobelli, D.E. Gresser,J.D. Yaszemski, M.J. (1995) '*Encyclopaedic Handbook of Biomaterials and Bioengineering*', Taylor & Francis, 1795

Woolley, G. R. G., J C Inst Civ Engr Proc (1984) 'Prestressed Precast Piling at Drax Power Station and the Use of Pulverized Fuel Ash Replacement in Concrete ' *International Journal of Rock Mechanics and Mining Science & Geomechanics Abstracts* 76, (5) 473-493

Yazici, H. (2008) 'The Effect of Silica Fume and High-Volume Class C Fly Ash on Mechanical Properties, Chloride Penetration and Freeze-Thaw Resistance of Self-Compacting Concrete.' *Construction and Building Materials* 22, (4) 456-462

Zhao, F.-Q., Ni, W., Wang, H.-J. and Liu, H.-J. (2007) 'Activated Fly Ash/Slag Blended Cement.' *Resources, Conservation and Recycling* 52, (2) 303-313

CONFIDENTIAL**GYPSUM WASTE REDUCTION. Mini-Waste Faraday Research Proposal.****Case For Support****Part 1 Previous Research Track Record****Recent work in area by the partners.**

Imperial College and Coventry University are currently working on the Landfill Barriers project (1,2) which has been funded with 0.5M pounds, primarily from landfill tax. In this work a very wide range of different mineral wastes are being mixed to make concretes and used to make barriers to act as liners below landfills to contain the leachate. Examples of the materials used are in table 1. The work has included some site trials, which contain 60 m³ of waste-derived concrete. Extensive physical and chemical testing of the concretes has been carried out.

Component in mix	Material	Source
Cementitious matrix	Soda Slag	Pyrometallurgical refining of lead
	Borax slag	Silver refining
	Lagoon Ashes	Power Generation (note that these are not classified ash which can be sold)
	Municipal Waste Ash	Waste incineration
	Cement Kiln Dust	Cement Manufacture
	Granulated Blastfurnace slag	Steel production (note that this is not the ground product which can be sold)
	Ground Glass	Waste glass which cannot be re-used
	Limex 70	Sugar refining
	Red Gypsum	Titanium oxide pigment manufacture
Mixture liquid	Sodium sulphate solution	Lead-acid batter recycling
Aggregates	Foundry sands	Metal casting moulds
	Ferrosilicate slag	Various applications in pyrometallurgy
	Chrome alumina	Chromium manufacture
	Crushed furnace bricks	Rotary furnaces linings

Table 1 Waste materials used in the Barriers project

Coventry University and Lafarge Plasterboard Ltd. are partners in the "Cleanlead" programme which is a major EU Framework 5 research project investigating ways of producing clean gypsum from spent acid from lead-acid batteries. This project is comparing a wide variety of systems including nanofiltration, diffusion dialysis, chemical precipitation, hydrocycloning and biological systems to remove contaminants. The project partners have also developed a very clear definition of the properties of gypsum which are required by different industrial users.

Coventry and Imperial are also working on a contract for Huntsman Tioxide to develop uses for red gypsum. This is a short 6 month contract ending in December 2003 which includes a small site trial of a controlled low strength material as a trench backfill and will provide useful initial data for the full investigation in the current proposal.

Birmingham University have undertaken research into stabilising soils for trench backfill and low cost roads. Trench backfill was funded by the EPSRC (grant references: GR/H 53389 – 1992 to 1995 and GR/M27210 – 1998 to 2001) and the DfID has provided funds for investigation into stabilisers for low cost roads. The last of the DfID projects is underway at present, wherein students based in Bangladesh are under training at the University of Birmingham. Dr Ghatora has most recently been involved with the improvement of stiffness of railway subgrade (EPSRC grant ref: GR/M/76508/01).

Our contribution to “UK PLC”

As an example, the Landfill Liners project is about to start its large scale demonstration phase. Both the industrial partners (Biffa PLC) and the Environment Agency have expressed confidence in the developed technology. When adopted, this technology will make use of 1.5 Mt of material in the UK alone that would otherwise have gone to waste each year and become part of the landfill inventory. This five year programme seeks to use waste to contain waste and has received very positive acclaim from both the waste management industry and regulatory authorities.

Specific expertise available**Coventry University**

Dr Peter Claisse is a Civil Engineer many years' experience in construction and in research into construction materials. He leads a group with interests in using secondary aggregates and novel cementitious binders as construction materials. Dr Esmail Ganjian is a Civil Engineer currently working on major projects on the production of concrete using waste materials.

Imperial College

Professor Alan Atkinson is a leading expert in cementitious materials and as Professor of materials chemistry heads a group concerned with many functional materials, with particular applications in energy and resource efficiency. Dr Mark Tyrer is a Geochemist with interests in pozzolanic cements, especially as applied to pollution control.

Birmingham University

Dr Gurmel Ghataora is a Geotechnical Engineer with interests in ground stabilisation and excavation backfill technology, using cementitious materials.

Lafarge Plasterboard

Steve Hemmings brings a wealth of knowledge in plaster products for the construction industry. Lafarge are the largest cement company in the world and major manufacturers of plaster and plaster products.

Huntsman – Tioxide

The Huntsman group is a major chemical company with world-wide interests and Dr Brian Noble directs research within their titanium dioxide plant on Teeside. His knowledge of both the process chemistry and commercial aspects of gypsum production add considerable value to the team.

The City of Birmingham is at the forefront of using recycled materials in road construction and backfill and will provide expertise and facilitate the site trials.

Specific Justification of the inclusion of Post-Doctoral Research Assistants at Spine Points 15 and 18

Two areas of this research rely on contributions from Named Researchers, Drs Ganjian and Tyrer. Together with Dr Claisse and Professor Atkinson, they have been instrumental in the research, which lead to this proposal.

The area of controlled low strength materials in its relative infancy and Dr Ganjian has been responsible for developing both novel compositional mixes and in optimising their rheology. This is an exciting and potentially commercial area of construction materials and one in which Dr Ganjian has considerable expertise. Dr Tyrer is very familiar with computational thermodynamics, particularly as applied to simulations of mineral interactions with aqueous solutions. Such expertise is necessary for the efficient optimisation of the process and the technique will ensure that the experimental programme concentrates on those systems predicted to have the highest impact on waste prevention and re-use. These researchers have complimentary skills and the Coventry-Imperial consortium has worked together successfully for six years.

Part 2. Description of research

Background. Introduction to topic and context: Past and current work.

Sources of by-product Gypsum

Flue gas desulphurisation at power stations is the single largest source of secondary gypsum with 600kt produced in the UK and 16Mt in the EC in 2000. After a temporary rise to 1.5Mt in 2005, UK arisings are expected to fall substantially as domestic coal supplies are replaced with low-sulphur imported coal by 2015.

Titanium oxide pigment production yields 250kt of “red” and 84kt of clean “white” gypsum per year in the UK. Worldwide production of red gypsum is 1.25Mt from one producer alone (Huntsman Tioxide). This material contains approximately 40% moisture, 16% iron oxides, 0.5% of both Mn and SiO₂, 0.2% of Al and TiO₂ and many other elements. These render it unacceptable to the plaster and cement industries, principally due to its iron content, which may cause staining in plaster products and adversely affects cement clinker chemistry.

Waste gypsum also arises from plasterboard off-cuts from construction sites and spent casting cores from foundries and very many areas of chemical manufacturing produce secondary gypsum from acid neutralisation. In order to meet demand, substantial amounts of quarried gypsum are also used in this country and the UK is a net importer of gypsum.

Current Uses of Gypsum

Clean gypsum such as flue gas gypsum and white by-product titano-gypsum finds a ready market in cement and plasterboard manufacture. Changes in building regulations requiring thicker plasterboard are creating increased demand. Limited amounts of plasterboard off-cuts can be used in new board manufacture but the paper content restricts the proportions and transport costs can be prohibitive. Lafarge’s estimated quantity of surplus waste board is 30kt per year.

Contaminated gypsum such as red titano-gypsum, waste plasterboard and spent casting cores is used as a soil conditioner but this is expected to end in 2004-05 due to environmental concerns and much of it is already landfilled. There is an urgent need to limit the waste of this material and this proposal seeks both to reduce red gypsum production through chemical processing and to establish new uses in the construction and casting industries.

Potential Uses of contaminated gypsum identified by the proposers.

Sulphate activated Pozzolans. The product formed from intergrinding blastfurnace slag and hemihydrate is known as supersulphated cement (SSC) and this was widely used in foundation engineering until the advent of speciality sulphate-resisting cements in the mid 20th century. The use of SSC has declined in recent decades for economic reasons, yet it remains an eminently viable engineering material.

A potential use for sulphate activated pozzolans is to make Controlled Low Strength Materials (CLSM) (3) which are low strength mortars and are used for trench-fill and other general backfill applications. These materials are rapidly gaining market share in the USA from conventional products such as foamed concretes. In the UK a study by TRRL in 1998 showed that about 70% of the problems with trench backfill resulted from inadequate compaction. These could be avoided with flowing backfill materials that do not require compaction (4,5).

Concretes for road foundations and sub-bases for car parks and other hard standing are other potential uses. Gypsum is already permitted in EU standard prEN14227-3 for road foundations containing ash.

Water-resistant gypsum plaster. Plaster products produced from coloured gypsum must be made water-resistant to prevent staining (in particular the discoloration of water-based paints). Conventional water resisting plasters (such as tile grouts) comprise hemihydrate grains whose surfaces have been coated in a hydrophobic compound, typically long chain aliphatics. On wetting, the hydration reaction occurs preferentially where the organic coating is thin or missing; at the grain boundaries. The hydrated product consists of a slightly porous mass of gypsum crystals, the organic compounds lining the surfaces of the pores, thus imparting a degree of water resistance on the product.

Self-heated product forming. In plaster manufacture the gypsum must be calcined to form hemihydrate before it may be formed into the desired shape by re-hydration. Recent work (6) suggests that a self-heated synthesis route exists by which products may be formed from a mixture of waste gypsum, free lime and sulphuric acid. This utilises the heat of neutralisation of the system to raise the temperature of the mixture (we speculate) above the thermodynamic phase boundary between gypsum and anhydrite. On cooling, the anhydrite reacts with its pore solution to produce gypsum which takes on the form of the mould into which the mixture is pressed.

Production of clean gypsum from the titanium oxide process.

A number of processes for the production of clean gypsum have been researched in the past, such as complexation with a chelating agent, or recovery of either gypsum and/or iron from the final red gypsum precipitate. These processes have not been implemented by the industry, on account of their low cost efficiency, poor scalability etc.

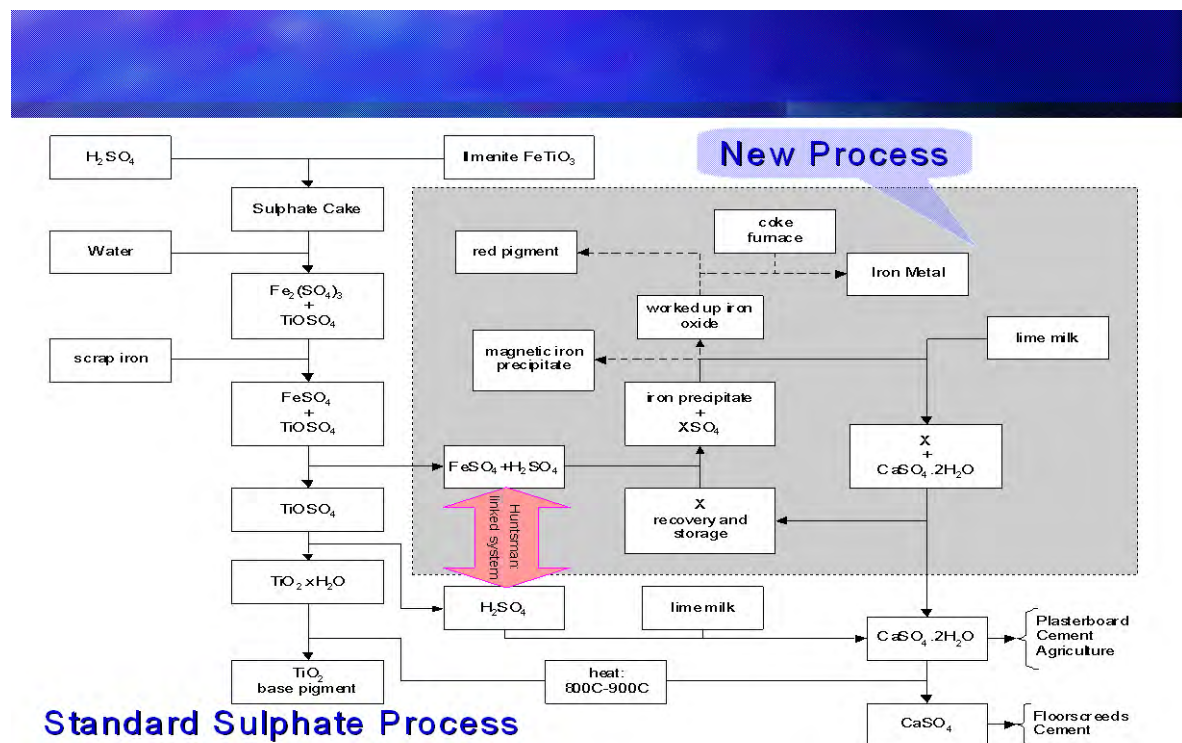


Figure 1. The new process for clean gypsum production.

The proposers have carried out preliminary work (including an initial lab trial) on a new system which addresses these problems by precipitating iron and gypsum in separate parts of the process. Prior to secondary gypsum formation, the iron is present as dissolved ferrous sulphate, which co-precipitates during acid neutralisation with limestone. The proposed process is shown in Figure 1 and introduces an intermediary process step, using a chemical agent (of which there are a variety that can be investigated) to remove the iron by precipitation. The resulting filtrate is then worked up, simultaneously recovering the chemical agent, which will be recycled in the process, and producing pure gypsum. The iron

precipitate could be introduced as feedstock in siderurgical operations, alternative uses in pigments and magnetic applications will also be investigated. Consequently, the process does not generate any additional waste streams

Aims:

The aims of this project are:

1. To develop uses for contaminated gypsum.
2. To develop processes to produce clean gypsum in place of contaminated gypsum.

Specific Objectives:

- 1a. Cementitious products will be developed and tested using sulphate activated pozzolanic mixes.
- 1b. Controlled low strength materials will be made using sulphate activated mixes and site trials will be carried out with them
- 1c. The self-heated route for product forming from waste gypsum will be developed and samples from it will be tested.
2. The new process for clean gypsum production from the titanium oxide process will be developed.

Programme and Methodology

At **Coventry University** research will be carried out on products made from sulphate activated pozzolans with contaminated gypsum. These will include blocks and other formed items such as coving for internal construction and mould materials for glass and metal casting. The developed products may contain fine aggregate such as spent foundry sand or metallurgical slags. The alkali will be lime-slaker dross or cement kiln dust. The pozzolanic material is most likely to be unclassified pulverised fuel ash, incinerator ash or slag although a full range of industrial by-products will be investigated.

Coventry University already has access to a very wide range of potential components for the mixes and a large number of different combinations of them will be used. The numbers of materials will be far too large to complete a “full matrix” of tests in which all combinations are mixed so initial formulations will be based on experience from previous projects and an understanding of the hydration processes. The procedure will include measurement of wet properties including viscosity and setting time and then, after curing, measurement of strength, permeability and leaching. In order to reduce leaching conventional hydrophobic compounds will be tested but mixes which inhibit leaching without them will also be sought. Different methods of air entrainment (admixtures and compressed air feed) will be tested to reduce the mass of the products.

Materials characterisation, both of the materials chemistry and microstructure of the component materials and of the trial mixes will be carried out using facilities at Coventry and Imperial. This will include analytical electron microscopy and x-ray diffraction and, if time permits, thermal analysis and surface analysis alongside classical techniques such as analytical chemistry and petrographic microscopy.

The hydration mechanisms will be investigated with particular emphasis on minor contaminants which may accelerate or poison the process. Effective limits on the constituents of the wastes will be proposed and a formalism established by which by-product gypsum may be selected for a specific use, based on its composition.

Birmingham University will work on the use of CLSM grouts in soil. They will continue the materials development work carried out by Coventry University on landfill barriers and in this contract and apply this to trench backfills. This will build on their existing expertise in ground improvement. Backfill grouts will be developed to comply with the strength and durability requirements in the existing HUAC specifications for highway use and anticipated revisions to it.

At least one field trial will be carried out and monitored through a winter season. The performance will be monitored by surveying and cores will be recovered from it for laboratory testing for strength. The performance of the trial will be compared with control sections constructed with standard techniques.

Imperial College will work on the self-heated synthesis of products from gypsum and on the production of clean gypsum from the titanium oxide process. Both of these chemical processes are at a very early stage of development and initial work will be based on trying to replicate previous results.

The self-heated synthesis has not been attempted on red gypsum and this will be done as soon as the process has been demonstrated on clean gypsum. Any effects of impurities will be investigated. Formed products will be sent to Coventry University for mechanical testing and measurements of leaching and permeability and conversely, Imperial will examine the chemistry and microstructure of CLSM materials produced at Coventry.

A bench-top process for the production of clean gypsum will be established and the properties of the products will be measured. The gypsum morphology and particle size and aspect ratio will be measured (these properties are critical to plasterboard production). Test panels of plasterboard will be made. In addition samples will be inter-ground with cement clinker using the ball mill at Coventry and the properties of the resulting cement will be examined.

If time permits trial batches of iron precipitates from the process will be investigated for siderurgical, pigment and magnetic applications. For this work potential users of the material will supply specifications and the physical and chemical properties will be matched to them. If this is successful samples from the process will be supplied to the users for further trials.

Programme

		Months	0-6	6-12	12-18	18-24	24-30	30-36
1a	Formed products (Coventry)	Mix designs and initial casting	*	*	*			
		Materials characterisation	*	*	*	*		
		Permeability and leach tests		*	*	*	*	
		Mechanical tests		*	*	*		
		Air entrainment trials			*	*		
		Microstructural analysis				*	*	
		Development of guidelines for mixes					*	*
1b	Controlled low strength materials (Birmingham)	Review of uses of CLSM and relevant standards	*	*				
		Laboratory mix design development		*	*	*		
		Field trial				*	*	
		Monitoring and further development				*	*	*
1c	Self-heated synthesis (Imperial/Coventry)	Pilot process development	*	*	*			
		Trials with contaminated samples		*	*	*	*	
		Product forming			*	*	*	
		Product testing				*	*	
2	Clean gypsum production. (Imperial)	Pilot process development	*	*				
		Sample analysis		*	*	*		
		Cement intergrinding trials			*	*	*	
		Plasterboard trials			*	*	*	
		Testing of precipitates				*	*	
	Final report						*	

Justification of methodology

The principal methods which are proposed for this project have been used with considerable success in the “Landfill Liners” and “Cleanlead” projects.

Timeliness and novelty

The various factors which are combining to increase demand and reduce supply of clean gypsum and to increase disposal costs of waste gypsum make this project of particular importance to UK industry. We are confident that no similar work has been carried out in this area.

Relevance to Beneficiaries

This threat of changes in the Waste Management Licensing Regulations (which will prevent agricultural use of waste gypsum) is significant to both producers of gypsum by-products and gypsum based-materials, and finding new viable uses for any type of gypsum by-product is essential. Without new uses for the red gypsum and waste plasterboard, the disposal costs will be increasingly significant. As the UK continues to import gypsum, there is no doubt that by-product gypsum produced to prevailing specifications will find a use, lowering the need for such imports and providing domestic economic growth.

The environmental impact of the work is potentially substantial. Lafarge plasterboard imported 440kt of natural mined gypsum and substantial amounts of plasterboard in 2000. Apart from the depletion of natural resources we estimate that this operation produced 240t of CO₂ and the UK produces around a million tonnes of by-product gypsum each year. The major portion of this is landfilled.

The larger impact will, however, be in replacing cement based products such as building blocks and foamed concrete with sulphate activated pozzolans. If 50% of the red gypsum arisings could be used to replace cement this would save 125kt of CO₂ emissions each year. Replacing fired clay would give similar benefits.

The plasterboard production process itself produced 67kt of CO₂ in 2000 and the self-heated product forming system has the potential to avoid a significant part of this.

The increasing use of the CLSM as a trench backfill will bring benefits to the public in the form of better road surfaces and more rapid re-opening of roads after trench excavations. This will also bring economic benefits to local authorities.

Impact of work

Contaminated gypsum is a very large volume waste stream. A single landfill site at Roxby on South Humberside, already contains over 1Mt of red gypsum. This work offers an opportunity to prevent further additions to this total and to reduce imports of natural gypsum at the same time.

The production of concrete is of particular value in that it uses wastes from different categories such as slags from the metals industries, waste plasterboard from construction and mineral wastes such as the red gypsum and combines them to produce a new product.

Likely benefits

As an example, current annual production of red gypsum at the Huntsman Tioxide Grimsby plant is 250,000 tonnes. The scope for reducing industrial waste is therefore considerable. The market for clean gypsum is substantial and expanding, so all of this material could be used if it was clean. The market for CLSM would be sufficient to use these quantities if it developed to the level currently found in parts of the USA. This project therefore has ample potential to have a significant impact on industrial waste arisings.

The training value of this project is high; three Ph.D. students will be eligible to become Faraday Associates and each will gain an understanding of the pigment, construction and waste management industries. The students will make planned visits to the other universities in order that they can become familiar with the different experimental techniques in use in the project. Before each of the six-monthly project meetings there will be a 1-2 day research seminar or training workshop in which they will present their results in detail and receive training in specific techniques at each host institution.

Collaboration with beneficiaries

This project will deliver environmental benefits of waste reduction and resource conservation, which will affect the wider community. However the immediate beneficiaries will be waste gypsum producers and gypsum users. The largest of these in the UK are project partners. The industrial partners will attend progress meetings every 6 months and will also provide technical assistance and information throughout the project.

Dissemination and exploitation

Because the work will be carried out in close collaboration with potential end users, all the results will be available for use as soon as they arise. The collaboration agreement between the partners will be worded to ensure that the IPR will benefit UK industry. The results will also be published in journals and conference proceedings. In addition, the project will culminate in a conference on The Use of Gypsum Wastes in Construction, hosted by the Society of Chemical Industry and will generate project titles to be offered to taught masters students.

Justification of resources

The resources for this project are almost entirely for staff costs, primarily for the 3 research students who will become Faraday Associates. The students will each have a separate area of work, but there will be considerable interaction between them. The supervision of the students will be the responsibility of the Investigators but the Recognised Researchers, who are established Research Fellows, will provide considerable additional resources to assist the students and help train them in research methods.

REFERENCES

1. E.Ganjian, P.A.Claisse, M.Tyrer and A.Atkinson, 'Selection of cementitious mixes as a barrier for landfill leachate containment', ASCE Journal of Materials in Civil Engineering, accepted for publication Aug 2003
2. Claissé, P A Atkinson A, Ganjian E and Tyrer M, "Recycled Materials in Concrete Barriers" ACI publication SP212-59. Proc. 6th Canmet/ACI conference on the Durability of Concrete, Thessaloniki, Greece, June 2003 pp.951-971.
3. ACI Committee 229, "Controlled low-strength materials, state of the art report". In "ACI manual of concrete practice, 2003", American Concrete Institute, Farmington Hills, MI, USA.
4. Ghatora G S, Alobaidi I M and Billam J . (2000) "The use of pulverised fuel ash in a trench backfill" ASCE Journal of Materials in Civil Engineering, Vol 12 No 3 pp.228-237.
5. Ghatora G S, Alobaidi I M Faragher W and Grant S (2004). Use of recycled granular materials in no-compaction trench backfill. In publication, ICE "Transport" Proceedings.
6. A. Kostic-Pulek, S. Marinkovic, V. Logar, R. Tomanec, S. Popov, "Production Of Calcium Sulphate Alpha-Hemihydrate From Citrogypsum In Unheated Sulphuric Acid Solution", Ceramics-Silikaty 44 (3) 104-108 (2000)

The results of XRD test on selected samples at 3, 7 and 28 days are shown in this Appendix. The discussion on these results is done in chapter 4 of this thesis.

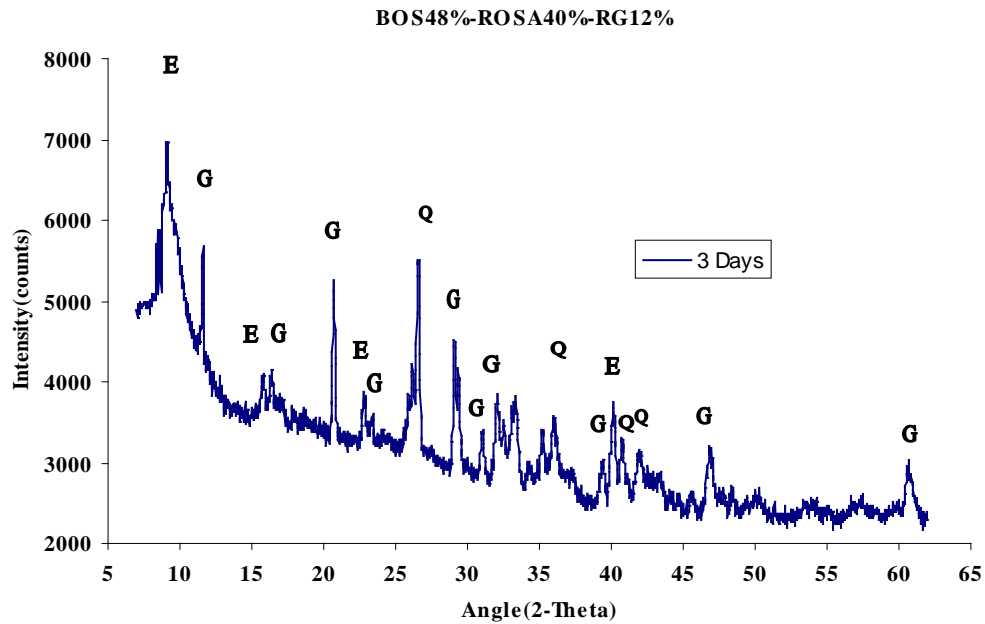


Figure B- 1 XRD of BOS-ROSA-RG at 3 days-E=Ettringite, G=Gypsum, Q=Quartz

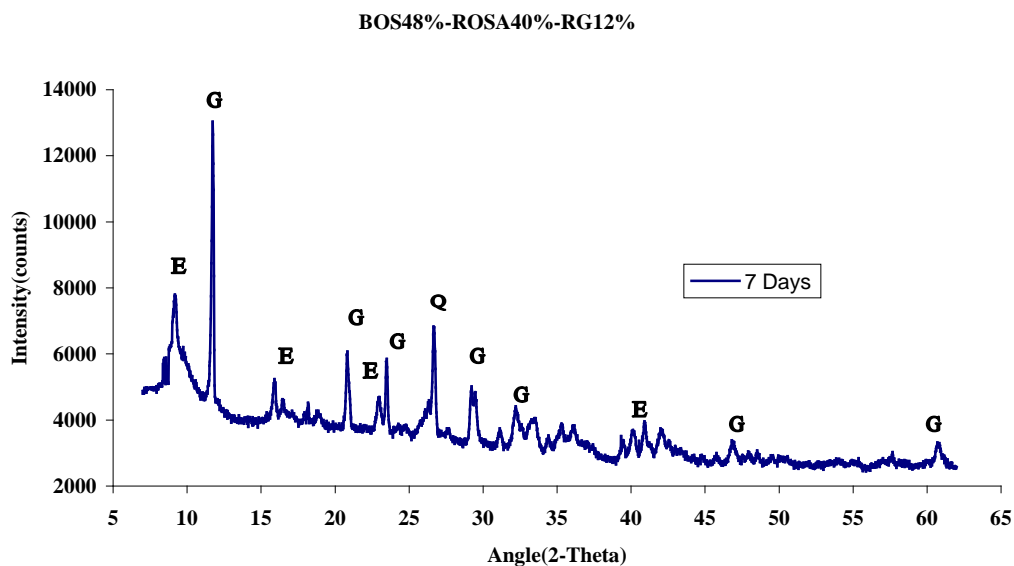


Figure B- 2 XRD of BOS-ROSA-RG at 7 days-E=Ettringite, G=Gypsum, Q=Quartz

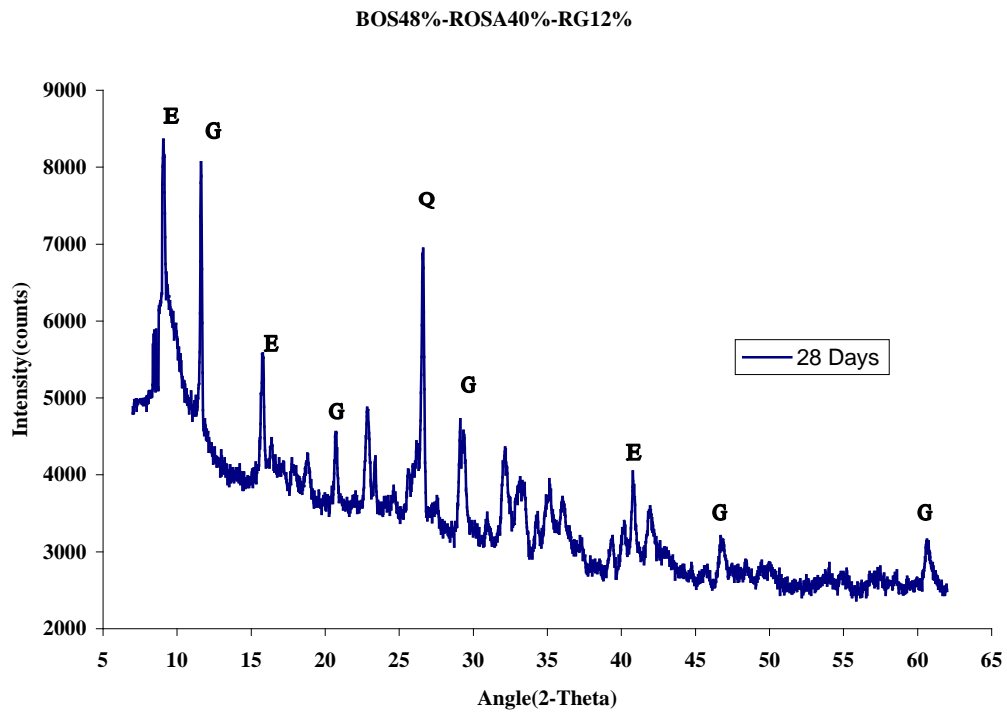


Figure B- 3 XRD of BOS-ROSA-RG at 28 days-E=Ettringite, G=Gypsum, Q=Quartz

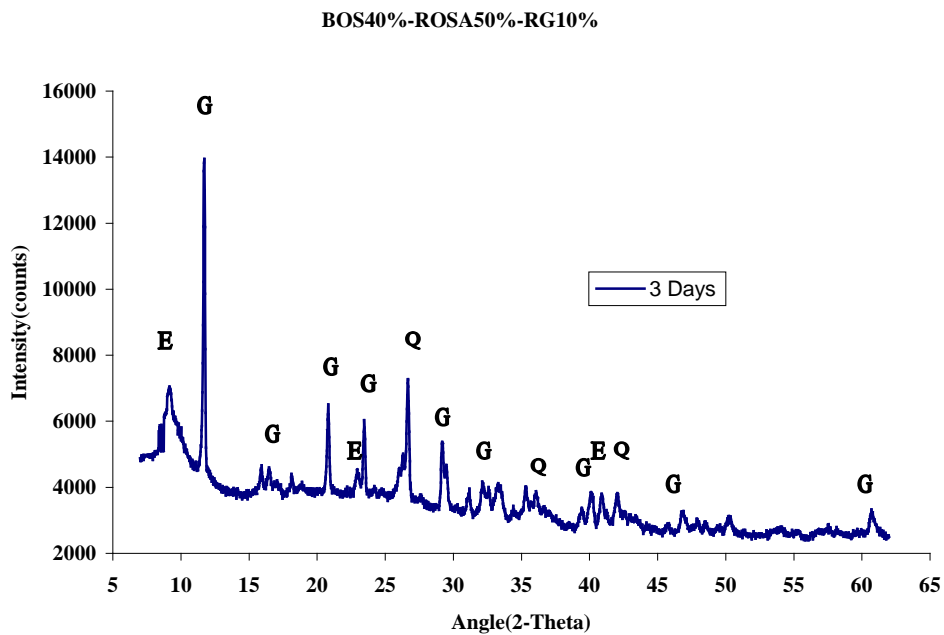


Figure B- 4 XRD of BOS-ROSA-RG at 3 days-E=Ettringite, G=Gypsum, Q=Quartz

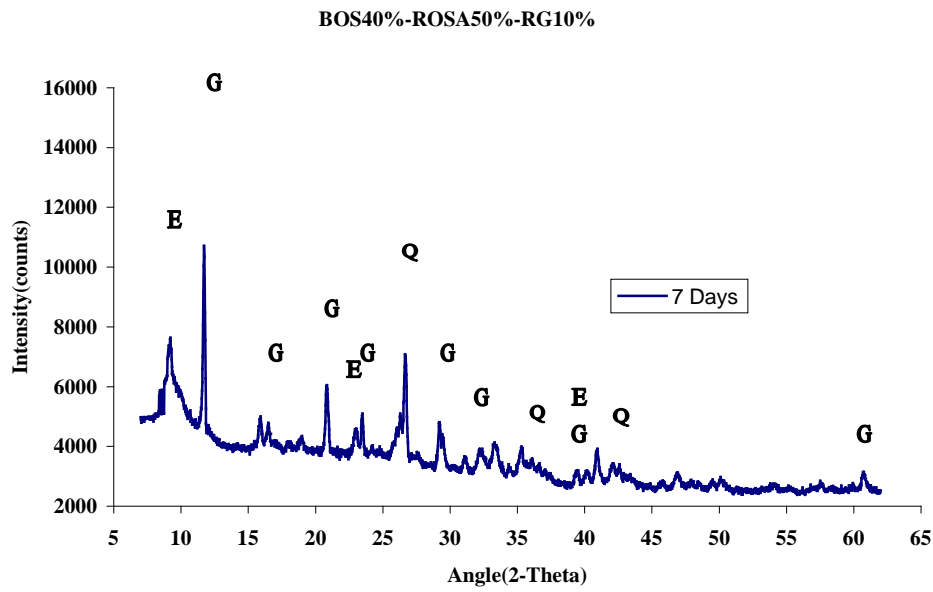


Figure B- 5 XRD of BOS-ROSA-RG at 7 days-E=Ettringite, G=Gypsum, Q=Quartz

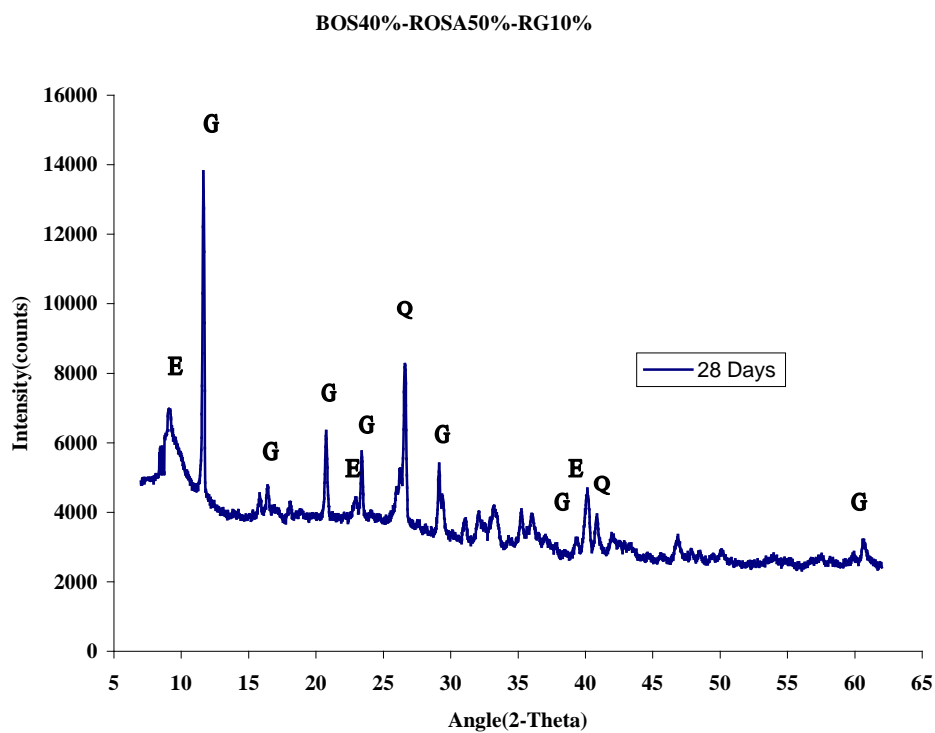


Figure B- 6 XRD of BOS-ROSA-RG at 28 days-E=Ettringite, G=Gypsum, Q=Quartz

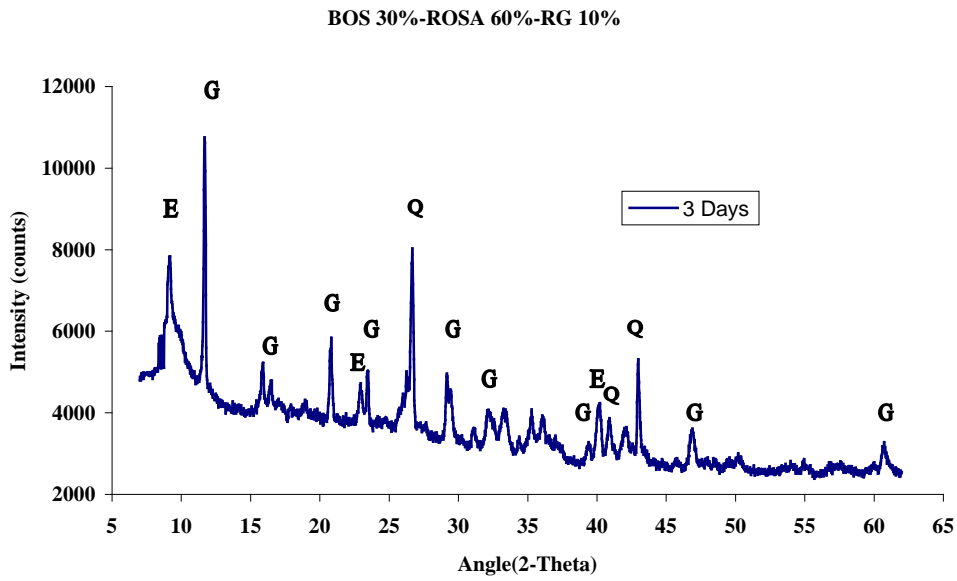


Figure B- 7 XRD of BOS-ROSA-RG at 3 days-E=Ettringite, G=Gypsum, Q=Quartz

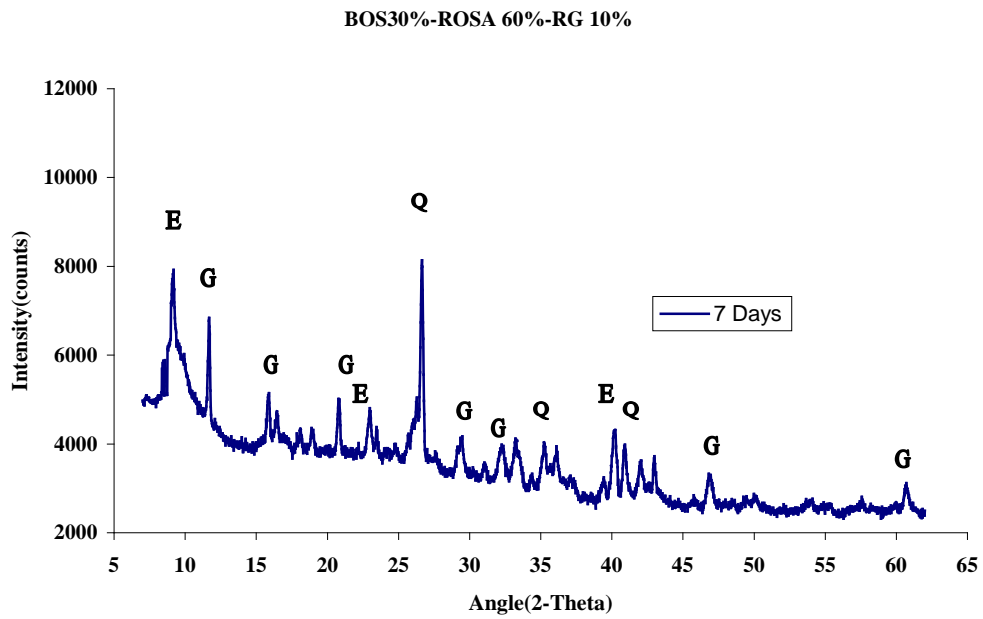


Figure B- 8 XRD of BOS-ROSA-RG at 7 days-E=Ettringite, G=Gypsum, Q=Quartz

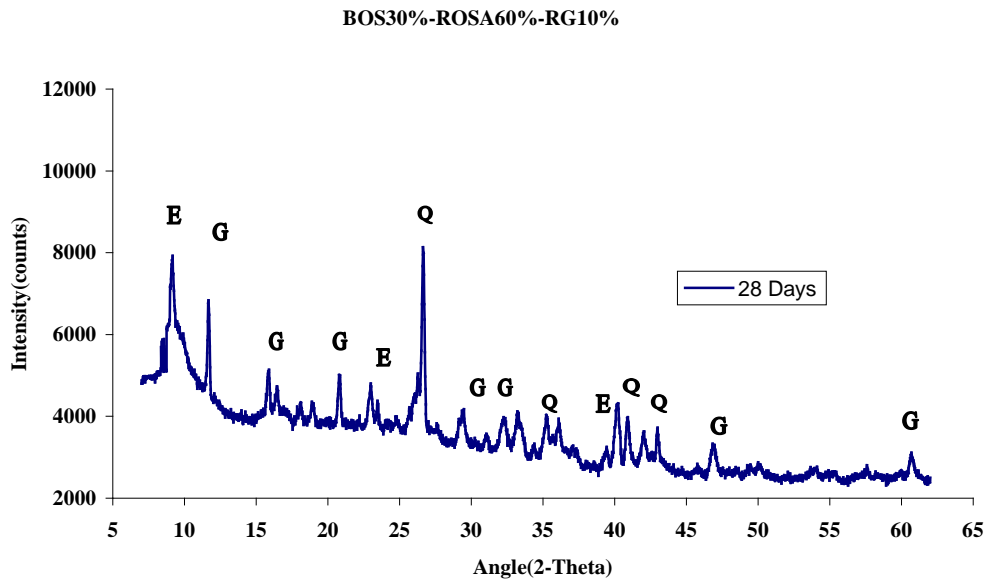


Figure B- 9 XRD of BOS-ROSA-RG at 28 days-E=Ettringite, G=Gypsum, Q=Quartz

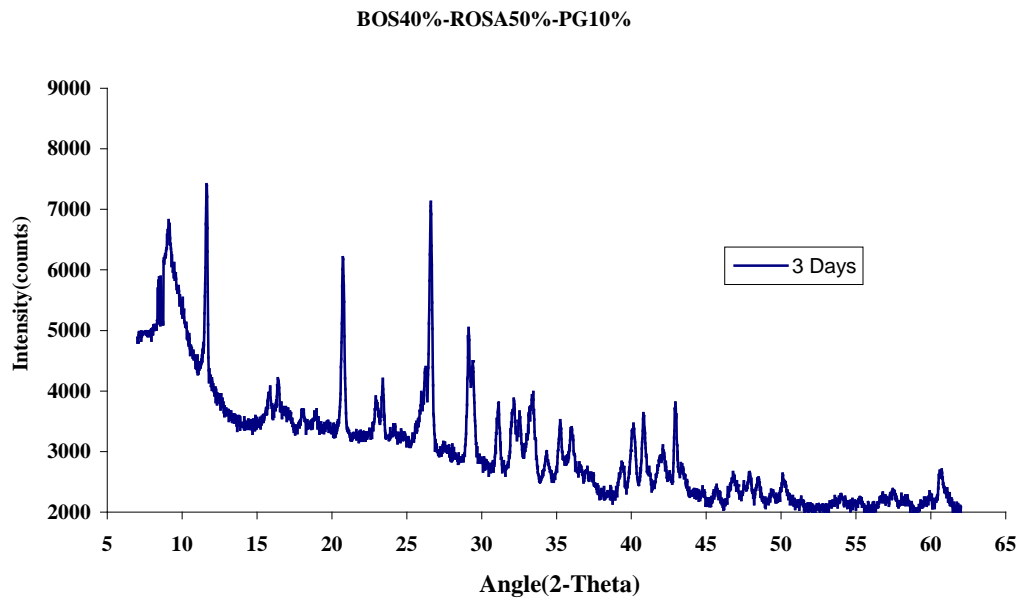


Figure B- 10 XRD of BOS-ROSA-PG at 3 days-E=Ettringite, G=Gypsum, Q=Quartz

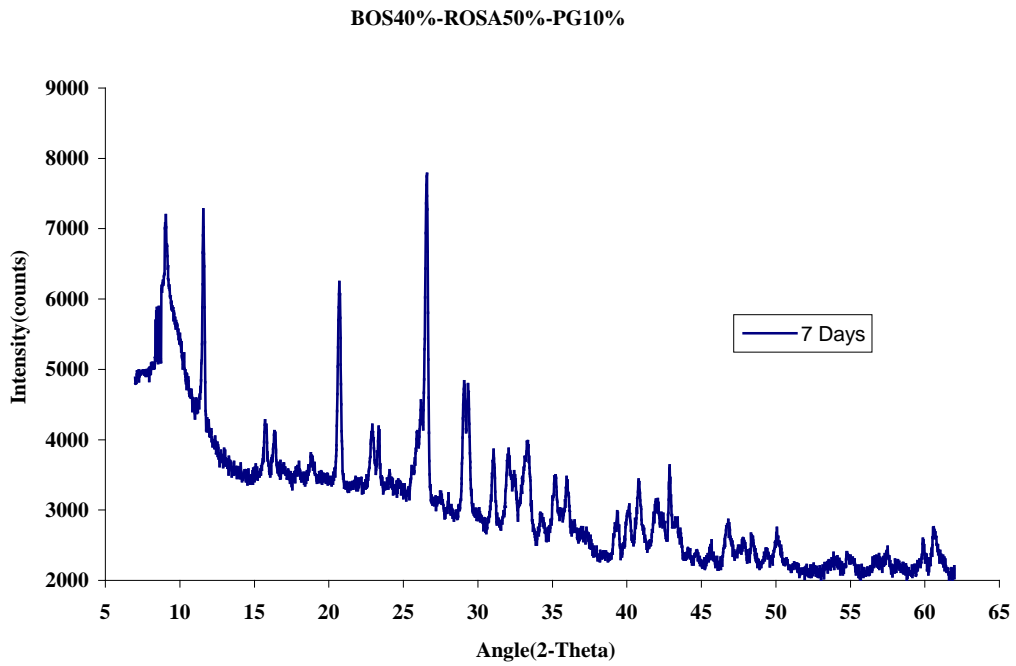


Figure B- 11 XRD of BOS-ROSA-PG at 7 days-E=Ettringite, G=Gypsum, Q=Quartz

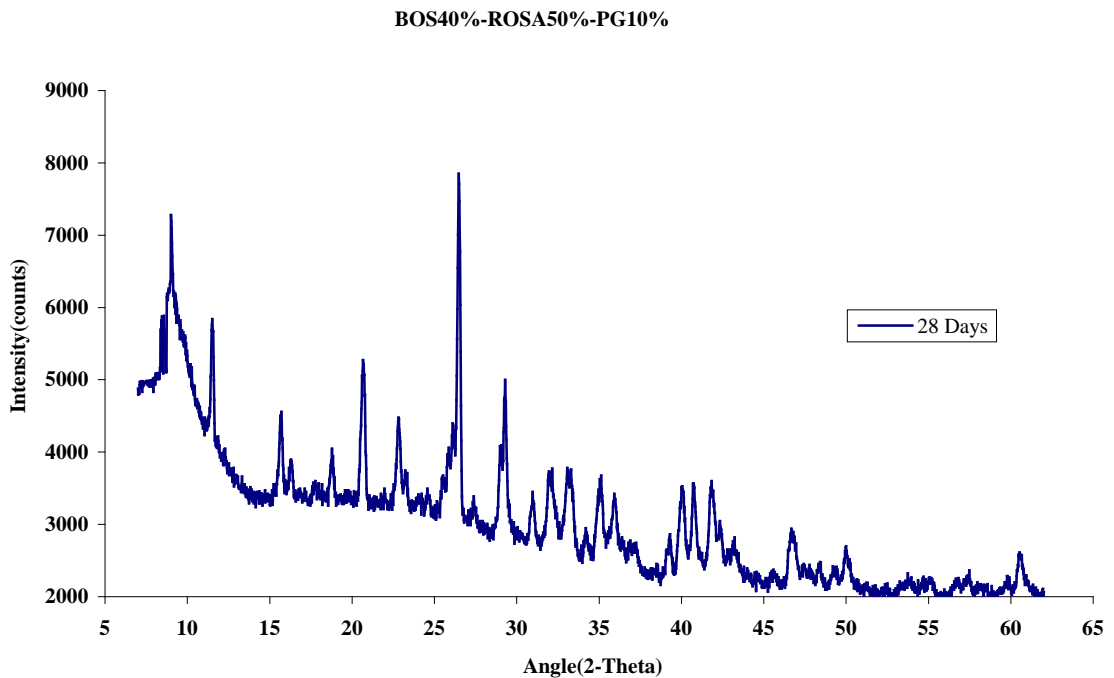


Figure B- 12 XRD of BOS-ROSA-PG at 28 days-E=Ettringite, G=Gypsum, Q=Quartz

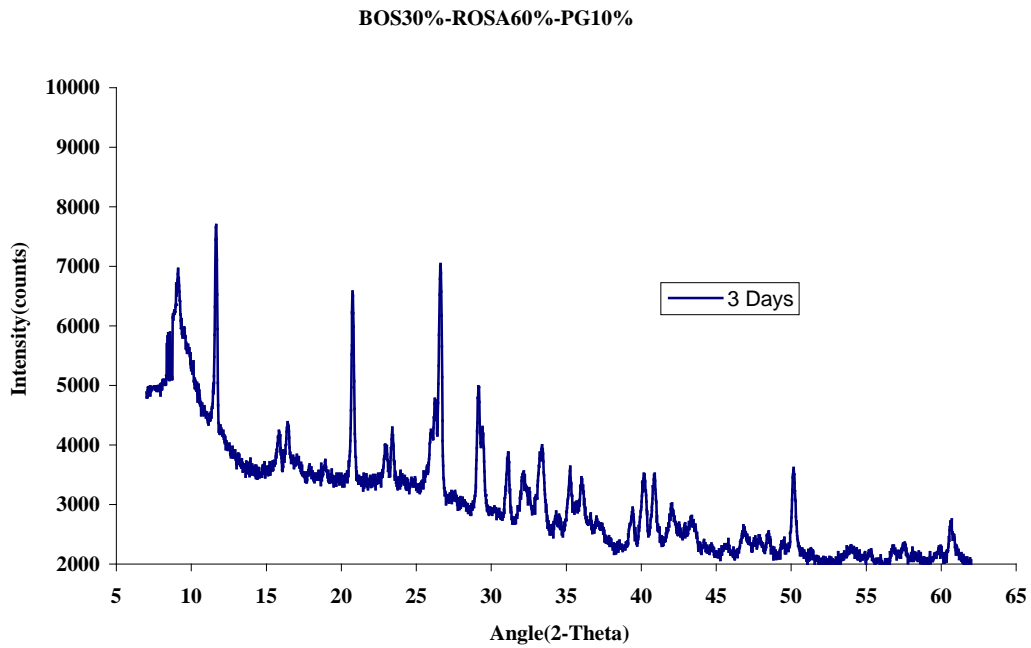


Figure B- 13 XRD of BOS-ROSA-PG at 3 days-E=Ettringite, G=Gypsum, Q=Quartz

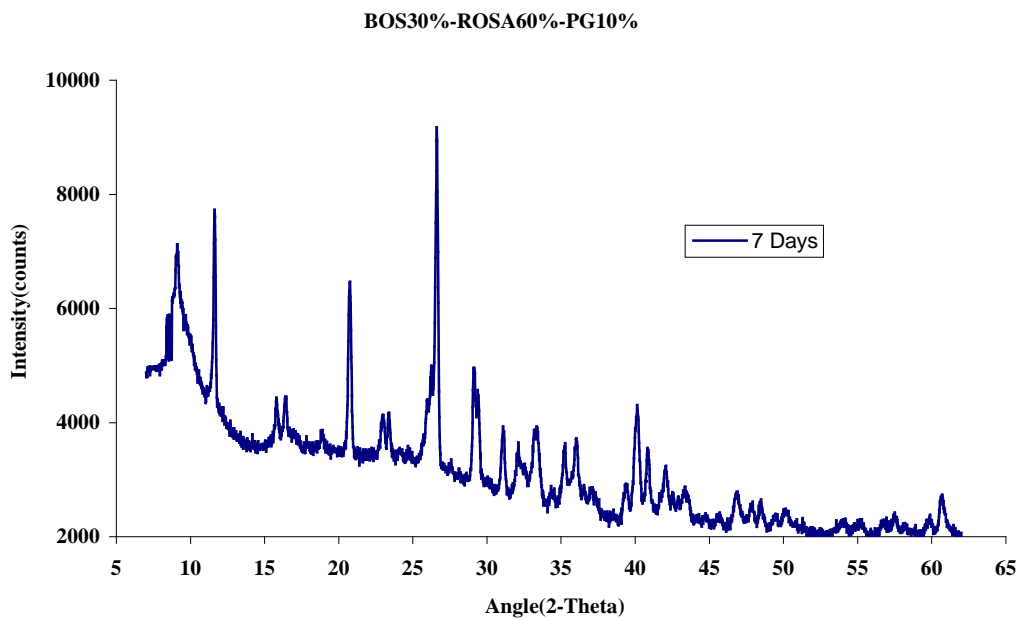


Figure B- 14 XRD of BOS-ROSA-PG at 7 days-E=Ettringite, G=Gypsum, Q=Quartz

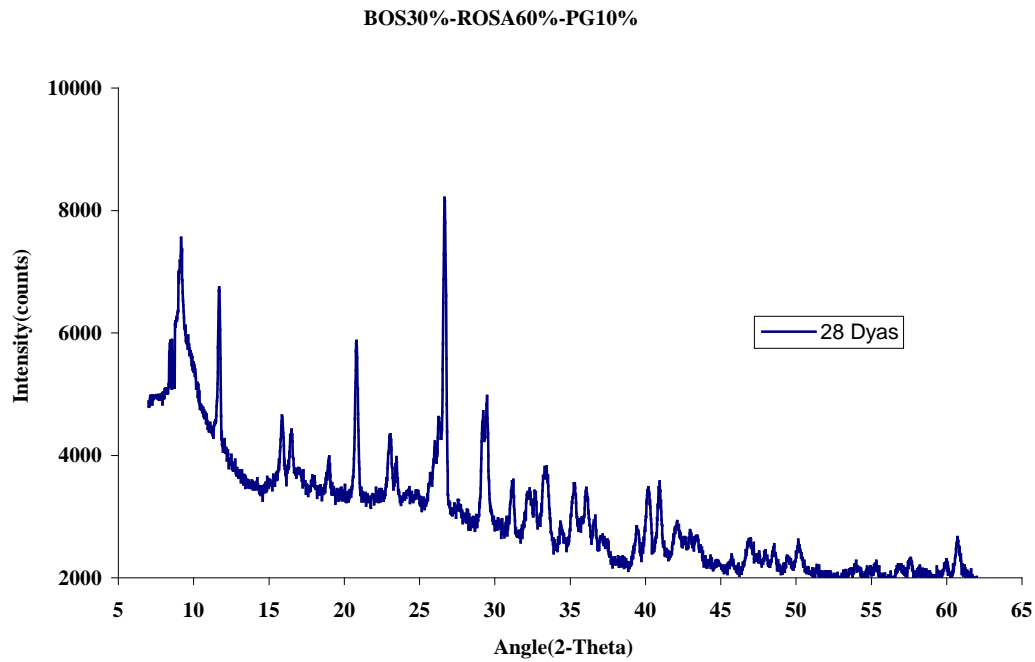


Figure B- 15 XRD of BOS-ROSA-PG at 28 days-E=Ettringite, G=Gypsum, Q=Quartz

Table B-1 Concrete samples for trials using cement and Super plasticiser

Mix PG as Agg	OPC	BOS	ROSA	RG	cement	super plasticiser%	3days	7days	28	density	w/c	supposed density
with cement	5	20	65	10	1000	2.0	1.35	3.5	7.4	1776	20%	1800
with cement	-	20	70	10	1000	2.0	0.93	1.7	6.2	1670	20%	1800
with cement	5	20	65	10	700	1.5	0.85	1.6	5.9	1690	20%	1800
Coventry blend	5				1000	1.0	0.77	1.2	2.6	1560	20%	1800
Coventry blend Coventry	5				1200	1.0	0.88	1.5	3.4	1656	15%	1800
blend+20%rosa	5				1200	1.0	0.50	0.9	3.7	1660	17%	1600

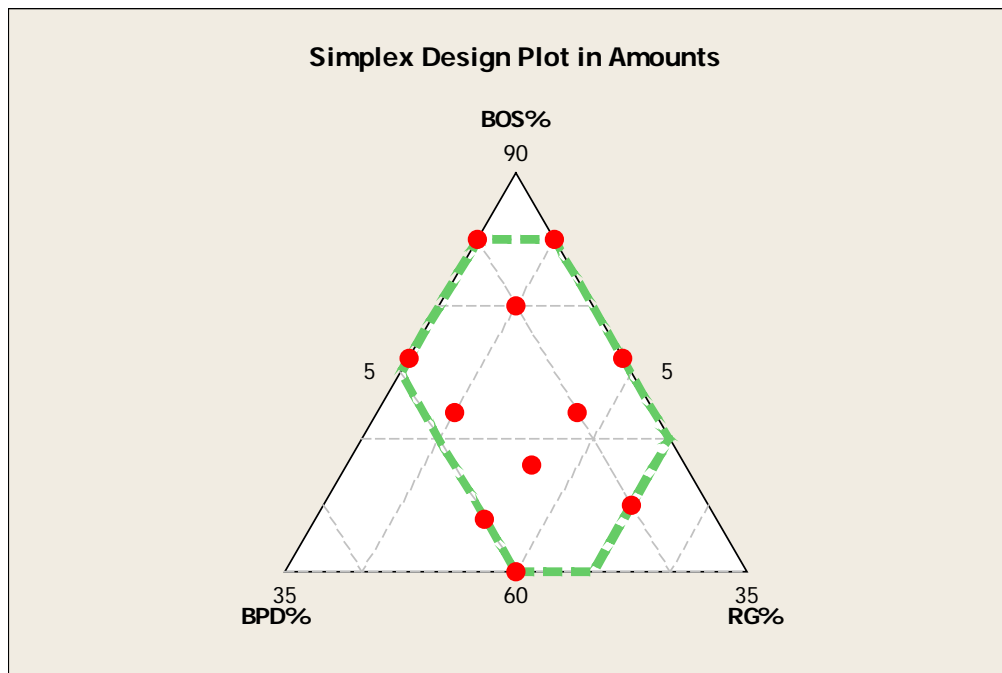
The results of RSM and ANNs are presented in this appendix. The glossary of basic neural network terminology is presented as a table in this appendix.

- BOS- BPD-RG**

Table C- 1 BOS- BPD-RG mixture design and compressive strength at 28 days

Mix No	BOS%	BPD%	RG%	28 days CS	Predicted Data	Error%
1	85	10	5	9.3	9.4	1.0
2	85	5	10	9.2	8.3	9.8
3	80	10	10	6.2	7.8	26.5
4	76	5	19	6.0	7.0	16.3
5	76	19	5	9.4	8.8	6.3
6	72	10	18	8.7	6.4	26.1
7	72	18	10	6.8	7.1	5.0
8	68	15	17	5.7	5.9	4.2
9	65	10	25	6.0	6.3	4.8
10	64	20	16	5.3	5.5	4.7
11	60	20	20	5.0	4.9	1.2
Testing Data	68	17	15	5.9	6.5	9.5

Error Average of training data=9.61%



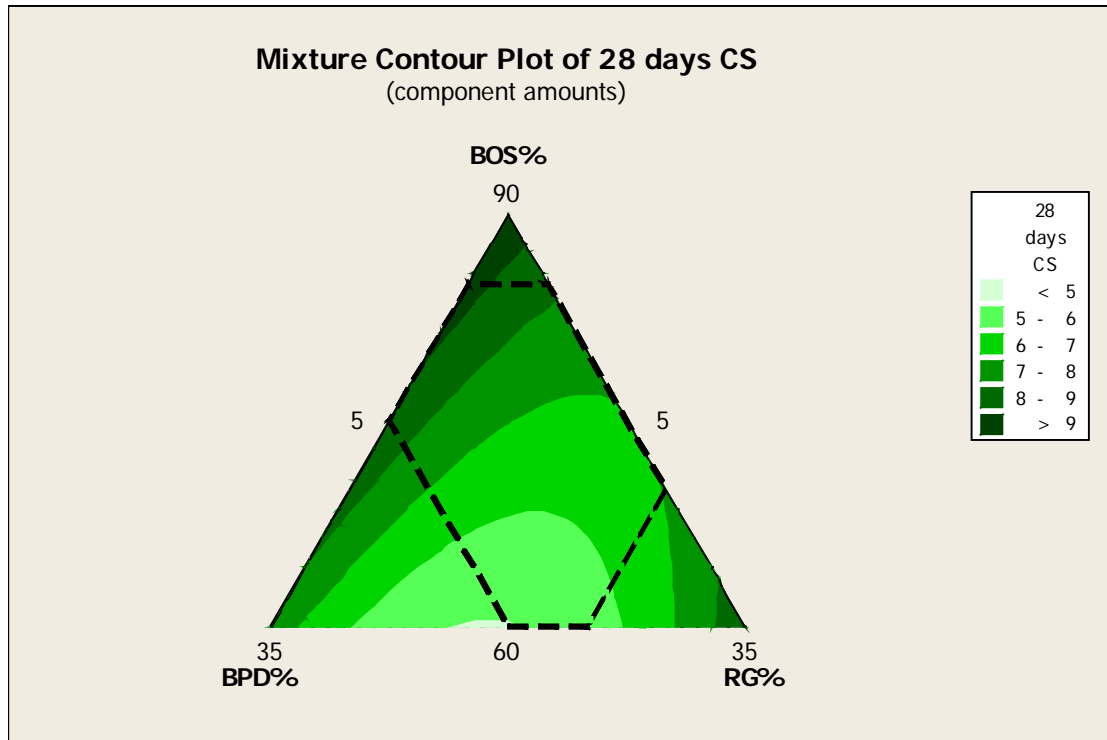


Figure C- 1 Mixture Design Plot and Mixture Contour Plot For Mix BOS- BPD- RG

Quadratic model Coefficients using MINITAB 14:

$$CS=0.12*BOS+0.05*BPD+0.73*RG+0.00037*BOS*BPD+ (-0.01)*BOS*RG+(-0.0146)*BPD*RG$$

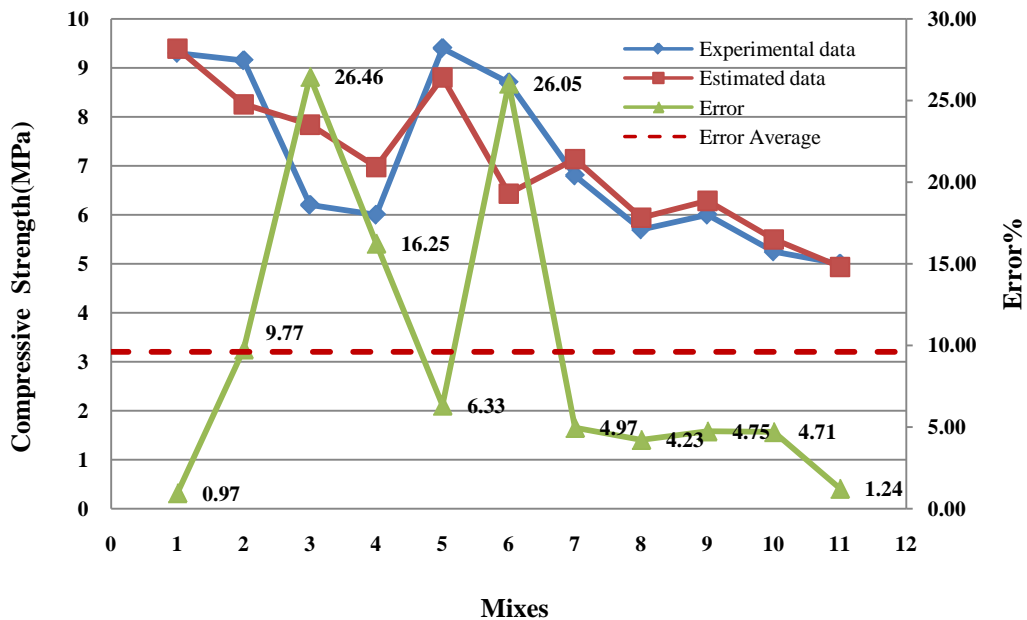


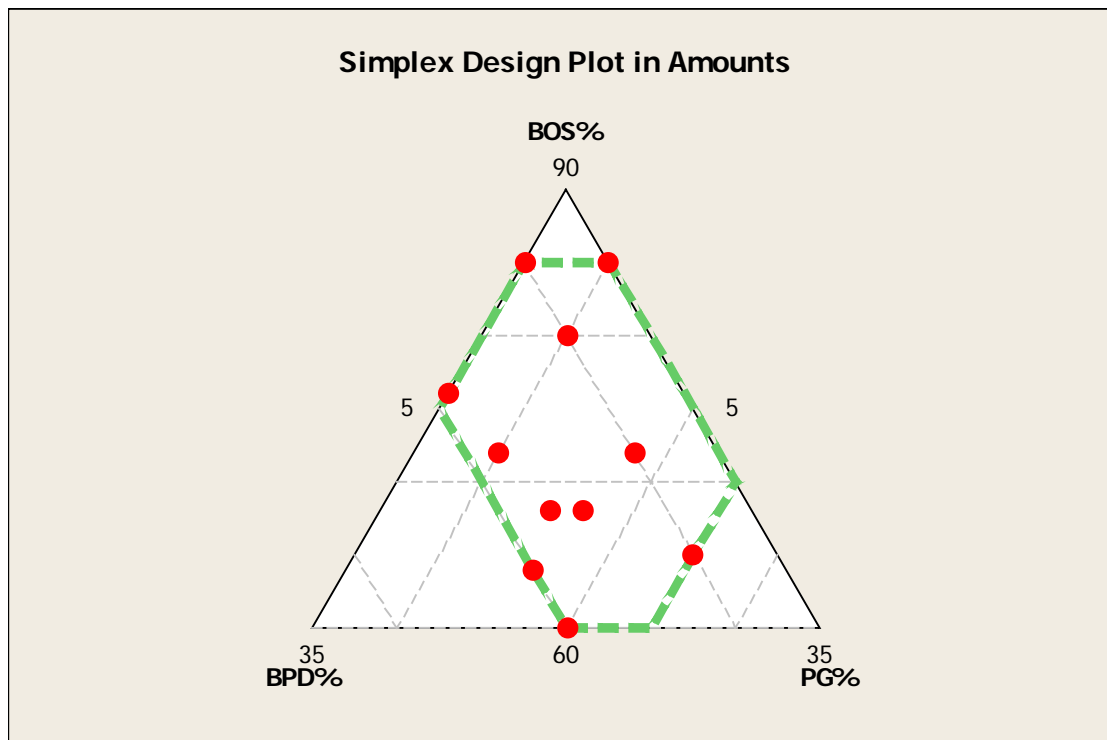
Figure C- 2 Comparison between Predicted and Experimental 28 days Compressive strength for BOS-BPD-RG Group

• **BOS- PBD-PG**

Table C- 2 BOS- PBD-PG mixture design and compressive strength at 28 days (laboratory data)

Mix No	BOS%	BPD%	PG%	28 days CS	Predicted Data	Error%
1	85	10	5	10.1	9.4	7.0
2	85	5	10	10.0	9.8	2.2
3	80	10	10	7.0	8.5	21.6
4	76	19	5	6.3	7.4	17.6
5	72	18	10	9.2	7.0	24.4
6	72	10	18	7.2	7.1	1.1
7	68	17	15	6.2	6.5	4.2
8	68	15	17	6.3	6.5	2.7
9	65	10	25	6.2	5.9	3.6
10	64	20	16	5.8	6.0	3.2
11	60	20	20	5.3	5.5	4.5
Testing Data	76	5	19	10.5	8.2	21.8

Error Average of training data=8.36%



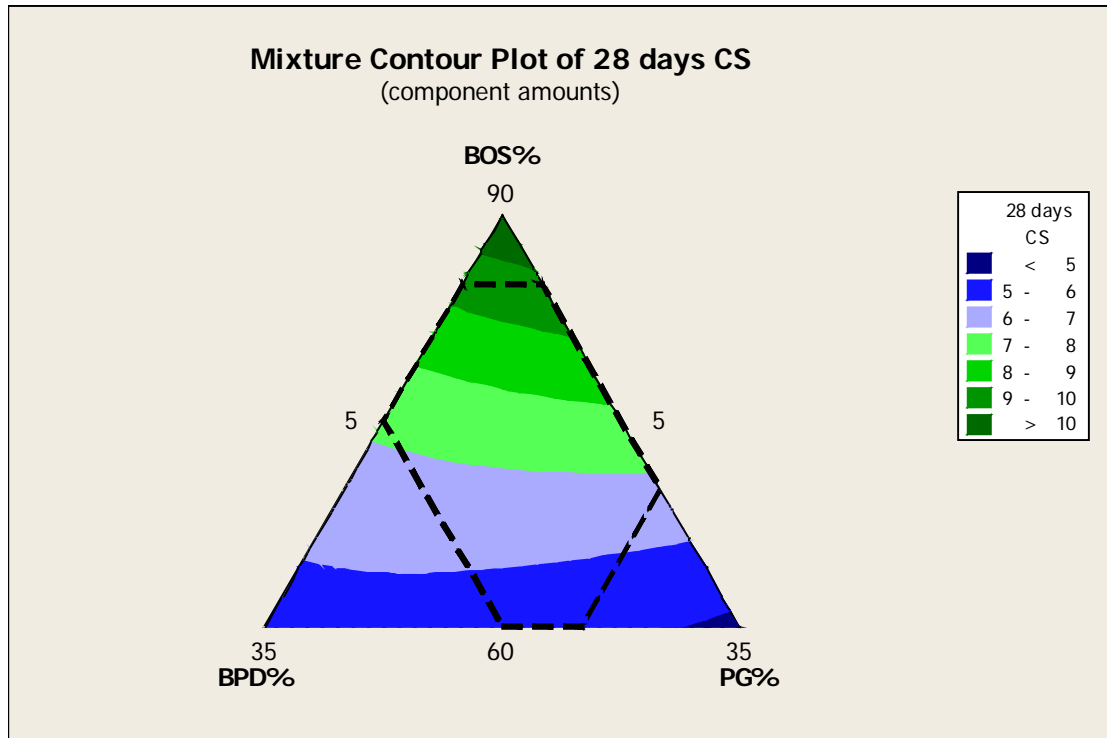


Figure C- 3 Mixture Design Plot and Mixture Contour Plot For Mix BOS- BPD- PG

Quadratic model Coefficients using MINITAB 14:

$$CS=0.14*BOS+0.21*BPD+(-0.08)*PG+(-0.0046)*BOS*BPD+(-1.83E-04)*BOS*PG+0.0013*BPD*PG$$

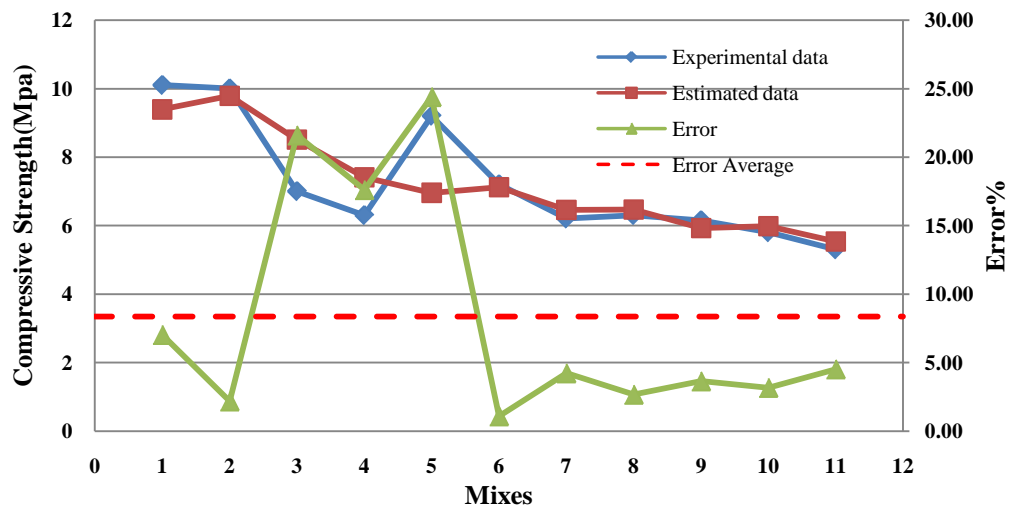


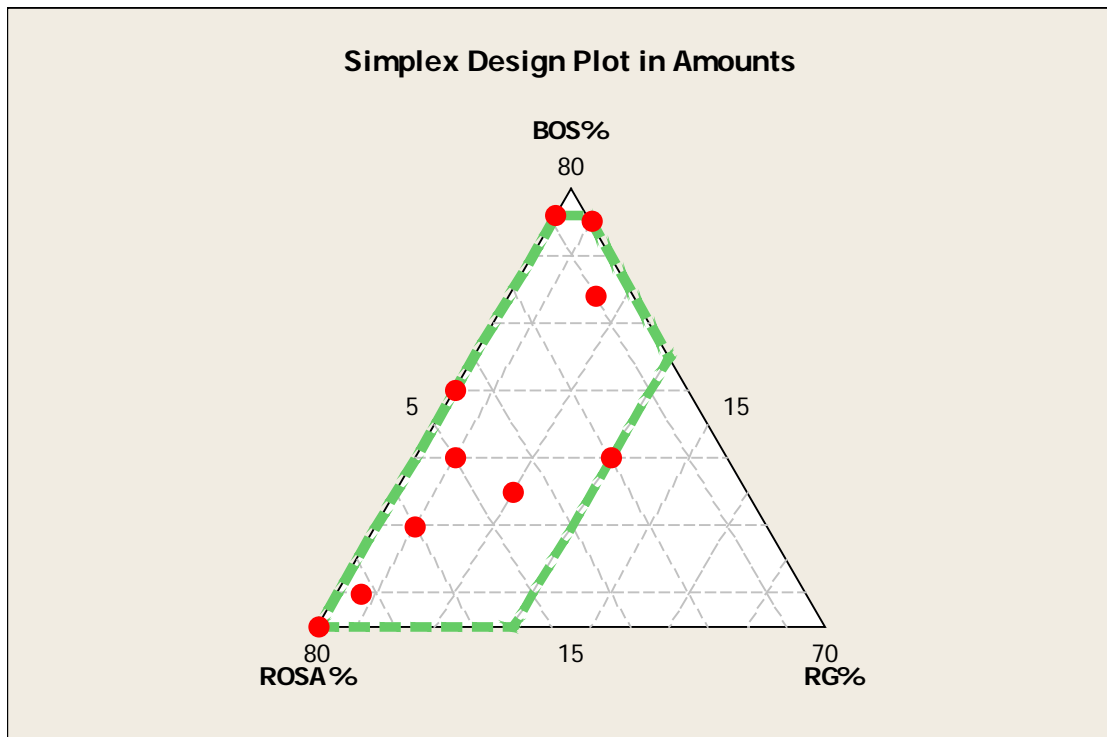
Figure C- 4 Comparison between Predicted and Experimental 28 days Compressive strength for BOS-BPD-PG Group

• **BOS- ROSA-RG**

Table C- 3 BOS- ROSA-RG mixture design and compressive strength at 28 days (laboratory data)

Mix No	BOS%	ROSA%	RG%	28 days CS	Predicted Data	Error%
1	76	19	5	6.7	7.1	6.3
2	75	15	10	9.7	8.1	16.2
3	64	20	16	11.8	13.2	12.0
4	50	45	5	13.8	15.6	13.0
5	40	30	30	17.9	17.0	5.1
6	40	50	10	19.3	17.1	11.2
7	35	45	20	15.4	17.8	15.8
8	30	60	10	18.9	16.3	14.0
9	20	72	8	12.5	13.3	6.7
10	15	80	5	10.2	10.6	3.9
Testing Data	48	40	12	17.6	17.0	3.4

Error Average of training data=10.42%



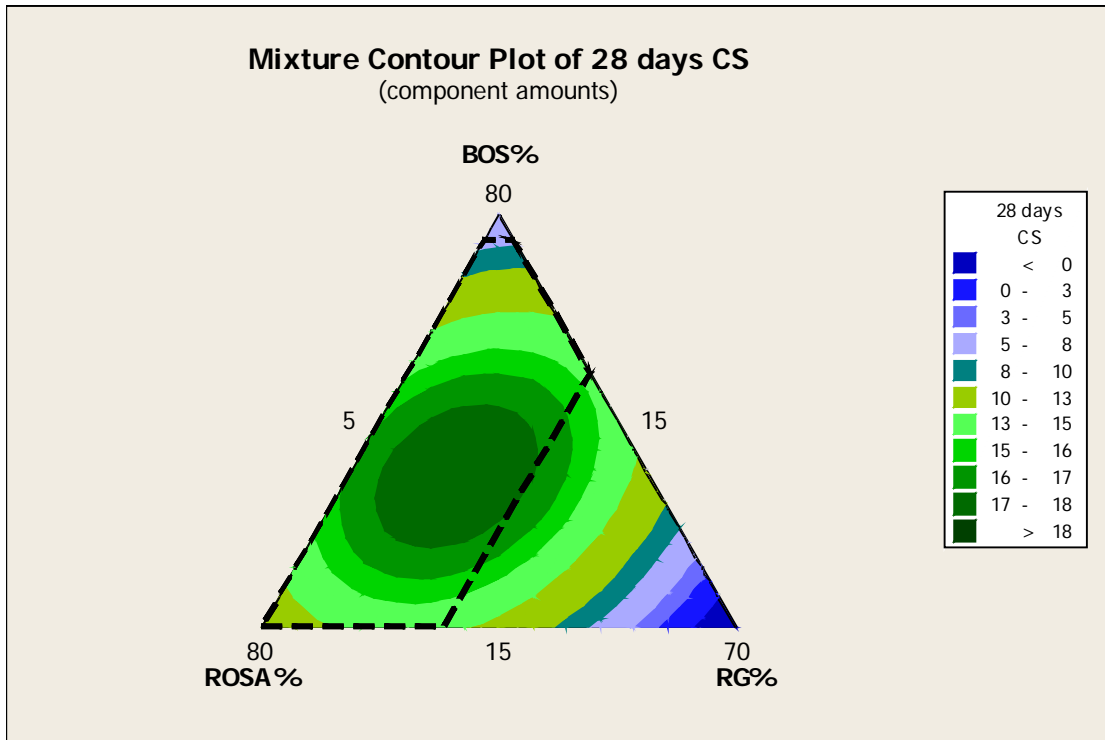


Figure C- 5 Mixture Design Plot and Mixture Contour Plot For Mix BOS- ROSA-RG

Quadratic model Coefficients using MINITAB 14:

$$CS = (-0.104) * BOS + 0.0058 * ROSA + (-0.39) * RG + 0.0077 * BOS * ROSA + 0.013 * BOS * RG + 0.0087 * ROSA * RG$$

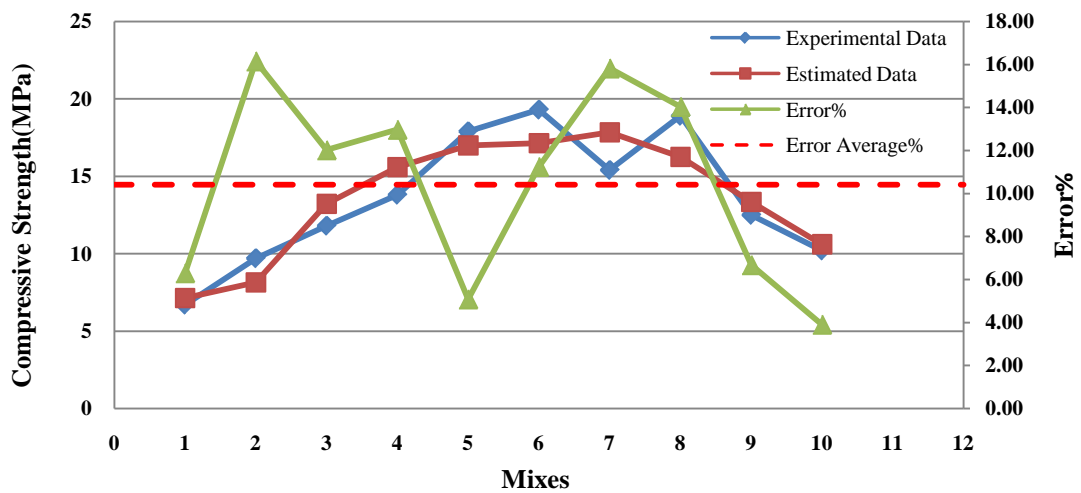


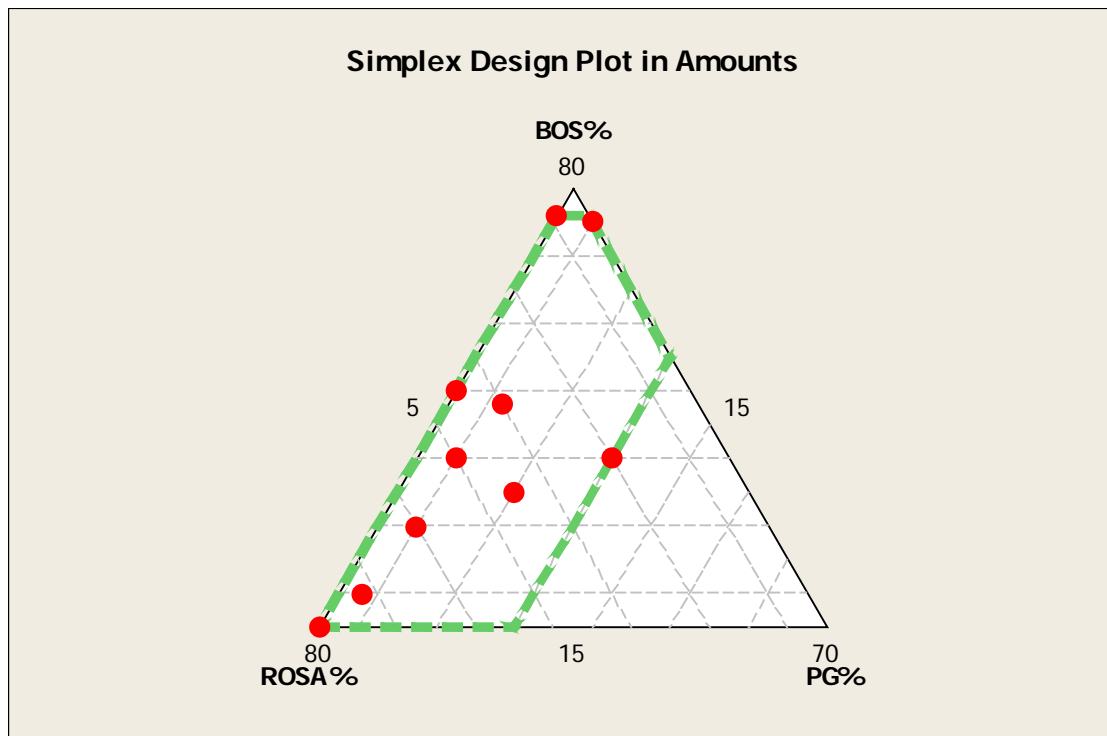
Figure C- 6 Comparison between Predicted and Experimental 28 days Compressive strength for BOS-ROSA-RG Group

• **BOS- ROSA-PG**

Table C- 4 BOS- ROSA-PG mixture design and compressive strength at 28 days (laboratory data)

Mix No	BOS%	ROSA%	PG%	28 days CS	Predicted Data	Error%
1	76	19	5	8.9	9.9	10.6
2	75	15	10	5.9	4.1	31.1
3	50	45	5	13.4	13.7	1.9
4	48	40	12	7.1	12.5	76.5
5	40	30	30	10.6	10.1	4.4
6	40	50	10	18.8	14.5	22.6
7	35	45	20	15.5	16.6	7.0
8	30	60	10	18.6	15.7	15.6
9	20	72	8	13.4	14.2	5.9
10	15	80	5	9.1	10.1	10.5
Testing Data	64	20	16	11.5	3.5	69.0

Error Average of training data=18.62%



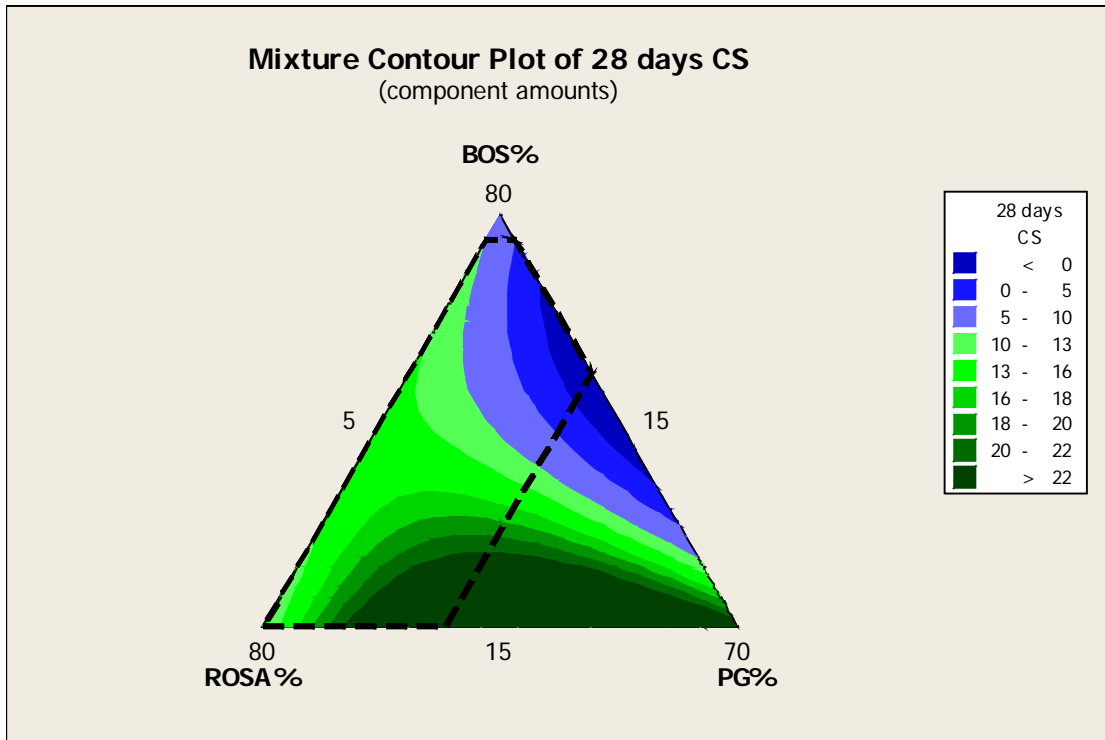


Figure C- 7 Mixture Design Plot and Mixture Contour Plot For Mix BOS- ROSA-PG

Quadratic model Coefficients using MINITAB 14:

$$CS = 0.12 * BOS + (-0.042) * ROSA + 0.36 * PG + 0.0041 * BOS * ROSA + (-0.019) * BOS * PG + 0.016 * ROSA * PG$$

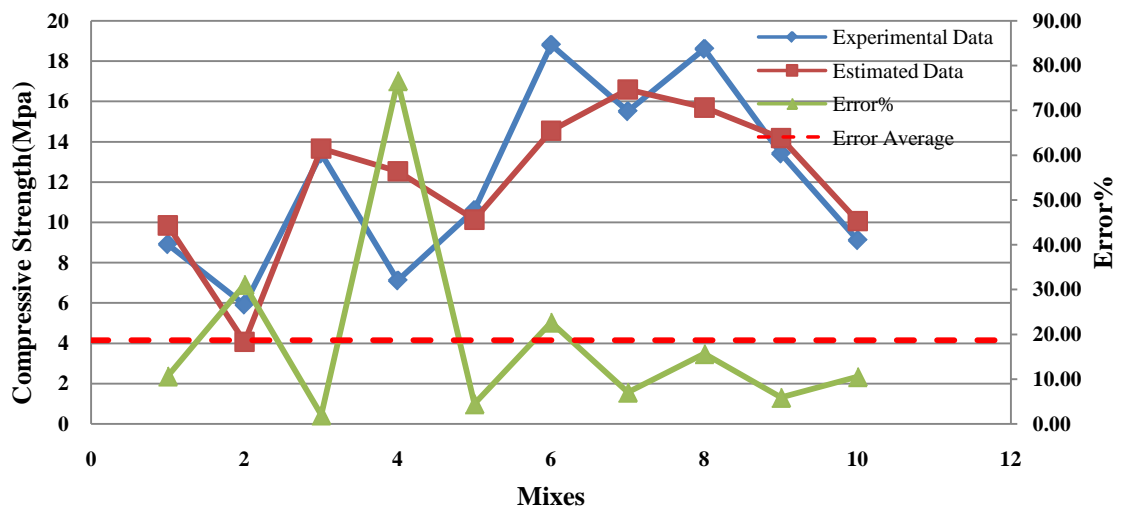


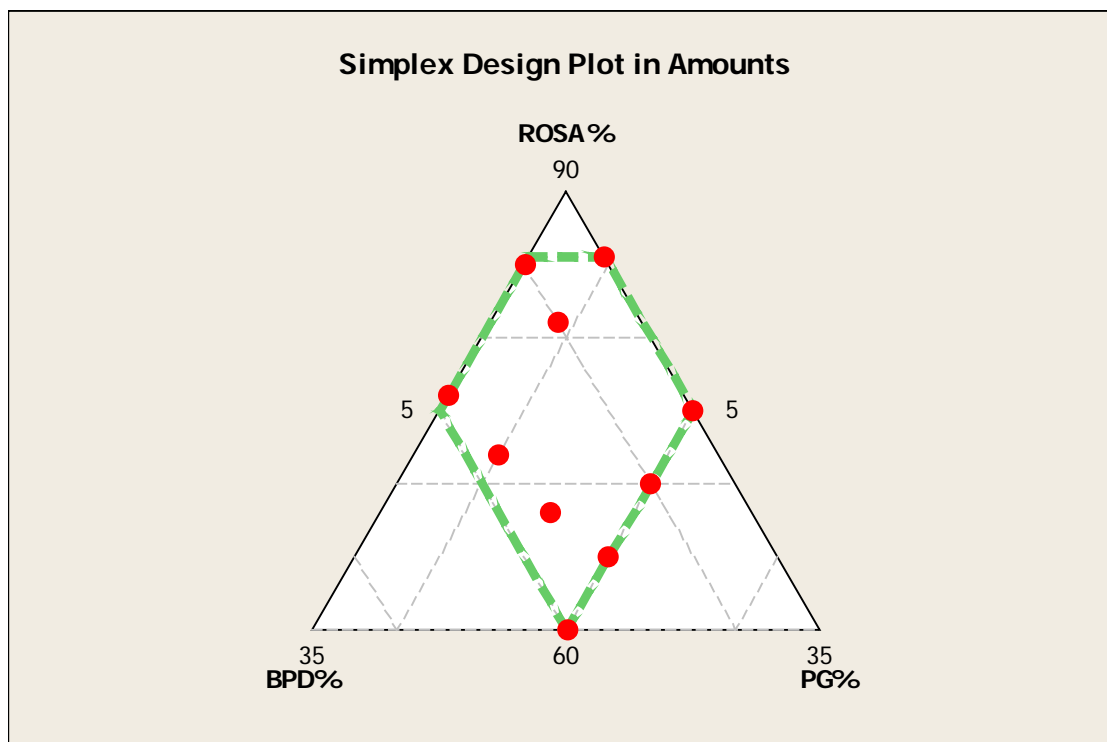
Figure C- 8 Comparison between Predicted and Experimental 28 days Compressive strength for BOS-ROSA-PG Group

• ROSA-BPD-PG

Table C- 5 ROSA-BPD-PG mixture design and compressive strength at 28 days (laboratory data)

Mix No	ROSA%	BPD%	PG%	28 days CS	Predicted Data	Error%
1	85.5	5	9.5	14.0	12.6	10.1
2	85	10	5	14.3	14.9	3.9
3	81	10	9	15.8	17.1	8.3
4	76	19	5	17.0	16.2	4.7
5	75	5	20	9.8	11.5	17.4
6	72	18	10	16.3	16.9	3.7
7	70	10	20	16.0	13.2	17.4
8	68	17	15	15.4	15.0	2.8
9	65	15	20	10.1	11.2	11.1
10	60	20	20	5.4	5.5	2.2
Testing Data	76.5	15	8.5	18.0	17.8	1.2

Error Average of training data=8.16%



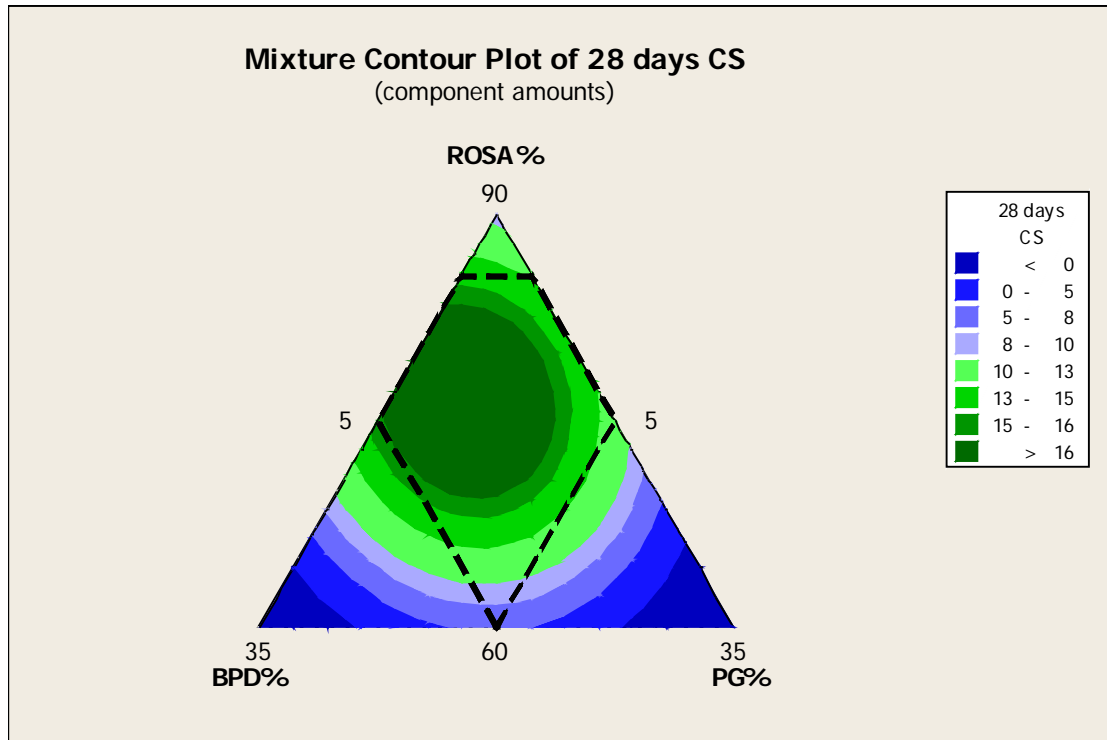


Figure C- 9 Mixture Design Plot and Mixture Contour Plot For Mix BPD- ROSA-PG

Quadratic model Coefficients using MINITAB 14:

$$CS = (-0.091) * ROSA + (-4.93) * BPD + (-4.23) * PG + 0.074 * ROSA * BPD + 0.061 * ROSA * PG + 0.079 * BPD * PG$$

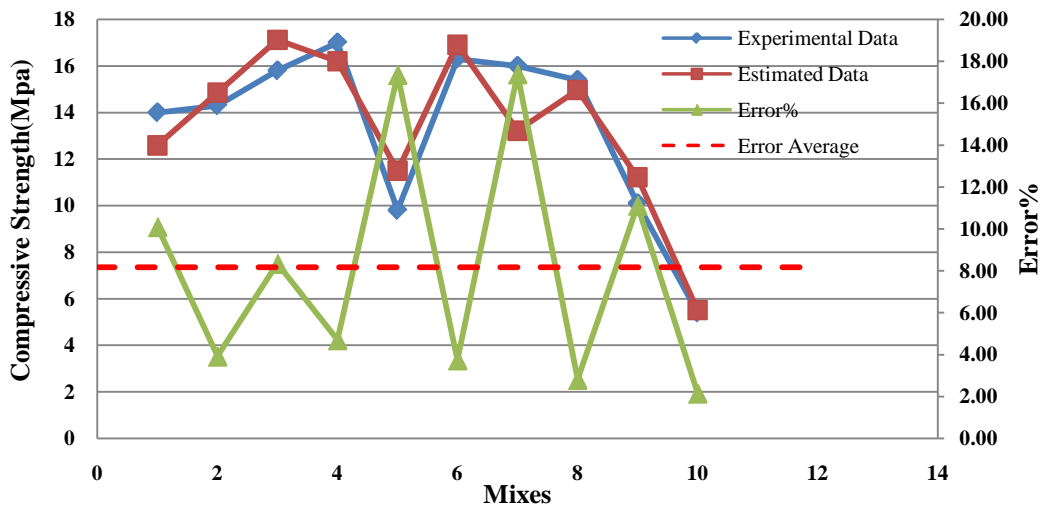


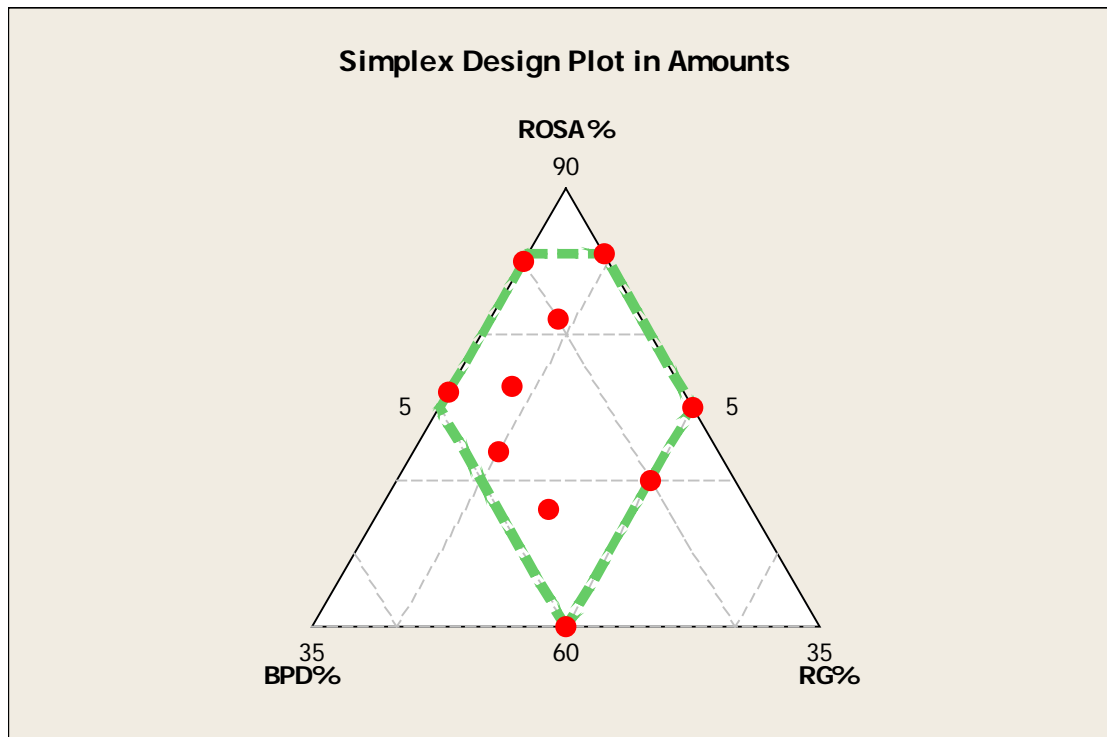
Figure C- 10 Comparison between Predicted and Experimental 28 days Compressive strength for ROSA-BPD-PG Group

• ROSA-BPD-RG

Table C- 6 ROSA-BPD-RG mixture design and compressive strength at 28 days (laboratory data)

Mix No	ROSA%	BPD%	RG%	28 days CS	Predicted Data	Error%
1	85.5	5	9.5	7.0	7.2	2.1
2	85	10	5	12.2	9.5	21.8
3	81	10	9	8.0	11.0	37.9
4	76.5	15	8.5	10.0	11.7	17.2
5	76	19	5	8.2	9.6	16.6
6	75	5	20	8.9	8.5	4.4
7	72	18	10	13.5	10.7	21.1
8	70	10	20	11.0	11.0	0.2
9	68	17	15	12.0	10.7	11.3
10	60	20	20	4.9	5.9	20.7
Testing Data	65	15	20	9.2	9.8	6.9

Error Average of training data=15.33%



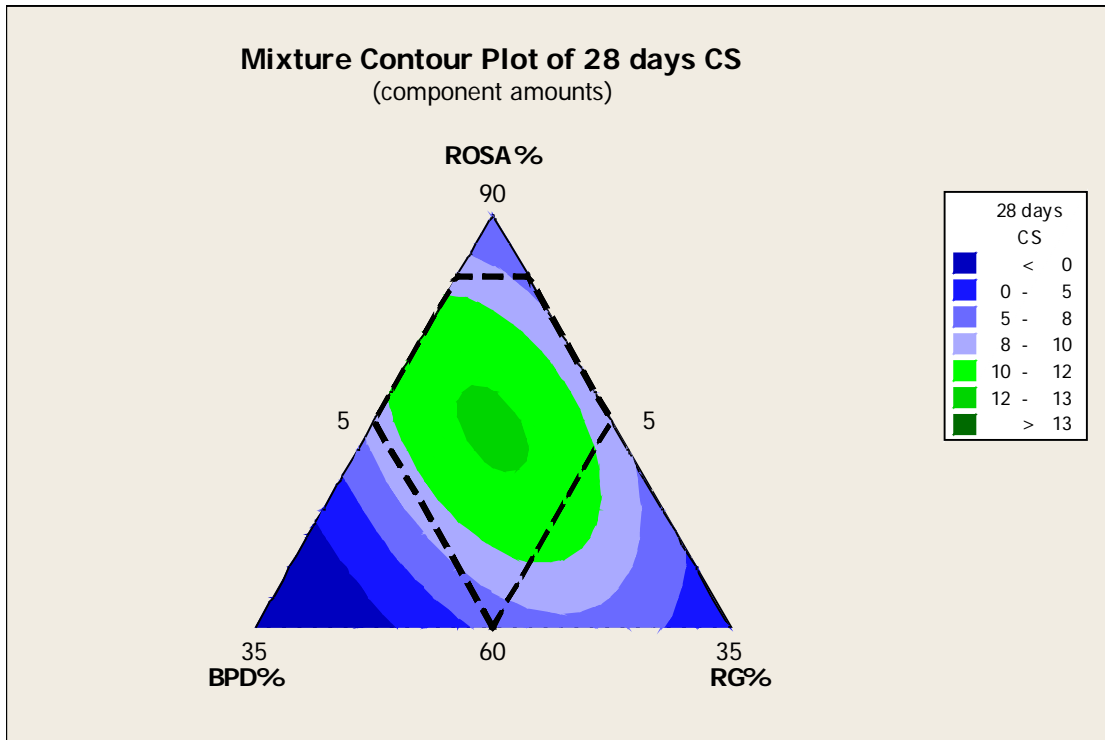


Figure C- 11 Mixture Design Plot and Mixture Contour Plot For Mix BPD- ROSA-RG

Quadratic model Coefficients using MINITAB 14:

$$CS = (-0.076) * ROSA + (-4.67) * BPD + (-1.58) * RG + 0.067 * ROSA * BPD + 0.025 * ROSA * RG + 0.062 * BPD * RG$$

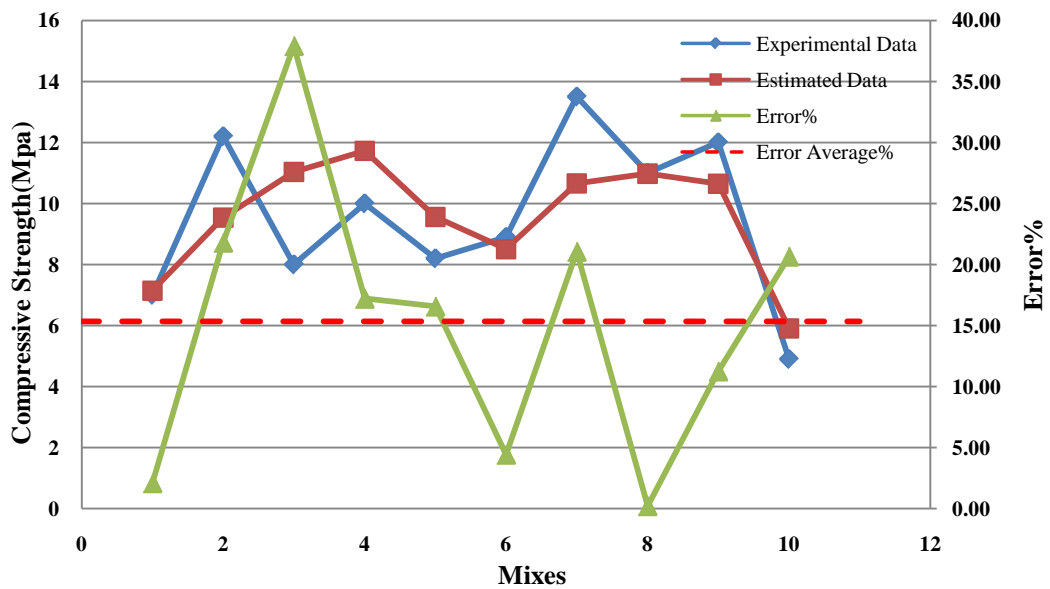


Figure C- 12 Comparison between Predicted and Experimental 28 days Compressive strength for ROSA-BPD-RG Group

Table C- 7 Glossary of basic neural network terminology (Buenfeld *et al.* 1999)

Term	Definition
Activation Function	A bounded function of infinite domain applied to the weighted and summed inputs to limit the amplitude of the output signal.
Architecture	The arrangement of cells in a neural network. Different architectures vary in the arrangement, type and number of their connections, and in their activation functions, types of learning and training algorithms.
bias	A weight parameter for an extra input whose activation is permanently set to +1
cell	A simple linear or non linear computing element that accepts one or more inputs, computes a function thereof, and may direct the result to one or more other cells
epoch	Each repeated entry of the full set of training patterns. Epoch=cycle
Error-backpropagation	A method for computing the error gradient, i.e. the derivatives of the error function with respect to the weights, for a feedforward network
Error function	An expression which describes the difference between the computed and target output. Typically the squared error, but sometimes linear error, absolute error or entropy
Feed forward	Uni-directional transfer of information
Gradient descent	The iterative changes in the weights during training are proportional to the negative of the first derivative of the total error
Input data	The vector of variables from which a prediction is intended to be made
layer	An arrangement of cells which process information in parallel, i.e., Typically one or more hidden layers are found between the input layer and the output layer

Learning rate	An iterative process that all patterns in the training set are presented in turn, several times, at the input to the network
Neural network	A class of flexible nonlinear regression and discriminant models, data reduction models, and nonlinear dynamical systems consisting of an often large number of neurons(i.e., cells) interconnected in often complex ways often organised into layers
over fitting	Construction or training of a network to fit the details of the training patterns rather than generalise well for new data
Over training	Over fitting of the training patterns by continuing to train without the use of an appropriate validation set
Regression	Prediction of the value of a continuous variable y from an input vector x
Sigmoid function	A strictly increasing function which exhibits smoothness and asymptotic properties, such as a logistic or hyperbolic tangent function
Supervised learning	Training in which the training patterns are divided into input data and output data, and the number of training iterations is dependent on the computed outputs and the target outputs for a set of test inputs
Target outputs	The output values provided to the network in supervised learning
Test set	A set of data which the neural network has not previously seen, which is used to test how well the neural network has learned to generalise
training	Using samples to adjust the weights on the connections in the neural network such that the network performs its task correctly. Learning is equivalent to minimisation of an error function
Training algorithm	The method by which the weights are adjusted during training
Training patterns	The data set used to train the neural network
Unsupervised learning	The neural network organises the training data and discovers its emergent collective properties
Validation set	A set of data used to test the performance of the network during training, but not used for modifying the weights of the network

Table C- 8 Training Data of ANN

BOS%	ROSA%	BPD%	RG%	PG%	28 days	TANSIG	Error%
76	19	5	0	0	0.28	0.28	0.50
72	18	10	0	0	0.25	0.24	5.07
48	12	40	0	0	0.08	0.08	3.35
32	8	60	0	0	0.01	0.01	23.00
35	55	10	0	0	0.71	0.71	0.19
0	85.5	5	9.5	0	0.17	0.17	0.11
27	68	5	0	0	0.25	0.25	0.20
30	30	40	0	0	0.37	0.37	0.68
76	0	19	5	0	0.33	0.31	6.00
15	80	5	0	0	0.24	0.24	1.65
18	10	72	0	0	0.12	0.12	0.26
76	19	0	5	0	0.15	0.17	12.48
75	15	0	0	10	0.09	0.10	7.72
16	20	64	0	0	0.25	0.25	0.03
12	40	48	0	0	0.54	0.54	0.10
8	60	32	0	0	0.95	0.94	0.92
85	0	10	5	0	0.32	0.32	0.01
85	0	5	10	0	0.31	0.27	13.33
80	0	10	10	0	0.11	0.19	66.02
0	76	19	5	0	0.25	0.26	3.36
0	60	20	20	0	0.03	0.03	6.93
72	0	18	10	0	0.16	0.12	22.85
68	0	15	17	0	0.08	0.14	77.35
65	0	10	25	0	0.10	0.10	2.32
64	0	20	16	0	0.05	0.06	22.54
85	0	10	0	5	0.38	0.38	0.43
85	0	5	0	10	0.37	0.34	9.24
72	0	10	0	18	0.18	0.19	4.64
68	0	17	0	15	0.11	0.09	17.90
68	0	15	0	17	0.12	0.11	10.38
65	0	10	0	25	0.11	0.11	2.43
64	0	20	0	16	0.09	0.10	18.40
60	0	20	0	20	0.05	0.06	6.19
75	15	0	10	0	0.35	0.32	8.92
64	20	0	16	0	0.49	0.50	1.84
50	45	0	5	0	0.63	0.64	1.17
40	30	0	30	0	0.91	0.90	0.41
40	50	0	10	0	1.00	0.95	5.11
35	45	0	20	0	0.74	0.75	1.67
30	60	0	10	0	0.97	0.95	2.03
20	72	0	8	0	0.54	0.54	0.34
15	80	0	5	0	0.39	0.39	0.48

APPENDIX C

76	19	0	0	5	0.30	0.29	1.85
64	20	0	0	16	0.47	0.46	2.64
50	45	0	0	5	0.60	0.60	0.26
40	30	0	0	30	0.41	0.41	1.35
40	50	0	0	10	0.97	0.94	2.25
35	45	0	0	20	0.74	0.75	0.45
30	60	0	0	10	0.95	0.96	0.76
20	72	0	0	8	0.60	0.60	0.22
15	80	0	0	5	0.31	0.31	0.42
0	85.5	5	0	9.5	0.64	0.65	1.25
0	85	10	0	5	0.66	0.69	3.87
0	81	10	0	9	0.76	0.71	6.48
0	76	19	0	5	0.84	0.81	3.69
0	75	5	0	20	0.36	0.41	13.96
0	70	10	0	20	0.78	0.62	20.27
0	68	17	0	15	0.74	0.75	1.64
0	65	15	0	20	0.38	0.48	25.67
0	60	20	0	20	0.06	0.03	49.35
0	85	10	5	0	0.52	0.51	1.46
0	81	10	9	0	0.24	0.25	4.02
0	76.5	15	8.5	0	0.37	0.36	3.40
76	0	19	0	5	0.12	0.13	2.86
72	0	18	0	10	0.32	0.30	4.62
0	75	5	20	0	0.30	0.30	0.24
0	70	10	20	0	0.44	0.44	1.03
0	68	17	15	0	0.51	0.52	1.90
0	72	18	10	0	0.61	0.61	0.79
0	72	18	0	10	0.80	0.83	4.25
48	40	0	0	12	0.18	0.18	3.32
72	0	10	18	0	0.28	0.17	40.31
60	0	20	20	0	0.03	0.02	44.65
76	0	5	19	0	0.10	0.14	41.78
80	0	10	0	10	0.17	0.22	27.81
76	19	5	0	0			9.17

Table C- 9 Test Data of ANN

BOS%	ROSA%	BPD%	RG%	PG%	28 days CS MPa	TANSIG	Error%
50.0	45.0	5.0	0.0	0.0	0.5	0.5	4.5
76.0	0.0	5.0	0.0	19.0	0.4	0.3	18.8
48.0	40.0	0.0	12.0	0.0	0.9	0.6	34.3
0.0	65.0	15.0	20.0	0.0	0.3	0.3	7.9
0.0	76.5	15.0	0.0	8.5	0.9	0.8	15.4
64.0	16.0	20.0	0.0	0.0	0.2	0.2	3.7
68.0	0.0	17.0	15.0	0.0	0.1	0.0	49.6
64.0	20.0	0.0	0.0	16.0	0.5	0.5	2.6
Average							17.1